Raquel Pereira Portela

MSc. in Biology

New studies in the resistance to β-lactams and in cell wall damage survival in *Staphylococcus aureus*: an integrated approach

A thesis submitted in partial fulfillment of the requirements
for the degree of Doctor of Philosophy

Supervisor: Rita Gonçalves Sobral de Almeida,
Assistant Professor,
Faculdade de Ciências e Tecnologia / Universidade NOVA de Lisboa

Jury:

Chairman: Professor Pedro Miguel Ribeiro Viana Baptista

Examination Committee: Professor Maria João Gracias Fernandes da Costa Catalão

Doctor Floriana Rosa Maria Campanille

Professor Rita Gonçalves Sobral de Almeida

Doctor Jorge da Silva Dias

Doctor Maria Leopoldina Caldeira Carvalhais Amorim Miragaia Ryder

FACULDADE DE CIÊNCIAS E TECNOLOGIA
UNIVERSIDADE NOVA DE LISBOA

September 2019

Aknowledgments

Firstly, to my supervisor, Professor Rita Sobral, for having given me the opportunity to pursue the PhD and to be involved in many projects. For her confidence in me and for all the knowledge I have learned from her. For being present at any time with genuine scientific interest and motivation. For always seeing further in the results and for the open minded and stimulating discussions. For the capacity to push me forward to always achieve better than before. Especially, for the friendship that has grown over the years. To Rita, a very special thank you.

To Professor Ana Madalena Ludovice, member of my thesis committee and member of the laboratory, for the scientific interest and the working discussions. For the lessons of scientific accuracy and rigor. For the kindness and support of her words in many moments and for the always warm criticism that made me improve. For the advices she offered me as a mentor and that I will take for life. For her, my deepest gratitude.

To Professor Mariana Pinho, member of my thesis committee, for her guidance and suggestions and for being always available to help me during this path.

To Professor Hermínia de Lencastre and Professor Alexander Tomasz, collaborators of the work presented in this dissertation and in whose laboratories this work emerged. To take part in their work is for me an immense privilege.

To Professor Isabel de Sá-Nogueira, coordinator of the PhD program in Biology, for all the support to the development of this Thesis. But especially for the kind way she received me since my first day at FCT and the care with which she accompanied me along the years. For her example and encouraging words. For all the pleasant moments and conversations inside and outside the lab, with her amazing perspicacity and disarming humor.

To Professor Pedro Almeida and Professor Catarina Leal, for a brilliant collaboration that extended boundaries and with whom the work was always performed in a friendly and motivating environment. For the opportunities they gave me and the confidence.

To Jorge Dias, for the support and the immeasurable help, firm motivation and for being always available. Mostly, for the friendship in all the moments.

To UCIBIO and to Departamento de Ciências da Vida da Faculdade de Ciências e Tecnologia da Universidade NOVA de Lisboa for having provided me all the conditions to perform this work.

To all the present and former Professors and Colleagues of Departamento de Ciências da Vida for having created a good and stimulating environment.

A special aknowledgment to the memory of Professor Ilda Sanches for her always positive and contagious view about life.

To Nicole, who always helped me with her precious work and always with a good mood.

To all the students that worked by my side in the different subjects of this thesis: Ricardo Lobo, Liliana Santos, Sérgio Torres, Ana Catarina Carvalho, Francisco Lopes and João Pedro SIlva. All of them motivated and pursued me to know more. With them I have learned a lot.

To Joana Bugalhão and Maria Cunha for the support and friendship in all moments. To Filipe Almeida, Inês Gonçalves and Inês Pereira and the “lunch team” for the always good environment.

To Teresa Figueiredo, for her friendship and the working nights at ITQB who made it so easy to handle.

To the members of the lab 330, Isabel, Lia, Viviana, Mário, Damien e Aristides who are the best partners I could ask for. For the special environment and friendship, for sharing the joys and complaints, for the team feeling. Once 330, forever 330! A special thanks to my partner Damien who listened to me when I needed, for the mutual confidence, for guessing my deepest feelings and for the adventures.

To the colleagues and friends of the Laboratory of Molecular Microbiology of Bacterial Pathogens: Inês Grilo, my colleague since my beginning in science, for the good moments shared these years and for the help and motivation; to Bárbara Gonçalves, a great friend and colleague, always genuinely interested and available to help and to listen me. To Gonçalo Cavaco who brought endless joy and good mood. To all for the exchange of knowledge and the stimulating environment.

To Cinthia, colleague and friend, for her words and support. For always cheering for me.

Aos meus amigos: Gabriela, Guida, Marisa, Hugo, Ana Rilo, Rute Cabrita, Ana Pena, Tiago, Rute Silva, Nuno, Ana Souto, Rafael, Maria e Idálio por uma bonita e longa amizade, por o tempo ser sempre pouco e por as memórias serem muitas. Por estarem sempre comigo e partilharem as minhas alegrias.

À Inês e à Rute, pela forte amizade e por me receberem sempre com alegria. Pelas noites de jogos e de partilha. Pelo companheirismo. À Inês, por gostar tanto de me ganhar!

À Marta, ao Afonso e ao meu sobrinho Bernardo por me receberem sempre, por haver sempre tempo, por uma grande amizade, sem reservas, e por me sentir sempre em casa.

À Irina, pelo incentivo, a dedicação e o carinho. Por me aconselhar e por me ouvir. Por me acompanhar e partilhar todos os bons momentos e pela paciência e conforto nos outros. Pelo que me ensina todos os dias. Por tudo, obrigada!

Ao meu irmão, Pedro, por acreditar e por me motivar sempre. Por ser um exemplo para mim. Por não serem precisas palavras. E porque ouvir “mana” irá encher-me o coração para sempre.

Aos meus pais, pela força, pela dedicação, pelo orgulho e pelo carinho que me transmitem. Pelo amor que me dedicam e a alegria partilhada em todas as conquistas. Pelos sonhos comuns e por todo o amparo no caminho. Por saber que qualquer direcção será em conjunto. A vocês o meu mais terno e profundo obrigada!

Para os meus avós, para quem todas as palavras não chegariam para expressar o meu amor e saudade.
O maior exemplo de coragem, de carácter e de ternura. Por tudo o que me transmitiram e pelo tanto que me motivaram. Porque não teria sido possível ser mais acarinhada e amada. Perdurarão para sempre comigo, no meu coração, a iluminar-me em qualquer caminho. Para vocês, o meu maior e mais sentido obrigada.

À vossa memória.

Abstract

In previous studies on *Staphylococcus aureus murF* gene, responsible for the addition of the terminal D-alanyl-D-alanine to the peptidoglycan stem peptide, the insertional mutant F9 was constructed and showed abnormal tripeptide incorporation, a damage described to be lethal and to impact resistance to β-lactams. Although unable to correct this defect, F9 survives with normal growth rate, suggesting the existence of a mechanism to overcome this damage. F9 belongs to a collection of thirty insertion mutants of which three showed the same phenotypes of F9 strain. All mutants harbored multiple chromosomal copies of the inserted plasmid arranged in tandem.

Whole genome sequencing of F9 and F9H, a highly resistant revertant strain, revealed a common loss-of-function mutation in *rho* gene, that encodes Rho transcription termination factor and one mutation unique to F9H, in *pheS* gene that encodes the phenylalanyl-tRNA synthetase. Through the construction of several mutants, we showed that Rho was responsible for amplification of the chromosomal plasmid copies, disclosing a new function for Rho in homologous recombination. Using genetic complementation, we demonstrated that *pheS* mutation promoted the reversion of the resistance phenotype by stringent response.

The transcriptome of F9 and F9H unveiled a new putative three-component-system, composed of two small proteins and a transmembrane protein, specific of staphylococcal species, that may be involved in the survival to an otherwise lethal damage. Functional characterization of this system was pursued by constructing and characterizing recombinant proteins and specific mutants. Although the two small proteins do not interact with one another, they associate to DNA and eventually to the cytoplasmic membrane. Their overexpression inhibits bacterial growth, suggesting that they must be tightly regulated. The transmembrane protein seems to impact bacterial growth upon challenge with oxacillin.

Altogether, our results provided new insights into the complex dynamic of cell wall metabolism and added new players to this equation.

Keywords: *Staphylococcus aureus;* Resistance to β-lactams; Peptidoglycan Biosynthesis; Stringent Response; Rho Transcription Termination Factor; Three-Component System.

Resumo

Em estudos anteriores sobre o gene *murF* de *Staphylococcus aureus*, responsável pela adição do terminal D-alanil-D-alanina do pentapéptido do peptidoglicano, foi construído um mutante de inserção, F9, que possui uma incorporação anormal de tripéptido, um dano descrito como letal e com impacto na resistência a β-lactâmicos. Apesar da incapacidade de corrigir o dano, o mutante F9 sobrevive e apresenta uma taxa de crescimento normal, sugerindo a existência de um mecanismo que permite à célula superar o dano.

O mutante F9 pertence a uma colecção de trinta mutantes de inserção dos quais três apresentam o mesmo fenótipo de F9. Todos os mutantes possuem múltiplas cópias do plasmídeo de inserção organizadas sequencialmente no cromossoma.

A sequenciação global de F9 e de F9H, um mutante revertente de F9 que apresenta elevada resistência a β-lactâmicos, revelou uma mutação comum no gene *rho* que codifica o factor de terminação da transcrição Rho, resultante em perda de função da proteína, e uma mutação única em F9H, no gene *pheS*, que codifica a fenilalanil-tRNA sintetase.

Através da construção de diversos mutantes demonstrou-se que a proteína Rho foi responsável pela amplificação das cópias de plasmídeo no cromossoma o que revelou uma nova função para o terminador da transcrição Rho no processo de recombinação homóloga.

Por complementação genética demonstrou-se ainda que a mutação no gene *pheS* promoveu a reversão do fenótipo de resistência através de um mecanismo de resposta restringente.

O transcriptoma de F9 e F9H revelou um novo putativo sistema a três componentes, constituído por duas proteínas de menor dimensão e uma proteína transmembranar, específico de *Staphylococcus* sp., que pode estar envolvido na sobrevivência a um dano que seria, de outra forma, letal. Para a caracterização funcional deste sistema procedeu-se à construção e caracterização de proteínas recombinantes e mutantes específicos. Apesar de as duas proteínas de menor tamanho não interagirem fisicamente, têm a capacidade de se associar a DNA e eventualmente à membrana citoplasmática. A sua sobrexpressão inibe o crescimento bacteriano sugerindo a sua forte regulação. A proteína transmembranar parece ter impacto no crescimento da bactéria aquando do crescimento com oxacilina.

Em suma, os resultados permitiram obter novos dados na complexa dinâmica do metabolismo da parede celular assim como adicionar novos elementos a este mecanismo.

Palavras-chave: *Staphylococcus aureus;* Resistência a β-lactâmicos; Biosíntese de Peptidoglicano; Resposta Restringente; Terminador de Transcrição Rho; Sistema a Três Componentes.

Table of Contents

Chapter 2 - Revisiting murF gene in *Staphylococcus aureus* - role of rho and stringent response in the phenotype of a cell wall mutant

Index of Figures

Index of Tables

Abbreviations and Acronyms

CAMP - Cationic Antimicrobial Pepetides
$CdCl_2$ – Cadmium Chloride
DSB – Double-Strand Breaks
GlcNAc - *N*-acetylglucosamine
HMM – High Molecular Mass
IPTG – Isopropyl β-D-1-thiogalactopyranoside
LMM – Low Molecular Mass
ManNAc - *N*-Acetylmannosamine
MRSA - Methicillin Resistant *Staphylococcus aureus*
MurNAc – *N*-acetylmuramic acid
NMR – Nuclear Magnetic Resonance
PBP – Penicillin Binding Protein
PFGE – Pulsed Field Gel Electrophoresis
ppGpp - Guanosine-5′-(di)phosphate-3′-diphosphate
pppGpp - Guanosine-5′-(tri)phosphate-3′- diphosphate
SCC*mec* - Staphylococcal Cassette Chromosome *mec*
Subsp – Subspecies
TCS – Two Component System
TEC – Transcription-Elongation Complex
TRC – Transcription-Replication Conflict
UDP - uridine-5'-diphosphate
WGS - Whole Genome Sequencing
WTA - Wall Teichoic Acids
X-Gal – 5-bromo-4-chloro-3-indolyl-β-D-galactopyranoside

Chapter 1
General Introduction

1.1. *Staphylococcus aureus*: an overview

Staphylococcus aureus are Gram-positive bacteria, firstly identified in 1881, isolated from pus, by the scottish surgeon Alexander Ogston (1). Due to its clustered appearance at the microscope, Ogston named the micrococci "staphylococci" from the greek *staphyle*, meaning bunch of grapes and *kokkos* meaning a grain or berry.

Later, in 1884, the German surgeon Anton J. Rosenbach, identified two types of staphylococci colonies with different pigmentations: white colonies and yellow colonies which were named by Rosenbach as *Staphylococcus albus* and *Staphylococcus aureus*, respectively. The name “aureus” was chosen after *aurum,* the latim name for gold, as a mention to the colour of the colonies. *Staphylococcus albus* would become, years later, *Staphylococcus epidermidis* (2).

Taxonomically, *S. aureus* belongs to the Phylum Firmicutes, Class Bacilli, Order Bacillales and Family Staphylococcaceae. *S. aureus* are facultative anaerobes that may grow by aerobic respiration or by fermentation, are catalase positive converting hydrogen peroxide to water and its cells are 0.5 to 1.5 µm in diameter. *S. aureus* tolerates temperatures from 15 to 45^{o}C and concentrations of NaCl of up to 10%. It has a low (<50 mol%) DNA G+C content (3).

The *Staphylococcus* sp. genus comprises, to date, more than 40 species. *S. aureus* can be distinguished from the other species for being able to ferment mannitol, a sugar alcohol, and for being coagulase and agglutination positive. Coagulase (Coa) and the von-Willebrand factor binding protein (vWbp) both are secreted and react with prothrombin and these complexes promotes the conversion of fibrinogen into fibrin, causing plasma to clot. An agglutination factor, clumping factor A (ClfA) in the bacterial envelope promotes the association of *S. aureus* with fibrin evading from phagocytosis (4).

Amongst all the staphylococcal species, due to their importance as human pathogens, more relevance has been given to *S. epidermidis* and to *S. aureus.*

1.2. Pathogenicity of *Staphylococcus aureus*

Staphylococcus aureus is a human commensal that can be found in several regions of the human body such as the skin and on its main reservoir, the anterior nares, where *S. aureus* expresses adhesion molecules that enable a successful colonization (5). It is estimated that 20 to 80% of the population are asymptomatic carriers, either in a persistent or in a transitory way. Of these, up to 30% of the carrier population is estimated to be of persistent carriers with the remaining concerning intermittent carriage (6). The nasal colonization seems to present a major risk for invasive infections, and the competition between *S. aureus* and the other constituents of the microbial flora of the nose for epithelial attachment sites or limited nutrients determines the success of the colonization process (7).

Under some circumstances, that remain largely unknown, *S. aureus* can evade the immune system and become an opportunistic pathogen, invading tissues and promoting diseases (8). One of the barriers responsible for the physical separation between the bacterial stages as commensal and as a pathogen is the skin, inhibiting bacteria to evade to other locations of the host, promoting infection. In burn patients, for instance, for who this barrier has been disrupted, the prevalence of infections caused by *S. aureus* is very high (9).

When *S. aureus* becomes a pathogen it can be responsible for a variety of diseases ranging from the mild-severe skin and soft tissue infections, like impetigo and cellulitis, to the immediately life-threatening severe diseases such as epidural abscess, toxic shock syndrome, osteomyelitis (infection of the bone), pneumonia or meningitis.

A high number of the infections caused by this pathogenic agent is related with the presence of devices that disrupt the cutaneous barrier allowing the entrance of bacteria to previously sterile locations, moreover because of the presence of biofilm communities in the surface of these devices that can act as reservoirs of bacteria. This is frequent for prosthetic cardiac valves, prosthetic joints and catheters (10).

The immense success of *S. aureus*, first as a colonizer and then as a pathogen, relies on two features related with genome's plasticity: the capacity to horizontally acquire resistance genes, which will be addressed later on this thesis (1.4. Resistance to antibiotics) and with the acquisition of a myriad of virulence determinants. These determinants are multifactorial and combine the actions of tissue adhesion, evasion of the immune system and injury of the host.

The first line of defense in an immune reaction is initiated by macrophages that release cytokines to gather neutrophils. However, *S. aureus* subverts the immune response through the production of a variety of specific toxins, by surviving intracellularly within immune cells and also by evading the capture by phagocytes (11).

Acting on the first part of this process, some virulence determinants are membrane bound factors that promote the bacterial adhesion such as collagen, fibronectin and elastin binding proteins. On the second stage of the process, the virulence determinants consist in secreted molecules helping the evasion of the immune system or damaging the host. This is the case of enzymes like coagulase and staphylokinase, of toxins such as enterotoxin, α-hemolysin and the potent shock syndrome toxin-1 (TSST-1). Other notable virulent factor of *S. aureus* is the panton-valentine leukocidin (PVL) a cytotoxin responsible for leukocyte destruction and tissue necrosis (12).

Additionally to the attack strategy, the success of *S. aureus* resides also in its protection from the host immune system. This is achieved by the production of antibody-binding proteins, cytolytic peptides, pore-forming toxins and polysaccharide capsules to confer protection against phagocytosis. The production of protein A (*spa*), is a very important step that prevents opsonization through the binding and neutralization of Fc region of immunoglobulin G (IgG). *S. aureus* also initiates a proinflammatory cascade by activating the tumor necrosis factor receptor 1 (TNFR1) (12).

The expression of these virulence factors is tightly controlled by transcriptional regulators. Some of them are at the same time regulators of metabolic pathways, interconnecting several key processes in the cell. For instance, the conversion from aerobic respiration to fermentation helps bacteria to evade

the immune radicals present at infection sites which are damaging to the respiratory enzymes (13). These regulators with combined activity are CcpA, that mediates catabolite regulation and also the expression of toxic-shock syndrome toxin 1 and CcpE, a fructose biphosphate that influences the expression of genes involved in iron acquisition, toxin production, pigmentation and capsule biosynthesis (14). The CodY, a general repressor, involved in amino acid biosynthesis also plays a role in virulence factor production (15). Other players are involved in the regulation of the expression of virulence factors: the *agr* quorum sensing system induces the expression of toxins and inhibits the translation of Rot. Rot is a repressor of the expression of toxins and regulator of extracellular proteases. The regulatory protein SarA represses the expression of *spa* and SigB is a stationary phase sigma factor that inhibits *agr* activity (16).

However, most of the regulation of virulence determinants is performed by two component systems (TCSs). The most relevant are: SrrAB that affects biofilm formation through the murein hydrolase Atl (17); SaeRS*,* that controls the production of hemolysins, leukocidins, superantigens and surface proteins (18) and the ArlRS, a regulator of autolysis which inhibits *agr* and induces MgrA which induces efflux pumps and capsule expression regulating a large number of secreted proteins (19).

1.3. *Staphylococcus aureus* cell envelope

The *S. aureus* first line of defense relies on the cell envelope, a multilayered structure, highly dynamic, that protects bacteria from the surrounding environment.

In *S. aureus,* the most outer layer of this envelope is composed by a polysaccharide capsule that helps masking the surface-associated proteins. To date, thirteen types of capsular polysaccharides (CP) have been identified, however, two main serotypes, CP5 and CP8, account for almost 80% of the clinical strains. The capsule is composed of trisaccharide repeating units of *N*-acetyl mannosaminuronic acid, *N*-acetyl-L-fucosamine and *N*-acetyl-D-fucosamine. The differences between capsules rely on the glycosidic links between sugars and the *O*-acetylation sites. The capsule thickness is highly variable and depends on environmental factors such as CO_2 availability (20, 21).

Internal to the capsule layer, are the cell wall and the inner membrane. The inner membrane is a lipidic bilayer that in *S. aureus* includes high amounts of lysyl-phosphatidylglycerol positively charged. Transmembrane proteins, lipoproteins and several two-component systems related with the sensing and response to external stimulus such as cell density and antibiotics, are attached to the cell membrane. Also attached to the membrane are lipotheicoic acids (LTAs), which consist in a chain of polyglycerol-phosphate anchored to a glycolipid inserted in the membrane (22).

In the outer layer is the cell wall whose composition and structure will be particularly focused below (1.3.1. *Staphylococcus aureus* cell wall).

1.3.1. *Staphylococcus aureus* cell wall

The cell wall of *S. aureus* is composed of a thick layer of peptidoglycan to which are covalently linked long anionic polymers called wall teichoic acids (WTAs). The cell wall is responsible for maintaining the structure and the elasticity of the cell, providing it with the ability to expand and relax. It has pores in its structure and at the same time withstands the osmotic pressure that can be of up to 20 atmospheres in Gram-positive bacteria (23).

The cell wall is constantly undergoing the processes of synthesis and degradation that parallels the growth and division of *S. aureus* and which allows for a rapid adaptation of bacteria to the exterior challenges. Studies using cryoelectron microscopy identified two distinct zones in the cell wall: one of low- and another of high-electron density. The low-electron density region is enriched in proteins and membrane-attached lipoteichoic acids. The high-electron density region appears as surrounding the first one and contains the polymeric peptidoglycan, the attached wall teichoic acids and cell wall proteins (24).

1.3.1.1. Wall teichoic acids

In *S. aureus*, wall teichoic acids (WTAs) consist in anionic polymers of 11 to 40 poly(ribitol-phosphate) repeating units and can account for as much as 60% of the total cell wall mass in Gram-positive organisms (25).

The biosynthesis of WTAs occurs in a set of sequential reactions catalyzed by dedicated enzymes and initiates in the cytoplasm with the synthesis of the linkage unit (Fig. 1.1). First, GlcNAc phosphate is transferred to an undecaprenyl phosphate carrier located at the membrane in a reaction catalyzed by TarO. Then, TarA transfers *N*-Acetylmannosamine (ManNAc) from UDP-ManNAc to the C4 hydroxyl of the GlcNAc residue forming a β-linked disaccharide. Phosphoglycerol is added to the C4 hydroxyl of ManNAc by TarB and the linkage unit is formed. The second series of reactions consists in the addition of a unit of glycerol-phosphate by TarF and the subsequent addition of the repeating ribitol phosphate units by TarL. The polymer is then exported to the exterior by TarGH, an ABC transporter (26). The last phase is the covalent linkage of the polymer by proteins of the the LCP family (LytR-CpsA-Psr) to the peptidoglycan via a disaccharide linkage unit to the C-6 hydroxyl group of the *N*-acetylmuramic acid residues (Fig. 1.1). After the assembly, the WTAs extend well beyond the peptidoglycan layer (27).

The WTAs suffer two kinds of modifications: D-alanylation and α- or β- glycosylation, in which the O-2 and O-4 positions of the ribitol residue are substituted with D-ala and N-acetylglucosamine (GlcNAc), respectively.

The D-alanylation consists in the introduction of D-alanyl ester residues in the ribitol groups in a process catalyzed by four proteins, DltABCD, encoded by the *dlt* operon. This process is a way for the bacteria to modulate the surface charge. Alanylation introduces positive charges to neutralize the negatively charged phosphates in the polymer backbone (28).

The α- or β-GlcNAc substitution at the O-4 ribitol residue is strain-specific, with some strains such as N315 exhibiting β-GlcNAc substitution at the O-3 ribitol residue (29). The glycosylation is performed by the α- and β- glycosyltransferases TarM and TarS, respectively. Recently, another β-glycosyltransferase was identified, the TarP (30).

The WTAs are important elements for the *S. aureus* cell since they contribute to several processes like bacterial adhesion, colonization, virulence and biofilm formation. Additionally, WTAs also play a role in cell division (29). In fact, in the absence of WTAs, *S. aureus* present a viable phenotype, however, it becomes impaired in the ability to colonize and to infect and present defects in the cell division. WTAs, namely their β-*O*-GlcNAc modifications, were found to mediate resistance to β-lactams in the Methicillin Resistant *Staphylococcus aureus* (MRSA) strains (31).

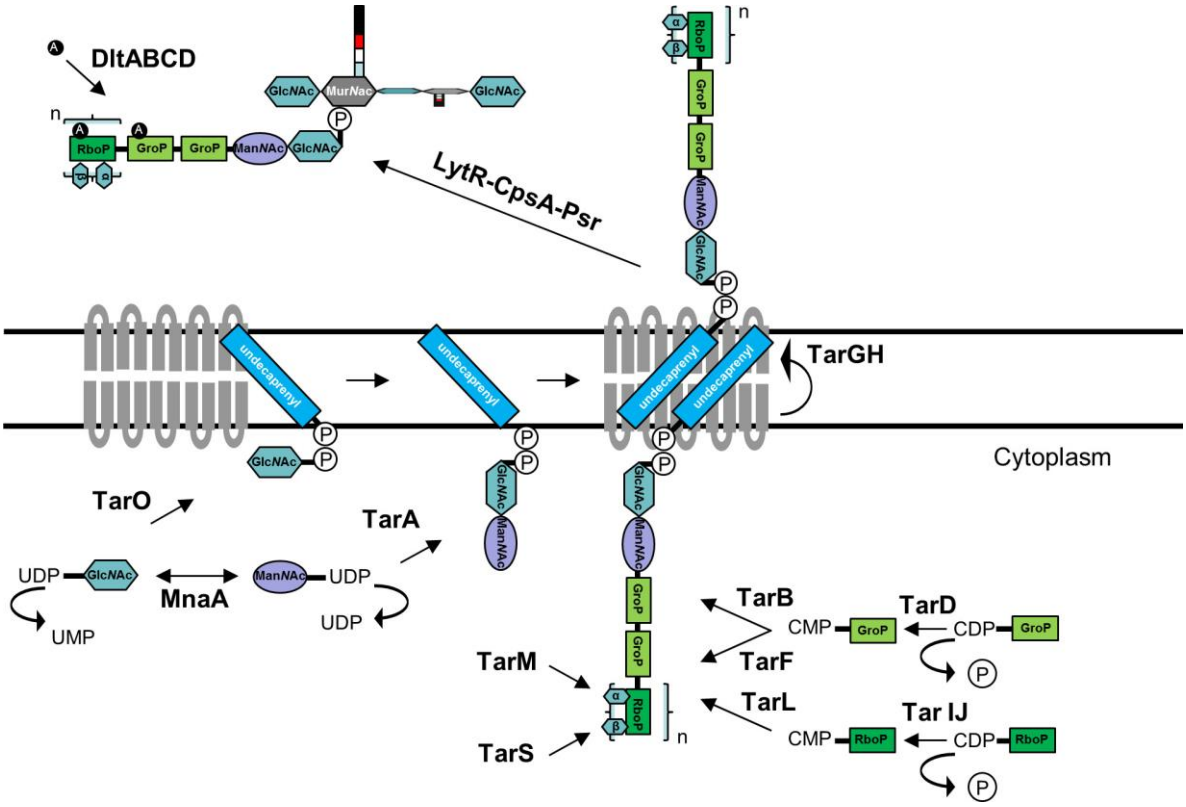

Fig. 1.1. Wall Teichoic Acids biosynthesis in *S. aureus*. WTA biosynthesis in a three-step process, starting in the cytoplasm with the formation of the anchor structure and binding to the membrane. The molecules of ribitol phosphate are then polymerized onto the anchor structure.
The glycosylation is performed by α- and β- glycosyltransferases and the whole structure is then flipped across the membrane. On the outer side of the membrane the polymer is covalently linked to the peptidoglycan. The enzymes involved in each step are indicated in the figure. (Reproduced from (32)).

1.3.1.2. Sortases – Peptidoglycan anchoring proteins

Despite its membrane location, sortases are important enzymes for the cell wall since they are responsible for linking the surface proteins, mostly virulence determinants, to the peptidoglycan during its assembly (33). The process of anchoring the proteins to the surface represents advantages for the

colonization and pathogenicity processes. *S. aureus* harbors two sortases, SrtA and SrtB, which recognize different sorting signals.

The surface proteins are synthesized in the bacterial cytoplasm with N-terminal signal peptides for Sec-mediated secretion and C-terminal sorting signal motifs. The signal peptide directs the export of the peptide through the Sec system. After translocation across the membrane, this signal is cleaved. Sequentially, SrtA cleaves the LPXTG motif of the sorting signal between the threonine (T) and glycine (G) residues. SrtB cleaves the NPQTN sorting signal. After cleavage, the protein is bound to the pentaglycine cross bridge in lipid II and incorporated into the nascent peptidoglycan (34).

So far, 21 proteins are known to be anchored to the peptidoglycan of *S. aureus* by SrtA, such as the protein A (Spa) and the clumping factors A and B (ClfA and ClfB), and 1 protein by SrtB, the iron-regulated surface determinant C (IsdC) that is linked to the cell wall when staphylococci are grown under iron starvation conditions, as occurs during host invasion (35).

1.3.2. *Staphylococcus aureus* peptidoglycan structure

The peptidoglycan is a net-like macromolecule, composed by linear glycan chains that are cross-linked by short peptides. The thickness of this layer ranges between 20 to 40 nm and represents about 50% of the cell wall (36). The glycan strains consists in alternating disaccharide units of *N*-acetylglucosamine (GlcNAc) and *N*-acetylmuramic acid (MurNAc) linked by β-1,4 glycosidic bonds (Fig. 1.2). The MurNAc is formed from a GlcNAc molecule with a D-lactoyl group linked to its C3 position that functions as the attachment site for the stem peptide.

About 85 to 90% of the *S. aureus* peptidoglycan consists of short glycan strands of 3 to 10 disaccharide units and only 10 to 15% consists of glycan strands with more than 26 disaccharide units (37).

Regarding the stem peptide, it is bound to the carboxylic group of the C3-lactoyl group of MurNAc through the amide bond of the α-amino group of the N-terminal L-Ala residue. The following residues are subsequently added: D-iso-glutamine (D-iso-Glu) at position 2, L-lysine (L-Lys) at position 3, and two D-alanine residues forming the L-Ala-ɣ-D-Glu-L-Lys-D-Ala-D-Ala pentapeptide precursor.

Specifically in *S. aureus*, the cross-linking responsible for conferring a net structure to the peptidoglycan, occurs between stem peptides from two adjacent glycan strands through a pentaglycine bridge (Gly_5) between the carboxylic group of D-Ala at position 4 and the free amino group of the L-Lys at position 3 of the adjacent stem peptide. This process is accompanied by the release of the last D-alanine (Fig. 1.2). About 20% of the terminal D-alanyl-D-alanine residues is estimated to remain uncrosslinked (38).

The inclusion of D-amino acids in the peptidoglycan is remarkably due to its rare abundance in nature (39). At the same time, these are the targets of an important class of cell wall antibiotics: the glycopeptides, precisely for its uniqueness.

The composition of the *S. aureus* peptidoglycan structure was elucidated through the combination of high performance liquid chromatography (RP-HPLC) with mass spectrometric analysis (40).

Peptidoglycan hydrolysis with M1 muramidase followed by reduction and separation by RP-HPLC allowed the identification of 21 distinct peaks (Fig. 1.3.). The first peaks eluted correspond to the monomeric structures composed of the two sugars, the stem peptide and variations in the number of glycines linked (Fig.1.3. Peaks 1 to 8). The second group of peaks correspond to the dimeric strcutures which are two monomers linked by the pentaglycine bridge and with variable number of glycines linked to one of the monomers (Fig. 1.3. Peaks 9 to 13). In the end of the chromatogram there is a “hump” of unresolved material that accounts for about 25% of the sample. This unresolved material represents the oligomers with higher degree of cross-linking (Fig. 1.3. peaks 15 to 21).

The peaks were identified to be monomers (disaccharide pentapeptides that represent 13% of *S. aureus* muropeptides), dimers (two monomeric structures crosslinked that correspond to 20%) and trimers to enneamers (40%) (37, 40-42).

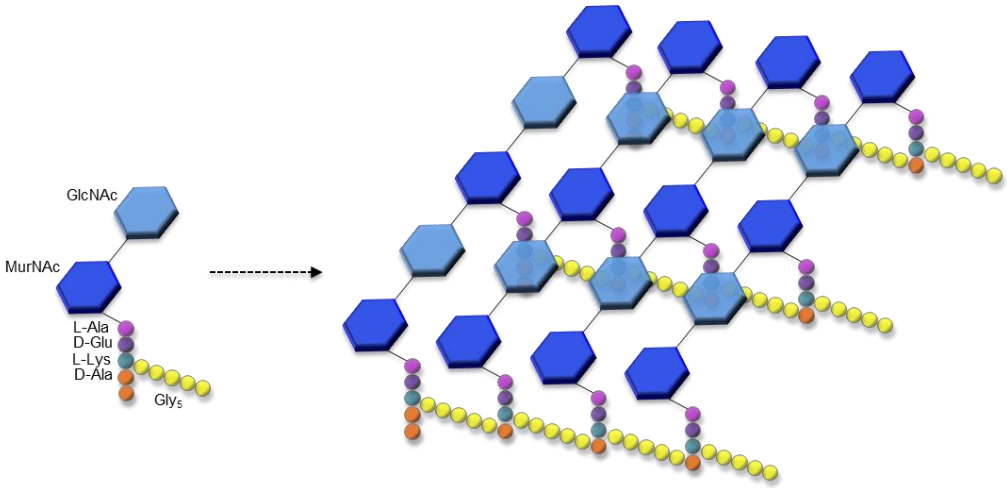

Fig. 1.2. Tridimensional structure of *S. aureus* peptidoglycan. Glycan chains are composed by two alternating sugars *N*-acetylglucosamine (GlcNAc) and *N*-acetylmuramic acid (MurNAc) linked by β-1,4 glycosidic bonds. To MurNAc is attached the stem peptide L-Ala-ɣ-D-Glu-L-Lys-D-Ala-D-Ala, cross-linked by a pentaglycine bridge.

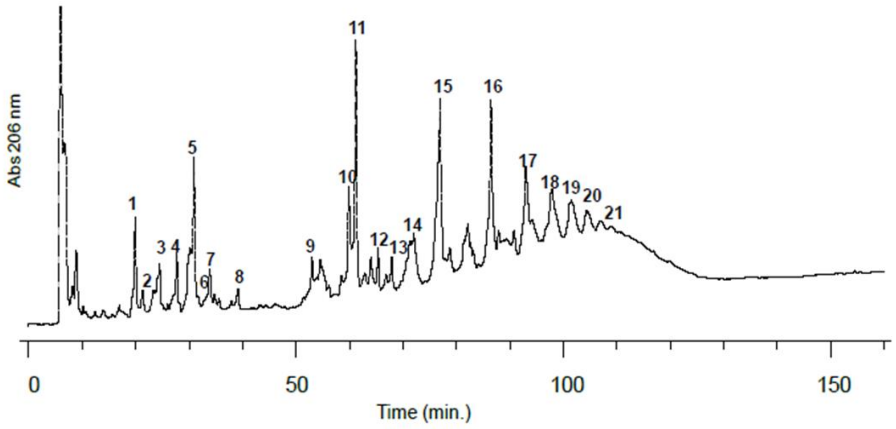

Fig.1.3. RP-HPLC profile of *S. aureus* peptidoglycan composition. Separation of *S. aureus* MRSA strain COL cell wall muropeptides, isolated, digested with muramidase and separated by reverse-phase HPLC. Adapted from (41).

1.3.3. *Staphylococcus aureus* peptidoglycan biosynthesis

The biosynthesis of the peptidoglycan occurs in a three-stage process, each taking place in a different cellular compartment (Fig. 1.4.). The assembly of the monomer unit occurs in the cytoplasm then it is transferred to the membrane and is finally translocated to the outer side of the cytoplasmic membrane, where the final step of assembly of the structure occurs. Each step will be described in more detail.

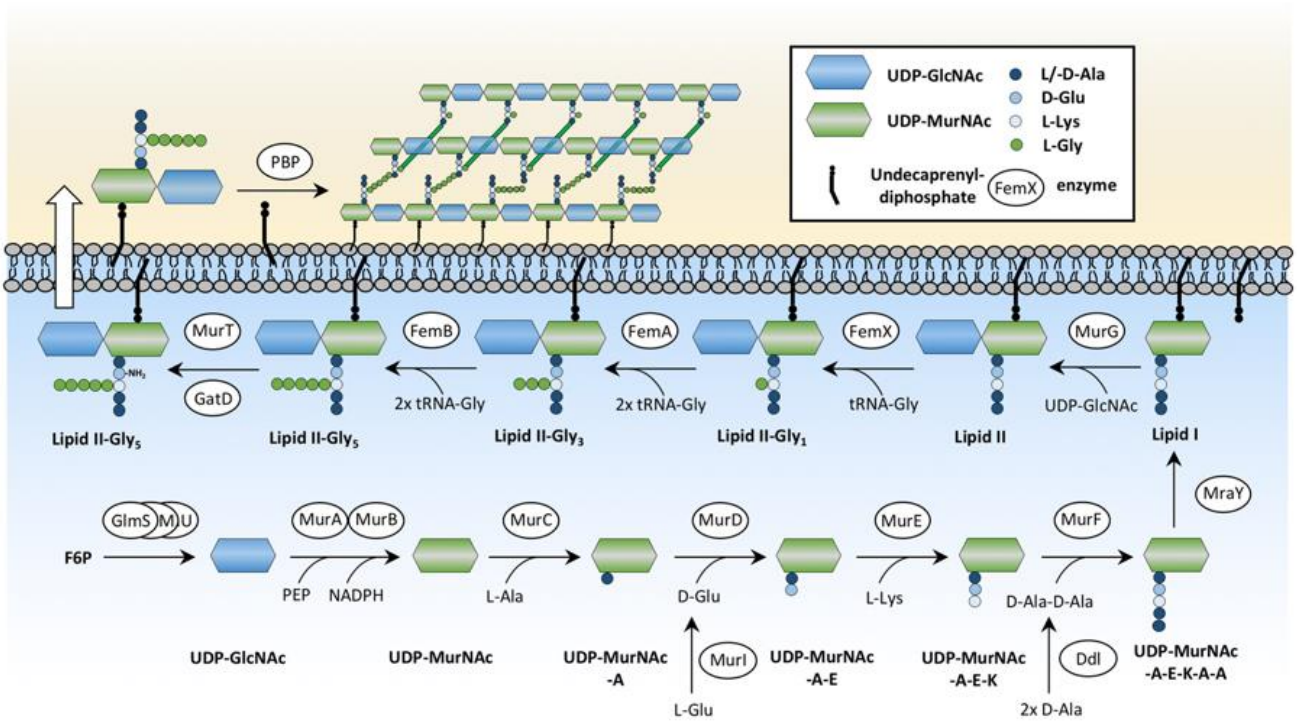

Fig. 1.4. The *S. aureus* peptidoglycan biosynthesis. Peptidoglycan biosynthesis occurs in a three-step process with each stage occurring in a different cellular compartment. The first step occurs in the cytoplasm and consists in the formation of the monomer. The second stage takes place at the cytoplasmic membrane, where the UDPMurNAc-pentapeptide precursor is linked to a membrane-associated lipid carrier forming lipid I to which is subsequently added GlcNAc forming lipid II. The third and last step includes the translocation of lipid II from the cytoplasm to the outer side of the membrane where the assembly occurs through transglycosylation and transpeptidation into the nascent peptidoglycan. Reproduced from (43).

1.3.3.1. Cytoplasmic steps – assembly of the monomer unit

The first cytoplasmic step consists on the formation of uridine-5'-diphosphate-*N*-acetylglucosamine (UDP-GlcNAc) in a series of successive reactions catalyzed by GlmS, GlmM and GlmU enzymes (Fig. 1.5.).

It begins with D-fructose-6-phosphate being converted into glucosamine 6-phosphate by the amidotransferase GlmS. Then, GlmM, a phosphoglucosamine mutase, catalyses the isomerization of glucosamine-6-phosphate to glucosamine-1-P and the bifunctional acetyltransferase-uridyltransferase GlmU synthesizes UDP-GlcNAc through acetylation using acetyl-coenzyme A (acetyl-CoA) and uridine triphosphate (UTP) in an uridylation process (44).

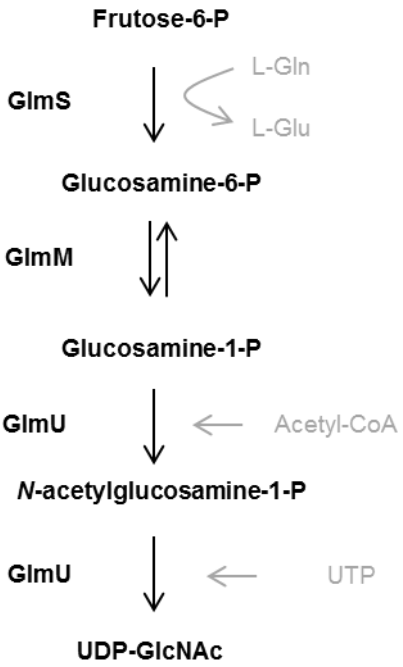

Fig. 1.5. Formation of UDP-GlcNAc. UDP-GlcNAc is formed from fructose-6-P, through the sequential action of GlmS, GlmM and GlmU enzymes.

After the formation of UDP-GlcNAc, the second step is devoted to the formation of UDP-MurNAc-pentapeptide which is called the Park nucleotide (45), the peptidoglycan building block. Once again, this occurs in a two-step process: first the formation of the UDP-MurNAc and then the subsequent addition of the stem peptide composed of five amino acid residues.

First, MurA enzyme transfers enolpyruvate from phosphoenolpyruvate (PEP) to the C3-position of UDP-GlcNAc. The resulting UDP-GlcNAc-enolpyruvate is reduced by MurB with NADPH yielding UDP-MurNAc. The second step is the sequential addition of L-Ala, D-Glu, L-Lys and the dipeptide D-Ala-D-Ala by the ATP-dependent amino acid Mur ligases MurC, MurD, MurE and MurF, respectively (Fig. 1.6). Most of the precursor synthesizing enzymes are essential and some of them are targets for known antibiotics (46).

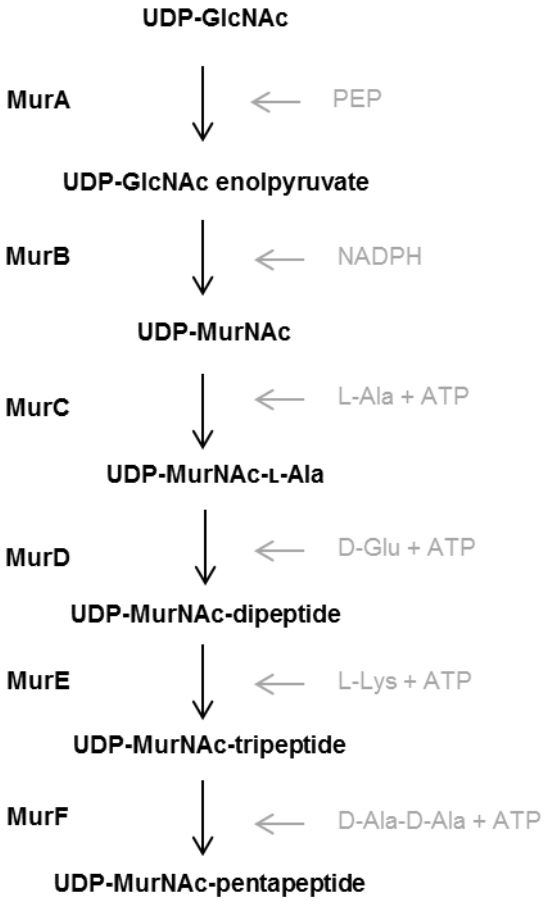

Fig. 1.6. Formation of UDP-MurNAc-pentapeptide. The UDP-MurNAc-pentapeptide is formed in the first stage of PG biosynthesis, occurring in the cytoplasm, through the consecutive action of Mur ligases.

1.3.3.1.1. Mur ligases

The Mur nomenclature was given to the cytoplasmic enzymes that take part in the murein (peptidoglycan) synthesis, from MurA to MurF (47). From MurC to MurF, the proteins belong to the Mur ligase family, due to the structural and functional common features (48). These enzymes are able to catalyze non-ribosomal peptide bond formation and to use D-amino-acids.

Structurally, Mur ligases have three domains: a N-terminal domain primarily responsible for recognition and binding of the UDP-MurNAc substrate, a central domain involved in the binding of ATP and a C-terminal domain that binds the incoming amino acid and transfers it to the substrate (Fig. 1.7) (49, 50). Functionally, the carboxyl group of the UDP precursor is activated by ATP and an acyl phosphate intermediate and ADP are formed, followed by the nucleophilic attack by the amino group of the amino acid or dipeptide to be added to peptidoglycan precursor, which removes the phosphate and forms a new amide bond (51).

Later, a new ligase was added to this family, MurT, responsible for the amidation of D-iso-glutamate into glutamine in the stem peptide (52, 53).

Despite the conserved domains, Mur ligases are highly specific and cross-activity was not documented.

In this work, the MurF ligase will be particularly focused. MurF is a 50 KDa protein and was firstly described in *S. aureus* in 1962 (54). The substrate of MurF is the UDP-MurNAc-tripeptide, to which the enzyme adds a terminal D-alanyl-D-alanine. The incorporation of D-alanyl-D-alanine is dependent on a first step of conversion of L-alanine to D-alanine which is catalyzed by alanine racemase, encoded by *alr* gene and a second step of dimerization of D-alanyl-D-alanine performed by D-alanine:D-alanine ligase DdlA with the consumption of ATP (55).

The MurF is able to use both UDP-MurNAc-L-Ala-D-Glu-L-Lys and UDP-MurNAc-L-Ala-D-Glu-*meso*-Dap being the less specific Mur ligase.

However, regarding the second substrate, other dipeptides can be accepted and transferred by MurF (56). For instance, *S. aureus* MurF is able to replace the terminal D-alanyl-D-alanine by D-alanyl-D-glycine if grown in medium rich in glycine (57).

The *murF* gene was shown to be an essential gene in *S. aureus* and an auxiliary gene, essential for the full expression of resistance to β-lactams (58, 59). Moreover, disturbance of the *murF* gene, was assessed by microarrays and showed to impact several metabolic pathways in the cell highlighting a link between cell wall synthesis, specifically at the MurF catalyzed step, and the metabolism of *S. aureus* (60).

To date, crystal structures of MurF homologs in *E. coli*, *Thermotoga maritima, Acinetobacter baumanii* and *Streptococcus pneumoniae* have been reported (61, 62). The structural elucidation would be of key interest potentiating the design of inhibiting compounds for a molecule of essential function for bacteria.

D-cycloserine is an inhibitor of the alanine racemase which converts L-alanine to D-alanine. Specifically of MurF, few classes of inhibitors are known. Initially, pseudo-tripeptide and pseudo-tetrapeptide aminoalkylphosphinic acids were developed but without significant antibacterial activity. The sulphonamides were also tested as MurF inhibitors (63). Thiazolylaminopyrimidines, 8-hydroxyquinolines and diarylquinolines were discovered but, once again, presented low antimicrobial activity (64).

A second generation of MurF inhibitors called cyanothiophene based MurF inhibitors were produced and, in relation to the inhibitors of first generation, reduced lipophilicity and increased solubility maintaining the enzyme inhibitory potency in micromolar range. However, these compounds achieve their antimicrobial action by a non-specific effect of damaging the cytoplasmic membrane. Prior to its development as drug candidates, the non-specific effect should be diminished (64).

The demand for bacterial inhibitors is a growing concern, and specifically at the Mur ligases level, several attempts have been made in order to discover a potent Mur ligase inhibitor. Different series of MurF inhibitors were sometimes described but, so far, still apart from clinical practice with the major obstacles encountered respecting to efflux pumps and permeability barriers (65, 66).

Fig.1.7. Ribbon model of the overall structure of MurF ligase of *S. aureus*. The three structural domains are colored to highlight the N-terminal domain (blue), the central domain (green), and the C-terminal domain (red). From: https://swissmodel.expasy.org/repository/uniprot/A0A0H2WWP1.

1.3.3.2. Membrane steps – formation of the lipid intermediate

After the formation of the monomer unit in the cytoplasm, the second stage comprises the linkage of the monomer to the lipidic carrier at the membrane. This process is accomplished through the formation of two lipid intermediates, lipid I and lipid II.

The lipid I is the membrane linked precursor formed after the transfer of UDP-MurNAc-pentapeptide to the undecaprenylphosphate molecule (C_{55}-P or bactoprenol), the lipid carrier embedded at the membrane (Fig. 1.4) (67). This transfer is catalyzed by the UDP-MurNAc-pentapeptide phosphotransferase MraY, an integral membrane protein (68, 69). Next, MurG, which is an *N*-acetylglucosaminyltransferase, transfers *N*-acetylglucosamine to lipid I resulting in the formation of lipid II. While linked to the membrane, through bactoprenol, the peptidoglycan precursor will undergo two modifications before the translocation: the addition of the pentaglycine bridge and glutamate amidation.

After these processes, that will be detailed further (1.3.3.2.1. and 1.3.3.2.2), the lipid II is translocated across the membrane with the mediation of the FtsW flippase (70).

1.3.3.2.1. Addition of the pentaglycine bridge to lipid II

The pentaglycine bridge is the trademark of *S. aureus* and it is necessary for the transpeptidation reaction occurring at the cell wall in the last stage of peptidoglycan assembly. It is responsible for the elasticity of the peptidoglycan and drives major processes in the cell, such as division and resistance to β-lactams.

The pentaglycine bridge links the L-lysine of the stem peptide of one peptidoglycan strand to the D-alanine in position 4 of the adjacent strand.

This addition occurs in the sequential order of the activity of specific peptidyltransferases: FemX encoded by *fmhB* gene adds the first glycine of the cross bridge, FemA encoded by *femA* adds the second and the third glycines and FemB encoded by *femB* gene, adds the fourth and the fifth glycines, respectively (71, 72). The construction of the pentaglycine bridge depends on glycyl-tRNAs as glycine donors (73).

The *fmhB* gene was already described as an essential gene, but *femA* and *femB* were only this year proven to also be essential (74). In previous works, *S. aureus femAB* null mutants resulted in growth defects, and it was suggested that *S*. *aureus* could survive with a peptidoglycan composed of a bridge formed by a single glycine since there was a reduction but not absence of cross-linking in these mutants. However, these mutants most likely had compensatory mutations (75, 76).

1.3.3.2.2. Amidation of the glutamate residue of the stem peptide

The glutamate amidation is a secondary modification of the peptidoglycan that consists in the amidation of the α-carboxyl group of the D-glutamate residue in Lipid II, forming D-isoglutamine. The reaction is catalyzed by the MurT and GatD enzymes. MurT is an enzyme of the Mur ligase family and GatD belongs to the family of CobB/CobQ-like glutamine amidotransferases (52, 53). The two enzymes act cooperatively, physically interacting through the C-terminal region of MurT, the DUF1727 domain, which is suggested to channel the ammonia from glutamine hydrolysis at the GatD active site, to the active site of MurT (77).

The amidation of peptidoglycan by this enzymatic complex is essential in *S. aureus* which may be due to an optimal transpeptidase activity of penicillin binding proteins (PBPs) when the stem peptides are amidated (78). Defects on amidation also impact resistance to β-lactams and increased susceptibility to lysozyme, the first line of the host's defense (79).

1.3.3.3. Extracytoplasmic steps: polymerization of peptidoglycan

The last step of peptidoglycan biosynthesis concerns the incorporation of the dissacharide-pentapeptide into the peptidoglycan layer on the extracytoplasmic side of the cellular membrane, mainly at the septum (80) (Fig. 1.2). This incorporation occurs through two different reactions: transglycosylation and transpeptidation.

Transglycosylation consists in the elongation of the glycan chains. The dissacharide-pentapeptide, which is linked to the lipidic carrier, bactoprenol, is in this way attached to the nascent peptidoglycan layer. The reducing end of the MurNAc of the nascent lipid-linked peptidoglycan strand is transferred onto the C-4 carbon of the glucosamine residue of the lipid-linked precursor, accompanied by the release of bactoprenol (81). Transglycosylation is catalyzed by the monofunctional glycosyltransferases (MGTs) (detailed in 1.3.3.3.1.) and the penicillin binding proteins (PBPs) (detailed in 1.3.3.3.2.).

The following step is transpeptidation (the reverse reaction is endopeptidation) which is the reaction responsible for the cross-linking between two stem peptides of adjacent glycan chains. Firstly, the D-alanyl-D-alanine bond is disrupted by a nucleophilic attack of the hydroxyl group of the active serine of the PBP domain, producing an ester-linked peptidyl enzyme with the concomitant release of the terminal D-Ala. This reaction provides the necessary energy for the next step which is the binding of the side chain amino group of the L-Lysine residue to the carboxylic group of D-Ala of an adjacent peptide (82). The transpeptidation reaction is exclusively catalyzed by PBPs.

1.3.3.3.1. Monofunctional glycosyltransferases (MGTs)

MGTs are membrane-bound enzymes with a transglycosylase domain. These enzymes are able to perform the transglycosylation and thus to elongate the glycan chains of peptidoglycan without cross-linking activity. Two MGTs were identified and characterized in *S. aureus*: MGT and SgtA (83, 84). Both enzymes are not essential, but, in the absence of PBP2, a PBP with transglycosylase activity, the cell depends on MGT to remain viable, suggesting different substrates for PBP2 and MGT. The interaction of both proteins was already demonstrated, indicating that they may work as a complex. MGT is able to compensate for the lack of PBP2 transglycosylase activity both in MSSA and in MRSA strains but it does not replace PBP2 upon challenge with high concentrations of oxacillin (83).

1.3.3.3.2. Penicillin binding proteins

PBPs are membrane associated enzymes responsible for the step of transpeptidation of the peptidoglycan which consists in the 4-3 cross-link between the side chain amino group of the L-lysine residue to the carboxylic group of the D-Ala at position 4 of an adjacent peptide. The PBP enzymes are the targets of the β-lactams class of antibiotics, inactivating them by acylation. The β-lactams covalently bind to the active site serine in the catalytic cleft of PBPs which results in an acyl-enzyme that is hydrolyzed at a very slow rate, thus reducing the capability of peptidoglycan cross-linking.

S. aureus has four native PBPs, PBP1, PBP2, PBP3 and PBP4 and one acquired, PBP2A exclusive of methicillin resistant strains (MRSA). Initially, they were described according to their molecular weight and then by the selective binding of different β-lactams and its concentrations (85, 86).

PBPs are divided into two categories: the high molecular mass (HMM) and the low molecular mass PBPs (LMM) (113). The HMM PBPs can belong to class A, having a bifunctional activity of transglycosylase and transpeptidase, or to class B, that are monofunctional and only exert transpeptidation activity. The LMM PBPs are single domain proteins with only a transpeptidase domain (87, 88).

HMM PBPs have a C-terminal penicillin-binding domain, responsible for the transpeptidase reaction and for β-lactam binding. In class A HMM-PBPs, the N-terminal domain is responsible for

their glycosyltransferase activity, in class B the N-terminal is presumably associated with cell morphogenesis by interacting with other proteins involved in the cell cycle.

PBP1 (*pbpA* gene) is a class B PBP that has only transpeptidation activity. It is an essential PBP and localizes at the division septum (89, 90). The impairment of PBP1 results in decreased viability but in a normal peptidoglycan. Moreover, PBP1 must be present even in the absence of its transpeptidase activity for the correct septum formation despite the fact that its activity is necessary for cell separation, which seems to suggest a dual role function for PBP1 (91, 92).

PBP2 (*pbpB* gene) is the only class A PBP of *S. aureus.* It has a transglycosylase and a transpeptidase domain. It is also the most abundant of all the native PBPs (93). Since its transpeptidase activity can be complemented by the acquired PBP2A, PBP2 is only an essential PBP in MSSA strains (94). Additionally, in the presence of β-lactams, PBP2 cooperatively functions with PBP2A. While the transpeptidation domain is inactivated by the antibiotic, the transglycosylase domain remains important for the expression of resistance to β-lactams (95). The PBP2 accepts stem peptides with pentaglycines, triglycines and monoglycines as substrates for transpeptidation (96).

PBP3 (*pbpC* gene) is a class B PBP, and among all the PBPs of *S. aureus* is, so far, the less well studied. It contains the common conserved motifs of transpeptidases in its C-terminal penicillin binding domain and an N-terminal of unknown function. The inactivation of PBP3 did not result in alterations in the peptidoglycan composition. The rates of autolysis were slightly decreased. However, in the presence of a sub-MIC of methicillin, the *pbpC* impaired mutant cells had an abnormal size and shape and disoriented septa, suggesting that other PBPs can take the function of PBP3 when it is unavailable (97). More recently, the C-terminal of PBP3 was found to bind and activate human plasminogen, which is the precursor of plasmin, a serine protease that dissolves blood clots, undisclosing a role for PBP3 in virulence (98).

PBP4 (*pbpD* gene) is a non-essential LMM PBP. Inactivation of PBP4 results in a normal growth and in a reduced fraction of highly oligomeric peptidoglycan structures which was suggested to be due to a secondary activity of PBP4 as a transpeptidase (99). PBP4 acts as a transpeptidase exclusively in pentaglycine muropeptides and can have other functions: incorporation of D-amino acids into peptidoglycan, cross-linking of partially cross-linked pentamers and of high oligomeric muropeptides which is useful for the repair of defects in cells (93, 100). Although previously it was thought that PBP4 was not necessary for resistance to β-lactams, it was shown that in community associated strains (CA-MRSA), its expression is necessary for resistance (101). Recent studies have shown that mutations in *pbpD* result in resistance to β-lactams independently of PBP2A (102).

PBP2A (*mecA* gene) is an acquired PBP of *S. aureus,* only with transpeptidation activity, responsible for the resistance to β-lactams in MRSA strains, due to its extremely low affinity for β-lactams, continuing transpeptidation in its presence (103). The serine at the catalytic site changes conformation to maintain preference for the peptidoglycan to the detriment of the β-lactam molecule (104).

PBP2A cross-links stem-peptides with pentaglycine branches, but also the triglycine-containing stem peptides. The monoglycine stem peptides are not cross-linked by PBP2A (96)

1.3.4. Modifications of the cell wall

S. aureus peptidoglycan undergoes several modifications with the intent of avoid the recognition of bacteria by host factors. Before the complete assembly of peptidoglycan, the precursors suffer two modifications: glutamate amidation (described in 1.3.3.2.2.) and the D-alanine esterification of teichoic acids (described in 1.3.1.1.). After the complete assembly of peptidoglycan, it undergoes another modification: the *O*-acetylation of MurNAc.

The *O*-acetylation is performed by OatA, an integral membrane *O*-acetyltransferase. This enzyme transfers an acetyl group of acetyl-CoA to the C-6 position of the muramic acid residue, only in pathogenic strains of *Staphylococcus* sp. (105). The *O*-acetylation sterically prevents the binding of lysozyme to peptidoglycan conferring resistance to this muramidase (106).

1.3.5. Peptidoglycan hydrolases

As important as the biosynthesis of the peptidoglycan is its disassembly, necessary for cell division and for the incorporation of new muropeptides, in a turnover process. Moreover, the release of peptidoglycan fragments can work as a signaling mechanism in inter-bacteria and bacteria-host communication as well as a trigger for adaptive responses (107). This process is accomplished by the autolytic activity of hydrolases, classified according to the type of bond cleaved. There are several classes of hydrolases and in *S. aureus*, three autolytic activities are described: *N*-acetylglucosaminidases, cleaving glycosidic bonds between GlcNAc and MurNAc in glycan strands, *N*-acetylmuramidases that cleave the bond between sequential MurNAc and GlcNAc residues and *N*-acetylmuramyl-L-alanine amidases, hydrolyzing the amide bond between the first amino acid of the stem peptide and the MurNAc (Fig 1.8) (107, 108). An example of an *N*-acetylmuramidase is lysozyme, the first line of defense of the innate immune host response against bacterial infection (109, 110).

Other peptidoglycan hydrolases are peptidases that can be classified into two groups: carboxypeptidases that remove the C-terminal amino acid of the stem peptide and endopeptidases that cleave within the peptide cross-links, which is the case of lysostaphin, a glycylglycine endopeptidase capable of cleaving the pentaglycine bridge specific of *S. aureus* (111, 112).

The zymogram analysis of the autolytic pattern of *S. aureus*, revealed more than 20 bacteriolytic bands, suggesting that *S. aureus* produces several peptidoglycan hydrolases (113). The four main characterized are: Atl, SleI, LytM and LytN.

The major peptidoglycan hydrolase is Atl, a bifunctional protein that is produced as a single polypeptide and is then proteolytically cleaved into an *N*-acetylmuramyl-L-alanine amidase and an *N*-acetylglucosaminidase with the ability to bind DNA, which may be related to the capture of extracellular DNA molecules. (114-116). Atl is involved in cell separation, cell wall turnover, antibiotic-

induced lysis and biofilm formation. Sle1 is an *N*-acetylmuramyl-L-alanine autolytic enzyme, involved in cell separation after division (117) .

Other four autolysins are known in *S. aureus*: LytM, LytN, LyA and LytH. LytM is a glycylglycine endopeptidase and the remaining are *N*-acetylmuramyl-L-alanine amidases (118, 119).

The regulation of hydrolases must be tight to avoid the possibility of uncontrolled lysis. In *S. aureus*, the regulation of the autolytic activity involves two-component systems such as ArlRS that mediates autolysis exclusively in methicillin susceptible strains of *S. aureus* (MSSA) and not in MRSA strains, through the repression of *lytN* (120).

Other examples are the two component systems LytRS (121) and the WalKR (122). Other global regulators involved in autolysis are MgrA, SarA and Agr (123, 124).

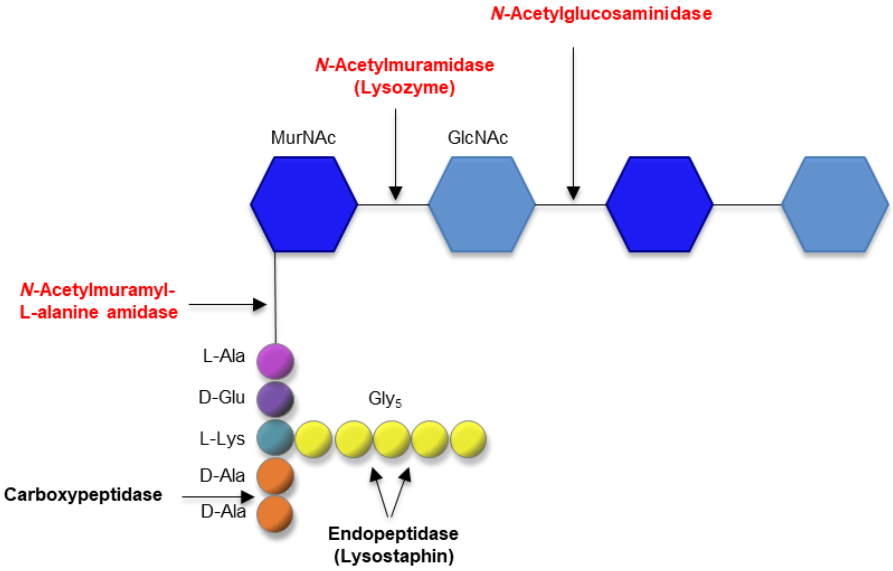

Fig.1.8. Activity of peptidoglycan hydrolases. Schematic representation of the cleavage sites of the hydrolases of the *S. aureus* peptidoglycan. In red are highlighted the peptidoglycan hydrolases produced by *S. aureus*.

1.4. Staphyloccocal resistance to antibiotics

The outstanding success of *S. aureus* as a pathogen is not only associated with the presence of several virulence determinants, but also with its unusual capacity of acquisition and maintenance of genetic determinants of resistance (125).

Due to the uniqueness of the peptidoglycan structure, without counterpart in any other structure of the host, the targeting of steps in its biosynthesis represents an advantage. The peptidoglycan has been one of the most interesting bacterial targets for the development of antimicrobials, such as the β-lactams and the glycopeptides.

Before the introduction of antimicrobials in the clinical practice, the prevalence of infections by *S. aureus* almost paralleled the rate of mortality, of about 80%, meaning that the infections were untreatable (126). With the introduction of penicillin, in the early 40's, this rate significantly decreased and almost all the isolates exhibited susceptibility to this antibiotic. However, soon after, penicillin-

resistant *S. aureus* expressing and secreting a β-lactamase were isolated and this resistance trait disseminated to almost all the *S. aureus* isolates (127-129).

To overcome the emergence of resistance to penicillin, methicillin, a semi-synthetic penicillin which is resistant to the action of β-lactamases, was clinically introduced in 1959 (130). However, soon after, resistance to methicillin also appeared, with the isolation of the first MRSA strain occurring in 1962 in the United Kingdom (131).

One of the first MRSA isolates was the *S. aureus* strain COL, isolated from the air of an operating-theatre in a hospital in Colindale, England (132). It was one the first isolates to be characterized and is a model for intrinsic methicillin resistance (133). It has a high and homogenous level of resistance to methicillin (MIC~800 μg/ml). COL strain does not carry functional *mecI/mecRI* regulatory genes, being the *mecA* expression constitutive. Its genome was sequenced and revealed a 7% of mobile genetic elements including a pT181 plasmid conferring tetracycline resistance, a prophage L54a integrated into the *geh* lipase gene and five pathogenicity islands mainly composed of toxins and virulence elements. COL has no transposons in its genome (134).

Contrarily to the mechanism of resistance to penicillin, the mechanism of resistance to methicillin confers a broad protection against all the β-lactams. This emergence of resistance to methicillin begun in the 60's and remained until nowadays associated with a high prevalence in nosocomial settings and in the community worldwide (135).

After the dissemination of resistance to β-lactams, the glycopeptides, that have been discovered in 1956 but not readily used, were introduced in the clinical practice in the 70's as the last resource for the treatment of MRSA infections. However, in the 80's, resistance to glycopeptides was detected in *Enterococcus* sp.. Shortly after, in 1997, the first vancomycin intermediate *S. aureus* (VISA) was isolated in Japan and in 2002 the first vancomycin resistant *S. aureus* (VRSA) was isolated in the United States (136). The mode of action of glycopeptides consists in the binding of the antibiotic molecule to the D-Ala-D-Ala terminus of the peptidoglycan structure inhibiting the cross-linking by PBPs. In VRSA strains, that acquired the genetic determinant *vanA* from *Enterococcus*, the terminus of the stem peptide is replaced by a D-Ala-D-Lac dipeptide which does not bind to the glycopeptide (137).

The more recent antibiotics that are in utilization against MRSA infections are: linezolid, an oxazolidinone that acts as a protein synthesis inhibitor; daptomycin, a cyclic lipopeptide acting on the membrane potential; tigecycline, a glycylcycline class of antimicrobial agents that binds to the bacterial 30S ribosome; telavancin, a lipoglycopeptide which is a glycopeptide derivative and ceftaroline and ceftobiprole, both fifth generation cephalosporins (138). However, with higher or lower prevalence, staphylococci have developed resistance to all of the antibiotics introduced in clinics (139-143).

Recently, it was demonstrated that a substantial fraction of the MRSA strains are susceptible to penicillins when used in combination with β-lactamase inhibitors. This is achieved through two different mutations, one in the *mecA* promoter region, reducing the expression of PBP2A and other increasing its affinity for penicillin in the presence of clavulanic acid (144). These findings can provide new treatment options for MRSA infections making use of collateral sensitivity and of antibiotics already available.

Despite the fact that *S. aureus* presents resistance mechanisms to several classes of antibiotics, the mechanism of resistance to β-lactams has been widely studied due to its historical and epidemiological significance and it has been paralleled by the study of the peptidoglycan structure and its biosynthesis.

Due to the scope of this thesis, resistance to β-lactams will be further addressed.

1.4.1. Mode of action of β-lactams and resistance mechanisms

The β-lactams are the most widely used class of antibiotics, due to their low toxicity, broad-spectrum activity and low cost. They are divided in four major classes: penicillins, carbapenems, monocyclic β-lactams and cephalosporins and, inside each class, synthetic and semi-synthetic derivatives were developed. Nowadays, the majority of the β-lactams are synthetic derivatives, however they all derive from natural products: Penicillin G from the *Penicillium notatum* mold; cephalosporin C from *Cephalosporium* sp. in sewage sludge; carbapenems from actinomycetes in soil samples and monocyclic β-lactams (monobactams) from bacteria from soil and water samples (145). Each new class of β-lactams has been developed with the aim to increase its spectrum of activity or to address new specific resistance mechanisms in the targeted bacterial population. The first group, the penicillins, includes the first antibiotic and first β-lactam clinically used, the penicillin G (benzylpenicillin), the penicillinase-stable methicillin, introduced in clinical practice in 1959 that was then discontinued and also oxacillin, the β-lactam routinely used in research laboratories (146) .

All β-lactams have in common the highly reactive four-membered β-lactam ring that structurally mimics the carboxy-terminal D-Ala-D-Ala of the stem peptide, the natural substrate of PBPs. Through the serine residue 403 of the active site, the PBPs bind irreversible to the β-lactam molecule, through an acylation reaction. This reaction forms a penicilloyl-β-lactam intermediate, which is stable and has a low rate of deacetylation. This bond prevents the PBP to bind to its natural substrate and blocks the transpeptidation reaction in the last step of PG biosynthesis (108).

Resistance to β-lactam antibiotics can occur, in *S. aureus,* by two main mechanisms: the degradation of the β-lactam ring of the antibiotic by the production of a β-lactamase enzyme and by the expression of a PBP with low affinity for β-lactams, PBP2A, that continues the transpeptidation step in the presence of the antibiotic (147). Mutations in the PBPs may also confer resistance to the β-lactams.

1.4.1.1. Resistance mediated by the production of β-lactamases

β-lactamases are versatile, ancient enzymes, whose existence is prior to the existence of antibiotics pressure. They are produced from many bacterial sources and have in common the ability to hydrolyze a β-lactam ring.

β-lactamases and PBPs are structurally and functionally similar, despite the difference in amino acid identities (148). Both present conserved patterns and preservation of the topology at the active site with the majority of the β-lactamases containing a serine in the active-site that can also be acylated by β-lactams, as it happens with PBPs (145). In fact, it is suggested that β-lactamases may have evolved from PBPs (82, 148). β-lactamases are still divided in four groups, according to the serotype of the strains in which they are expressed and differences in hydrolysis of selected β-lactam substrates. They can be plasmid borne or located in the chromosome (149, 150). Today, 17 functional groups associated with four molecular classes have been distinguished.

In *S. aureus,* the β-lactamase is expressed by activation of the *blaZ* gene (151). Two adjacent regulatory elements control the expression of *blaZ*, the antirepressor signal sensor/transducer *blaR1* and the repressor *blaI* (126, 152). The expression of the BlaZ β-lactamase is not constitutive but is induced by the presence of β-lactam antibiotics (153).

When β-lactams are absent, the repressor BlaI is bound to the promoter region, repressing the transcription of both *blaZ* and *blaRI-blaI*. When bacteria are challenged with β-lactams, the antibiotic is sensed by binding to the extracellular part of transmembrane sensor transducer, BlaRI. The association of the antibiotic to the sensor induces a conformational modification that activates its cytoplasmatic domain as a protease, that cleaves itself and also the repressor, BlaI, inhibiting its attachment to the *bla* operator (154). In the absence of the repressor, the *blaZ* is transcribed and the β-lactamase is synthesized (155, 156).

1.4.1.2. *mecA*-dependent resistance to β-lactams

Additionally to the β-lactamase production, another mechanism of expression of resistance to β-lactams is through the expression of an exogenous gene, *mecA*. The strains expressing resistance through this mechanism are the so-called methicillin resistant *S. aureus* strains - MRSA.
The *mecA* encodes an extra HMM class B PBP, PBP2A, of 78 KDa, with a low binding affinity for β-lactams (157). In the presence of β-lactams, PBP2A retains the transpeptidase activity, by the the presence of key catalytic residues, but at the same time, has low affinity for the substrates, which are both the muropeptides and the β-lactams. Bacteria containing the *mecA* gene continue the peptidoglycan synthesis relying on the cooperative function between the transpeptidase activity of PBP2A and the transglycosylase domain of the native staphylococcal PBP2 (94, 103, 157).

The majority of MRSA strains possess the *mecA* gene but other genetic determinant exists in *S. aureus*, namely the *mecC* gene. The *mecC* gene is also found in other species of the genus like *S. xylosus*, *S. sciuri* subsp. *carnaticus*, and *S. stepanovicii.* The *mecC* gene has a 69% nucleotide

sequence identity with *mecA* and also encodes a low affinity PBP but seems limited to few *S. aureus* clonal lineages (CC130 and ST425) and poorly associated with human infection, so far (158, 159).

Additionally, more distant phylogenetically, but sharing a 62% nucleotide sequence identity with *mecA*, are the *mecB* and the *mecD* genes from *Macrococcus caseolyticus*, a colonizer of animal skin.

The *mecB* was found located in a plasmid in *M. caseolyticus* and also in a ST7 strain of *S. aureus* infecting a human (160). The *mecD* gene is carried within one of two resistance islands inserted at 3' end of the conserved *rpsI* gene. The resistance island also contains genes for an integrase of the tyrosine recombinase family and one putative virulence-associated protein (*virE*).

The resistance island $MecRI_{mecD}$ encodes a site-specific recombinase which suggests the risk of transference of this genetic determinant to new hosts across genus barriers (161).

All the four *mec* genetic determinants confer resistance to β-lactams through the expression of a low affinity PBP. The most prevalent and more studied to date has been the most successful one, the *mecA* gene.

1.4.1.2.1. *mecA* origin

It is known that the *mecA* gene of *S. aureus* is of exogenous source and a lot of efforts have been made to track the evolutionary origin of *mecA*. In the beginning of this demand, structural studies have proposed that the *mecA* gene could have been originated from the recombination between a PBP (from *E. coli* or from *Enterococcus hirae*) with a β-lactamase encoding gene (162, 163).

Later, a *mecA* homolog was found in *S. sciuri*, *mecA1*, which is the most ancestral form of *mecA,* sharing 85% of homology in nucleotide sequence with the *S. aureus mecA*. Other homologs were found in *S. vitulinus,* the *mecA2*, with 94% of homology with the *S. aureus mecA* and in *S. fleuretti,* the *mecAf*, with 99% homology with the *S. aureus mecA* (164, 165). The *mecAf* gene from *S. fleuretti* is the only homolog which, in fact, confers resistance to β-lactams.

All these homologs are differentially located, 200 Kb apart, in the genomes in which they are comprised, in comparison with the native localization of *mecA* in *S. aureus*, which is in the SCCmec localized at the *orfX* (165).

It is suggested that the *mecA1* from *S. sciuri* is the evolutionary precursor of the *S. aureus mecA*. Most probably, the primary function of *mecA* was related with cell wall biosynthesis, as a native PBP and, during the course of evolution, it has evolved to resistance-related functions in a step-wise process that comprised: the structural diversification of the non-binding domain of native PBPs, altering the structure of the active site to promote the exposure of Ser403; alterations in the promoters of *mecA* homologs, either by mutations or by insertion of IS256, resulting in increased expression of the protein; ultimately resulting in the acquisition of SCC*mec* (166).

1.4.1.2.2. SCC*mec*

The *mecA* gene is carried in a large mobile genetic element called staphylococcal cassette chromosome *mec* (SCC*mec*) which can ranges in size from 20 to 70 Kb, according to the elements that are present and their organization (167). The SCC*mec* integrates in the chromosome of susceptible strains at a precise location: the 3' end of *orfX* (now *rlmH*), which is located near the origin of replication (*oriC*) and encodes a staphylococcal ribosomal methyltransferase (168).

Flaking the SCC*mec* cassette are characteristic nucleotide sequences: inverted repeats (attL and attR) and direct repeats (DR-left downstream *orfX*, and DR-right at SCC*mec* end).

The cassette is composed by two central elements. The first element is the *mecA* gene complex, containing *mecA* and its regulators *mecI* and *mecRI* and the cassette chromosome recombinase (Ccr) gene complex, containing the site-specific recombinases responsible for the integration and excision of SCC*mec* in and from the chromosome (167).

The Ccr recombinases recognize a specific sequence in the chromosome, attB, with a minimum of 14-bps at the 3′ end of *orfX* gene which is also present on the SCC*mec* element, attS. The Ccr recombinases bind the two sites bringing them together and forming attSCC which triggers DNA cleavage and exchange of the sites. The process generates the hybrid sites attL and attR (169).

The second element is a group of J regions, for "joining" regions, composed of non-essential components such as antibiotic and metal resistance genes and genes of unknown function. A new anti-repressor of the *mecA* gene, *mecR2*, was described to exist downstream of *mecI* (170).

Up to now, thirteen different structural types of SCC*mec* have been described in *S. aureus* which correspond to the combination of the class of the *mec* complex (A-E), the presence or absence of regulatory genes and insertion sequences and the type of *ccr* allotypes *ccrAB* and *ccrC*. Some SCC*mec* type variants are also defined by differences in the J regions (171, 172).

The SCC*mec* is currently diversifying and one of the main reasons pointed out for this diversification is the pressure of β-lactams and glycopeptides (173).

1.4.1.2.3. Regulation of *mecA* gene

The regulation of the expression of the *mecA* gene is somehow similar to the one of *blaZ* gene, responsible for the expression of β-lactamases. The elements of the *mecA* gene complex *mecR1-mecI-mecA* are homologous of the elements *blaR1-blaI-blaZ* (152, 174). However, the induction of expression of *mecA* only by MecR1 is very inefficient and slow. In order to fully express *mecA*, the system requires an additional anti-repressor, MecR2, forming a three-component system. The *mecR2* is co-transcribed with the functional complementary elements *mecR1-mecI.*

In the presence of the β-lactam, the system is activated through the acylation of the cytoplasm domain of the sensor partner MecR1. This activation induces a conformational change that results in the intracellular activation of a proteolytic domain on the opposite extremity of MecRI. After activation,

the MecRI protease cleaves the MecI repressor bound to the promoter region of *mecA* gene, allowing the transcription of *mecA* (155, 175). The MecR2 interacts directly with MecI, destabilizing its binding to the promoter and fostering its proteolytic cleavage by native cytoplasmatic proteases (Fig.1.9.).

In the absence of the antibiotic, MecI forms dimers that remain bound to the *mecA* promoter, inactivating its transcription. A residual number of copies of MecR1 is present at the membrane (170).

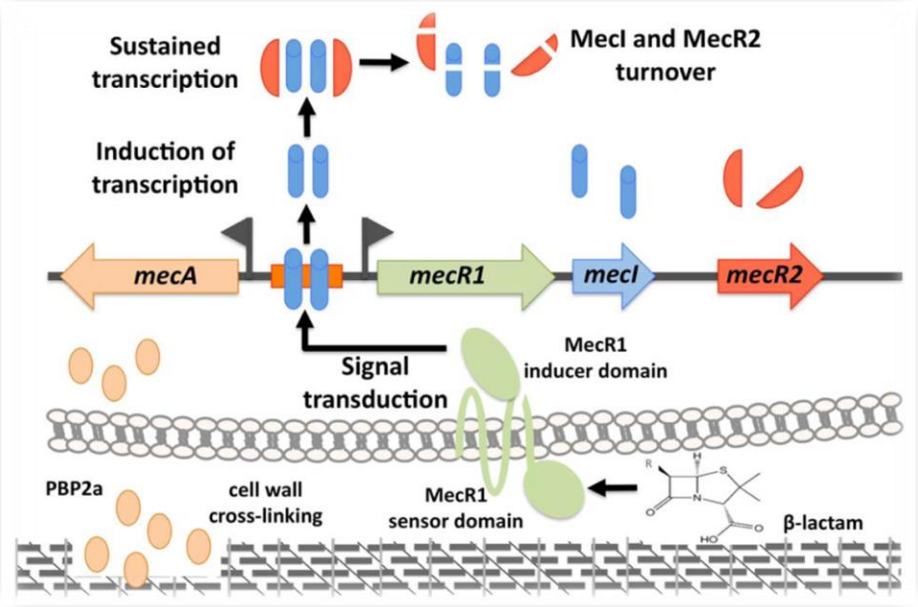

Fig.1.9. Model for the *mecA* induction of expression by the MecR1-MecI-MecR2 three-component system. When a β-lactam antibiotic is present, it is sensed by MecR1 which is activated and cleaves the repressor MecI. MecI, which is bound to the *mecA* promoter, is cleaved allowing *mecA* transcription. MecR2 interacts with MecI and destabilizes its interaction with the promoter, fostering its cleavage by native proteases (Reproduced from (170)).

1.4.1.2.4. Role of auxiliary genes in resistance to β-lactams

The study of resistance to β-lactams showed that the *mecA* gene and the corresponding product PBP2A is the essential determinant of resistance even though it is not the exclusive determinant. In some cases, the level of PBP2A expression detected does not correspond to the level of resistance observed in the MRSA strains and the exclusive presence of *mecA*, *per se*, it is not sufficient to explain the variation in the phenotypic levels of methicillin resistance (176-178).

Furthermore, the oxacillin susceptible MRSA strains (OS-MRSA) that present susceptibility to the β-lactams despite the presence of *mecA* and the absence of the *mecI* repressor, clearly highlight the importance of the genetic background in the expression of resistance (179, 180).

Moreover, the *mecA* gene provided in trans in strains that never had *mecA*, was not able to confer resistance, in contrast to strains in which *mecA* was excised and the expression of resistance was restored (181).

To identify the additional factors that underly the resistance mechanism, a transposition library was performed and mutants with decreased methicillin resistance were selected. This strategy allowed the

identification of a large number of genes involved in resistance which were named *fem* genes (for factors essential for methicillin resistance) and later *aux* genes (for auxiliary) (182, 183).

Most of these genes were later found to be related with the cell wall synthesis. This was the case for the *femAB* mutants, involved in the formation of the pentaglycine interpeptide bridge amongst others such as the glutamine synthetase *glnRA* operon (76, 184).

The number of genes related with resistance was then reassessed in order to select for mutants that exhibited a phenotype of decreased resistance that was not as drastic as in the case of the *fem* mutants. This reassessment rendered 20 to 30 new genetic auxiliary determinants which were also related with the biosynthetic process of the cell wall (185). This strategy allowed the identification of *murE* and *murF* as auxiliary mutants, with accumulation of abnormal dipeptide and tripeptide, respectively in the peptidoglycan. In these auxiliary mutants, the level of PBP2A was affected suggesting that the expression of PBP2A can be directly or indirectly under the control of these genes (58, 186, 187). Additionally, the *pbpb* was discovered to be an auxiliary gene as PBP2 cooperates with its transglycosilase domain of the PBP2A in the presence of antibiotic, as described above (1.3.3.3.2) (94, 95).

Despite the unconditional advances in the identification of auxiliary resistance genes offered by these libraries, the major pitfall of this strategy is that it only allows the detection of non-essential genes. To circumvent this issue, another approach was followed that consisted in the genome-wide antisense fragmentation in which the genes are targeted with anti-sense RNAs. Using this approach even more genes related with β-lactam resistance were added to the pre-existent list such as the essential factors of cell division (*ftsZ* and *ftsA*), protein secretion (*spsB*), wall teichoic acid biosynthesis (*tarL*) and signal transduction system (*pknB*) (188).

Yet, the exact mechanism (or mechanisms) through which the auxiliary genes are involved in the phenotype of full resistance to β-lactams resistance remains elusive.

Besides the direct mechanisms of resistance, such as those of β-lactams and glycopeptides previously described, that rely on the modification of the target of the antibiotic molecule or on its cleavage, bacteria employ other complementary strategies to circumvent the antibiotic challenge, resisting to the damage. These mechanisms are more indirect and may involve a complex signaling cascade interconnecting different pathways and in which the players are not all known. These are the cases of the two-component systems and of stringent response, a mechanism that is intimately related with the regulatory roles of tRNAs in bacteria. These examples will be further detailed.

1.5. Two-component systems (TCSs)

TCSs are regulatory elements, widespread among microorganisms that sense and respond, directly or indirectly, to physical and chemical environmental stimuli. These stimuli range from small molecules, ions, toxins, gases, pH, temperature, osmotic pressure, light or the redox state of the cell to unknown signals.

Despite the innumerous variations found, canonically, a TCS comprises a sensor histidine kinase and its cognate cytoplasmic response regulator. Response regulators always comprise a receiver (REC) that can be phosphorylated, and may harbour additional domains, including an effector domain. The REC domain can have regulator protein-binding capacity and the effector domain may function as DNA-binding transcription factors, RNA-binding, protein-binding or possess enzymatic activities (189).

In the MRSA strain MW2, 16 TCS were identified (190), and collaborate with transcriptional regulators to regulate several processes in the cell such as virulence and pathogenesis, as is the case of the TCS SaeRS and ArlRS (see section 1.2. Pathogenesis of *S. aureus*), and adaptation to environmental conditions like oxygen levels, cell density or nutrient availability (191, 192).

Moreover, TCSs are activated by bacterial pathogens in order to adopt alternative ways to circumvent antibiotics in addition to the well-known resistance mechanisms. This is the case of VraSR, GraRS and WalKR that are involved in resistance to antibiotics (193).

VraSR was identified for being activated by vancomycin challenge and its regulon overlaps the cell wall stimulon which is the core of genes known to transcriptionally respond to cell wall damage in an attempt to resist the antibiotic challenge and to repair the cell wall (194, 195). The VraSR mediates resistance to methicillin in a yet unknown mechanism although *mecA* independent (196).

An example of the complexity of these systems is the GraSR (glycopeptide resistance-associated). GraSR is a multicomponent system involved in resistance to cationic antimicrobial peptides (CAMP), which increases the net cell charge through the D-alanylation of teichoic acids (*dltABCD* operon) and lysylination of phosphatidylglycerol (MprF). This increase in the net charge of the cell wall contributes to the electrostatic repulsion of CAMP. For its function, the system depends on an accessory protein, GraX and on the ABC transporter VraFG forming a five-component system.

The CAMPs are sensed by the VraFG ABC transporter and the signal is transduced to GraS through the interaction between VraG and GraS. The GraS activates the response regulator GraR which promotes the transcription of the *dlt* operon and the *mprF* gene, leading to CAMP resistance (Fig. 1.10) (197). The regulon of this system overlaps the WalKR regulon.

The WalKR is an essential TCS for the viability of *S. aureus* (198). It is involved in the regulation of cell wall metabolism which is accomplished through the positive modulation of the autolytic activity of most of the cell wall hydrolases, including the Atl and LytM which has direct implications in the reduction of the degree of cross-linking through the Atl endopeptidase activity, biofilm formation, and vancomycin resistance (199).

Another example of a TCS associated with resistance to antibiotics, is the BraSR, involved in resistance to bacitracin and nisin, two membrane targeting antibiotics. Similarly to GraSR, the functioning of BraSR depends on the interaction with two ABC transporters: BraDE and VraDE. The BraDE senses the antibiotic and activates signaling through BraSR. The VraDE is a detoxification module and is sufficient to confer resistance to nisin and bacitracin antibiotics when it is independently expressed. The transcriptional activation of the *vraDE* operon is controlled by BraR (200).

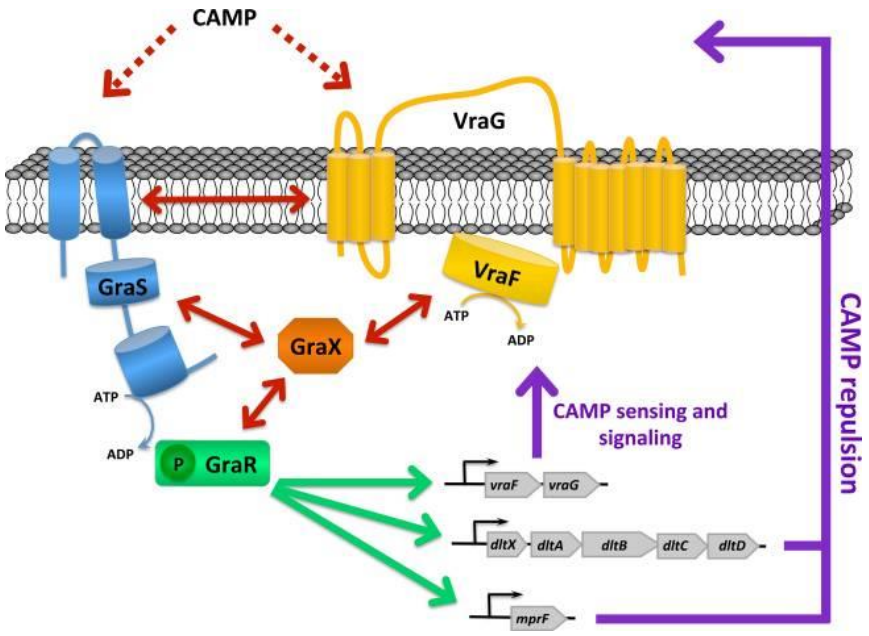

Fig. 1.10. Mode of action of the multicomponent system GraXSR/VraFG. The GraXSR/VraFG controls CAMP sensing and resistance through the activation of the *dlt* operon and of *mprF* gene. Double-headed arrows indicate protein-protein interactions, green arrows indicate activation of transcription, and purple arrows indicate protein synthesis and phenotypes. Reproduced from (197).

1.6. Regulatory roles of tRNAs

Many bacterial regulatory networks profit from the high specificity of aminoacyl t-RNA synthetases in charging tRNAs and also from the acetylated-tRNA/deacetylated-tRNA ratio, since the aminoacylation status of the tRNA provides a measure of the balance between the pathways that use amino acids, like translation, and the central metabolism. Ultimately, the cell can also profit from the tRNA charged status to circumvent antibiotic challenge. Therefore, tRNAs play a key role in regulatory functions acting as a sensors of the metabolic and the transcriptomic status of the cell.

In fact, besides the canonical role played by tRNAs in translation, by providing amino acids for protein synthesis, there are other non-canonical functions associated with tRNA molecules.

One example of the regulatory roles of tRNAs is transcription attenuation, a form of control of some operons which results in a premature termination of transcription. Transcription attenuation can occur by a mechanism of ribosome-mediated attenuation as in the case of the regulation of the tryptophan operon in *E. coli.* In this case, an mRNA sequence in the 5' leader region encodes a protein with high abundance of tryptophan residues. In the presence of low abundance of tryptophan, the ribosome will be stalled in this region due to the presence of non-acylated tRNAs and two other regions will form a hairpin structure that inhibits the formation of the hairpin structure for transcription termination and thus transcription of the operon proceeds. Another mechanism of attenuation of transcription can also occur through the binding of the non-aminoacylated tRNA to a T-box riboswitch which prevents the formation of the transcription terminator and allows downstream transcription, usually of aminoacyl-tRNA synthetase operons (201).

Another example is the modification of molecules such as the aminoacylation of lipids or the addition of amino acids to peptides, as for the synthesis of the pentapeptide bridge of peptidoglycan. Actually, one pathway that uses large amounts of aa-tRNAs is the peptidoglycan biosynthesis of Gram-positive bacteria which is related with antibiotic resistance. In *S. aureus*, the cross-linking between the two adjacent pentapeptides of peptidoglycan, formed by a pentaglycine bridge, is synthesized by the action of three enzymes, FmhB, FemA and FemB that are t-RNA dependent aminoacyl ligases. In this peptide-forming pathway alternative to translation, the Gly-tRNA^{Gly} is sequestered to donate glycine residues to other purposes than protein synthesis (202). In this way, according to the acylated/non-acylated ratio of these tRNAs, the cell can identify damages in peptidoglycan biosynthesis and adapt to the new conditions.

1.6.1. tRNAs in induction of stringent response

Besides the aforementioned examples, one of the major roles of tRNAs in regulatory mechanisms is the triggering of the stringent response. In stringent response, a decrease in amino acid availability promotes the binding of deacetylated tRNAs to ribosomes which in turn transfer PPi from ATP to GDP or GTP forming guanosine-5′-(di)phosphate-3′-diphosphate (ppGpp) and guanosine-5′-(tri)phosphate-3′-diphosphate (pppGpp), both are hyper-phosphorylated versions of GDP and GTP, respectively, commonly designated as (p)ppGpp. Biosynthesis of (p)ppGpp occurs in a reaction catalyzed by the RSH (RelA/SpoT homolog from *E. coli*) enzymes. RSH is a bifunctional enzyme that contains a synthase domain, responsible for the synthesis of (p)ppGpp and a hydrolase domain, responsible for its hydrolysis. RSH is essential in *S. aureus*, but only its hydrolytic domain (203), suggesting that (p)ppGpp can be synthesized by the small alarmone synthases RelP and RelQ, which are monofunctional enzymes only capable of the synthetic process of (p)ppGpp (204).

The (p)ppGpp molecules are alarmones which are involved in a range of physiological processes, from metabolism of amino acids and nucleotides to the regulation of the synthesis of sRNAs and tRNAs, allowing a quick reprogramming of transcription (205). In Firmicutes, in which pp(G)pp does not directly binds RNA polymerase (RNAP), (p)ppGpp regulates transcription through the regulation of the concentration of the initiating nucleotide of transcription (iNTP, or position 1) which can be GTP or ATP for instance. The (p)ppGpp accumulation usually leads to a sharp drop in the GTP level that is accompanied by an increase in the ATP pool and culminates in the relief of the global metabolic repressor CodY that regulates mainly stress tolerance and virulence (206).

1.6.2. The role of stringent response in β-lactam resistance

The study of stringent response in *S. aureus* is intimately related with the search for the genetic determinants of heteroresistance to β-lactam antibiotics. Almost all the MRSA isolates present a phenotype of heteroresistance: the majority of the cells in the population exhibit a low or moderate

resistance level to β-lactams and a small fraction of the population exhibits high resistance. This phenomenon is common to isolates from different origins suggesting that the basis for heteroresistance is genetically determined and of high importance for the bacteria. Such behavior would benefit the population as a whole, by limiting the high resistance phenotype to a small number of specialized individuals, sparing the remaining population from the fitness cost it represents.

In a study on heteroresistance, the MSSA strain 476 was provided with copies of *mecA* gene in a thermosensitive plasmid. A heterogeneously resistant strain was obtained with the majority of cells exhibiting low level of resistance to β-lactams and a small fraction of the population exhibiting high-resistance. Whole genome sequencing of the highly resistant subpopulation revealed two point mutations in the *relA* gene (encoding RSH). One of the mutations inserts a premature stop codon and deletes two domains of *relA* (ACT and TGS). The disruption of the same domains in the *relA* ortholog of *Mycobacterium segmatis* is known to produce increased levels of (p)ppGpp (207). The second mutation was found after the new stop codon in a noncoding nonfunctional sequence.

The heteroresistance phenotype is known to occur in most clinical strains, with varying levels of methicillin resistance according to the clonal lineage, independently of the *mecA* regulatory elements it possesses. This fact suggests that heteroresistance is not related with the *mecA* regulatory elements. Assuming this, isolates from the archaic clone (SCC*mec* type I and absence of *mecA* regulatory elements) were screened for mutations in β-lactam resistant subpopulations. The whole genome sequencing of the sub-population of highly resistant bacteria revealed 27 mutations in genes of diverse functional categories but all involved in the (p)ppGpp biosynthetic pathway (208).

In the MRSA USA300 clonal lineage, the genetic determinants responsible for high level resistance were mostly related with the guanine pathways. Four genetic determinants were common to those found in the archaic clone and one (*gmk*) found in the LGA251 *mecC* harboring strain, suggesting a role for the guanine pathway in stringent response. An increase in the (p)ppGpp level results in inhibition of Gmk, the enzyme responsible for the conversion of GMP to GDP during *de novo* synthesis of GTP. This consequently leads to a decrease in the cellular pool of GTP which helps bacteria to increase resistance (209).

The production of (p)ppGpp seems to be responsible for the high resistance phenotype, but the process triggered by the alarmone to achieve resistance, remains elusive. This question was addressed through the measurement of transcription and translation of *mecA* upon activation of stringent response by mupirocin, an isoleucyl t-RNA homologue, in the MRSA strain N315. In this strain, contrarily to the massive shut-off of transcription that is triggered by stringent response, the level of transcription of *mecA* gene is up-regulated in the presence of oxacillin to relief the repression of MecI over *mecA*. The amount of PBP2A that is translated in conditions of stringent response was also highly increased. This up-regulation suggests that *mecA* is not under stringent control or that stringent control regulates the transcription of *mecA* in the opposite direction of the majority of the genes. The high resistance level induced by stringent control is only attained through the concomitant expression of the native PBP2 which fits the cooperative model of β-lactam resistance. Experiments with ZOX3, an MSSA strain with a mutation in the native *pbpB* that confers β-lactam resistance, showed that stringent response cannot induce full resistance in this strain unless if copies of *mecA* are

provided to ZOX3 in a plasmid, corroborating that the mechanism through which stringent response induces resistance, despite yet elusive, involves *mecA* (210).

Studies on *S. aureus* LGA251 strain carrying the *mecC* gene (SCC *mec* XI), which typically confers low resistance to β-lactams, if it is expressed in the background of a highly resistant strain such as COL-S (MRSA strain COL in which *mecA* was excised) is able to confer a high and homogeneous resistance level. However, when *mecC* is provided in a plasmid to the MSSA strain RN450, it only confers a moderate resistance level, but the treatment with mupirocin allows the strain to exhibit high and homogeneous resistance. On the other hand, a mutation in the transpeptidase domain of *mecC,* that confers high levels of resistance in LG251, when transduced to the MSSA strain RN450 does not confer high levels of resistance when challenged with mupirocin being the mutated gene exempt from stringent control (211).

The study of stringent response in COL revealed, through comparison of its genome with the 27 genes found to be mutated in homostar subpopulations (208), that COL shares 4 mutations in genes related with stringent response. The genes are *prsA* (ribose-phosphate pyrophosphokinase), *gltX* (glutamyl-tRNA synthetase), *rplK* (ribosomal protein L11), and *rpoB* (the β-subunit of RNA polymerase).

In COL strain the mutation in *rpoB* induces a constitutively “on” state of stringent response without the presence of external inducers. In auxiliary mutants, some mutations result in the shut-off of the *rpoB*-mutation-induced stringent response and consecutively lower (p)ppGpp which decreases the level of PBP2A without affecting *mecA* transcription leading to a decrease in resistance (212).

In the case of the *femAB* genes (whose protein products add the last four glycines to the stem peptide of peptidoglycan), their deletion results in a decrease of resistance to methicillin which results from the fact that PBP2A cannot use lipid II with only one glycine added to the stem peptide as a substrate (213). Contrary to what is observed for other auxiliary genes, the stringent response does not correct the level of oxacillin resistance in this mutant. This must occur since the stringent response induces an increase in the level of PBP2A, however, in this case the substrate of PBP2A is not present, thus preventing the correction of the β-lactam resistance level.

Despite elusive in several aspects, stringent response has the ability to recover resistance to β-lactams in a PBP2A dependent manner.

1.7. Transcription terminator factor Rho

Transcription termination is one of the major forms of regulation of gene expression in bacteria and it is important for the regeneration of RNA polymerase (RNAP). There are two mechanisms of proper transcription termination of a given gene: an intrinsic, or Rho-independent, and a Rho-dependent mechanism. An additional form of transcription termination is the Mfd - dependent termination but it occurs only as a way of dissociate elongation complexes at sites of DNA damage, initiating a transcription-coupled repair mechanism. In this repair process, in order to protect the DNA replication fork from blockage, the Mfd protein in an ATP-dependent translocation mechanism, moves

towards the stalled elongation complex and the RNAP translocates, dissociating from the transcript. The system UvrABC is then recruited to repair the damage in the DNA chain (215, 216).

In the intrinsic termination mechanism, the newly formed mRNA molecule has two main elements: a guanine and cytosine (GC)-rich region that will form an RNA hairpin and a segment, at 7–8 nt from the end of the sequence, of predominantly uridine (U) nucleotides, that acts as a RNAP pausing site.

When RNAP reaches the U-rich region, it is forced to pause, providing time for the hairpin to be formed and then both the RNA transcript and the enzyme, forming the elongation complex (EC), are dissociated from the template DNA and the transcription process stops (214).

The second mechanism of transcription termination is protein-mediated, involving Rho termination transcription factor (215). Rho is an ATP-dependent, RNA translocase/helicase from the RecA-family, formed by an hexamer of identical 47-kDa monomers with the six subunits packed laterally forming a ring (216). Rho is responsible for termination of transcription at specific locations in the chromosome and widely at undefined sites. The mechanism of Rho transcription termination has three main steps: the binding of Rho to the mRNA molecule, the translocation across the mRNA until it catches the RNAP, and the release of the transcript (217).

Rho has the conformation of an open ring and when in this conformation, it binds to an mRNA molecule at the so-called *rut* site (for Rho utilization). The *rut* site is indispensable for the binding of Rho, however, the mechanism by which it is recognized remains unknown. The *rut* site is a C-rich region lacking secondary structures and with 60-90 bps of the transcript being ribosome free. Upon binding to the *rut* site, the RNA molecule occupies the primary binding site of Rho. Then, it engages and occupies the secondary binding site of Rho and this promotes a conformational change of Rho into a closed ring. In this conformation, Rho is translocase-competent. The second step is the translocation of Rho towards the elongation complex in an ATP-dependent process. When Rho reaches the elongation complex, it promotes its dissociation, stopping the transcription process (218). This final step is dependent on the helicase activity of Rho which unwinds the RNA:DNA hybrid to release the nascent RNA transcript (219) (Fig.1.10). The NusG protein is a cofactor of Rho. NusG is a transcription elongation factor, known to associate with RNAP and to accelerate the elongation process through its antipausing activity. NusG facilitates Rho action at several Rho dependent terminators and regulates the action of Rho in termination of the transcription (220). The function of NusG seems to be to increase the rate of RNA release at termination sites and from stalled elongation complexes (221, 222).

Contrarily to what happens in *E. coli* and *B. subtilis,* little is known about the functioning of Rho in *S. aureus.* Rho was identified in *S. aureus* in 2001 as a 443-amino-acid protein with 50 kDa and 53% identity to *E. coli* Rho and 66% identity to *B. subtilis* Rho (223). Similarly to what happens in *B. subtilis,* Rho is not essential for the viability of *S. aureus.* Moreover, Rho was not needed for the virulence of this pathogen in a mouse infection model (223).

More recently, a wide transcriptomic study of a *rho* knock-out mutant of *S. aureus*, the mutant HG001Δ*rho*, derived from the MSSA strain NCTC8325, established an unparalleled repertoire of transcription units and non-coding RNAs in this strain. This study allowed to classify the promoters

according to their dependence on sigma factors and revealed the low abundance of antisense RNAs in *S. aureus*, which was shown to be only 6% overlapping the coding genes.

Furthermore, this extensive transcriptomic data revealed that Rho transcription termination factor is responsible for the suppression of the pervasive antisense transcription occuring from spurious transcription (224). This result evidenced that Rho ensures physiological roles in bacteria others than termination of transcription.

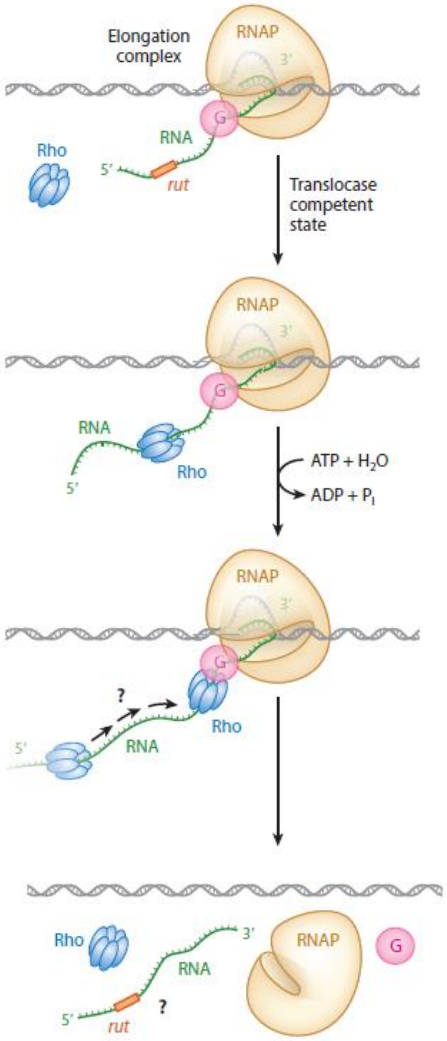

Fig.1.11. Mode of action of Rho in transcription termination. Rho binds to the mRNA molecule in the *rut* site and translocate in the mRNA molecule towards the elongation complex in an ATP-dependent process. When Rho reaches the elongation complex, the RNAP is dislodged and the transcript is released. All the process is assisted by the NusG protein (G). The question mark indicates the processes of Rho translocation and of release of the transcript, whose mechanisms are currently under debate. Reproduced from (219).

1.7.1. Additional regulatory functions of Rho

The study of Rho has deciphered several additional physiological roles for Rho in bacteria. Actually, its known role as terminator of the transcription process seems to be one of the smallest parts of its competences.

In *E. coli*, Rho is responsible for the release of an obstructing transcription-elongation complex to the passage of the replisome maintaining the integrity of the chromosome, which happens even in operons wherein transcription is Rho-independent (225). Additionally, Rho prevents the accumulation of R-loops that usually occur upstream of the elongation complexes. The R-loops are hybrids of DNA:RNA in a three-stranded structure which are formed when the nascent RNA transcript binds the transiently exposed DNA template. This structure promotes strand-breaks in the DNA and consequently, genome instability, which again, may be linked to the inability of the replication fork to proceed (226-228).

The suppression of the pervasive transcription is another major role of Rho. Pervasive transcription refers to the non-canonical transcription in the genome. Frequently, these transcripts are non-coding, are not demarked by gene boundaries and are mainly antisense. Pervasive transcription could arise from spurious promoters across the genome but these transcripts are not necessarily noise, and could function as regulatory modules, a theory increasingly accepted. As antisense RNAs are complementary to sense transcripts, they have the potential to interfere with gene expression and must be tightly regulated (229).

Rho is not only related with transcription-related functions but also with translation and the coupling of both functions is responsible for transcriptional polarity. In prokaryotes transcription and translation occurs concomitantly. When the level of translation of an mRNA is low, Rho accesses the *rut* site in the same mRNA molecule which is being poorly translated and stops transcription of the mRNA which is not being translated. This phenomenon affects also the downstream genes in the same operon which will have their expression decreased. Transcriptional polarity, mediated by Rho, results in decreased synthesis of inefficiently translated mRNAs assuring the transcription-translation coupling (230).

In a different scope, Rho is also associated with the protection of the cell from exogenous DNA. Several prophages and some horizontally transferred genes have a Rho-dependent termination mechanism. This seems to act as a protection for the cell in order to tightly regulate the transcription of genes acquired from the exterior, that can offer benefits, but at the same time can also present a menace (231). However, this may not be a Universal role of Rho since in *B. subtilis*, the lack of Rho does not induce the expression of prophage-related genes (232).

The mentioned examples resume and highlight several functions of Rho in bacteria other than the termination of transcription, which for some bacteria, can even not be its main role in the cell.

Differences in the essentiality and on the prevalence of Rho in the different species suggest alternative pathways of regulation involving Rho which may be species-specific. New roles and mechanistic pathways remain to be disclosed, especially in the *S. aureus* pathogen in which, so far, little is known.

In summary, despite the growing concern about the Staphylococcal infections, namely those derived from MRSA strains and the efforts to eradicate the problem, the lack of strategies to deal with its high prevalences and dissemination in nosocomial and community settings demand further studies on this harmful pathogen and its metabolism and several levels to fill the missing links on its intricate physiological pathways.

Chapter 2

Revisiting *murF* gene in *Staphylococcus aureus* - role of *rho* and stringent response in the phenotype of a cell wall mutant

2.1. Introduction

Previous studies on the *S. aureus murF* gene relied on the characterization of two different *murF* mutants – an insertion mutant and a conditional mutant, both constructed in the background of the early MRSA strain COL. In the conditional mutant COLspac*murF,* the chromosomal *murF* gene was placed under the control of the inducible promoter Pspac which have demonstrated that *murF* is an essential gene. At suboptimal concentrations of the inducer, abnormal tripeptide was incorporated in the peptidoglycan accompanied by a decrease in the oligomerization degree of the peptidoglycan (59). The *murF* insertion mutant F9 was constructed through the insertion of the integrative plasmid pRS2 harboring the terminal 1057 bps of the *murF* gene, excluding the last 6 bps and the stop codon.

After recombination and integration of the plasmid, the last 6 bps of *murF* gene were replaced by 85 bps of plasmid sequence. Restriction mapping revealed that the pRS2 vector inserted into the chromosome of F9 in the form of 6 tandem copies (58).

The F9 mutant exhibited decreased resistance to oxacillin with a minimum inhibitory concentration (MIC) of 0.75 µg/mL and a highly heterogeneous resistance profile. The resistant sub-populations, that retained the ability to grow in the presence of high concentrations of oxacillin, were present at a frequency of 10^{-3}. One colony from these resistant sub-populations was isolated, the stable homostar mutant F9H, and its oxacillin resistance profile was indistinguishable from the one of the parental strain COL (58).

The reverse-phase high-performance liquid chromatography (RP-HPLC) analysis of the composition of the peptidoglycan of the insertion mutant F9 and the homostar F9H, showed structural differences from that of the parental strain COL, namely the appearance of 2 new peaks corresponding to monomeric structures and the decrease of oligomeric structures of high retention times. Three new structures were identified by mass spectrometry, all corresponding to derivatives of the disaccharide tripeptide without oligoglycine branches.

The percentage of disaccharide tripeptide for mutant F9 was approximately 9% while for the homostar F9H, it decreased to 2%. The analysis of the precursor pool of F9 and of F9H mutants revealed that the accumulation of the abnormal tripeptide in the cytoplasm was similar for both mutants suggesting a different incorporation of this altered structure into the cell wall of F9 and F9H.

This result suggested that the reversion of the phenotype observed in F9H did not occur at the level of *murF* gene but at the step of tripeptide incorporation into the cell wall (58).

In this work, in order to understand the phenotype of decreased β-lactam resistance of F9 and the reversion mechanism of this phenotype in F9H, the genomes of the two mutants, F9 and F9H were compared by whole genome sequencing and the single nucleotide polymorphisms identified were addressed by genetic complementation. A comprehensive analysis of the transcription pathways

related with the genes found to be mutated was addressed by a microarray transcriptome analysis of the two mutants. In brief, we describe two different strategies of the bacterial cell to overcome an otherwise fatal cell wall damage; a new role for *rho* gene in the amplification of repeat regions by homologous recombination, a molecular event that allowed to re-establish the full *murF* gene and stringent response, which is a mechanism triggered in the cell as a response to nutrient limitations, resulting in a remodeling of transcription and shut off of non-essential functions in the cell (233).

2.2. Materials and Methods

2.2.1. Bacteria strains and growth conditions

Bacterial strains used in this study are listed in Table 2.1. *S. aureus* strains were grown at 37°C with aeration in tryptic soy broth or agar (TSB/TSA) (Difco Laboratories, Detroit, MI). *E. coli* DH5α was grown at 37°C with aeration in lysogeny broth or agar (LB/LA) (Difco). Erythromycin (10 μg/ml and 5 μg/ml), ampicillin (100 μg/ml), neomycin (50 μg/ml), kanamycin (50 μg/ml), IPTG (100 μM) and $CdCl_2$ (0.2, 1 and 1.8 μM) were used as recommended by the manufacturer (Sigma, St. Louis, MO) for the selection and maintenance of *S. aureus* and *E. coli* and for the induction of *S. aureus* mutants.

2.2.2. DNA manipulation

DNA manipulation was performed using standard methods. FastDigest Restriction enzymes were used as recommended by the manufacturer (Thermo Fisher Scientific, Waltham, MA, USA).

Routine PCR amplification was performed with NZYTaq DNA polymerase (NZYTech, Portugal). Unless otherwise described, amplification of DNA fragments with cloning purposes was performed with Phusion High Fidelity DNA polymerase (Thermo Fisher Scientific) or Pfu DNA polymerase (Stratagene, Heidelberg, Germany) following the manufacturer's instructions. The purification system NZYMiniprep (NZYTech) was used for plasmid extraction. Digestion products were purified using NZYGelpure (NZYTech). Ligation reactions were performed using T4 Ligase (Thermo Fisher Scientific).

Transformations of *E. coli* strain DH5α were performed as follows: ligation mixtures (1:5 molar ratio) of vector and fragment were incubated with DH5α competent cells on ice for 30 min. A heat shock was performed at 42ºC during 90 sec followed by a 5 min incubation on ice. Fresh LB medium was added to the mixture and incubated for 1h at 37ºC. The cells were then plated on LA + Amp (100μg/ml).

Electroporations were performed using a Gene Pulser apparatus (Bio-Rad, California) following the conditions described in (234).

Transductions were performed with the 80α phage as described in (114).

2.2.3. Construction of the mutants

2.2.3.1. Construction of *murF* insertion mutants and respective backcrosses

The insertion mutants F1 to F30 were constructed as described in (58) for mutant F9. Briefly, a 1057-bp *murF* fragment was amplified by PCR with Pfu DNA polymerase (Stratagene, Heidelberg, Germany), using specific primers pmurFup2 and pmurFdownsalI (Table 2.2). The reverse primer pmurFdownsalI was designed at 6 nucleotides before the *murF* stop codon and was engineered to carry a *Sal*I restriction sequence.

Both the amplified fragment and the integrative plasmid pSP64E were digested with *Hin*dIII and *Sal*I and subsequently ligated. The mixture was used to transform *E. coli* DH5α competent cells and to obtain plasmid pRS2.

The pRS2 plasmid was then electroporated into electrocompetent cells of *S. aureus* RN4220 (234). The correct insertion of pRS2 into the chromosome was confirmed by PCR and sequencing using an internal *murF* primer pmurFup4 and a primer for the plasmid (pUCM13 rev) (Table 2.2). The construct was transduced from RN4220 into the background of strain COL with phage 80α (114). Thirty independent insertion mutants were isolated, named F1 to F30.

A single colony of the F9 mutant capable of growing on agar containing 200 µg/ml oxacillin was isolated and named F9H (58). Later, two more independent highly resistant revertant colonies from F9 were isolated and named F9H1 and F9H5.

To isogenize the insertion in *murF* gene, new transductions, or backrosses were performed of F9 and of F9H to COL, generating mutants F9T and F9HT, respectively. The sequencing of the interrupted *murF* gene was performed for F9, F9H and F9HT.

2.2.3.2. Construction of *rho* overexpression plasmid and mutants

The *rho* gene and its RBS sequence were amplified from COL using primers p93 and p94 (Table 2.1) designed to include BamHI and EcoRI restriction sites, respectively. The amplified PCR product and the replicative vector pBCB8 were digested and ligated with the fragment placed under the transcriptional control of the inducible promoter pcad. The ligation mixture was transformed to DH5α competent cells and plasmid pBCB8*rho* was obtained (Table 2.1). PCR colony screening and plasmid digestion with the enzymes used for cloning were performed to confirm the insertion of the fragment.

Plasmid from a positive clone was used to transform electrocompetent cells of *S. aureus* RN4220 by electroporation. The correct construction was sequenced using primers of the pcad promotor (pcadF) and of the fragment (p94) (Table 2.2).

After confirmation of the presence of pBCB8*rho* in RN4220, the plasmid was transduced from RN4220 into strains COL, F9, F9T, F20, F26 and F9H with phage 80α.

For control purposes, the empty replicative vector pBCB8 was also electroporated to RN4220 and subsequently transduced to the same background strains with phage 80α.

2.2.3.3. Construction of transposon insertion *rho* mutants

The *S. aureus* NE149 is a transposition mutant with the transposon Tn *bursa aurealis* (3.2 Kb) inserted in *rho* gene available and is part of the Nebraska Transposon Mutant Library (NTML) (235). The NE149 mutant was used to transduce the transposon Tn *bursa aurealis* into the background strains COL, COL-S, HDE288 and COLpcad*murF* with the 80α phage. Chromosomal DNA of the transductants was extracted using the Wizard Genomic DNA purification Kit (Promega, Wisconsin, USA) and the correct insertion of the transposon was verified by PCR using the primers upstream and buster from the Tn *bursa aurealis* and the internal primers for *rho* gene p50 and p54 (Table 2.2), in the four possible combinations to detect the correct insertion and orientation of the transposon.

2.2.3.4. Construction of *pheS* overexpression plasmid and mutant

The *pheS* gene and the RBS sequence were amplified from COL using primers p91 and p92 (Table 2.2) designed to include BamHI restriction sites. The amplified PCR product and the replicative vector pBCB8 were digested and ligated with the fragment placed under the transcriptional control of the inducible promoter pcad generating plasmid pBCB8*pheS* (Table 2.1). The ligation mixture was transformed to DH5α competent cells. PCR colony screening and plasmid extraction and digestion with the enzymes used for cloning were performed to confirm the insertion of the fragment. Plasmid from a positive clone was used to transform electrocompetent cells of *S. aureus* RN4220 by electroporation. The correct construction was validated by Sanger sequencing using primers of the pcad promotor (pcadF) and of the fragment (p92) (Table 2.2).
After confirmation of the presence of pBCB8*pheS* in RN4220 the construct was transduced from RN4220 into the background of F9H with phage 80α.

2.2.3.5. Construction of *pheS* conditional mutant

A fragment of 706 bps of *pheS* and the corresponding RBS sequence were amplified from COL using primers p85 and p86 (table 2.2), designed to include SmaI restriction sites. The amplified PCR product and the integrative vector pBCB20 were digested and ligated generating the pBCB20*pheS* plasmid. The ligation mixture was transformed into DH5α competent cells. PCR colony screening and plasmid extraction and digestion with the enzymes used for cloning were performed to confirm the insertion of the fragment. Plasmid from a positive clone was used to transform electrocompetent cells of *S. aureus* RN4220. To verify the correct Campbell type integration of the plasmid in the

chromosome of RN4220, chromossomal DNA of RN4220::pcad-*pheS* was extracted using Wizard Genomic DNA purification Kit (Promega, Wisconsin, USA) and PCR was performed using primers pcadF and p92, a primer outside the cloned region (Table 2.1). After confirmation of the correct insertion of pBCB20*pheS* in RN4220 the construct was transduced from RN4220 into the background of F9 with phage 80α.

Table 2.1. List of strains and plasmids used in this study

Strain/Plasmid	Description	Source or Reference
E. coli		
DH5α	*recA endA1 gyrA*96 *thi*-1 *hsdR*17 *supE*44 *relA*1 Φ80 Δ*lacZ*ΔM15	Invitrogen
S. aureus		
COL	Homogeneous Mc^r, Em^s	Rockefeller University
RN4220	Mc^s , restriction negative	R. Novick
F1-F30	COL (*murF*::pRS2), Em^r	This study
F9	COL (*murF*::pRS2), Em^r	(58)
F9H1	COL (*murF*::pRS2), Em^r , Homo*	This study
F9H	COL (*murF*::pRS2), Em^r , Homo*	(58)
F9H5	COL (*murF*::pRS2), Em^r , Homo*	This study
F9T	COL (*murF*::pRS2), Em^r , transductant backcross	(58)
F9HT	COL (murF::pRS2), Em^r Homo*, transductant backcross	This study
COLpcad*murF*	COL with *murF* gene under pcad control, Kan^r, Neo^r	(79)
COL-S	COL with SCCmec excised; Mc^s	(90)
HDE288	MRSA Low level Mc^r (Scc*mec*IV)	(236)
NE149	USA300-JE2 with Tn *bursa aurealis* insertion in *rho* gene	(235)
Rho mutants:		
RN4220 + pBCB8	RN4220 with replicative vector pBCB8	This study
RN4220 + pBCB8*rho*	RN4220 with *rho* under pcad control in replicative vector pBCB8, Kan^r , Neo^r	This study
COL+ pBCB8*rho*	COL with *rho* under pcad control in replicative vector pBCB8, Kan^r , Neo^r	This study
F9+ pBCB8*rho*	F9 (*murF*::pRS2) transductant with *rho* under pcad control in replicative vector pBCB8, Em^r , Kan^r , Neo^r	This study
F9T+ pBCB8rho	F9T (*murF*::pRS2) transductant backcross with *rho* under pcad control in replicative vector pBCB8, Em^r , Kan^r , Neo^r	This study
F20 + pBCB8*rho*	F20 (*murF*::pRS2) transductant with *rho* under pcad control in replicative vector pBCB8, Em^r , Kan^r , Neo^r	This study
F26 + pBCB8*rho*	F26 (*murF*::pRS2) transductant with *rho* under pcad control in replicative vector pBCB8, Em^r , Kan^r , Neo^r	This study
F9H + pBCB8*rho*	F9H (*murF*::pRS2) Homo* transductant with *rho* under pcad control in replicative vector pBCB8, Em^r , Kan^r , Neo^r	This study
COL + pBCB8	COL with replicative vector pBCB8 Kan^r , Neo^r	This study
F9 + pBCB8	F9 with replicative vector pBCB8 Em^r, Kan^r , Neo^r	This study
F20 + pBCB8	F20 with replicative vector pBCB8 Em^r, Kan^r , Neo^r	This study
F26 + pBCB8	F26 with replicative vector pBCB8 Em^r, Kan^r , Neo^r	This study

COL Tn::*rho*	COL with Tn *bursa aurealis* insertion in *rho* gene	This study
COLpcad*murF* Tn::*rho*	COLpcad*murF* with Tn *bursa aurealis* inserted on *rho* gene	This study
COL-S Tn::*rho*	COL-S with Tn *bursa aurealis* inserted inn *rho* gene	This study
HDE288 Tn::*rho*	HDE288 with Tn *bursa aurealis* inserted in *rho* gene	This study
PheS mutants		
RN4220 + pBCB8*pheS*	RN4220 with *pheS* under pcad control in replicative vector pBCB8, Kan^r , Neo^r	This study
RN4220::pcad*pheS*	Conditional mutant RN4220 with chromosomal *pheS* under pcad control Emr , Kanr , Neor	This study
F9::*pcad-pheS*	Conditional mutant F9 with chromosomal *pheS* under pcad control Em^r , Kan^r , Neo^r	This study
F9H + pBCB8*pheS*	F9H with *pheS* under pcad control in replicative vector pBCB8, Em^r Kan^r , Neo^r	This study
Plasmids		
pBCB8	*S. aureus* replicative vector with pcad inducible promotor, Amp^r , Kan^r	R. Sobral and M. Pinho (unpublished)
pBCB20	*S. aureus* integrative vector with pcad inducible promotor, Ap^r , Kan^r	(52)
pBCB8*rho*	pBCB8 vector with *rho* rbs and *rho* fused to pcad promotor, Amp^r , Kan^r	This study
pBCB8*pheS*	pBCB8 vector with *pheS* rbs and *pheS* fused to pcad promotor, Amp^r , Kan^r	This study
pBCB20*pheS*	pBCB20 vector with pheS RBS and the first 705 bps fused to pcad promotor, Ap^r , Kan^r	This study

Table 2.2. Primers used in this study

Primer ID	Sequence 5'→3'	Source or Reference
Insertion mutants and confirmation of *murF* restoration		
pmurFup2	GAAAATGTTGACGGTCATCG	(58)
pmurFdownsalI	CGCGTCGACTAAAGCATTTACCACTTC	(58)
pmurFup4	GTATGCGTATGGAACAACA	(58)
p112	GAAGTGGTAAATGCTTTAATTTCATAG	This study
pucM13	CGCCAGGGTTTTCCCAGTCACGAC	(237)
General cloning		
pcadF	GCACTTATTCAAGTGTATTT	R. Novick
Construction of *pheS* conditional mutant		
p85	CACCCGGGAGGTCAGTGACATATGTC	This study
p86	CACCCGGGTTCAAATCACTCATTTTAACG	This study
Construction of *rho* overexpression mutant		
p93	TAAGGATCCAAATGGGTGTAAACTAATGC	This study
p94	GCCGGAATTCTATTAAATTATAGGTCGA	This study
Construction of *pheS* overexpression mutant		
p91	CAGGATCCGAATAGTTCGAATAGGGAGG	This study

p92	CAGGATCC TGCGCGTAATACGTTCTGCC	This study
Tn::*rho* insertion mutants		
Upstream	CTCGATTCTATTAACAAGGG	(235)
Buster	GCTTTTTCTAAATGTTTTTTAAGTAAATCAAGTAC	(235)
p50	AAAAATAATGAAATGGGTGTAAAC	This study
p54	TATTTTCAGCTCCTTTGCCC	This study
RT-PCR		
p0033-F	ACCGAAACAATGTGGAATTGG	This study
p0033-R	TGCCTATCTCATATGCTGTTCCTGTA	This study
p0095-F	CAGCAAACCATGCAGATGCTA	(60)
p0095-R	CACCAGTTTCTGGTAATGCTTGAG	(60)
p0677-F	GCTAACGGCAAACAAACAGAATTT	This study
p0677-R	CAGGGTTAATGTTAGCGAATCGA	This study
p1032-F	TCGACCAGCATTTGATGATGA	This study
p1032-R	CGAATTATTTCACTACCGTTTCTTTG	This study
p1216-F	TCGATTGAAGAGGCCGTTTTA	(60)
p1216-R	ACCAGCTGCATTTGCTAACTTG	(60)
p1490-F	CAGAAACCAAGCAACAGATCCTC	(238)
p1490-R	TTCAATGGCAGGTCCATACG	(238)
p2073-F	TGTTGACGGTCATCGCTTTG	(60)
p2073-R	GCCCCAGCACCATCTTGTA	(60)
p2689-F	AGTATGAACCGCTTGCCATGT	(60)
p2689-R	CTCCCAATGTTTCTGGAACCA	(60)
Northern blotting probe		
pmurFnorthF	CGCGAGGGGATTGCTAAAGC	This study
pmurFnorthR	TGCTTTTTCGACATGTTGC	This study

2.2.4. Restriction mapping

The number of pRS2 plasmids present in the chromosome of the insertion mutants F1 to F9 and of strains F9H, F9T, F9HT, F9+pBCB8*rho* (grown with 0 and 1 μM $CdCl_2$) and F9H+pBCB8*rho* (0 and 1 μM $CdCl_2$) was assessed by restriction mapping. DNA agarose plugs were prepared as described (239) and were digested with EcoRV enzyme, which has no restriction site inside the sequence of pRS2 plasmid. The separation of the chromosomal DNA digested with EcoRV was performed by Pulsed Field Gel Electrophoresis (PFGE) using the following conditions: 1 sec initial pulse, 12 sec final pulse, 6V/cm, 11.3 ºC during 15 hours in TBE 0.5 X buffer. The ladders used were the Mid Range PFGE Marker and the Lambda ladder PFG marker (New England Biolabs, Ipswich, MA, USA). The approximate number of inserted plasmids was calculated for each strain by dividing the estimated molecular weight of the band by the molecular weight of pRS2 plasmid (5.2 Kb).

2.2.5. Determination of *S. aureus* oxacillin resistance

Cultures of *S. aureus* were grown in TSB with the appropriate concentration of the inducer and of antibiotic. Overnight cultures were harvested by centrifugation 5.000 x *g* during 2 min and ressupended in the same volume of fresh medium, three times, to remove traces of antibiotic and/or of inducer from the O/N culture. The washed cultures were swabbed on TSA and TSA supplemented

with the appropriate concentration of the inducer. Oxacillin (Sigma) diffusion disks (1 mg) were placed on the plates and incubated at 37°C for 48 h and the growth inhibition halos were measured. For the determination of oxacillin minimum inhibitory concentration (MIC), the same procedure was used with E-test M.I.C. evaluator strips (Oxoid) instead of the oxacillin disks.

2.2.6. Determination of antibiotic resistance by population analysis profiles (PAPs)

Overnight cultures were washed as described above and plated at various dilutions on TSA plates containing increasing concentrations of oxacillin (0, 0.75, 1.5, 3, 6.25, 12.5, 25, 50, 100, 200, 400, and 800 µg/ml). Bacterial colonies were counted after incubation of the plates at 37°C for 48 h.

2.2.7. Whole-genome sequencing (WGS)

Chromosomal DNA preparations isolated from F9 and F9H were sequenced and compared to the DNA sequence of strain COL. The complete genomic sequence (no contig gaps) for COL is available at the NCBI. The 454 platform was used for the sequencing of the genome and *de novo* assemblies of the reads were done using the NCBI's complete genomic sequence for COL as the reference. The methods for the sequencing, assemblies, and polymorphism detection were described previously (240-243).

2.2.8. Microarrays

Cultures of COL, F9 and F9H were grown overnight in TSB. For F9 and F9H the medium was supplemented with erythromycin (10 µg/ml).

The overnight culture was washed three times to remove the antibiotics and then back diluted to an optical density at 620 nm (OD_{620}) of 0.01 into fresh preheated medium. The culture was incubated until the OD_{620} reached 0.7 (mid-log phase). At the time of sampling, a double volume of RNAprotect Bacteria reagent (QIAGEN, Hilden, Germany) was added to the culture. The mixture was incubated for 5 min at room temperature, the cells were centrifuged for 10 min at 3500 rpm and 4°C, and the pellets were frozen in dry ice and kept at -70°C.

Total RNA was extracted as described previously (60). Briefly, cells were resuspended in Trizol reagent (Gibco BRL, Maryland) and the lysing procedure applied was mechanical disruption using silica beads and a FastPrep FP120 apparatus (Bio 101, La Jolla, California, USA). A chloroform extraction was performed, and the RNA was recovered by precipitation with isopropyl alcohol, washed with 80% ethanol, and resuspended in diethyl pyrocarbonate (DEPC) treated water.

The RNA quality and quantity was determined by agarose gel electrophoresis and by measuring the absorbance at 260 and 280 nm. Each of the cultures grown was repeated three times.

Total RNA from all samples were treated with DNase I by using the RNase-free DNase set protocol and RNeasy minikit protocol (QIAGEN, Hilden, Germany). Total RNA was quantified using the Nano-Drop spectrophotometer (Nanodrop Technologies, Wilmington, DE, USA). The protocols for array processing, data quality control and statistical analysis are described in (60).

2.2.9. Microarray validation by Real-time qPCR (RT-qPCR)

Total RNA preparation was performed exactly as described for the microarray assay. Residual DNA was removed from the samples by performing two on-column DNase digestion steps with RNase-free DNase (QIAGEN, Hilden, Germany). cDNA was synthesized with TaqMan reverse transcription reagents (Applied Biosystems, Foster City, CA) and random hexamers. Specific primers for the genes tested and for 16S rRNA, used as endogenous control, were designed using Primer Express software (Applied Biosystems) (Table 2.2). Real-time PCR was performed with the ABI PRISM 7000 sequence detection system (Applied Biosystems) and SYBR green technology. The three biological replicates were analyzed in duplicate and normalized against 16S rRNA gene expression. For the three strains, the amounts of target and control genes were determined from the appropriate standard curve. In order to obtain a normalized relative gene expression value, the amount of target gene for each condition was divided by the respective amount of control gene.

2.2.10. Northern Blotting

Cells were grown in TSB at 37°C to an optical density at 620 nm of 0.7 to 0.8 (log-phase growth). Prior to harvesting the cells, RNAprotect Bacteria reagent (QIAGEN,) was added to the culture. Total RNA preparation was performed exactly as described for the microarray assay. The RNA samples were run in an agarose gel under denaturing conditions (0.66 M formaldehyde - 1× morpholinepropanesulfonic acid [MOPS]; Sigma) and were blotted onto Hybond N+ membranes (Amersham, Buckinghamshire, UK). The DNA probe used for the hybridization was internal to *murF* and was amplified by PCR with the respective primers described in Table 2.2. The DNA probes were labeled with [α-32P] dCTP (Amersham Life Sciences, New Jersey, USA).

2.2.11. Peptidoglycan purification

Cell wall isolation was performed as described previously (77). Briefly, cultures of COL, F9, F9T and the respective complemented F9+pBCB8*rho* and F9T+pBCB8*rho* and COLpcad*murF* and its *rho* transposon mutant COLpcad*murF* Tn::*rho* were grown in the presence of the respective antibiotics and in the absence or in the presence of $CdCl_2$ inducer up to an OD_{620nm} of 0.3. The cells were harvested by centrifugation, rapidly chilled in an ice-ethanol bath, and boiled in 4% SDS, to remove

the cell wall associated proteins, for 30 min. The cells were disrupted using 106 mm glass beads (sigma) and subsequently treated with DNase (10 g/ml; Sigma-Aldrich), RNase (50 g/ml; Sigma-Aldrich), and trypsin (200 g/ml; Worthington Biochemical Corporation, USA). Teichoic acids were removed by treatment with 49% hydrofluoric acid (Merck, Germany) for 48 h at 4°C. The peptidoglycan was then washed to remove any traces of hydrofluoric acid and lyophilized.

2.2.12. Muropeptide analysis by RP-HPLC.

Identical amounts of peptidoglycan of each sample were digested with mutanolysin (1 mg/ml; Sigma).

The resulting muropeptides were reduced with sodium borohydride powder (Sigma) and separated by RP-HPLC using a Hypersil octyldecyl silane (Runcorn, Cheshire, UK) column and a linear gradient from 5% to 30% methanol in 100 mM sodium phosphate buffer, pH 2.5, at a flow rate of 0.5 ml/min as described previously using a Shimadzu Prominence system and Shimadzu LC solution software. The peaks of the chromatograms were identified by assessing the relative retention times according to previous works (58, 244). The peaks were integrated, and the values are presented as the area percentages of the total area of the chromatogram. The baseline used for the integration of the individual peaks was the same as the one used for the whole chromatogram.

2.2.13. Purification of staphylococcal membrane fraction

The cultures of COL, F9, F9HT and F9+pBCB8*rho* (1µM $CdCl_2$) were grown in 250 ml of TSB at 37˚C with aeration to an OD_{600nm} of 0.7. Cells were harvested, washed and ressuspended in buffer A (50 mM Tris pH 7.5, 150 mM NaCl, 5 mM $MgCl_2$) with 0.5 mM phenylmethylsulfonyl fluoride (PMSF) and submitted to freeze-thaw cycles. All subsequent steps were performed at 4˚C. Lysostaphin (100 µg/ml), Lysozyme (50 µg/ml), DNase (10 µg/ml), RNase (10 µg/ml), PMSF (0.5 mM) and β-mercaptoethanol (10 mM) were added and the cell suspensions were incubated on ice for 30 min, followed by 5 cycles of sonication of 30 s and 2 min intervals. Unbroken cells and cellular debris were removed by centrifugation of 5 min at 5000 x *g* and the resulting supernatants were centrifuged at 50.000 x *g* for 1h and washed in 50 mM phosphate buffer, pH 7.0. The obtained membrane fraction was resuspended in buffer B (25 mM phosphate buffer pH 7.0, 1% Triton X-100, 10 mM $MgCl_2$, 20% glycerol). Total protein concentration was determined using the BCA assay (Pierce, Thermo Scientific, USA).

2.2.14. Detection of PBP2A by western blotting

Membrane preparations (10 µg) were separated by SDS polyacrylamide gel electrophoresis (8% acrylamide-0.06% bisacrylamide) at a constant current of 20 mA. The proteins were transferred onto

nitrocellulose Hybond-ECL membranes (GE Healthcare Life Sciences, USA) using the semi-dry blotting system (Bio-Rad, USA) for 15 min. Membranes were kept on PBS-Tween with 4% low-fat milk O/N. The membranes were then incubated with rabbit polyclonal anti PBP2A antibody (raised against the synthetic peptide NH2-CGSKKFEKGMKKLGVGEDIPSDYPF; RayBiotech) at 1:1000 dilution for 1 hour. After two washes with PBS-Tween the membranes were incubated with the anti-rabbit secondary antibody conjugated to horseradish peroxidase (PerkinElmer, USA) at 1:5000 dilution for 1 hour. The chemiluminiscent signal was detected using Western Lightning Plus-ECL (PerkinElmer) and Amersham hyperfilm ECL (GE Life Sciences). The membrane was incubated in stripping buffer (25 mM glycin, 1% SDS, pH 2.2) at RT for 15 min and re-hybridized with polyclonal antibody raised against the amidase domain of *S. aureus* Atl protein, at 1:1000 dilution for 1h.

2.3. Results

Thirty independent *murF* insertion mutants (F1 to F30) were constructed by cloning a 1057 bp *murF* fragment in the integrative plasmid pSP64E generating plasmid pRS2 (Fig. 2.1). The pRS2 plasmid was then electroporated into *S. aureus* RN4220 and subsequently transduced from RN4220 into the background of strain COL with phage 80α.

Thirty independent insertion mutants were isolated, named F1 to F30.

A highly resistant revertant strain of F9, named F9H, capable of growing on agar containing 200 μg/ml oxacillin was also isolated.

The backross mutants F9T and F9HT were obtain by the transduction of F9 and of F9H to COL, respectively, to isogenize the mutation in *murF*.

2.3.1. Characterization of a collection of independent *murF* insertion mutants

The restriction mapping involved the digestion of the chromosomal DNA with EcoRV, an enzyme with no restriction sites inside the sequence of pRS2 plasmid, allowing to obtain a fragment of DNA containing the several copies of the plasmid. The restricted DNA was then separated by Pulsed Field Gel Electrophoresis (PFGE), since the molecular weight of the bands containing the pRS2 copies ranged in from >33.5 to 145.5 Kb .

Restriction mapping of the 30 transduction mutants showed that for 21 independent transductants, the number of copies of pRS2 was similar to the one of RN4220::pRS2 (>27; Fig. 2.2). For six of the insertion mutants (F1, F11, F12, F14, F16 and F21) the number of copies of pRS2 was lower (between 9 and 27) than in these 21 transductants. The insertion mutants F9, F20 and F26 had fewer copies of pRS2 in the chromosome (F9 ~6 copies, and F20 and F26 ~7 copies) than the remaining insertion mutants.

Besides F9, six more mutants (F1, F10, F16, F20, F26 and F28) were chosen to verify the insertion of the pRS2 plasmid by PCR and sequencing. The six mutants, similarly to F9, presented the *murF*

gene with the last 6 bp replaced by 85 bps of pRS2 plasmid, and downstream, the insertion in tandem repeats of the *murF* fragment used for cloning, in as many copies as the ones of the inserted plasmid (Fig. 2.1, Fig. 2.2). The result obtained for these mutants suggested that all the remaining mutants also had the insertion of pRS2 at 6 bps of the stop codon.

The resultant altered MurF protein translated from this genetic arrangement should consist in a protein with the two last C-terminal residues substituted by a sequence of 28 residues (Fig.2.3). Other genetic rearrangements in the chromosome leading to the translation of alternative versions of MurF cannot be discarded.

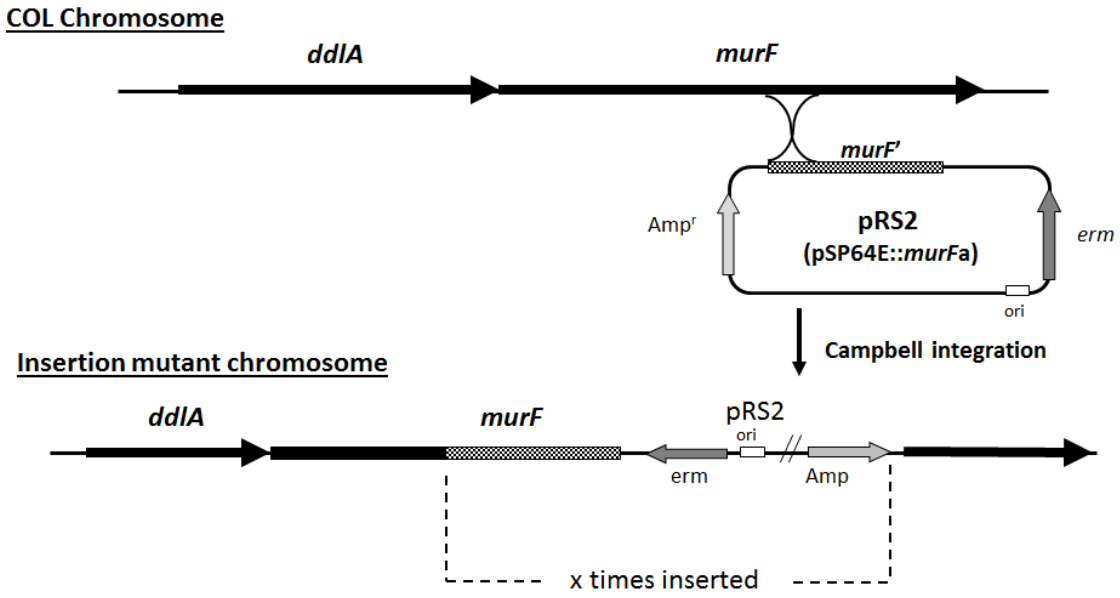

Fig. 2.1. Construction of the mutants F1 to F30. The mutants were constructed by insertion of pRS2 plasmid at 6 bp from *murF* stop codon and insertion of variable pRS2 copies in tandem. The x represents the number of plasmids inserted for each independent mutant. Adapted from (58).

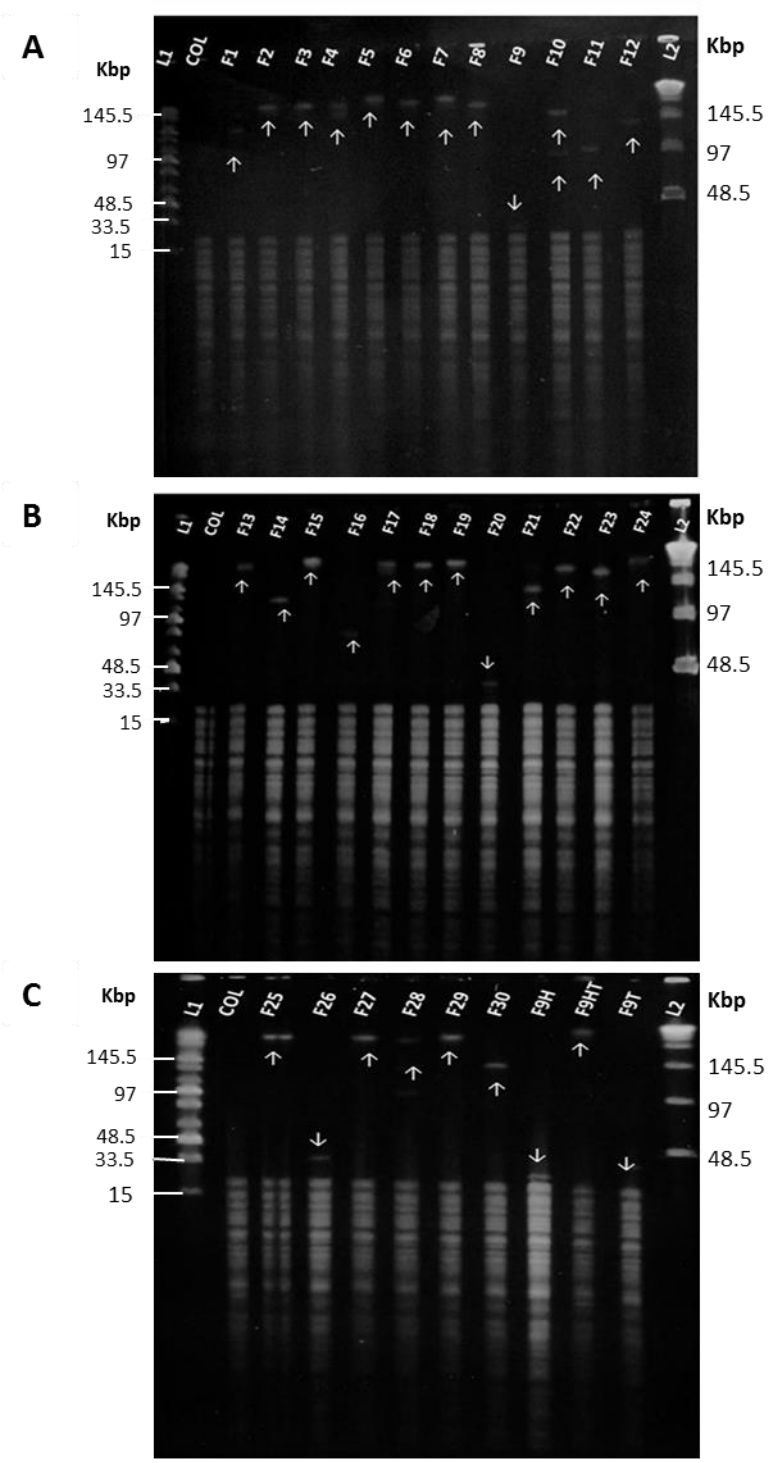

Fig. 2.2. Restriction mapping of mutants. Total DNA of COL and the insertion mutants, digested with EcoRV and separated by Pulsed Filed Gel Electrophoresis (PFGE). **A)** Strain COL and mutants F1 to F12; **B)** Strain COL and mutants F13 to F24 and **C)** Strain COL and mutants F25 to F30, F9H, F9HT and F9T. L1 correspond to the Mid Range PFGE Marker (New England Biolabs) and L2 correspond to the Lambda ladder PFG marker (New England Biolabs). Arrows indicate the position in the lane of the band corresponding to the multiple copies of pRS2 vector.

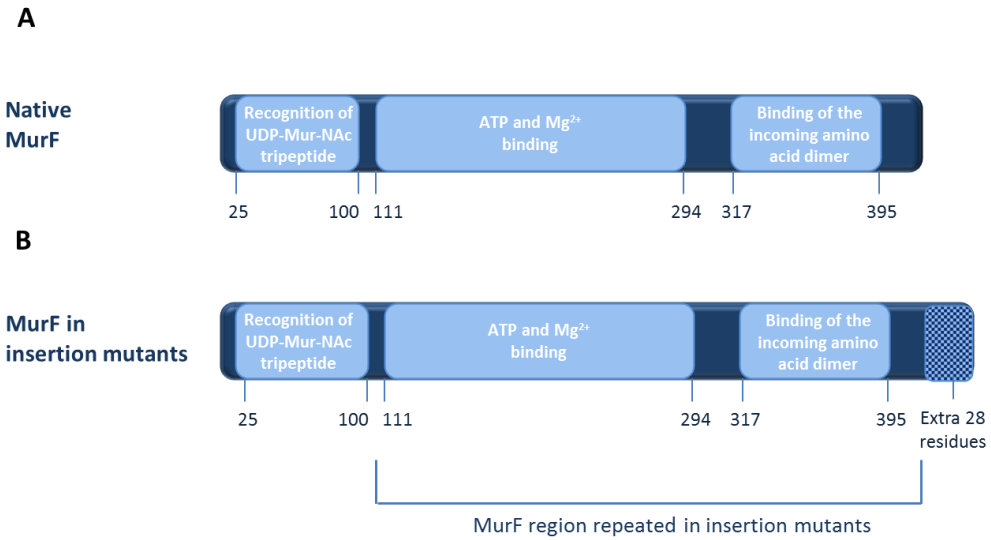

Fig. 2.3. MurF protein domains. **A)** Wild-type MurF protein and **B)** Altered MurF protein version present in insertion mutants F1 to F30 with an extension of 28 residues.

2.3.2. Oxacillin resistance phenotype of the insertion mutants

Three of the thirteen insertion mutants exhibited a decrease in oxacillin resistance: strains F9 (58), F20 and F26 while the remaining mutants showed unaltered high level resistance to oxacillin (Table 2.3). The three mutants with decreased oxacillin resistance exhibited a heterogeneous oxacillin resistance profile (Fig. 2.4), indicating the existence of revertant populations. Also, these three mutants showed the lower number of copies of pRS2 plasmid (6 to 7) (Fig. 2.2) (58). The mutants with higher number (9 to >27) of pRS2 insertions, showed a resistance profile identical to the parental strain COL (Table 2.3). This indicates a correlation between the number of copies of pRS2 inserted in the chromosome of the insertion mutants and the phenotype of oxacillin resistance.

For the homostar mutant F9H (58), despite being a subpopulation of F9 with high level resistance to oxacillin, restriction mapping revealed a number of pRS2 insertions similar to F9 (Fig. 2.2), suggesting that for this strain, the number of pRS2 copies is not responsible for the resistant phenotype.

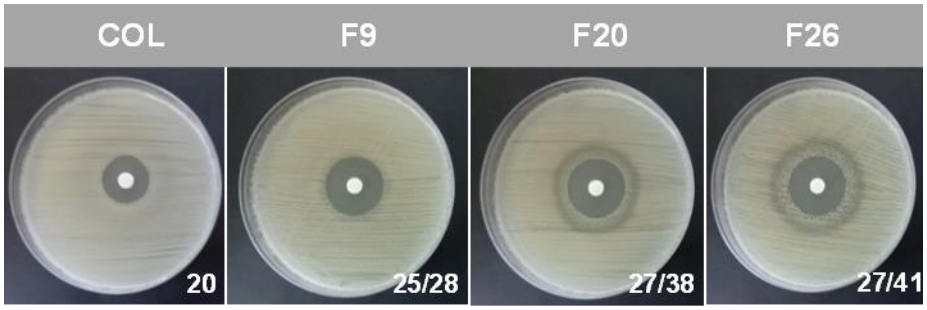

Fig. 2.4. Growth inhibition halos of susceptible insertion mutants. Growth inhibition halos for oxacillin (1mg) obtained by disk diffusion for the parental strain COL and the susceptible insertion mutants F9, F20 and F26. The values presented correspond to the diameter in mm.

2.3.3. Expression of the *murF* gene in the insertional mutants

The level of *murF* expression in the insertion mutants F1 and F9 as representatives of a resistant and of a susceptible mutant, respectively, was determined by Northern blotting using a *murF* probe of 500 bps that hybridizes to the terminal region of the gene, at 129 bp from the stop codon. The sequence of the DNA probe includes the region of the *murF* gene cloned in pRS2 and repeated in tandem in the chromosome of the mutants. The *murF* transcription pattern of COL consisted on a single band of 2.5 Kb, compatible with the co-transcription of the *murF* and *ddlA* genes in a single mRNA molecule (59). The *murF* transcription profiles of F1 and F9 showed a smear with a strong signal intensity compatible with the presence of mRNA transcripts of several sizes, with higher intensity for mutant F1 (Fig.2.5). The insertion of a high number of plasmids containing the 1057 terminal fragment of the *murF* gene could lead to multiple transcripts, explaining the strong signal transcription profiles of the mutants. In accordance, the insertion mutant F1 showed more than 18 copies of pRS2 in the chromosome, while F9 showed only 6 copies.

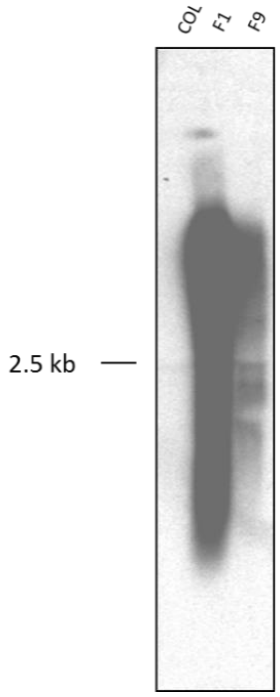

Fig. 2.5. F1 and F9 *murF* northern blotting. Northern blotting analysis of strain COL and the insertion mutants F1 and F9 with a *murF* ^{32}P radiolabeled specific probe.

2.3.4. Restoration of *murF* full sequence by the tandem amplification event

Since the insertion mutants with high number of tandem copies of pRS2 (9 to >27) maintained the high level of resistance to oxacillin of the parental strain COL, we hypothesized that the full *murF* sequence could have been restored upon the genetic amplification event. To address if the *murF* gene

was restored in this mutants, the *murF* gene was amplified by PCR and the amplification product was sequenced.

Two amplifications were performed by PCR: 1) the amplification of *murF* gene with primers pmurFup2 that hybridizes with *murF* 5' end in a region not cloned in pRS2 and p112 (Table 2.2) that hybridizes to the 3' end of the *murF* sequence, finishing at the stop codon and 2) the amplification of a fragment with primers pmurFup4 which hybridizes with a *murF* region that is cloned in pRS2 and pUCM13 (Table 2.2), which hybridizes with the plasmid sequence as depicted in Fig.2.6.

Both amplifications were performed for F1 (oxacillin highly resistant mutant) and for F9 (oxacillin susceptible mutant) and subsequently sequenced. The amplification and sequencing of fragment number 2 was performed for mutants F1, F10, F16, F20, F26 and F28 The amplification and sequencing of fragment number 2 in F9, had already been performed (58).

The results showed that most probably, in F1, a canonical copy of *murF* was fully restored while in the mutant F9, with decreased oxacillin resistance, the gene was not restored.

Sequencing of the first amplification products, from F1 and from F9, showed that in F1 the sequence terminated exactly at the stop codon while in F9 the sequence terminates abruptly at the location of the plasmid insertion, at 6 bps from the stop codon. The results seem to suggest that the amplification of the tandem repeats may have resulted in the generation of a complete copy of *murF*, responsible for the high level of resistance of these mutants.

In both types of mutants (resistant and susceptible) truncated versions of *murF* were present, a direct consequence of the insertion of pRS2. In all, the insertion occurred at 6 bp from the stop codon as previously found in F9 (58).

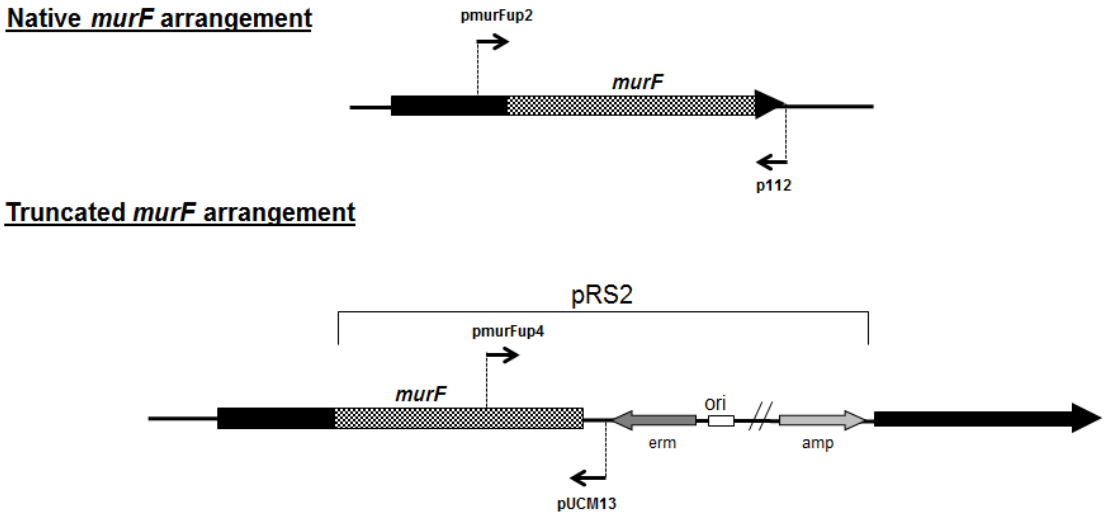

Fig. 2.6. PCR amplification strategy of the *murF* gene. Amplification for **A)** Chromossomal arrangement of *murF* in COL and in insertion mutants with a restored copy of *murF* and **B)** chromosomal arrangement of *murF* gene truncated by the insertion of pRS2. The primers used for the amplification of *murF* in different arrangements in the chromosome are identified and listed in Table 2.2.

2.3.5. Whole genome sequencing of the insertion mutant F9 and the homostar F9H

The genomes of mutant F9 and its homostar revertant mutant F9H were compared by whole genome sequencing (WGS). All the polymorphisms identified by WGS were confirmed through Sanger re-sequencing to detect possible sequencing or assembly errors.

The F9 and the F9H genome sequences were compared with the available genome of the parental strain COL (134) and 4 polymorphisms were identified, 3 common to F9 and F9H and one only present in the F9H genome: (i) the expected Campbell-type integration of pRS2 vector in the terminal region of the *murF* gene in F9 and F9H strains; (ii) a single-nucleotide substitution of a cytosine by a thymine in position 2137992 bps of the chromosome, corresponding to position 915 bps of the coding sequence of DEAD/DEAH box helicase (SACOL2072) but resulting in an amino acid synonymous substitution (Y305Y) in the helicase protein; (iii) a single-nucleotide substitution of a guanine by a thymine in position 2173340 bps of the chromosome, corresponding to position 227 bps of the coding sequence of *rho* gene (SACOL2113), that should result in the substitution of glycine 76 for a valine residue (G76V) in the Rho protein; (iv) a single-nucleotide polymorphism was unique to F9H and corresponds to the substitution of a cytosine for a thymine in nucleotide position 523 (C523T) of the coding region of *pheS* gene (SACOL1148), in position 1156068 bps of the chromosome. This mutation should result in the substitution of leucine 175 to a proline (P175L) in PheS protein (Table 2.3).

Since the polymorphism found in the DEAD/DEAH box helicase was a same-sense mutation in the coding region we have decided to focus on the role of the mutations in *rho* and in *pheS* genes.

2.3.6. Isogenization of the mutants F9 and F9H by backcross

To isogenize the mutants F9 and F9H from the polymorphisms other than the Campbell type integration of pRS2, the mutants were backcrossed to the parental strain COL using the 80α phage, producing the backcrosses F9T and F9HT, respectively. The transductant F9T showed a similar oxacillin resistance profile and the same number of pRS2 copies inserted in the chromosome of the parental strain F9 (Fig.2.2, Fig.2.7). The transductant F9HT exhibited an intermediate oxacillin resistance profile between F9 and F9H (Fig. 2.7) and a substantially increased (>27) number of plasmids copies compared to the F9H parental strain (Fig. 2.2).

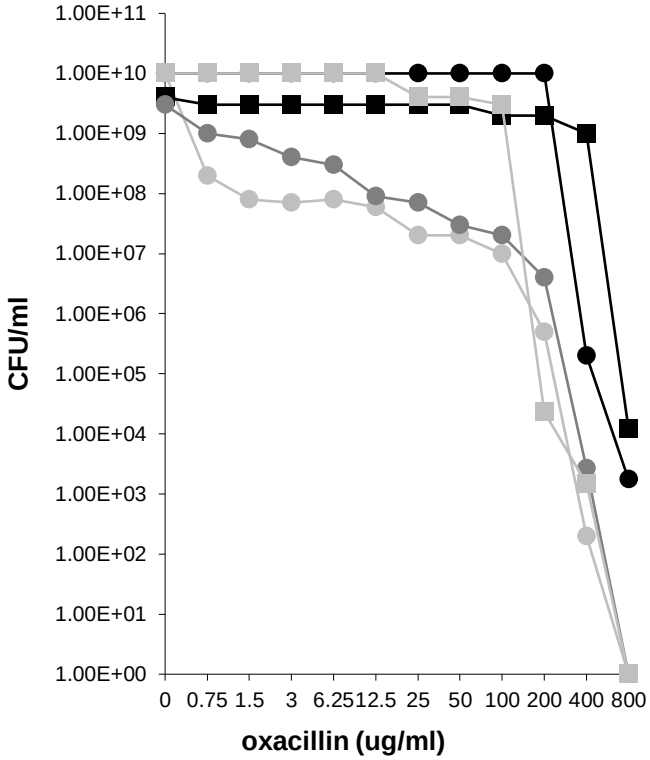

Fig. 2.7. Population analysis profiles (PAPs). PAPs of strains COL (●), mutant F9 (●), homostar mutant F9H (■) and of the respective backross mutants F9T (●) and F9HT (■) in the presence of growing concentrations of oxacillin.

Table 2.3. Main characteristics of the insertion, homostar and backcross mutants. Oxacillin resistance phenotype, number of pRS2 insertions in the genome and presence of *rho* and *pheS* polymorphisms.

			Polymorphisms			
Strain	**Oxacillin Resistance**	**Number of pRS2 insertions**	***rho***		***pheS***	
			DNA	Protein	DNA	Protein
Parental Strain						
COL	Homogeneously resistant	-	wt	wt	wt	wt
Insertion mutants						
F1	Homogeneously resistant	>18	wt	wt	wt	wt
F11, F12, F14, F16 and F21	Homogeneously resistant	9-27	wt	wt	n.d.	n.d.
F2 to F30*	Homogeneously resistant	>27	wt	wt	n.d.	n.d.
F9	Heterogeneous, decreased	~6	G227T	G76V	wt	wt
F20	Heterogeneous, decreased	7-8	ΔT228	Truncated - 77 aa	n.d.	n.d.
F26	Heterogeneous, decreased	7-8	ΔC569	Truncated - 189 aa	n.d.	n.d.
Homostar mutante						
F9H2	Homogeneously resistant	~6	G227T	G76V	C523T	P175L
Backcrosses						
F9T	Heterogeneous, decreased	~6	G227T	G76V	wt	wt
F9HT	Heterogeneous, intermediate	>27	wt	wt	wt	wt

* - except for strains F9, F20, F26, F11, F12, F14, F16 and F21.
n.d. – not determined
wt – wild-type

2.3.7. The *rho* mutation in F9 and in F9H insertional mutants

Rho, the transcriptional terminator factor, is not essential for viability or virulence in *S. aureus.* It catalyzes the release of the RNA molecule from the transcription complex for a DNA sequence that includes a Rho-dependent termination motif. Rho is an hexamer ring-shaped protein composed of identical 47 KDa monomers and has RNA-dependent NTPase activity, which is required for transcript release and helicase activity that allows unwinding of the DNA-RNA hybrid duplex structure (223).

Rho binds to a cytosine rich region named Rut (for Rho Utilization) in the nascent mRNA transcript and moves in an ATP dependent reaction towards the RNA 3′-end. At this end it promotes the dissociation of the transcription elongation complex (223).

Besides the transcription termination of Rho-dependent segments, one of the major roles of Rho is preventing pervasive transcription, mainly antisense transcription. When there is an increase in the pervasive antisense transcription, since the anstisense transcript is complementary to the sense transcript, it leads to a negative regulation of the sense transcription showing an influence of Rho in gene expression (245). In *S. aureus*, the deletion of *rho* results in widespread transcription in the cell

that is originated mainly from three processes: i) presence of spurious promoters; ii) read-through of Rho-dependent and independent transcription terminators and iii) the higher expression of specific coding regions (246).

The mutation present in F9 mutant should result in the substitution of a glycine for a valine in the position 76 (G76V) of the Rho protein. The analysis of the sequences of the Rho protein of *B. subtillis* and *E. coli* showed that G76 of *S. aureus* corresponds to G67 of *B. subtillis* and G63 of *E. coli*, the first of four conserved residues (GFLR) among the three amino acid sequences (223). Moreover, the structure of the *E. coli* N-terminal of Rho in complex with a 9-base polycytidylic RNA oligonucleotide, showed that residue F64 is directly involved in the interaction with RNA (247). The F64 residue corresponds to the F77 residue in the sequence of Rho of *S. aureus*, immediately following the substituted G76 in the F9 mutant (Fig. 2.8).

This suggests that G76 should be crucial for the interaction between Rho and the RNA molecule, anticipating that the function of Rho protein should be impaired in the F9 mutant.

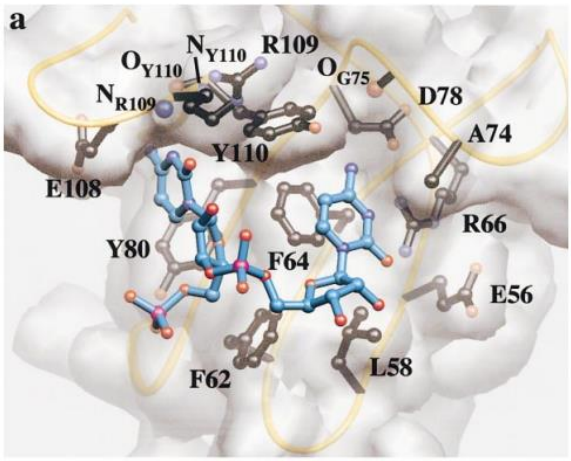

Fig. 2.8. Specific interactions between the *E. coli* 13 KDa N-terminal of the Rho protein with RNA. The RNA moiety (blue sticks) is shown on a surface representation of the Rho13N C-terminal subdomain. Residues and atoms that interact directly with the RNA are colored black and labeled. Reproduced from (247).

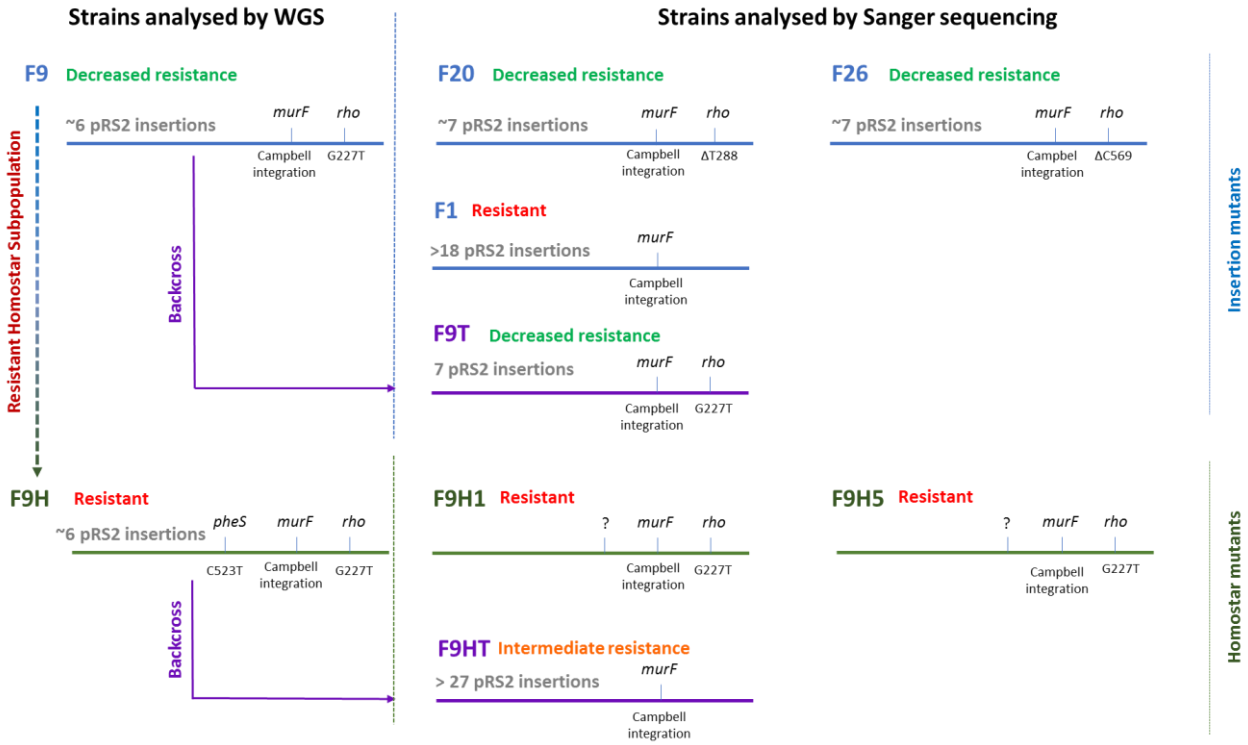

Fig. 2.9. Summary of the mutants described in this work. The mutants are represented regarding the relation between mutants, the mutations present on their genomes, the number of pRS2 insertions, and their phenotype of oxacillin resistance.

2.3.8. Detection of the *rho* polymorphisms in F1, F20 and F26 insertional mutants and in F9T and F9HT backcrosses

The *rho* gene was sequenced for the other *murF* insertion mutants that presented decreased resistance to oxacillin (F20 and F26) and the F1 insertion mutant as a representative of the insertion mutants that presented unaltered resistance to oxacillin.

The mutants with decreased resistance to oxacillin, F20 and F26 showed two different polymorphisms, while the F1 resistant mutant did not have any alteration in the *rho* gene sequence.

For mutant F20, the *rho* gene presented a non-sense mutation corresponding to the deletion of thymine in nucleotide position 228, resulting in a premature stop codon and consequently a truncated Rho protein with only 77 of the native 438 residues. For mutant F26, the *rho* gene presented a frameshift mutation due to the deletion of cytosine 569, resulting in a truncated Rho protein with 183 of the native 438 residues and 6 extra residues (Table 2.3). In the backcross mutant F9T the sequencing analysis revealed that the mutation in *rho* gene (G227T) was present, as in F9 mutant. Since the nucleotide distance between *rho* and *murF* in the COL genome is of 31.4 Kb, the mutation in *rho* was transferred with the *murF* mutation upon transduction by phage 80α (encapsidation capacity of 43.8 Kb) (248). In the backcross mutant F9HT, the mutation in *rho* gene was not transferred in the transduction process.

Interestingly, the results showed that 3 out of the 30 insertion mutants isolated have polymorphisms in the same gene (*rho*), which represents an unusually high rate (10%) of mutation in the same gene.
Additionally, and reinforcing the importance of the mutation in *rho,* the three polymorphisms found were different for each of the mutants (Fig.2.9).

2.3.9. Wild type *rho* gene complements the oxacillin resistance phenotypes in the susceptible insertion mutants

The observation that the insertion mutants with decreased oxacillin resistance (F9, F20 and F26) all harbored polymorphisms in the *rho* gene, suggested that Rho could play a role in the oxacillin resistance phenotype of these mutants. To address this question, the mutants were complemented with a replicative plasmid carrying a copy of the wild-type *rho* gene under the transcriptional control of a cadmium inducible promoter, generating strains F9+pBCB8*rho*, F20+pBCB8*rho* and F26+pBCB8*rho*.

As controls, strains F9+pBCB8, F20+pBCB8 and F26+pBCB8 harboring the empty plasmid were constructed. In the presence of 1μM of $CdCl_2$ the diameter of the growth inhibition halos of the mutants was restored to the value of the parental strain COL (Fig. 2.10, C), while the resistance profile of the control strains was not affected (Fig. 2.10, A and B). For the parental strain COL, the overexpression of *rho* did not affect resistance to β-lactams (Fig. 2.10, C; COL+pBCB8*rho*).

In summary, the resistance profile of the insertion mutants F9, F20 and F26 was restored by the expression of the wild-type *rho* gene, suggesting that Rho plays an important role in the phenotype of oxacillin resistance of these mutants.

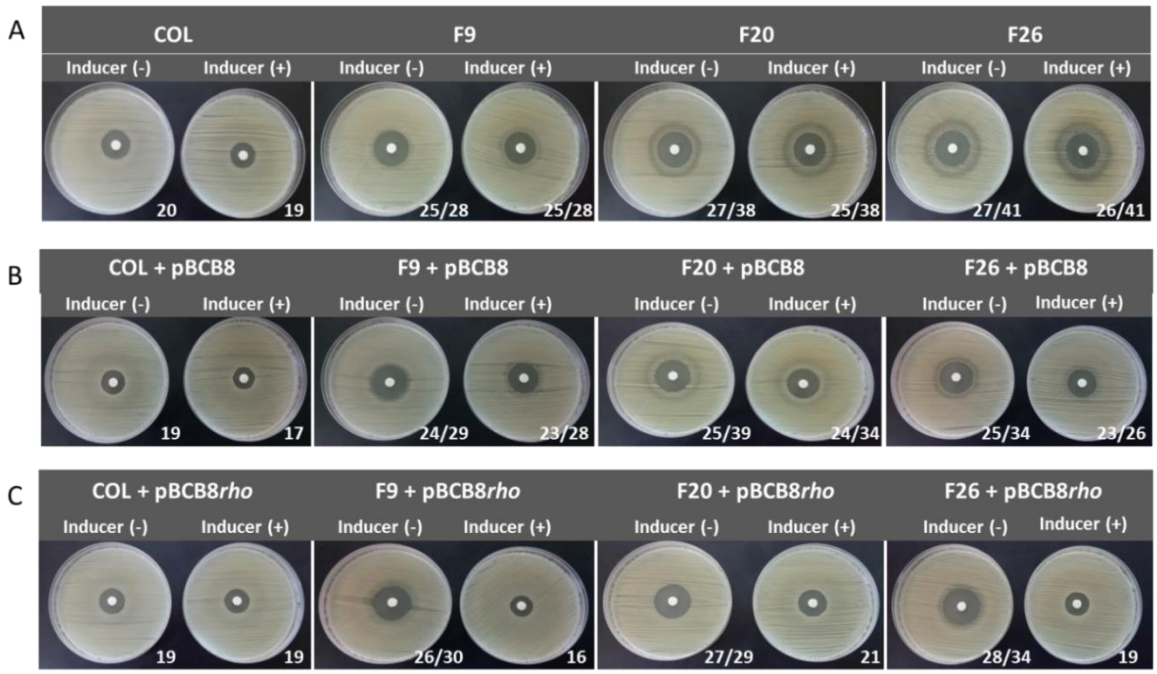

Fig. 2.10. Growth inhibition halos for *rho* overexpression mutants. Growth inhibition halos of oxacillin (1mg) obtained by disk diffusion: parental strain COL and the insertion mutants F9, F20 and F26 with the replicative vector pBCB8 (middle panels) and with pBCB8*rho*, carrying the *rho* gene under the control of the inducible pcad promoter (lower panels). The values presented correspond to the diameter in mm in the absence (-) of the inducer and in the presence (+) of 1µM of $CdCl_2$.

2.3.10. Consequences of the *rho* impairment in different strain backgrounds

The *rho* genetic complementation strategy has shown that mutants F9, F20 and F26 recover the parental strain resistant phenotype, once the wt *rho* gene is expressed. In this way, a loss-of-function mutation in *rho* gene seems to be responsible for decrease in resistance that occurs in these *murF* mutants. To understand if *rho* gene is directly involved in the oxacillin resistance mechanism of COL strain, we used the Tn *bursa aurealis* transposon mutant NE149 (*rho* inactivated) from the Narsa Transposon Mutant Library (235). The *rho* transposon insertion was transduced into strain COL and the oxacillin resistance profile of the mutant was determined by E-test (Range: 0.016-256 µg/mL). The impairment of *rho* gene did not affect the oxacillin high resistance level of COL (Fig. 2.11, A).

To verify whether the high and homogeneous resistance of COL could mask the effect of the interruption of *rho* and to address the function of *mecA* regulatory elements in this response, the *rho* gene was interrupted in the low level resistant MRSA strain HDE288 (SCC*mec* type IV). However, the oxacillin resistance phenotype of the HDE288 Tn::*rho* mutant was not affected (Fig. 2.11, B).

Additionally, to verify if the impact of *rho* impairment is dependent on the *mecA* gene in the PBP2A dependent-MRSA oxacillin resistance, the transposon insertion was transduced into the COL-S strain, a derivative of strain COL in which the SCC*mec* cassette was excised (90). The oxacillin resistance phenotype of the COL-S Tn::*rho* mutant was also not affected (Fig. 2.11, C).

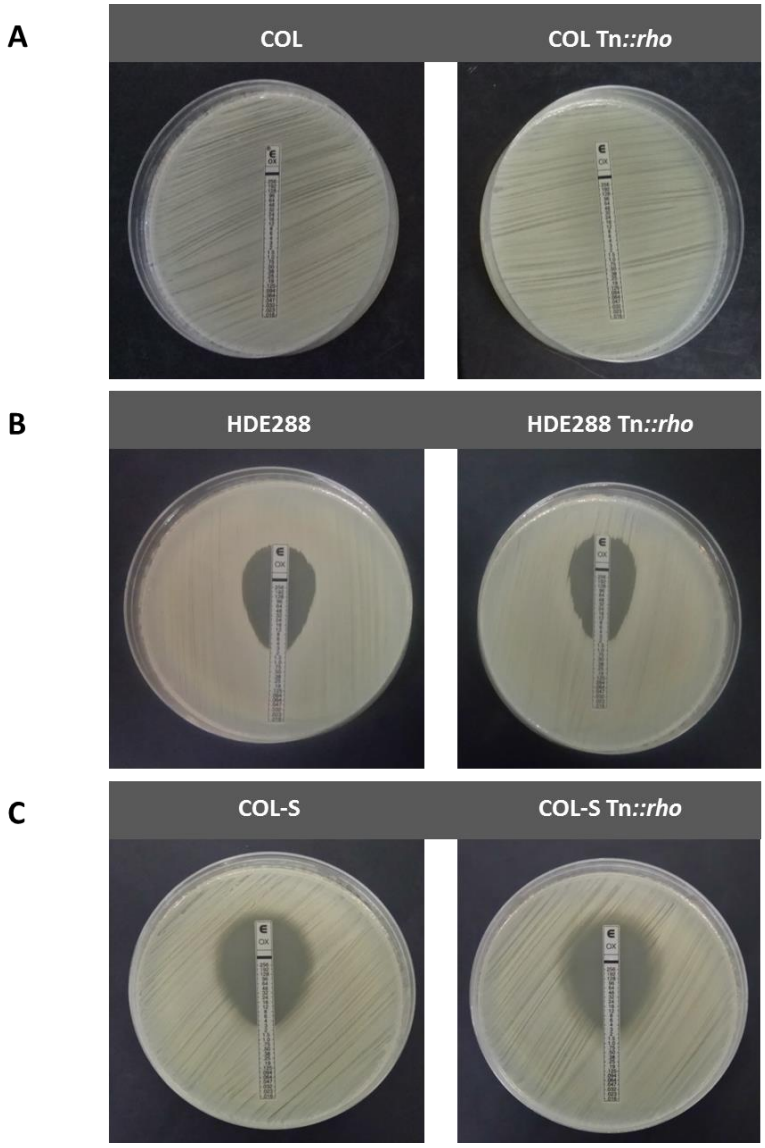

Fig. 2.11. Oxacillin Etests for *rho* transposition mutants. A) strain COL (left panel) and its isogenic Tn::*rho* mutant (right panel); **B)** strain HDE288 (left panel) and its isogenic Tn::*rho* mutant (right panel) and **C)** strain COL-S (left panel) and its isogenic Tn::*rho* mutant (right panel).

2.3.11. Impact of *rho* impairment in the transcription of PBP2A

To address if the mechanism through which Rho reverts the oxacillin susceptibility of mutant F9 is related with the production of PBP2A or with the high number of pRS2 copies, membrane fractions of the mutant F9+pBCB8*rho* grown in the presence of 1μM $CdCl_2$ and of COL, F9 and F9HT (which presents intermediate resistance to β-lactams) were prepared. The membrane protein extracts were separated in a SDS-polyacrylamide gel, transferred to a nitrocellulose membrane and Western blotting was performed with an anti-PBP2A antibody.

The results showed that the amount of PBP2A present in the membrane fraction of all the mutants tested was the same as for the parental strain COL (Fig. 2.12). Western blotting of the same

membrane was performed with an anti-AM antibody, as a control (Fig. 2.12). The amidase AM is one of the two domains of the *S. aureus* Atl autolysin, and its expression is known not to be altered.

The overexpression of Rho did not induce a higher expression of PBP2A, which showed that the mechanism through which Rho restored the resistance to oxacillin in the susceptible insertion mutants did not rely on PBP2A protein levels. In fact, even for F9 mutant, with decreased oxacillin resistance, no alterations in the PBP2A production level were found in comparison to COL (Fig. 2.12). The same result was observed for F9HT that produces the same amount of PBP2A than the parental strain COL and of the mutants F9 and F9+pBCB8*rho* in the presence of 1µM $CdCl_2$. These results suggest that the production of PBP2A is not affected neither by the overexpression of Rho neither by the increased number of copies of pRS2 in tandem present in F9HT.

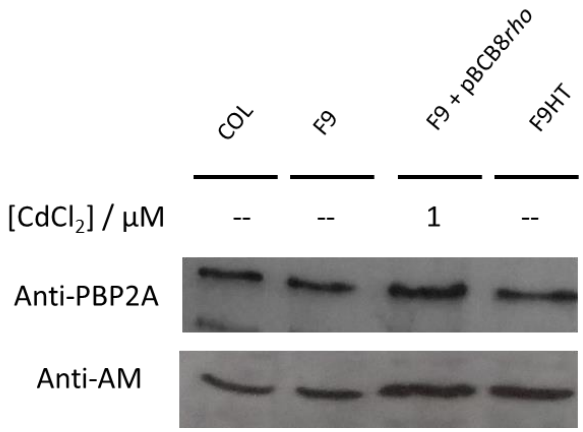

Fig. 2.12. Western blotting of PBP2A expression. of the membrane fraction of strain COL and mutants F9, F9HT and F9+pBCB8*rho* in the presence of 1µM of $CdCl_2$ using a polyclonal antibody raised against *S. aureus* PBP2A and a polyclonal antibody raised against the amidase (AM) domain of *S. aureus* Atl protein.

2.3.12. Effect of the impairment of *rho* in combination with *murF* impairment

Since the impairment of Rho, *per se,* was not responsible for an alteration in the oxacillin resistance level of different genetic backgrounds, it raised the question whether the impact of *rho* impairment on oxacillin resistance would be associated with the impairment of *murF* gene.

To address this question we constructed a different *murF-rho* double mutant. The *rho* transposon insertion was transduced into the conditional COLpcad*murF* mutant (79), generating mutant COLpcad*murF* Tn::*rho* and its resistance to oxacillin was determined using an Etest M.I.C. evaluator strip (Fig. 2.13). In the absence of inducer, a high number of resistant subpopulations emerged, probably due to the leaky nature of the pcad promotor. The results showed that both in the presence and in the absence of *murF* expression, the impairment of *rho* did not alter the oxacillin resistance level. This suggests that the mechanism by which *rho* conferred resistance in the insertion mutants F9, F20 and F26 is not related with the level of transcription of *murF* (Fig. 2.13).

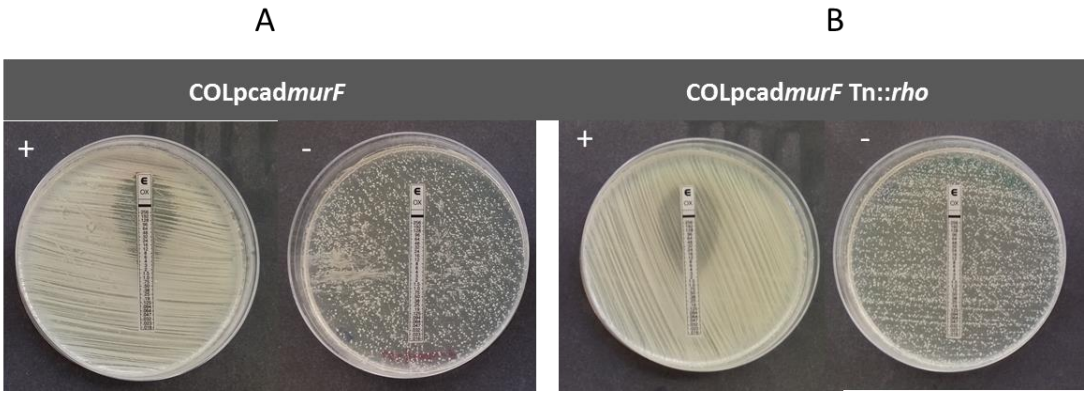

Fig. 2.13. Oxacillin Etests for mutant COLpcad*murF* and respective transposition mutant. Oxacillin Etest for COLpcad*murF* (A) and its isogenic double mutant COLpcad*murF* Tn::*rho* (B) in the presence (+) and in the absence (-) of the inducer (0.2 µM $CdCl_2$).

2.3.13. Peptidoglycan composition of the different insertional *murF* mutant strains

2.3.13.1. Effect of genetic complementation with *rho* in the cell wall composition of the insertion mutants

The complementation of the insertion mutants F9, F20 and F26 with the *rho* gene reverted the low level of resistance to the high level of the parental strain COL. To address if the mechanism of reversion by *rho* includes the repair of the cell wall damage, the cell wall of the parental strain COL, of the insertion mutants F9 and of the respective complemented mutants F9 + pBCB8*rho* grown in the presence of 1µM $CdCl_2$, were extracted, the peptidoglycan was purified, digested with muramidase and the muropeptides were analyzed by RP-HPLC (Fig. 2.14).

For the insertion mutant F9 (Fig. 2.14) the expression of *rho* from a replicative vector resulted in a decrease in the accumulation of disaccharide tripeptide, from 4.5% to 1.8% of relative peak area for F9 (Table 2.4), corresponding to approximately 60% reduction in both cases.

These results suggest that the mechanism through which the transcription terminator Rho rescues the phenotype of methicillin resistance in a MurF impaired mutant ultimately results in the decrease of the abnormal tripeptide accumulated in the cell.

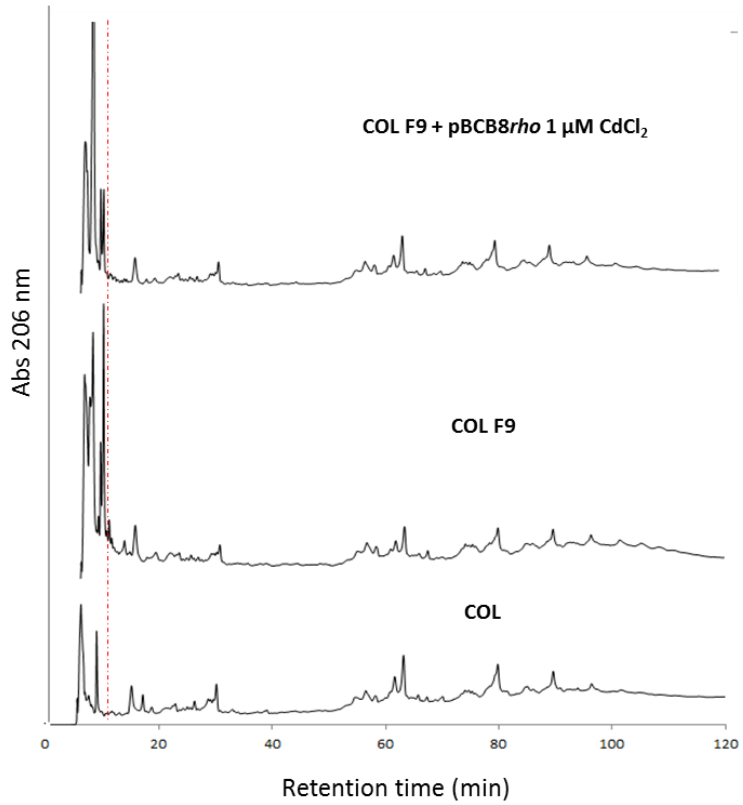

Fig. 2.14. RP-HPLC profiles of *rho* overexpression mutant. RP-HPLC of purified peptidoglycan digested with mutanolysin of strain COL, F9 insertional mutant and the overexpression mutant F9 + pBCB8*rho* grown in the presence of 1µM of the inducer $CdCl_2$.
The red dot lane indicate the peak corresponding to the disaccharide tripeptide (previously identified by mass spectrometry in (58)).

2.3.14. The impairment of *rho per se* did not affect tripeptide accumulation regardless of the *murF* integrity

The overexpression of Rho restored the methicillin resistance and promoted the decrease of the abnormal tripeptide present in the *murF* impaired mutant F9, suggesting that the loss-of-function mutation in *rho* contributes to the cell wall damage in these mutants.

To determine whether the loss-of-function mutation in *rho* affects the level of tripeptide incorporation in the cell wall peptidoglycan in a mutant with the same cell wall damage but with a different genomic impairment, the peptidoglycan of the *murF* conditional mutant COLpcad*murF,* grown in the absence of inducer, was compared to the peptidoglycan of COLpcad*murF* Tn*::rho* double mutant (Tn *bursa aurealis* transposon inserted in *rho* gene) (Fig. 2.15). In the absence of inducer, the expression of *murF* is inhibited and the tripeptide accumulates to 9.7% in the peptidoglycan of the conditional mutant COLpcad*murF* (Table 2.4), as had been previously shown for the other *murF* conditional COL*spacmurF* mutant, previously characterized (59). For COLpcad*murF* Tn*::rho* grown in the absence of inducer (0 µM $CdCl_2$), both the *murF* and the *rho* genes are impaired, as for F9 mutant.

In this background, the impairment of *rho* had a small effect on the tripeptide incorporation (from 9.7% to 7.7%, a 21% reduction) (Table 2.4).

To determine if the loss-of-function mutation in *rho, per se,* resulted in the accumulation of tripeptide, peptidoglycan of the *murF* conditional mutant COLpcad*murF* Tn*::rho,* grown in the presence of optimal concentration of inducer (0.2 µM), was compared to the peptidoglycan of strain COL (Fig. 2.15). The integration of the peaks revealed that upon impairment of *rho* there is no tripeptide accumulation if the *murF* is optimally expressed (COLpcad*murF* Tn*::rho* with 0.2 µM $CdCl_2$), showing that the *rho* impairment *per se* is not responsible for accumulation of tripeptide.

As a conclusion, although the complementation with *rho* led to the reversion of the decreased oxacillin resistance in the insertion mutants and to the decrease in the accumulation of abnormal tripeptide in the cell wall, the impairment of *rho* was not the responsible for the accumulation of tripeptide and consequently the decrease in the oxacillin resistance. Additionally the results showed that *rho* impairment did not affect the incorporation of tripeptide at the cell wall, regardless of the *murF* integrity and the genomic impairment leading to the cell wall damage.

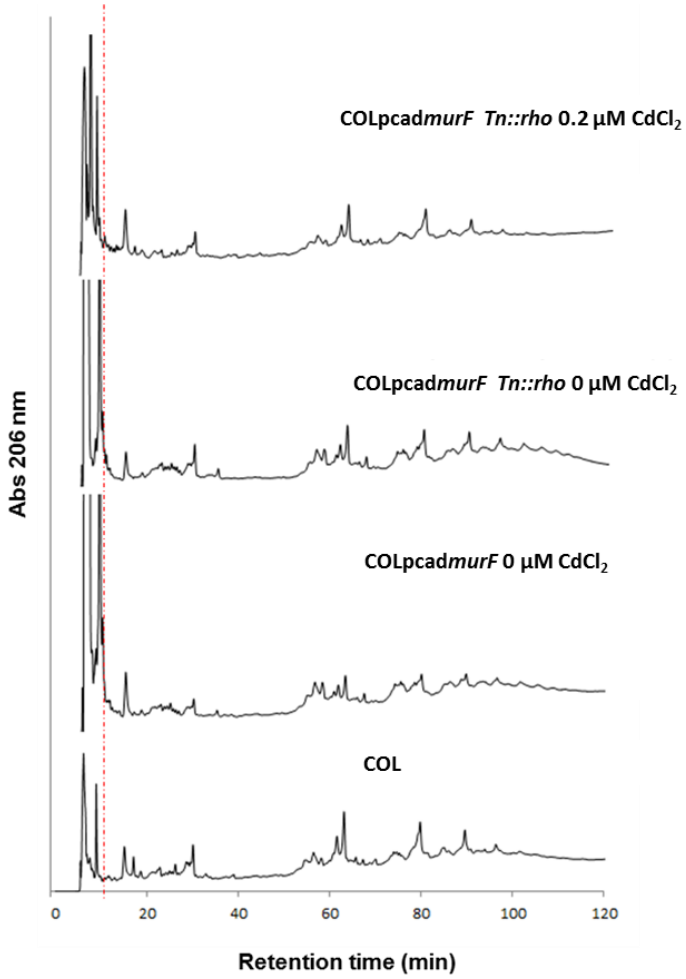

Fig. 2.15. RP-HPLC profiles of COLpcad*murF* Tn::*rho* transposition mutant. RP-HPLC profiles of purified peptidoglycan digested with mutanolysin of strain COL, of the conditional mutant COLpcad*murF* grown in the absence of the inducer and of the conditional mutant COLpcad*murF* Tn::*rho* grown in the absence and in the presence of the optimal inducer concentration (0.2 µM). The Red dot lane indicates the peak corresponding to the disaccharide tripeptide (previously identified by mass spectrometry in (58)).

Table 2.4. Tripeptide contents of the peptidoglycan. Tripeptide incorporation of the parental strain COL, the insertion and conditional *murF* mutants and the respective *rho* overexpression and *rho* impairment mutants.

Strain	$CdCl_2$ Concentration (μM)	Tripeptide Incorporation (relative peak area %)
COL		0.4
F9		4.5
F9 + pBCB8*rho*	1.0	1.8
COLpcad*murF*	0.0	9.7
COLpcad*murF* Tn*::rho*	0.0	7.7
COLpcad*murF* Tn*::rho*	0.2	1.0

2.3.15. Role of Rho in plasmid tandem amplification

The first step in the construction of the mutants was the electroporation of pRS2 integrative plasmid into the restriction/modification negative strain RN4220. Restriction mapping of the electroporation mutant RN4220::pRS2 showed that a high number of copies of pRS2 (>27) was present in the chromosome (data not shown). The two hypotheses for this high number of pRS2 copies were: i) the electroporation and integration of a multimer of pRS2, or ii) the integration and subsequent amplification in tandem of the plasmid in the chromosome (249).

After electroporation, the pRS2 insertion was transduced to COL using the 80α phage and 30 independent transductants were isolated.

Restriction mapping of the 30 transduction mutants showed that for 21 independent transductants, the number of copies of pRS2 was similar to the one of RN4220::pRS2 (>27; Fig. 2.2). For six of the insertion mutants (F1, F11, F12, F14, F16 and F21) the number of copies of pRS2 was lower (between 9 and 27) than in these 21 transductants. The insertion mutants F9, F20 and F26 had fewer copies of pRS2 in the chromosome (F9 - 6 copies, and F20 and F26 – 7 to 8 copies) than the remaining insertion mutants.

The pRS2 plasmid size is 5.2 Kb and the 80α phage is able to encapsidate approximately 43.8 Kb of DNA (248) thus, the 80α phage could not have transduced all the pRS2 copies found in the insertion mutants with high copy numbers (>48.5 Kb), corroborating the hypothesis of duplication in tandem after the integration in the chromosome.

Tandem amplification usually occurs by recombination between two homologous regions in the chromosome which will create a duplication in the first round of replication. In subsequent rounds of replication the number of amplification events will be increased accordingly (250). In this particular case, the *murF* fragment of 1057 bp that was cloned in pRS2 and its homologous sequence in the chromosome should have served as long direct repeats that, through homologous recombination during the replication of the bacterial chromosome, have amplified in copy number (Fig. 2.16).

However, for the insertion mutants F9, F20 and F26, the number of copies of plasmids in tandem did not exceed 7, corresponding to 36.4 Kb, a value approximate to the transducing capacity of the 80α phage. Our hypothesis is that the phage transduced a maximum of 8 copies of pRS2 vector which were subsequently amplified by homologous recombination during the following rounds of replication.

For mutants F9, F20 and F26, the amplification by homologous recombination was inhibited and the 6 to 7 copies of pRS2 in the chromosome reflect the initial Campbell type integration of the maximum number of plasmids. Interestingly, in the backcross strain F9T only 7 copies of pRS2 were found in the genome of the mutant suggesting the incapacity to amplify the vector after its integration while in F9HT, >27 copies of pRS2 were found. Genome sequencing showed that F9, F20 and F26 had a mutation in *rho* gene. F9T had the same mutation in *rho* than F9 and F9HT had the *rho* gene unaltered. These results suggested that amplification in tandem in the chromosome occurred due to the presence of a functional copy of *rho* gene.

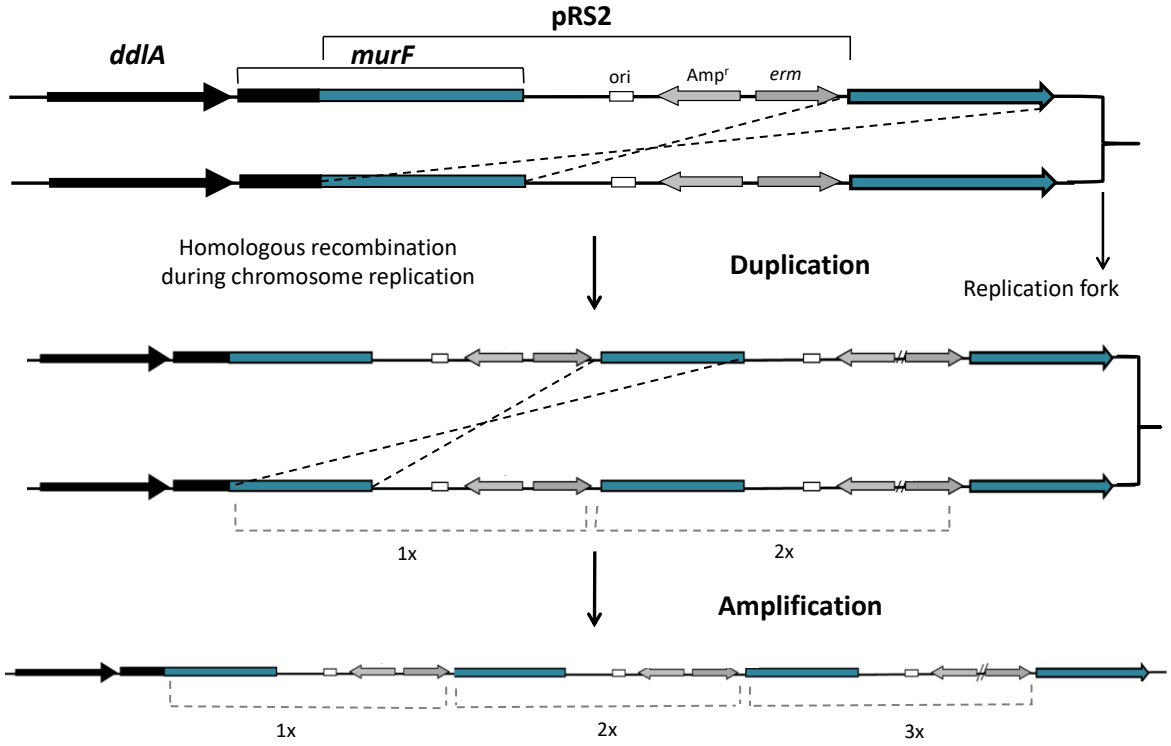

Fig. 2.16. Tandem amplification by homologous recombination. Schematic representation of the amplification of the pRS2 vector in the chromosome of the insertion mutants during replication, by subsequent events of homologous recombination between the 1057 bp fragment of the *murF* gene.

To address whether the mutation in *rho* gene was responsible for the limitation in the tandem amplification of pRS2 in the chromosome, restriction mapping of the mutants F9 and F9H complemented with a replicative plasmid with a copy of *rho* gene under the transcriptional control of pcad promotor (F9+pBCB8*rho* and F9H+pBCB8*rho*) was performed by PFGE (Fig. 2.10).

The results showed that, for both F9 and F9H, the presence of the plasmid copies of wt *rho* gene, resulted in the increase of the size of the band corresponding to the pRS2 copies (In F9 from 6 to 7

and in F9H from 6 to between 9 and 18 approximately). The fact that the number of copies of pRS2 also increased in the absence of the inducer (F9: from 6 to 7 and F9H from 6 to 8 approximately) is probably due to the leaky nature of the promoter pcad that allowed for residual expression of *rho* complementation copy. These results show that Rho is responsible for the tandem amplification of the plasmid in the chromosome, suggesting an important role for Rho in the process of homologous recombination.

However, in the presence of 1µM of inducer, the number of copies was much higher for the F9H complementation mutant (9-18 copies Fig. 2.17 – orange arrows) than for F9 complementation mutant (7 copies Fig. 2.17 – green arrows). Although for F9H, Rho undoubtedly mediates the homologous recombination events allowing the amplification in tandem of a region of the chromosome, for F9, there seemed to be a threshold for the number of copies that could be amplified. Since the growth rate of F9 complemented with *rho* is lower than that of F9H complemented with *rho* (Fig. 2.18), the lower number of pRS2 copies in F9 mutant may be due to fewer replication cycles and consequently fewer amplification events.

Rho is described to contribute to the resolution of conflicts between transcription and replication (227) which can explain the observed homologous recombination events that resulted in the *murF* tandem amplification.

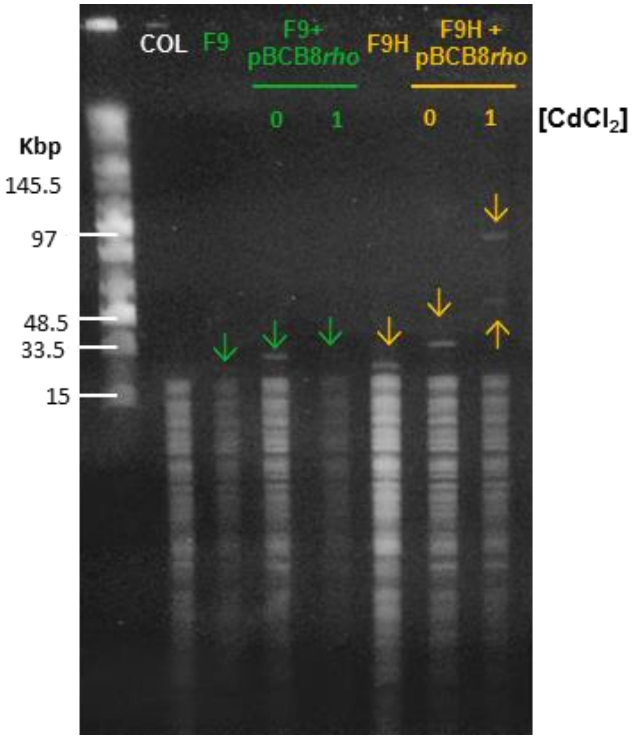

Fig. 2.17. Restriction mapping of *rho* overexpression mutants. Pulsed Filed Gel Electrophoresis (PFGE) of total DNA, digested with EcoRV of Strain COL (White)**,** Mutant F9 and *rho* complemented mutant F9+pBCB8*rho* in the absence (0) and in the presence (1) of inducer (Green),Mutant F9H and *rho* complemented mutant F9H + pBCB8*rho* in the absence (0) and in the presence (1) of inducer (Orange). Lane 1 correspond to the Mid Range PFG Marker (NEB). Arrows indicate the position in the lane of the excised band corresponding to the pRS2 vector.

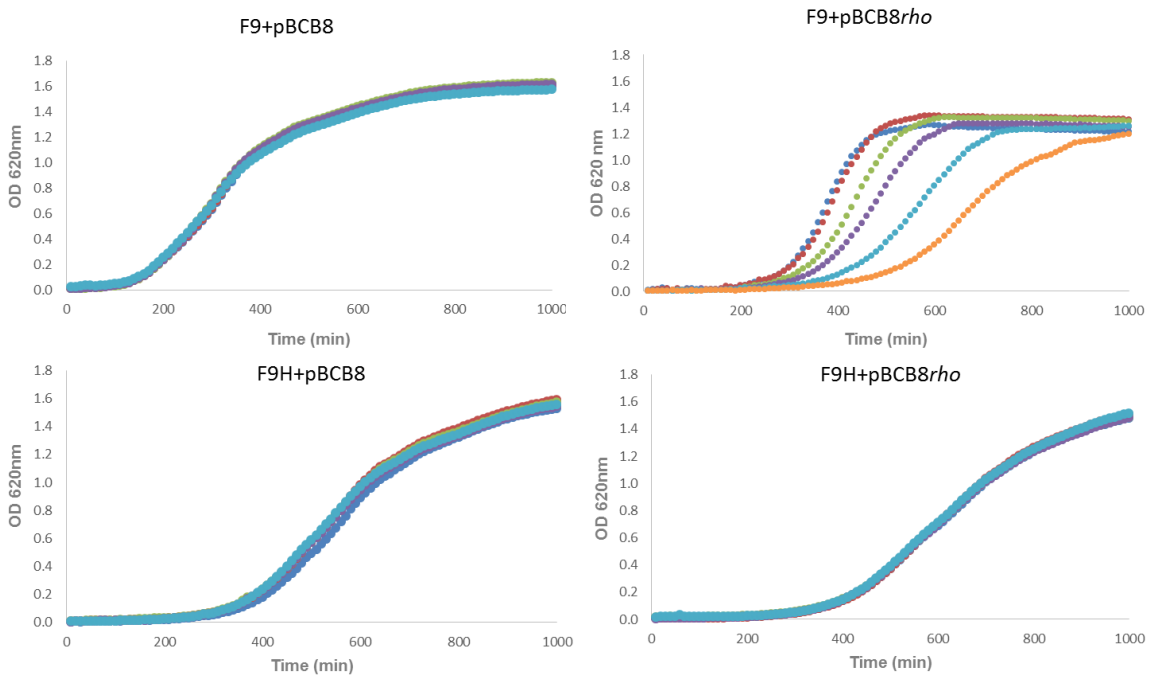

Fig. 2.18. Growth curves of *rho* overexpression mutants. Growth curves of insertion mutants F9 and F9H and the respective *rho* overexpression mutants F9+pBCB8*rho* and F9H+pBCB8*rho* in the absence and in the presence of growing concentrations of the $CdCl_2$ inducer. Legend: ● 0μM $CdCl_2$; ● 0.2μM $CdCl_2$; ● 0.4μM $CdCl_2$; ● 0.6μM $CdCl_2$; ● 0.8μM $CdCl_2$ and ● 1μM $CdCl_2$.

2.3.16. The mutation in *pheS* gene in F9H homostar

The mutation identified in *pheS* gene (C523T) resulting in a P175L protein substitution was unique to the revertant mutant F9H.

The *pheS* gene was sequenced for the other *murF* insertion mutants that showed decreased resistance to oxacillin (F20 and F26) and the F1 insertion mutant as a representative of the insertion mutants that presented unaltered resistance to oxacillin. None of the insertion mutants showed polymorphisms in the *pheS* gene (Table 2.3). Additionally, the *pheS* gene was sequenced for other two independent homostar mutants isolated, F9H1 and F9H5, but no mutations were found (Fig. 2.9).

In the case of F9HT, a backcross mutant of the homostar F9H, no mutation was found in *rho* and *pheS* genes, confirming the isogenization of *murF* mutation.

The exclusivity of the *pheS* mutation in F9H, a highly resistant revertant mutant, made the *pheS* emerge as a possible key determinant in the mechanism of reversion of the β-lactam resistant phenotype.

The *pheS* gene encodes the α-subunit of the Phenylalanyl-tRNA synthetase (PheRS). PheRS is responsible for the charging of the $tRNA^{Phe}$ with L-phenylalanine. PheRS is an heterotetrameric enzyme composed of two α-subunits and two larger β-subunits, these latter encoded by *pheT* gene, which belongs to the same operon as *pheS* (251).

Although the structure of PheRS in *S. aureus* is not available, an homology model was constructed using resolved structures from other species (252). The proline in position 175 is located immediately

adjacent to one of the three conserved motifs that constitute the active site pocket where the binding of ATP and phenylalanine occurs to form phenylalanyl-adenylate (Phe-AMP) as well as the interaction with the CCA end of the acceptor stem of $tRNA^{phe}$ (252). This pocket is a hydrophobic cavity formed by, among others, the Thr171, His172, Ser174 and Gln177 residues. Ser174 establishes hydrogen bonding with phenylalanine. The substitution of Pro175 by a leucine residue, although both are non-polar amino acids, occurs between residues of the hydrophobic cavity of the active site and immediately adjacent to a residue that establishes a hydrogen bond with the amino acid to be charged.

It is therefore likely that this substitution will have an impact in the correct charging of the phenylalanine residue on its cognate tRNA.

2.3.17. Impact of the *pheS* gene mutation in the oxacillin resistance phenotype

To further investigate if the mutation in the *pheS* gene is responsible for restoring the resistant phenotype in the homostar F9H, two different strategies were designed: (i) abolishment of *pheS* expression in the F9 mutant and (ii) overexpression of *pheS* in the homostar F9H.

The chromosomal copy of *pheS* was placed under the control of the cadmium inducible promoter pcad and the conditional mutant F9::pcad*pheS* was obtained. The oxacillin resistance of F9::pcad*pheS* was determined by disk diffusion and, in the presence of inducer (1.8µM $CdCl_2$) the growth inhibition halo was similar to the one of mutant F9. However, in the absence of inducer, and so in the absence of *pheS* expression, the oxacillin resistance level was restored to the high level of the parental strain COL (same resistance level of F9H homostar strain), confirming the involvement of *pheS* in the mechanism of reversion of the phenotype of oxacillin susceptibility (Fig. 2.19, A). Removal of *pheS* expression was sufficient to re-establish the resistance level of the F9 mutant to the high level of the parental strain COL.

The expression of the wt *pheS* gene in the homostar F9H was performed by the introduction of a replicative plasmid with the *pheS* gene placed under the control of the pcad promoter in this strain. The resulting mutant F9H+pBCB8-pcad*pheS* was tested for oxacillin resistance by disk diffusion. In the presence of copies of *pheS* wild-type gene, the level of oxacillin resistance of F9H homostar strain decreased to the level of resistance of mutant F9 (Fig. 2.19, B), confirming the previous observation, that a mutation in *pheS* gene is responsible for the reversion of mutant F9 into homostar F9H.

Since the *pheS* gene encodes the α-subunit of the phenylalanyl t-RNA synthetase and could impair the charging of the correct residue, phenylalanine, onto its cognate $tRNA^{phe}$, the results indicate that the mutation in *pheS* may have triggered a mechanism of stringent response. Stringent response is a mechanism of response to conditions of nutrient starvation which are sensed by bacteria through the ratio of deacylated tRNAs. This response induces a global transcriptomic rearrangement in the cell in order to shut off non-essential functions. Stringent response was already reported to be responsible for the reversion of the β-lactams resistance phenotype in a subpopulation of an MSSA strain to which were provided copies of *mecA* gene in a thermosensitive plasmid (207).

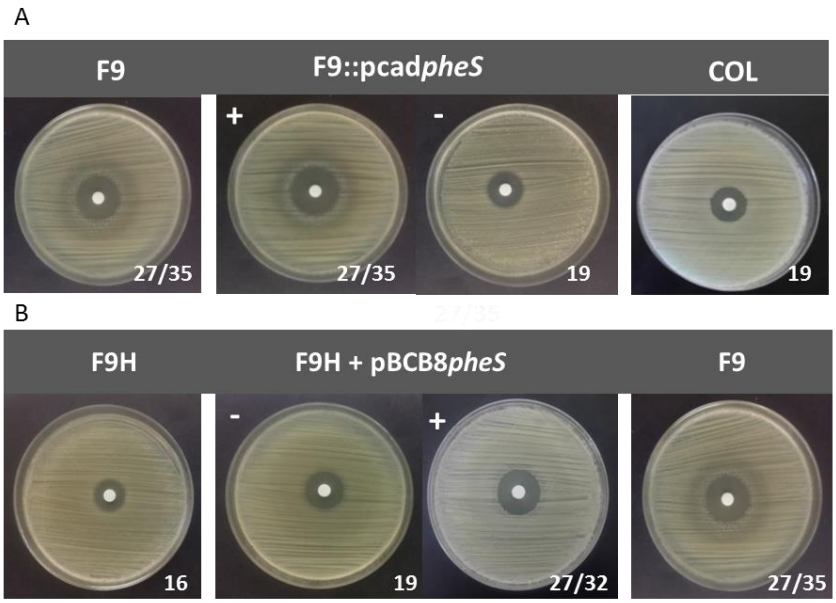

Fig. 2.19. Growth inhibition halos of *pheS* conditional and overexpression mutants. Growth inhibition halos for oxacillin (1mg) obtained by disk diffusion: **A)** conditional mutant F9::pcad*pheS* in the absence (-) and in the presence (+) of 1µM $CdCl_2$ inducer **B)** homostar overexpression mutant F9H+pBCB8*pheS* in the absence (-) and in the presence (-) of 1.8 µM $CdCl_2$ inducer. The values correspond to the diameter of the halos in mm. Oxacillin susceptibility halos for COL, F9 and F9H strains were used as controls.

2.3.18. Reversion of the oxacillin resistance phenotypes in absence of *pheS* expression is *rho* independent

Even though in the F9::pcad*pheS* mutant, the abolishment of *pheS* expression re-establishes the oxacillin high resistance level and the overexpression of *pheS* in the homostar mutant F9H+pBCB8::*pheS* led to a decrease in the level of resistance, the presence of a mutation in the *rho* gene in both mutants could still contribute to the mechanism of reversion of the resistance phenotype.

The overexpression mutant F9H + pBCB8*rho* was constructed providing *rho* in the same replicative plasmid as before. The results showed that, in the presence of the wt *rho* gene, the high level of resistance to oxacillin was unaltered, confirming that the mutation in *rho* gene is not involved in the F9H oxacillin resistance reversion phenotype (Fig. 2.20).

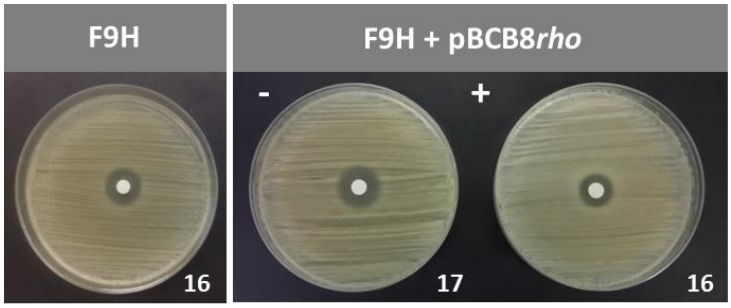

Fig. 2.20. Growth inhibition halos of *rho* overexpression mutant in F9H background. Growth inhibition halos for oxacillin (1mg) obtained by disk diffusion for F9H and F9H+pBCB8*rho* in the absence (-) and in the presence (+) of 1µM $CdCl_2$ inducer.

2.3.19. Microarrays transcriptomic analysis of the F9 and F9H mutants

To identify the transcription pathways through which the *rho* and *pheS* genes are involved in the expression and or activity of MurF and consequently how they impact cell wall tripeptide accumulation and the β-lactam resistance, transcriptomic comparative analysis was performed for COL, F9 and F9H. The comparison between these three strains allowed the identification of 168 genes differentially expressed in F9 in comparison with COL strain and 160 genes differentially expressed in the homostar F9H in comparison with COL. Differences in expression in intergenic regions were not accounted and a log fold change of ± 1.5 was used as the cut off value.

Transcriptomic data was already available in the literature for HG001Δ*rho,* a *rho* deletion mutant constructed in the MSSA strain HG001, a derivative of the NCTC8325 strain in which the SigB-activating phosphatase RsbU is active (253). The transcriptomic profile of F9 and F9H was compared with the transcriptomic profile of HG001Δ*rho* grown in TSB medium to the exponential phase, as this was the condition that best related to our experiment. A total of 171 genes were found to be differentially expressed in the HG001Δ*rho* mutant in this specific condition (253).

The overall comparison allowed to establish three distinct groups of genes: i) the genes responding to the *murF* damage - "*murF*-related"; ii) the genes related with the *rho* impairment/deletion – "*rho*-related" (Fig. 2.21, A) and iii) the genes that were affected by the *pheS* mutation – "*pheS*-related" (Fig. 2.21, B).

The genes whose expression pattern is common for F9 and F9H but different for HG001Δ*rho* or without counterpart in this mutant were included in the "*murF*-related" group of genes. The genes whose expression is common to the three mutants were considered to be "*rho*-related". The genes that were differentially expressed only in the F9H mutant and genes whose expression was different in F9 in comparison to F9H were assigned as "*pheS*-related".

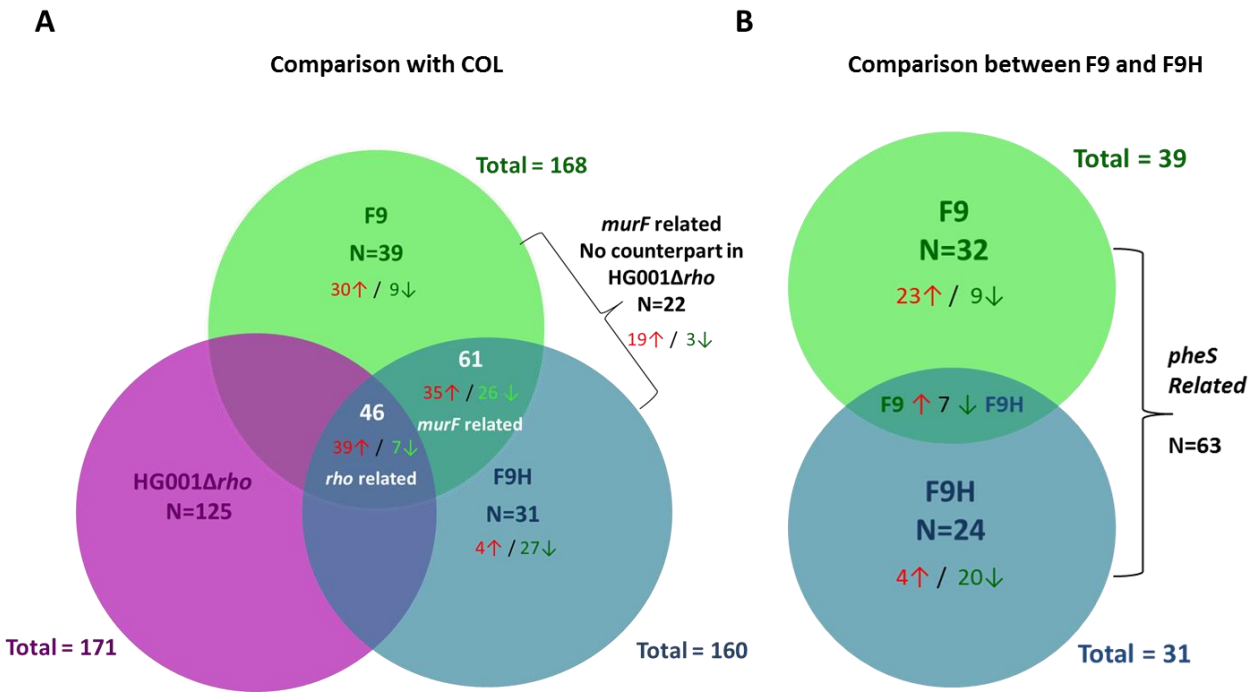

Fig. 2.21. Venn diagram of the number of genes differentially expressed obtained with transcriptomic studies. A) Genes differentially expressed in F9 (green), F9H (blue) and HG001Δ*rho* (purple) (253) in comparison to COL. **B)** Genes differentially expressed between F9 and F9H mutants. The total numbers are indicated outside the circles. Inside the circles are represented the numbers of genes of each group accordingly to its overlapping position among the different mutants. Numbers in red correspond to overexpressed genes and green correspond to under expressed genes.

2.3.19.1. Genes differentially expressed as a consequence of *murF* impairment – "murF-related"

The MRSA strain COL and the MSSA NCTC8325 parental strains have different genetic backgrounds that account for the fact that 22 genes found to be differentially expressed in F9 and/or in F9H have no counterpart in the HG001Δ*rho* genome (Table 2.5). The majority of the genes with no counterpart in the HG001 genome are transposable elements from the pathogenicity island υSa1 that include virulence factors and one transcriptional regulator from the Cro/CI repressors family. It also includes the recombinase genes of the SCC*mec* cassette element that contains the *mecA* resistance determinant. All these genes were up-regulated in F9 and F9H with the exception of the enterotoxin B that is downregulated in F9H.

Regarding the genes whose expression can be compared with the data obtained for HG001Δ*rho*, 61 genes were found to be differentially expressed in F9 and in F9H but not in HG001Δ*rho* disclosing a possible direct association between these genes and *murF* impairment (Table 2.6). Of these, 35 genes were overexpressed and 26 genes were under expressed in both mutants (Fig. 2.21, A).

Unexpectedly, the expression of the genes from the "core cell wall stimulon" was not altered by *murF* impairment (194). This fact is intriguing since these genes had their expression altered upon

challenge with D-cycloserine, bacitracin and oxacillin in NCTC8325 strain (194), with vancomycin in N315 (195), and in COLspac*murF* conditional mutant at suboptimal inducer concentrations (60).

The majority of the "*murF*-related" genes overexpressed were ABC (ATP binding cassette) transporters and other membrane transporters related with different substrates such as ions, iron compounds and amino acids. Genes encoding virulence factors were also found to be overexpressed upon *murF* impairment. From the five genes overexpressed (*spa*, *sdreE*, *clfA*, *sarY* and *clfB*) only *sdreE* is absent from the transcriptomic data from COLspac*murF* at sub inhibitory concentrations of inducer (60). Genes from the pathogenicity island ΦSa1 (Table 2.5) were overexpressed while in COLspac*murF* these were downregulated. However, in the conditional mutant, far more virulence genes were differentially expressed (n=79, including genes from four pathogenicity islands) in comparison with the five genes whose expression is altered in F9 and F9H.

Still related with virulence, the *murF* damage resulted in the repression of genes of the *icaADBC* operon, responsible for the production of PIA (polysaccharide intercellular adhesion), which may result in a decrease in the biofilm production. The repression of this operon was already observed in the transcriptomic analysis of the conditional COLspac*murF* mutant in the presence of suboptimal concentrations of the inducer (60).

Some pathways of synthesis of BCAAs (branched chained amino acids) were also down-regulated both in F9 and in F9H disclosing a connection with *murF* impairment, but since their down-regulation is higher in the F9H mutant, this issue will be covered in the point about genes differentially expressed as a consequence of *pheS* impairment. However, this down-regulation of an amino acid biosynthetic behavior seems to be specific for BCAA amino acids since the *putA* gene, that encodes the enzyme proline dehydrogenase, involved in the biosynthesis of arginine and proline, was overexpressed.

2.3.19.2. Genes differentially expressed as a consequence of *rho* impairment – "*rho*-related"

The genes whose expression was altered due to the impairment of *rho* were considered to be the 46 genes that were differentially expressed (39 up-regulated and 7 down-regulated) in the three mutants, F9, F9H and HG001Δ*rho* (Fig. 2.21, A and Table 2.7). In this group of genes, the direction of altered expression was the same for the three mutants.

The genes down-regulated in response to *rho* impairment were limited to the putative lytic transglycosylase *sceD* and the Ess cluster, known to be involved in the synthesis and secretion of the toxins EsxA and EsxB that are secreted by the ESAT-6-like secretion system (Ess) and are involved in the intracellular infection of *S. aureus* (254). In *S. aureus* the *sceD* and *isaA* both encoding autolytic enzymes, are described to be partially mutually compensatory (255). In our transcriptomic data, however, we were not able to found *isaA* transcription altered.

All the other genes were overexpressed in response to *rho* damage (Table 2.7) and included genes involved in different cellular functions such as transport and binding proteins, protein degradation, resistance to antibiotics and the metabolism of DNA and of fatty acids. The high up regulation of several genes of different functional categories was already expected since depletion of *rho* is known

to cause a high increase in overall transcription in *S. aureus*. This increase in transcription due to *rho* depletion results from: the increase in transcription of Rho-dependent genes; the higher transcription of coding genes due to Rho direct or indirect regulatory effects other than transcription termination; and absence of suppression of pervasive transcription (253).

One of the most overexpressed genes common to the three mutants (Log fold changes: F9-8.54, F9H-9.34, HG001Δ*rho* 2.49), was *sigS* encoding the RNA polymerase sigma factor σ^S involved in response to cell wall disruption and DNA damage (256), which is in accordance with an increase in transcription.

Another overexpressed pathway was the pathway of biosynthesis of riboflavin (vitamin B2) by the *rib* operon. Riboflavin is the precursor of the essential coenzymes flavin mononucleotide (FMN) and flavin adenine dinucleotide (FAD). Curiously, the feedback regulation of the expression of genes of the riboflavin biosynthesis relies on transcription attenuation, a *rho*-independent transcription termination mechanism (257). This result suggests that the Rho damage triggers the up-regulation of the *rib* operon through a *rho*-mediated regulatory effect independent of the transcription termination mechanism of the operon, disclosing the importance of the up-regulation of the *rib* operon for the cell, probably as intermediary metabolites in key cellular functions.

Among the list of genes that were overexpressed, the ones that presented a higher level of overexpression (>10 fold) were the *comEC* and *comK* genes, that are related with the process of genetic competence. ComEC is proposed to form a channel for the entrance of exogenous DNA into the cells and ComK1 is a transcriptional activator and a major regulator of competence that acts synergistically with sigma factor SigH to increase the transcription of members of the SigH regulon (258). The log fold change of these genes were 36.12 in F9 and 35.81 in F9H for *comK1* gene and 12.77 in F9 and 10.24 in F9H for *comEC* gene (Table 2.7, Black box) suggesting that the DNA uptake machinery is “activated” specifically in the two mutants. One hypothesis is that genetic competence is triggered by the impairment of *rho* but even more enhanced in the cell wall defective mutants.

The *radC* gene was found to be up-regulated (3.82 in F9, 5.38 in F9H and 1.18 in HG001Δ*rho)* upon *rho* damage (Table 2.7). RadC is annotated as a DNA repair protein in studies on *E. coli* and its function is still under debate (259) but was reported as specifically involved in recombinational repair of DNA strand breaks associated with the replication fork. RadC action was shown to prevent deletions at chromosomal tandem repeats induced by replication fork defects (260).

Additionally to the aforementioned examples, the most overexpressed gene related with *rho* impairment is SACOL0676 encoding a protein of unknown function, with a dramatic log fold change of approximately 140 and 190 for F9 and F9H respectively, in comparison to the parental strain COL. In the HG001Δ*rho* mutant, this gene is also one of the most highly up-regulated genes (5.92 fold change).

2.3.19.3. Genes differentially expressed as a consequence of *pheS* impairment – "*pheS*-related"

Contrarily to what was observed for the impairment of *rho* gene, the major effect of the *pheS* mutation was the down-regulation of the expression of several genes or at least the return to basal levels of expression similar to the ones found in parental strain COL. This expression behavior is in accordance with the standard concept of stringent response that promotes the switch-off of non-essential functions in the cell. A total of 63 genes were differentially expressed between F9H and F9 (Table 2.8) independently of being differentially expressed in comparison to COL. This list included genes that were not differentially expressed in F9H or in F9 in comparison to COL, since *pheS* impairment in F9H altered the expression of genes that had basal levels of expression in F9 or reverted the expression of genes that had altered levels of expression in F9 to basal levels in F9H (Fig.2.21, B). Most of these genes showed similar transcription patterns between F9 and HG001Δ*rho* reinforcing that the alteration in their expression levels was related with the mutation in *pheS* and are suggested to play a role in the reversion of F9 resistance phenotype.

One case in which the mutation in *pheS* restored the basal levels of transcription found in COL strain was the pathway of biosynthesis of pyrimidines that was down-regulated in F9 and de-repressed in F9H. The level of expression of this operon was also basal in HG001Δ*rho* similarly to what happens in F9H. This behavior suggests that the pathway of biosynthesis of pyrimidines was inhibited upon cell wall damage, and this inhibition was reverted by the mechanism of stringent response, triggered by the *pheS* mutation in order to solve the problem in the cell.

Regarding virulence-related genes, the mutation in *pheS* gene did not cause alterations in their expression, except for a group of genes that were up-regulated in F9 and presented basal levels of expression in F9H.

Although the link between stringent response and virulence remains poorly described, previous works identified a positive association, mainly in intracellular bacteria for which stringent response is in some cases mandatory for infection (261). In *S. aureus,* stringent response is known to activate the expression of toxic phenol-soluble modulins (PSMs) in neutrophils and promote survival after phagocytosis in a CodY-independent process (262). Although induction of the expression of virulence genes mediated by the de-repression by CodY could be expected, this was not observed as a result of the mutation in *pheS.* However, the results showed inhibition of genes encoding fibrinogen binding proteins, hemolysins and leukocidins in F9H transcriptome in comparison to F9. Our results are in accordance with a study that describes the triggering of stringent response through growth of *S. aureus* HG001 strain in chemical defined medium lacking leucine and valine and, similarly, almost none of the *codY* regulon genes were affected (262). The authors suggested that the higher or lower response of genes to CodY activity could explain the absence of activated virulence genes.

In *B. subtillis*, genes of the CodY regulon respond differentially to the GTP pool in the cell. Since the genome of the F9H mutant was sequenced and no mutation were found in the *codY* gene, other hypotheses are that the pool of virulence genes that respond to stringent response is very limited in *S. aureus* or that they are triggered under very specific conditions or at very narrow time-lapses.

Concerning the down-regulated pathways, genes related with the cell envelope and with transport were found to be repressed and were also identified routes related with the synthesis of amino acids and of branched chain amino acids (BCAAs) (Table 2.8). Genes involved in the synthesis of tryptophan (*trpE* and *trpB*) or the *lysC* gene that encodes an aspartate kinase involved in the synthesis of methionine, lysine and threonine were also down-regulated. These results are in contrast to a previous work that describes the up-regulation of genes related with amino acid and BCAA biosynthesis in a HG001 *rsh-codY* double mutant in which stringent response was triggered by the depletion of isoleucine and valine (262). According to this study, genes involved in amino acid and BCAAs biosynthesis are upregulated in stringent response in a CodY-dependent process. In fact, the majority of genes from this functional category belong to the CodY regulon and are repressed by it (263). The down-regulation observed for the genes of these functional categories in F9H seems to indicate that CodY is activated in F9H which is not expected in stringent response. In stringent response, ribosomes are stalled due to nutrient deprivation, the tRNAs become uncharged and the synthesis of the alarmone (p)ppGpp is activated at the expenses of the GTP pool that decreases and releases CodY, activating the transcription of several genes of its regulon like BCAAs biosynthetic genes (15). Additionally, it was reported for *Rhodobacter capsulatus*, a Gram-negative bacteria, that the BCAAs valine and isoleucine bind to the ACT domain of Rel, the (p)ppGpp synthase/hydrolase, activating the hydrolase domain which consequently leads to a decrease in the levels of (p)ppGpp, in this way controlling the level of the alarmone in the cell (264).

One hypothesis for the repression of the BCAAs found in F9H could be that the CodY-mediated de-repression of amino acid and BCAAs biosynthesis occurs very rapidly as an immediate response to stringency conditions. Later, the level of the amino acids pool is reset and the binding of BCAAs to CodY activates it leading to the normal repression of genes. This hypothesis is corroborated by the absence of up-regulation of genes of these pathways in a *codY* mutant of UAMS-1 strain in the post-exponential phase while the up-regulation is massive in exponential phase (263). The sampling of F9H for transcriptome analysis could have been done in a time frame in which *codY* was no longer de-repressing its dependent genes.

Table 2.5. Differentially expressed genes in F9 and/or in F9H mutant without counterpart in the data from HG001Δ*rho.*

COL ID	Gene function	Gene name	Fold change in gene expression* F9	F9H	
Transposable elements					
0028	IS431mec, transposase		4.07	2.92	
0885	pathogenicity island protein, integrase		2.57	1.82	
0886	staphylococcal enterotoxin	*sek*	2.09	1.52	
0887	staphylococcal enterotoxin type I	*sei*	2.05	1.57	Pathogenicity Island υSa1
0888	pathogenicity island, lipoprotein, putative		2.20	1.52	
0889	pathogenicity island protein		2.29	1.67	
0890	transcriptional regulator, Cro/CI family		2.62	1.96	
1425	IS1272-related, transposase, degenerate		4.20	3.07	
2172	IS1272-related, transposase, degenerate		2.18	1.81	
Virulence					
0610	SdrE adhesin	*sdrE*	2.49	3.02	
Resistance					
0041	cassette chromosome recombinase B	*ccrB*	3.00	2.18	
0042	cassette chromosome recombinase A1	*ccrA1*	4.42	3.31	
Hypothetical					
0030	hypothetical protein		7.31	5.79	
0043	hypothetical protein		5.29	3.54	
0044	hypothetical protein		8.72	5.59	
0286	hypothetical protein		-1.53	-2.25	
0287	hypothetical protein		-1.53	-2.18	
0289	hypothetical protein		-1.59	-2.30	
0355	hypothetical protein		3.88	2.65	
0493	hypothetical protein		2.97	1.84	
1755	hypothetical protein		4.42	2.53	
2005	hypothetical protein		8.16	2.68	

* Color red indicates the up-regulated expression and the color green indicates the down-regulated expression. In black are expression levels that were considered to be not altered.

Table 2.6. Differentially expressed genes in F9 and in F9H mutants but not differentially expressed in HG001Δ*rho,* related with the impairment of *murF* gene - "*murF*-related".

COL ID	Gene function	Gene name	Fold change in gene expression*		
			F9	F9H	
Transport and binding proteins					
0178	PTS system, IIBC components	*murP*	2.14	1.77	
0261	drug transporter, putative		2.35	1.78	
0630	amino acid permease		2.00	1.83	
0682	Na+/H+ antiporter, MnhD component, putative		2.28	1.69	
0688	ABC transporter, substrate-binding protein		2.03	1.63	
0689	ABC transporter, permease protein		2.24	1.61	
0690	ABC transporter, ATP-binding protein		2.31	1.62	
2066	K+-transporting ATPase, C subunit	*kdpC*	2.27	1.61	
2067	K+-transporting ATPase, B subunit	*kdpB*	3.23	2.45	
2452	amino acid ABC transporter, permease protein		1.57	2.22	
2572	copper-translocating P-type ATPase		2.16	1.54	
2655	arginine/ornithine antiporter	*arcD*	2.12	1.73	
Virulence/Pathogenesis					
0095	immunoglobulin G binding protein A precursor	*spa*	4.26	2.11	
0856	clumping factor A	*clfA*	1.73	2.44	
2289	staphylococcal accessory regulator Y	*sarY*	2.49	1.53	
2652	clumping factor B	*clfB*	2.09	3.78	
Cell Envelope					
2073	UDP-N-acetylmuramoyl-tripeptide--D-ala-D-ala ligase	*murF*	-2.68	-1.94	
2074	D-alanine--D-alanine ligase	*ddlA*	-2.11	-1.84	
2689	intercellular adhesion protein A	*icaA*	-5.11	-5.50	PIA Production
2690	intercellular adhesion protein D	*icaD*	-4.56	-4.56	
2691	intercellular adhesion protein B	*icaB*	-3.87	-5.13	
2692	intercellular adhesion protein C, authentic frameshift	*icaC*	-2.73	-2.73	
Aminoacid biosynthesis					
1816	proline dehydrogenase	*putA*	2.37	1.76	
2044	acetolactate synthase, small subunit, truncation	*ilvN*	-1.65	-3.49	BCAAs biosynthesis
2046	2-isopropylmalate synthase	*leuA*	-1.51	-3.47	
2047	3-isopropylmalate dehydrogenase	*leuB*	-1.51	-3.21	
2048	3-isopropylmalate dehydratase, large subunit	*leuC*	-1.55	-3.35	
2049	3-isopropylmalate dehydratase, small subunit	*leuD*	-1.64	-3.70	
2050	threonine dehydratase	*ilvA*	-1.71	-3.70	
Energy Metabolism					
0877	glycine cleavage system H protein	*gcvH*	-1.58	-2.17	
1094	cytochrome d ubiquinol oxidase, subunit I	*cydA*	2.36	1.78	
1095	cytochrome d ubiquinol oxidase, subunit II	*cydB*	2.16	1.70	
Other cellular functions					
0491	cobalamin synthesis protein, putative		4.40	3.22	
0813	*comF* operon protein 1, putative	*comFA*	3.18	2.67	
0869	phosphoglycerate mutase family protein		2.85	2.19	

1643	DNA polymerase III, delta subunit	*holA*	2.89	2.34
1708	type III leader peptidase family protein		2.11	3.07
Hypothetical				
0272	hypothetical protein	*esaA*	-1.81	-2.40
0273	hypothetical protein	*essA*	-1.98	-2.17
0274	hypothetical protein	*esaB*	-2.33	-2.42
0275	hypothetical protein	*essB*	-2.11	-2.52
0285	hypothetical protein		-1.79	-2.65
0299	hypothetical protein		-1.63	-2.00
0300	hypothetical protein		-1.72	-2.09
0334	hypothetical protein		3.36	1.54
0436	hypothetical protein		3.63	3.04
0463	hypothetical protein		2.10	1.91
0675	hypothetical protein		2.38	3.35
0922	hypothetical protein		4.42	4.31
1529	hypothetical protein		-2.29	-2.44
1530	hypothetical protein		-2.41	-2.44
1531	hypothetical protein		-2.27	-2.31
1532	hypothetical protein		-3.02	-2.36
1533	hypothetical protein		-3.19	-2.75
2338	hypothetical protein		-1.52	-2.13
2373	hypothetical protein		2.79	1.99
2377	hypothetical protein		5.41	5.94
2547	hypothetical protein		1.86	3.54
2592	hypothetical protein		2.07	1.78
2681	hypothetical protein		2.40	2.57
2733	hypothetical protein		4.94	3.64

* Color red indicates the up-regulated expression and the color green indicates the down-regulated expression. In black are expression levels that were considered to be not altered.

Table 2.7. Differentially expressed genes in common in F9, F9H and HG001Δ*rho* mutants related with *rho* impairment – "*rho*-related".

COL ID	NCTC8325 ID			Fold change in gene expression*			
SACOL	SAOUHSC	Gene function	Gene name	F9	F9H	HG001Δ*rho**[1]	
Biosynthesis of cofactors: Riboflavin, FMN, and FAD							
1817	01886	riboflavin synthase, beta subunit	*ribH*	3.38	2.49	1.76	*rib* operon
1818	01887	3,4-dihydroxy-2-butanone-4-phosphate synthase/GTP cyclohydrolase II	*ribA*	2.93	2.23	1.75	
1819	01888	riboflavin synthase, alpha subunit	*ribB*	2.66	2.30	1.55	
1820	01889	riboflavin biosynthesis protein RibD	*ribD*	2.19	2.22	1.41	
Transport and binding proteins							
0070	00042	permease, putative		3.64	2.58	1.60	
0090	00062	integral membrane domain protein		5.53	2.90	2.08	
2068	02312	K+-transporting ATPase, A subunit	*kdpA*	3.99	2.47	1.29	
2279	02557	transporter, putative		2.99	2.04	1.49	
2376	02661	PTS system, sucrose-specific IIBC components	*scrA*	5.10	4.96	2.30	
Protein degradation							
1055	00986	cysteine protease	*sspC*	4.57	3.35	1.03	
1056	00987	cysteine protease precursor	*sspB*	4.44	3.24	1.20	
1057	00988	V8 Protease	*sspA*	4.71	3.20	1.37	
1830	01900	exosortase E/protease putative		4.39	4.33	2.16	
2385	02670	heat shock protein, Hsp20 family		4.30	2.94	1.51	
2563	02862	ATP-dependent Clp protease, putative	*clpL*	2.10	1.77	1.56	
Regulatory functions							
0980	00913	transcriptional regulator, LysR family		3.17	1.64	1.94	
2388	02674	transcriptional regulator, MerR family, putative		5.55	3.39	1.01	
1827	01897	RNA polymerase sigma-70 putative	*sigS*	8.54	9.34	2.49	
2256	02530	transcriptional regulator, MarR family, putative		3.04	2.90	1.87	
Virulence/Pathogenesis							
0468	00383	superantigen like protein, putative		3.74	2.40	1.02	
0858	00816	secretory extracellular matrix and plasma binding protein	*emp*	4.97	4.87	2.88	
0271	00257	EsxA toxin	*esxA*	-1.72	-2.45	-1.11	ESAT-6 system
0276	00262	putative EssC/YukB component of type VII secretion system	*yukA*	-2.01	-2.62	-1.37	
0277	00264	hypothetical protein	*esaC*	-2.35	-2.66	-2.38	
0278	00265	EsxB toxin	*esxB*	-2.12	-2.79	-1.14	
0279	00266	hypothetical protein		-2.29	-2.55	-2.17	
0280	00267	hypothetical protein		-2.31	-2.70	-2.49	
Competence							
1032	00961	ComK family protein	*comK1*	36.12	35.81	2.21	
1644	01691	competence protein ComEC/Rec2	*comEC*	12.77	10.24	1.79	
Resistance							
0064	00036	metallo-beta-lactamase family protein		5.18	2.88	1.79	
2257	02531	drug transporter, putative		3.96	3.47	1.78	

DNA metabolism						
0441	00352	integrase like protein, putative		6.61	4.35	2.29
1707	01763	DNA repair protein	*radC*	3.82	5.38	1.10
Transposable elements						
0464	00378	transposase, IS3 family		3.07	3.07	2.11
Fatty acid metabolism						
0317	00300	lipase precursor, interruption	*geh*	3.38	1.66	1.59
Other cellular functions						
2088	02333	transglycosylase, putative	*sceD*	-2.91	-1.99	-1.34
2648	02958	alkaline phosphatase family protein		4.30	2.23	1.04
Hypothetical						
0025	00026	hypothetical protein		2.20	1.50	2.58
0063	00035	hypothetical protein		4.70	2.92	1.82
0071	00043	hypothetical protein		3.91	2.33	1.75
0129	00106	hypothetical protein		2.69	1.90	1.36
0676	00622	hypothetical protein		140.11	189.96	5.92
1828	01898	hypothetical protein		9.56	10.34	2.68
2387	02672	hypothetical protein		6.56	3.24	1.25
2502	02794	hypothetical protein		2.09	1.63	1.24
2503	02795	hypothetical protein		4.61	3.98	1.62

* Color red indicates the up-regulated expression and the color green indicates the down-regulated expression. In black are expression levels that were considered to be not altered.
*[1] – Log fold changes obtained from (253).

Table 2.8. Differentially expressed genes in F9H, related to *pheS* impairment – "*pheS*-related".

COL ID			Fold change in gene expression*	
SACOL	Gene function	Gene name	F9	F9H
Pyrimidine ribonucleotide biosynthesis				
1210	pyrimidine operon regulatory protein	*pyrR*	-3.03	1.11
1211	uracil permease	*pyrP*	-7.22	1.12
1212	aspartate carbamoyltransferase	*pyrB*	-6.76	1.07
1213	dihydroorotase	*pyrC*	-7.14	1.08
1214	carbamoyl-phosphate synthase, small subunit	*carA*	-6.75	1.05
1215	carbamoyl-phosphate synthase, large subunit	*carB*	-6.14	1.01
1216	orotidine 5-phosphate decarboxylase	*pyrF*	-6.46	-1.03
1217	orotate phosphoribosyltransferase	*pyrE*	-6.94	-1.08
Amino acid biosynthesis				
0772	ExsB protein	*queC*	1.13	-2.3
1403	anthranilate synthase component I	*trpE*	-1.26	-2
1408	tryptophan synthase, beta subunit	*trpB*	-1.27	-2.47
1428	aspartokinase, alpha and beta subunits	*lysC*	-1.12	-2.09
2042	dihydroxy-acid dehydratase	*ilvD*	-1.36	-2.87
2043	acetolactate synthase, large subunit, biosynthetic type	*ilvB*	-1.43	-2.97
2045	ketol-acid reductoisomerase	*ilvC*	-1.38	-3.27
Cell envelope				
0052	glycosyl transferase, group 1 family protein		2.14	1.33
0119	cell wall surface anchor family protein		-1.27	-5.03
2002	map protein, authentic frameshift	*map*	2.81	-1.56
2493	Staphylococcus tandem lipoprotein		-1.25	-2.1
Virulence/Pathogenesis				
0089	antigen, 67 kDa		2.94	1.44
0907	staphylococcal enterotoxin B	*seb*	2.39	-1.54
1164	fibrinogen binding-related protein		2.45	-1.13
1168	fibrinogen-binding protein	*efb*	3.48	1.01
1169	fibrinogen-binding protein precursor-related protein		3.53	-1.01
1173	alpha-hemolysin precursor	*hlY*	2.49	1.22
1880	leukotoxin	*lukD*	2.58	1.13
2004	leukocidin subunit precursor, putative		3.17	-1.13
2006	aerolysin/Leukocidin family protein		3.02	-1.72
2418	IgG-binding protein SBI		2.55	-1.48
2421	gamma hemolysin, component C	*hlgC*	3.89	1.03
2422	gamma hemolysin, component B	*hlgB*	2.3	-1.24

Transport and binding proteins				
0884	ABC transporter		-1.11	-2.13
2525	ABC transporter		1.23	-3.09
2451	amino acid ABC transporter		1.39	2.04
2453	amino acid ABC transporter		1.47	2.11
Metabolism				
0222	L-lactate dehydrogenase	*ldh*	2.12	1
0407	glycerol-3-phosphate transporter	*glpT*	2.02	1.24
1782	formate--tetrahydrofolate ligase	*fhs*	-1.25	-2.47
Regulatory functions				
2258	staphylococcal accessory regulator V	*sarV*	-1.1	-2
2290	transcriptional regulator, AraC family		2.21	1.4
Fatty acid and phospholipid metabolism				
2003	phospholipase C	*hlb*	2.42	-1.82
Protein degradation				
1970	cysteine protease precursor SspB	*sspB*	2.08	-1.33
2659	zinc metalloproteinase aureolysin	*aur*	-1.16	-2.72
DNA metabolismo				
0860	thermonuclease precursor	*nuc*	1.34	-4.02
Other cellular functions				
0415	Dyp-type peroxidase family protein		-1.31	-2.03
Hypothetical				
0055	hypothetical protein		2.17	1.42
0065	hypothetical protein		2.28	1.49
0208	hypothetical protein		2.42	1.28
0327	hypothetical protein		1.61	2.09
0480	hypothetical protein		2.11	-1.53
0625	hypothetical protein		-1.28	2.14
0641	hypothetical protein		-1.21	-2.67
0767	hypothetical protein	*saeQ*	2.7	-1.34
0768	hypothetical protein	*saeP*	2.68	-1.55
0879	hypothetical protein		-1.45	-2.31
0908	hypothetical protein		2.11	-1.77
1165	hypothetical protein		2.21	-1.2
1170	hypothetical protein		2.3	1.23
1218	hypothetical protein		-2.81	1.03
1659	hypothetical protein		-1.47	-2.06
1811	hypothetical protein		3.53	-1.34
1856	hypothetical protein		1.02	-2.08
2491	hypothetical protein		2.03	-1

* Color red indicates the up-regulated expression and the color green indicates the down-regulated expression. In black are expression levels that were considered to be not altered.

2.3.20. Validation of the F9 and F9H microarray results

In order to validate the microarray results, the differential expression of nine genetic determinants was confirmed by real-time RT-PCR for both the F9 and the F9H mutants (Table 3.7). The genes chosen are spread along the chromosome to avoid differential transcription of discrete regions of the chromosome.

The genes chosen included the ones which expression was more affected, such as SACOL0676, coding for a hypothetical protein, found by microarray to be highly up-regulated in both the mutant (140.11) strain and in its homostar (189.96). Real-time RT-PCR did not only confirm this result (F9: 937.16 fold; F9H: 773.07 fold) but further demonstrated that the microarray technology has limitations concerning the threshold value above which it no longer distinguishes differences in the signal intensity.

The second more overexpressed gene *comK* (F9: 36.12 fold; F9H: 35.81 fold), which encodes for a competence related protein, was also chosen for validating the microarray results.

For *spa* gene (F9: 4.26; F9H:2.11) coding for the major *S. aureus* virulence factor protein A, differential expression was confirmed by the RT-PCR method.

The *pyrF* (F9: -6.41 F9H:-1.03) and *icaA* (F9: -5.11; F9H:-5.5) genes were chosen for validation purposes for two main reasons, the fact that they are considerably down-regulated and the fact that they belong to operons in which more than one gene is being regulated. The coordinated altered expression of members of the same operon is *per se* an internal validation for the microarrays methodology.

The transcription pattern of the two cell wall related genes *mecA* and *pbpB*, was also confirmed by real-time RT-PCR. These two genes were previously reported to be under-expressed in mutant F9 when comparing to COL by Northern blotting (58). Unexpectedly, the microarray approach showed no detectable change neither for the mutant nor for the homostar. The real-time RT-PCR analysis confirmed this result as the change value determined was below the threshold value considered (1.5).

Table 2.9. Log fold change of the expression of nine genes used as controls for validation of the microarrays results by RT-PCR.

		Microarrays experiments		**RT-PCR validation**	
Gene	**COL ID**	**F9 vs COL**	**F9H vs COL**	**F9 vs COL**	**F9H vs COL**
mecA	**0033**	---	---	-1.05	-1.44
spa	**0095**	4.26	2.11	9.4	1.43
	0677	210.08	293.43	937.16	773.07
comK	**1032**	36.12	35.81	38.79	72.25
pyrF	**1216**	-6.46	-1.03	-5.77	-2.79
pbpB	**1490**	---	---	-1.32	-1.26
murF	**2073**	-2.68	-1.94	2.18	1.88
icaA	**2689**	-5.11	-5.5	-3.19	1.05

2.3.20.1 Analysis of *murF* expression

A discrepancy of the expression values of *murF* gene, obtained using microarrays (F9: -2.68; F9H: -1.94) and RT-qPCR (F9: 2.18; F9H: 1.88) (Table 2.9, black box) was observed. A negative log fold change was obtained both for F9 and F9H mutants, by microarrays, indicating the downregulation of the gene. In contrast, the result obtained by RT-PCR, suggested that the gene was overexpressed in the same mutants. The differences in the expression values obtained with each technique were probably related to the specificities of strand detection of each method and to the possibility of anti-sense transcription of the *murF* cloned fragment.

The pRS2 plasmid has the SP6 promoter, that upon integration of the plasmid in the chromosome remained located upstream of the *murF* cloned sequence and should be responsible for the production of transcripts of undefined size that englobe the *murF* truncated copy. The results of Northern blotting obtained both for F1 and F9 showed a smear that must probably represent the transcription of fragments of variable sizes which was compatible with spurious transcription controlled by the SP6 promoter. Additionally, we hypothesize the existence of a putative promotor, located on the minus strand in pRS2 that could regulate the transcription of an anti-sense *murF* mRNA molecule.

The Affymetrix GeneChip array used had 20 different probes of 25 nts each that hybridize with the *murF* mRNA transcript that is transcribed from the coding strand (Fig. 2.22, green). The down-regulation obtained by microarrays confirmed the impairment of *murF* through the insertion of the pRS2 plasmid. The transcription of anti-sense *murF* would not have been detected by the microarray assay since only the coding strand is detected by this technique, however, the Northern blotting technique is able to detect transcripts from both strands, which is in accordance with the strong smear signal obtained using an internal probe of 500 bps that hybridizes with the region of *murF* that is repeated in tandem in the chromosome of the mutants (Fig.2.22, red).

In the case of RT-PCR, the fragment amplified was located on the tandem repeat region thus it should be amplified from the template mRNA regulated by the native promotor and also from the expression of the truncated *murF* fragment, under the presumptive control of promotor SP6 (Fig. 2.22, blue). Moreover, by RT-PCR the detection of transcript molecules occurs without any strand specificity, so it is possible that if *murF* anti-sense transcription was occurring, it was amplified by RT-PCR accounting for the higher log ratio in comparison with the one found in microarrays

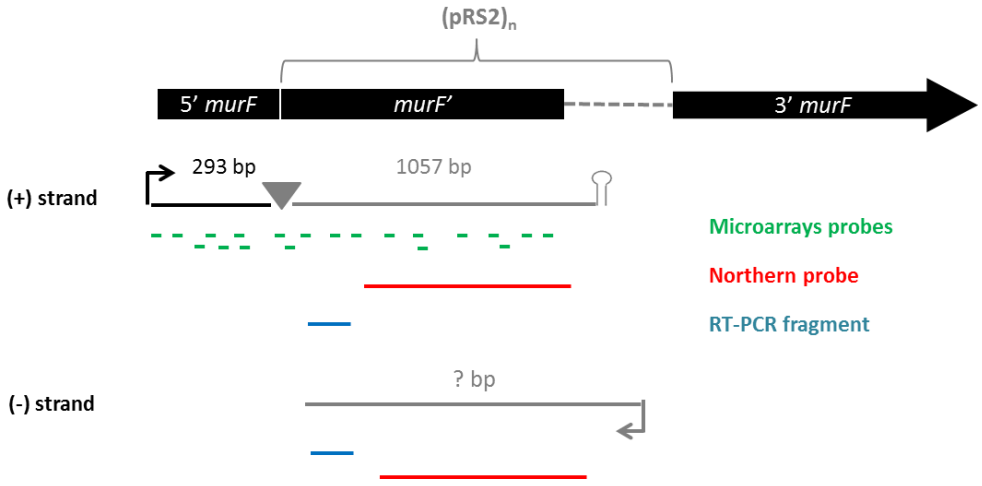

Fig. 2.22. Mapping of the probes for transcription analysis. Mapping of the probes used in the different transcription analysis techniques to genomic sequence of *murF* in the insertion mutants. The probe set sa_c4313s3667_a_at (Affymetrix GeneChip *S. aureus* array) used in microarrays experiment (green lines); the ~500 pbs probe used for Northern blotting (red line) and the fragment amplified by RT-PCR (blue line). The probe set of the microarrays only hybridizes to the mRNA transcript from the coding strand while the probe used for Northern blotting and the RT-PCR assay detect transcription from both strands. The triangle represents the location of the insertion of pRS2. The loop represents a putative transcription termination motif of the (+) strand inside the pRS2 plasmid. The black arrow represents the native promotor of *murF* gene. The grey arrow represents a putative promotor, present in pRS2 in the (-) strand that could be responsible for the transcription of antisense mRNAs, detected by Northern blotting and RT-PCR. (?) - Represents the unknown size of the putative transcripts originated from the antisense strand.

2.4. Discussion

The subject of this study was a collection of 30 isogenic mutants produced by the insertion of pRS2 plasmid in the genome of the MRSA strain COL, as a genetic strategy performed to impair the enzymatic activity associated to *murF* gene. MurF is the enzyme responsible for the insertion of the terminal D-alanyl-D-alanine of the stem peptide of the peptidoglycan. Of these 30 independent mutants, three showed a decreased in the level of resistance to oxacillin (F9, F20 and F26) while the remaining 27 showed the high and homogeneous level of resistance of the parental strain COL. The mutant F9 presented subpopulations of revertants, exhibiting homogeneous high resistance to β-lactams. One of these subpopulations, F9H, was isolated.

In this work, the whole genome sequencing of F9 and F9H was performed to identify the polymorphisms that could explain the reversion of the phenotype of oxacillin resistance observed in the F9H homostar mutant.

This strategy allowed the identification of two polymorphisms of interest: a point mutation in the *rho* gene, found in F9 and in F9H; and a point mutation in the *pheS* gene only present in F9H.

The subsequent work focused in unveiling the role of each of these two genes in the phenotypes of the insertion mutants studied.

The mutation in *rho* gene (G227T) is most probably a loss-of-function polymorphism. The *rho* sequence of the other two mutants with decreased resistance (F20 and F26) also presented loss-of-function mutations. Curiously, two different deletions; a non-sense mutation, resulting in a premature

stop codon and consequently in a truncated Rho protein with 77 residues (F20) and a frameshift mutation resulting in a truncated Rho protein with 183 of the native 438 residues (F26).

In the three mutants, genetic complementation with the native *rho* gene in a replicative vector reverted the phenotype of resistance to oxacillin (F9 + pBCB8*rho,* F20 + pBCB8*rho* and F26 + pBCB8*rho*) showing that the lack of Rho function was involved in the oxacillin susceptible phenotype of the three *murF* mutants.

To address the impact of the impairment of *rho* in the resistance phenotype, a *rho* transposition mutant was constructed in the background of strain COL. The impairment of *rho* did not translate into an impact on the oxacillin resistance level of the strain. The same mutation was transferred to strain COL-S, a derivative of strain COL with the SCC*mec* cassette excised, and to strain HDE288, a low level resistant strain with *mec* regulatory elements which lack in COL. The lack of *rho* gene did not show an impact on the resistance levels of any of these mutants.

To understand why the impairment of *murF* gene did not have the same impact on the oxacillin resistance phenotype of the other 27 of the 30 insertion mutants, amplification of the full length *murF* was performed for F1 as a representative of the 27 insertion mutants with decrease resistance to oxacillin. Despite the insertion of pRS2 has been confirmed by PCR amplification to have occurred at 6 bps of the *murF* stop codon*,* similarly to in F9, the full *murF* gene was also amplified with a primer that hybridizes precisely at the end of the gene encompassing the last base pairs and the stop codon suggesting that at least one copy may have been restored. Since the amplification of the full *murF* gene, with this PCR amplification strategy, was not possible for F9, the result suggested that a full *murF* copy might have been restored in F1 and, possibly in all the mutants with increased resistance to β-lactams. The fact that these mutants seem to have a *murF* restored copy, is most probably the reason for the maintenance of the oxacillin resistance phenotype.

The restriction mapping of all the insertion mutants revealed that the pRS2 plasmid exists in multiple copies in the chromosome, displayed in tandem repeats. However, the mutants with decreased oxacillin resistance showed a much lower number of pRS2 repeats than the mutants that retained the high and homogeneous level of resistance. This observation suggested a relation between the number of copies of pRS2, the integrity of *rho* gene and the resistance to β-lactams.

Supporting these evidences, the analysis of the backross mutants, constructed to isogenize the *murF* mutations, revealed the same behavior. The mutant F9T (backcross of F9 into COL strain) showed decreased resistance to oxacillin, low numbers of pRS2 repeats in the chromosome and the same polymorphism in *rho* as F9. The F9HT (backcross of F9H into COL strain) showed intermediate resistance to oxacillin, a very high number of pRS2 insertions and no mutations in *rho*.

The analysis of the peptidoglycan composition of the *murF* mutant F9 complemented with a native copy of *rho* gene revealed that providing copies of a functional *rho* gene in trans, results in the decrease of the amount of tripeptide accumulated in the cell wall. On the opposite hand, the impairment of *rho* was not, by itself, responsible, for the accumulation of tripeptide. Moreover, the impairment of *rho,* in the absence of *murF* expression in a conditional mutant, also did not show a considerable difference in the tripeptide found to be accumulated in the cell wall. Altogether these

results showed that the impairment of *rho, per se*, did not affect tripeptide accumulation, except in the F9 mutant.

To uncover the mechanism through which Rho protein is able to revert the susceptibility to β-lactams of the F9 mutant, the level of PBP2A produced was assessed for the F9 strain and its *rho* complemented derivative. No alterations were observed in the PBP2A translation levels of the F9 mutant complemented with *rho*, showing that the mechanism of resistance reversion in these strains is *mecA*-independent

The absence of a direct mechanism of phenotype reversion, suggests that it could be mediated by an indirect mechanism triggered by Rho. Since the mutants with decreased resistance had loss-of-function mutations in *rho* and also had low numbers of pRS2 insertions, we hypothesized whether Rho could be the responsible for the mechanism of tandem amplification of pRS2 in the chromosome during replication events.

To address this question, restriction mapping was performed for strains of F9 and F9H complemented with *rho* both in the absence and in the presence of the inducer. The results showed that, in fact, the complementation with *rho* triggered the amplification in tandem of pRS2 in the chromosome which could potentiate a recombination event that would culminate in the restoration of the *murF* gene and the consequent reversion of oxacillin resistance phenotype.

The results also showed that this amplification was more efficiently achieved in F9H than in F9. The overexpression of *rho* conferred a clear advantage to the cell in terms of oxacillin resistance, since it allowed the necessary recombination to restore *murF* and repair the cell wall. However, we observed that the cost of the *rho* overexpression, in F9, occurred at the expense of a critical reduction of fitness which was translated in a marked decrease in the growth rate, which did not happen in F9H in which the overexpression of *rho* did not affect growth.

Since F9 + pBCB8*rho* has a lower growth rate than F9H + pBCB8*rho*, the lower number of pRS2 copies could be due to a different time-lapse in replication events in both strains. The same time of growth did not correspond to the same number of generations and consequently to the same number of replication events.

The mechanism through which Rho mediates the tandem amplification is not yet understood but the answer may rely in the role of Rho as a mediator in transcription-replication conflicts (TRCs).

Considering that the replication fork progresses at an approximate rate of 600 nts/s (nucleotides per second), and that the progress rate of the RNA polymerase (RNAP) is around 20 nts/s, transcription-replication conflicts often occur, namely in highly transcribed regions (225), as is the case of the *murF* gene fragments, demonstrated by northern blotting of mutants F1 and F9. If these collisions are not properly solved, the result is highly damaging for the cell and could generate fork collapse.

When transcription elongation complexes (TEC) are stalled in these regions, the backtrack of the RNAP, which is the spontaneous sequence-dependent back and forth sliding of the elongation complex, is induced, leading to the displacement of the 3' end of the nascent RNA (265). Once free, the mRNA molecule can hybridize with DNA forming a three strand hybrid of DNA:RNA named R-loop (266). Additionally, when RNAP hits the replication fork it induces double strand breaks (DSB) or

ssDNA gaps. In the presence of this DSB or gaps in the DNA, the replication fork cannot progress and usually recombination events solve this problem allowing the restart of replication. R-loops can be used as primers for the DNA synthesis in this process (267).

Mutants unable to repair the collapsed replication forks, are more dependent on Rho activity. In *E. coli*, the inhibition of Rho induces DSB in the DNA and Rho is also known to prevent the formation of R-loops (268). Rho also triggers the dissociation of the stalled RNAP, allowing for the replication to resume or, in case of a DNA lesion, to be repaired. This rapid removal of the RNAP is critical to avoid the transcription-replication conflicts (TRC) (227). It was suggested that Rho has been maintained during evolution in Gram-positive bacteria to prevent the conflicts between TEC and replication (225).

It is possible that, upon cell intake of several copies of *murF* by transduction and homologous recombination, the high level of transcription in this region of the chromosome causes TRC that, in the presence of Rho, undergo a hyper-recombination process. In the mutants in which *rho* is mutated, the process of recombination was impaired (resulting in the small number of copies in F9, F20 and F26 mutants) and in the presence of functional copies of Rho, the process of recombination, and so, the amplification of the pRS2 copies, was re-established suggesting that Rho may be directly involved in the process of homologous recombination by a yet not described mechanism.

In contrast to *E. coli,* in which the abundance of Rho molecules corresponds to 38 to 64% of the abundance of RNAP, in Gram-positive bacteria this ratio is estimated to be 0.8 to 5% of the level of RNAP, according to different studies (269). This difference suggests that, while in *E. coli* Rho may be present at almost all the loci where RNAP is catalyzing transcription, in Gram-positive bacteria, the mechanism of Rho to prevent TRC should be broader and more indirect.

In our work, a set of microarrays performed for F9 and for F9H, combined with the results from the transcriptomic analysis of a *rho* deletion mutant (246) allowed to gain a more detailed view of the genes which expression was altered due to *rho* impairment. This approach may disclose a pathway through which *rho* acts to modulate the recombination process and consequently, to allow the reversion of resistance phenotype.

Curiously, *radC* gene was up-regulated in F9 and F9H mutants and also in the *rho* deletion mutant. RadC is specifically involved in recombinational repair of DNA strand breaks associated with the replication fork and it was shown to prevent deletions at chromosomal tandem repeats induced by replication fork defects (260). The up-regulation of *radC* was shown to result from the *rho* impairment and strengthens the importance of Rho in the *murF* tandem process. The function of *radC* in the process of tandem amplification of the plasmid insertion should be further characterized in the future.

In *E. coli*, Rho was appointed has having the function of silencing the horizontally transferred DNA, since treatment with bicyclomycin, which is an antibiotic that inhibits the function of transcription terminator of Rho, induces the expression of prophage genes, almost functioning like an “immune mechanism” for protection against phage-related or xenogenic DNA, being the horizontally transferred genes “hot-spots” to Rho-dependent termination (269). In fact, prophages could be harmful to the cell but they can also be beneficial and so the bacterial hosts have developed strategies to maintain them. Prophages integrate and excise from the host chromosome through site-specific recombination, a process that seems related with Rho regulation at the level of gene expression (270). It is conceivable

that a mechanism that regulates site specific-recombination in a prophage context exists and could be used by the *murF* insertion mutants to allow recombination in order to amplify a determinant that could rescue the cell from severe cell wall damage.

The massive overexpression of a small ORF, annotated as a hypothetical protein, SACOL0676, upon the impairment of *rho* may allow to deeply characterize the role of *rho*. This ORF showed an up-regulation of 210 fold and 293 fold in F9 and in F9H respectively, a result confirmed by RT-PCR to be even higher, with 937 fold to F9 and 773 fold to F9H. The high overexpression of this ORF in three mutants with the *rho* gene impaired suggested that the ORF *rho*-triggered overexpression may be involved in the survival of the cell to a lethal damage or in the pathway through which the inhibition of *rho* could affect the homologous recombination.

The further characterization of this ORF will be addressed in the chapter 3 of this thesis.

The *pheS* mutation reverted the oxacillin resistance in F9H

The mutation found in *pheS* gene, since was only present in the chromosome of the homostar F9H, emerged as the putative responsible for the reversion of oxacillin resistance observed in F9H. This reversion may occur at the level of the tripeptide incorporation since F9H does not incorporate tripeptide in the peptidoglycan. The analysis of the oxacillin resistance phenotype of a F9 *pheS* conditional mutant (F9::pcad*pheS*) and a F9H *pheS* overexpression mutant (F9H+pBCB8*pheS*) revealed a direct link between *pheS* and oxacillin resistance. Not only overexpressing the *pheS* gene in a mutant in which the same its mutated (F9H+pBCB8*pheS*) decreases its level of resistance for the levels of the parental strain, as also inhibiting its expression in a strain with a cell wall damage (F9::pcad*pheS*) is sufficient to restore the level of resistance. Our results showed that the impairment of *pheS* is responsible for the reversion of an important damage in the cell wall, that is lethal to the cell, as shown by the characterization of the *murF* conditional mutant COLspac*murF* (59), and manage to decrease the tripeptide incorporated which culminates in the restoration of resistance levels (58).

Due to the localization of the residue that was substituted (P175L) adjacent to the active center, the correct charging of the phenylalanine residue on its cognate tRNA is expected to be impaired, which suggests that the mechanism through which the mutation in *pheS* reverts the β-lactams resistance is stringent response.

Stringent response is triggered by the presence of non-acylated tRNAs that, once inside the ribosome, lead to the transfer of PPi from ATP to GDP or GTP forming (p)ppGpp in a reaction catalyzed by the RelA/SpoT enzymes. The presence of p(ppGpp) modulates a quick reprogramming of transcription and leads to the shut-off of non-essential functions in the cell. This mechanism is in accordance with the results of the microarrays assay in which 63 genes were found to be differentially expressed in F9H in comparison to F9, among which only 4 were found to be up-regulated suggesting a massive shut-off of cellular functions. However, among these 63 genes, 31 were also differentially expressed in comparison to COL strain, which suggests that these alterations are part of a normal response triggered in stringency conditions. However, the remaining 32 genes were only differentially expressed in F9H in comparison to F9, being most probably altered by the process of stringent

response as a mechanism to survive the damage in the cell wall since otherwise these genes were not altered in their expression in relation with COL.

The most evident case was the pathway of biosynthesis of pyrimidines. The *pyr* operon was highly downregulated in F9 and returned to basal levels in F9H suggesting that stringent response specifically targets the biosynthesis of pyrimidines to solve the damage at the cell wall level. The pathway of biosynthesis of pyrimidines is related with the integrity of the cell wall in *Lactococcus lactis.*

It was shown that the conversion of l-aspartate (l-Asp) to *N*-carbamoyl-l-aspartate, by PyrB, reduces the amount of l-Asp available for peptidoglycan synthesis causing a reduction in the cross-linking wich reduces the thickness and rigidity of peptidoglycan. The authors hypothesize that the common utilization of the substrate I-Asp by the pyrimidines pathway and the peptidoglycan biosynthesis pathway may regulate the flexibility of the peptidoglycan according to the growth phase (271). Moreover, 2'-Deoxyuridine 5'-triphosphate (dUTP), a pyrimidine derivative, is of vital importance for the formation of uridine-5'-diphosphate-*N*-acetylglucosamine (UDP-GlcNAc) in the first cytoplasmic step of the peptidoglycan biosynthetic pathway. In F9, a cell wall mutant, the pyrimidines pathway is down regulated. After triggering of the stringent response, the *pyr* operon returns to its basal level of expression. Previous studies showed that in the absence of *guaA,* a gene encoding an enzyme involved in the synthesis of GTP which subsequently is converted in (p)ppGpp, the *pyr* operon is downregulated suggesting a relation between stringent response, the expression of *pyr* operon and its importance for cell wall structure and properties (271). Additionally, we anticipate also the importance of the hypothetical protein SACOL1218 located immediately downstream of *pyrE* gene and with the same pattern of transcriptomic response.

This reversion in the transcription levels of the *pyr* operon may be, together with other yet unknown players, the responsible for the reestablishment of the cell wall of F9H and probably to be related with the reversion of β-lactams resistance in this mutant.

Despite the fact that the mechanism through which stringent response is able to revert β-lactam resistance in *S. aureus* is not yet fully understood*,* several advances have been made and it is thought that the oxacillin resistance phenotype is reverted by an increase in the levels of PBP2A, mediated by an increase in *mecA* transcription.

In this work, we were able to show that the mechanism through which stringent response reestablishes the cell wall damage is independent of Rho since in F9H, if copies of *rho* wild-type are provided, the high level of resistance to oxacillin is maintained.

The two mechanisms, the impairment of *rho* gene and the impairment of *pheS* gene, seem to be independent and alternative pathways that allowed the cell to circumvent cell wall damage. Through the activity of Rho protein, in a *mecA* independent process and through stringent response in a *mecA* dependent manner.

Chapter 3

Functional studies of an uncharacterized system of *Staphylococcus aureus*, SACOL0677-76-75, involved in *rho* response to cell wall damage

3.1. Introduction

In Chapter 2 of this Thesis, it was demonstrated that the impairment of the *rho* gene had a negative impact on the capacity of *S. aureus* to repair a cell wall damage caused by a plasmid insertion in the *murF* gene, in the F9, F20 and F26 mutant. In the presence of a functional Rho factor, tandem amplification of the inserted plasmid containing a truncated fragment of *murF* gene occurred by homologous recombination. In one or more of these recombination events, the *murF* gene was restored and the other 27 *murF* insertion mutants maintained the level of resistance to oxacillin. This finding undisclosed a direct or indirect role for Rho in homologous recombination in *S. aureus.* However, the mechanism by which Rho intersects the homologous recombination pathway remains unknown.

The transcriptomic analysis, of the F9 insertion mutant and of its F9H homostar resistant revertant mutant, revealed the massive overexpression of two small neighboring ORFs, consecutively located in the chromosome, most likely forming an operon: SACOL0676 and SACOL0677 due to their genetic organization and the presence of a single putative promoter upstream of SACOL0677. SACOL0677 was overexpressed 140 fold in F9 and 190 fold in F9H and SACOL0676 was overexpressed 210 fold in F9 and 293 fold in F9H. RT-PCR for SACOL0677 confirmed the overexpression by RT-PCR to be of 937 fold in F9 and 773 fold in F9H. Such expression values evidenced the importance of these genes in a mutant that is facing a cell wall damage by accumulating abnormal tripeptide in the peptidoglycan layer. This specific damage has been previously shown to be lethal for *S. aureus*, through the study of the conditional mutant COLspac*murF*, impaired in the same gene and with a similar resulting phenotype (59). The F9 mutant also showed decreased oxacillin resistance but, in contrast, was completely viable and with a growth profile that overlaps the one of the parental strain COL. In accordance with this contrasting behavior, F9 presented a transcription profile completely distinct from COLspac*murF*, as in the case of the overexpression of SACOL0676-0677. Additionally, downstream of these genes, was located another gene, SACOL0675, encoding for a transmembrane protein, also, although slightly, overexpressed in F9 and F9H.

The transcriptomic data suggested that these three unknown genetic determinants play an important role in the adaptation of bacteria to a lethal cell wall stress.

The SACOL0676 gene was also identified to be highly overexpressed in the transcriptomic analysis by RNAseq of the *rho* knockout mutant HG001Δ*rho,* a strain derivative of NCTC8325 with the SigB-activating phosphatase RsbU active (246). In this study, the authors showed that this gene (SAOUHSC_00622 in NCTC8325) was upregulated in the *rho* defective mutant but this upregulation was neither due to the lack of an intrinsic terminator, thus being Rho-dependent, nor due to read-through transcription over the terminator, but due to other regulatory role of *rho*. The results of this work combined with our transcriptomic data strongly suggested that the massive transcription of these

genes is triggered by the impairment of Rho. A more recent publication focused on the proteomic analysis of the same *rho* knockout mutant HG001Δ*rho,* showed that SAOUHSC_00622 protein (SACOL0676) was overexpressed both in the cellular and in the extracellular fractions of the knock-out mutant, but no overproduction was found upon inhibition of Rho with bicyclomycin (224). Bicyclomycin inhibits the function of transcription termination of Rho by interfering with its ATPase activity and impacts the capacity of Rho to reach and dissociate the RNA polymerase from its DNA template (272).

This data showed that the overproduction of the SACOL0676 protein is triggered by a specific cellular activity of Rho other than its role as transcription terminator.

Curiously, these works only refer to SACOL0676, and never to SACOL0677, which may be due to the databases annotation that consider the presence of a single gene (SAOUHSC_00622) for the strain NCTC8325 and of two genes (SACOL0676 and SACOL0677) in the same nucleotide sequence for COL, according to different ATG codons considered by different algorithm predictions.

In this chapter we aim to understand the function of the SACOL0677-0676 genes in order to reveal the mechanism through which the overexpression of these genes, triggered by *rho* impairment, were related with the capacity of *S. aureus* to resist to an otherwise lethal cell wall damage.

Several approaches were followed in parallel attempting to unveil the function of these proteins. We have first addressed the discordant database annotation to understand whether one or two proteins are translated from the same nucleotide sequence. We tested the physical interaction between SACOL0677 and SACOL0676; we addressed the effect of the overexpression of SACOL0677-0676 and of its deletion on *S. aureus* growth and resistance to antibiotics, and also the effect of the inhibition of SACOL0675 in the absence and in the presence of antibiotic challenge. We also performed preliminary studies on the structural elucidation of SACOL0676 by NMR and explored the possibility of protein-DNA interactions using electrophoretic mobility shift assays.

3.2. Materials and Methods

3.2.1. Bacterial strains and growth conditions

The bacterial strains used in this study are listed in Table 3.1. *S. aureus* strains were grown at 37°C with aeration in tryptic soy broth or agar (TSB/TSA) (Difco Laboratories, Detroit, MI, USA). *E. coli* strains were grown at 37°C with aeration in lysogeny broth or agar (LB/LA) (Difco). Antibiotics erythromycin (10 μg/ml), ampicillin (50 μg/ml and 100 μg/ml), neomycin (50 μg/ml), kanamycin (30 μg/ml and 50 μg/ml) and inducers isopropyl β-D-1-thiogalactopyranoside IPTG (100 μM and 1 mM) and $CdCl_2$ (1 μM) were used as recommended by the manufacturer (Sigma, St. Louis, MO, USA) for the selection, maintenance and induction of *S. aureus* and of *E. coli* strains.

The monitorization of culture growth was performed in 96 well plates with a volume of culture of 200 μL per well with agitation at 37ºC and the OD at 620nm was measured at discrete time points (10 min intervals) with a SpectraMax190 Absorbance Plate Reader (Molecular Devices, San Jose, CA, USA).

3.2.2. DNA manipulation methods

DNA manipulation was performed using standard methods. FastDigest and non-fast digest restriction enzymes were used as recommended by the manufacturer (Thermo Fisher Scientific, Waltham, MA, USA) and Routine PCR amplification was performed with NZYTaq DNA polymerase (NZYTech, Lumiar, Portugal). Amplification of DNA fragments for cloning purposes was performed with Phusion High Fidelity DNA polymerase (Thermo Fisher Scientific) following the manufacturer's instructions. PCR and digestion products were purified using NZYGelpure kit (NZYTech). The purification system NZYMiniprep (NZYTech) was used for plasmid extraction from *E. coli* strains. For *S. aureus* stains, the protocol of plasmid extraction included an extra step of incubation of the cells with lysostaphin (10 µg/ml) (Ambi Inc. Los Angeles, CA, USA) at 37ºC for 1 hour. Ligation reactions were performed using T4 DNA Ligase (Thermo Fisher Scientific).

E. coli strain DH5α was transformed as following: ligation mixtures (1:5 molar ratio) of vector and DNA fragment were incubated with DH5α competent cells on ice for 30 min. The cell suspension suffered a heat shock at 42ºC during 90 sec followed by an incubation of 5 min on ice. A volume of 1 ml of fresh LB was added to the suspension and incubated for 1h at 37ºC with agitation. The cells were then plated on LA supplemented with the appropriate antibiotic.

E. coli strain BL21 (DE3) was transformed with 20 ng of the purified plasmid using the same conditions described above. Electroporation of *S. aureus* was performed using a Gene Pulser apparatus (Bio-Rad, CA, USA) following the conditions described in (234).

Transduction was performed with the 80α phage according to the described in (114). Briefly, for the preparation of the phage lysates, the donor strain was grown in Brain-Heart Infusion (BHI, Oxoid, UK) agar slants supplemented with the appropriate antibiotic. The donor culture was collected in TSB and supplemented with $CaCl_2$ (5 mM). The cell suspension was mixed with different phage 80α dilutions and topped off with 3 ml of phage-Top medium supplemented with $CaCl_2$ (5 mM). This mixture was then poured onto phage-Bottom plates and incubated at 30ºC or 37ºC overnight. 2 ml of phage-Buffer were poured onto selected plates, that presented phage-induced lysis, and incubated at 4ºC for 60 min. The phage-Top and phage-Buffer were collected and cleared by sequential centrifugations at 4ºC at 9.000 x *g*. The supernatant was filtered through a 0.45 µm filter and the phage lysate was kept at 4ºC.

For the infection, the recipient strain was grown overnight at 37ºC in BHI agar slants. Recipient culture was thoroughly collected in TSB and supplemented with $CaCl_2$ (5 mM). Cell suspension were mixed with different volumes of transduction lysate and incubated at 30ºC for 20 min with agitation.

These mixtures were topped off with 3 ml of 0.3 GL Top and poured onto 0.3 GL Bottom plates with a bottom-top erythromycin gradient. Transductants were isolated onto TSA plates supplemented with the appropriate antibiotics and incubated at 30ºC or 37ºC until there were no signs of phage contamination.

3.2.3. Construction of SACOL0677, SACOL0676 and SACOL0677- 0676 recombinant proteins

The SACOL0677 gene from COL was amplified using primers p1 and p2 and SACOL0676 gene was amplified using primers p3 and p4 (Table 3.2). The amplified products were purified and digested with NcoI and XhoI restriction enzymes. The pET28a expression vector was also digested with NcoI and XhoI restriction enzymes, and ligated to the PCR product using T4 DNA ligase (New England Biolabs, Ipswich, MA, USA). The restriction sites were chosen to generate SACOL0676-His_6 N-terminal and SACOL0677-His_6 N-terminal fusion proteins.

In order to clone the two genes together originating both C-terminal fusion proteins and N-terminal fusion proteins, a DNA fragment encompassing SACOL0677-SACOL0676 genes was generated in two independent PCR amplification reactions. In one were used the primers p1 and p4 and in the other were used the primers p5 and p6 (Table 3.2). Both amplification products were purified and the first one was digested with NcoI and XhoI restriction enzymes and the second digested with NdeI and XhoI restriction enzymes. Two independent batches of pET28a plasmid were digested with the same combinations of restriction enzymes. The fragments were ligated into pET28a vector using T4 DNA ligase to generate: SACOL0677-0676-His_6 N-terminal and SACOL0677-0676-His_6 C-terminal fusion proteins.

E. coli DH5α was transformed with the ligation mixture and positive transformants were screened by PCR and sequenced. The correct recombinant plasmid was subsequently extracted and used to transform the *E. coli* BL21(DE3) expression host.

3.2.4. Construction of *S. aureus* mutants

3.2.4.1. Construction of SACOL0677, SACOL0676 and SACOL0677-0676 overexpression mutants

The SACOL0677 gene from COL was amplified using primers p13 and p14 (Table 3.2) designed to include BamHI and EcoRI restriction sites, respectively; the SACOL0676 gene from COL was amplified using primers p15 and p16 (Table 3.2) containing SmaI restriction sites. Both genes SACOL0677-SACOL0676 were amplified together using primers p75 and p77 (Table 3.2) designed to include PstI and BamHI restriction sites, respectively. Primers p13 and p15 were designed to include the RBS sequence. The amplified PCR product and the replicative vector pBCB8 were digested with the corresponding restriction enzymes and ligated with T4 DNA ligase.

DH5α competent cells were transformed with the ligation mixture. PCR colony screening and plasmid digestion and sequencing were performed to confirm the correct insertion of the fragment. Plasmid from a positive clone was used to transform electrocompetent cells of *S. aureus* RN4220 by electroporation. Subsequently, the plasmids pBCB8-0676, pBCB8-0677 and pBCB8-0677-0676 were transferred to strain COL by transduction with phage 80α. The plasmid pBCB8-0677-0676 was also transduced to the mutant strain COLspac*murF.*

3.2.4.2. Construction of the *S. aureus* conditional mutant COLpcad0675

The construction of the COLpcad0675 conditional mutant was performed in a two-step procedure. First, the SACOL0675 gene was amplified from COL genome by PCR using primers p106 and p107 (Table 3.2), containing BamHI and EcoRI restriction sites. These were designed to include the native RBS but to exclude its native putative promoter and the transcription terminator. Both the amplification product and pBCB8 vector were digested with BamHI and EcoRI and ligated with T4 DNA ligase. *E.coli* DH5α cells were transformed with the ligation mixture. PCR colony screening, plasmid digestion and sequencing were performed to confirm the correct insertion of the fragment and the construction of plasmid pBCB8-0675.

In a second step, the plasmid pBCB80675 was used as template for the amplification by PCR of the fragment pcad::0675 using primers p105 and p106 (Table 3.2). The upstream region of SACOL0675 (up0675) was amplified from COL by PCR using primers, p103 and p104. The two amplification products were fused together by PCR overlap using primers p103 and p106 generating a 2239 bp fragment. Both the fragment and pMAD thermosensitive vector were digested with EcoRI and NcoI and ligated with T4 DNA ligase. Competent cells of *E. coli* DH5α were transformed to obtain pMADupSACOL0675::pcadSACOL0675 transformants. The absence of point mutations was confirmed by sequencing.

Electrocompetent cells of the *S. aureus* RN4220 strain were transformed with pMADup0675::pcad0675 by electroporation. Subsequently, the plasmids were transferred to strain COL by transduction with phage 80α producing strain COL+ pMADup0675::pcad0675.

The chromosomal integration of pMADup0675::pcad0675 was performed as described by Arnaud and colleagues (273). Briefly, COL+ pMADup0675::pcad0675 was grown overnight at 30ºC on TSB supplemented with erythromycin (10 µg/ml). The overnight culture was diluted 1:1000 in the same medium and incubated at 30ºC for 6 hours with aeration. After incubation, the culture was diluted 1:1000 in fresh TSB medium and grown overnight at 42ºC to promote plasmid integration. The overnight culture was sequentially diluted (10^{-4}, 10^{-5}, 10^{-6}) in TSB and plated on TSA plates supplemented with erythromycin (10 µg/ml) and X-gal (80 µg/ml) and grown overnight at 42ºC. Blue colonies, indicating clones in which pMADup0675::pcad0675 integrated into the chromosome by a single recombination event were selected and restreaked onto new TSA plates supplemented with erythromycin (10 µg/ml) and X-gal (80 µg/ml) and grown overnight at 42ºC.

To promote plasmid excision through the second event of recombination, positive blue clones were grown overnight at 30ºC in TSB with aeration. The overnight culture was diluted 1:500 in the same medium and incubated at 30ºC for 6 hours. After incubation, the culture was sequentially diluted (10^{-3}, 10^{-4}, 10^{-5}) in the same medium and grown overnight at 42ºC on TSA plates supplemented with X-gal (80 µg/ml) to ensure the loss of the excised plasmid.

White colonies, indicating clones which have lost pMADupSACOL0675::pcadSACOL0675, were restreaked onto TSA plates supplemented with X-gal (80 µg/ml) and grown overnight at 42ºC. The same colonies were also restreaked onto TSA + erythromycin (10 µg/ml) plates.

To confirm the excision of pMADup0675::pcad0675 by the second event of homologous recombination, the white colonies that also did not grow on TSA + erythromycin plates were selected. Genomic DNA was extracted and PCR was performed in order to confirm the correct construction of COLpcad0675 conditional mutant.

3.2.4.3. Construction of the *S. aureus* SACOL0677- 0676 deletion mutant

The amplification of a DNA fragment of 931 bp downstream of SACOL0677-0676 operon was performed using primers p18 and p20 (Table 3.2). The amplification of a fragment of 913 bp upstream of SACOL0677-0676 operon was performed using primers p17 and p19 (Table 3.2). Primer p20 was designed to include a BamHI restriction site and p19 to include a NcoI restriction site.

The two fragments were purified and fused together by an overlap PCR using primers p19 and p20 (Table 3.2). The DNA fragment and the pMAD plasmid were digested with NcoI and BamHI restriction enzymes and ligated with T4 DNA ligase. Competent cells of *E. coli* DH5α were transformed with the ligation mixture. PCR colony screening and plasmid sequencing were performed to confirm the correct insertion of the fragment. Electrocompetent cells of *S. aureus* RN4220 were transformed with plasmid from a positive clone by electroporation. Subsequently, the plasmid was transferred to strain COL by transduction with phage 80α generating mutant COL+pMADΔ0677-0676. The subsequent events of integration of the plasmid in the chromosome of COL and the second event of recombination that results in the loss of the plasmid and consequently to the deletion of SACOL0677 and SACOL0676 genes from the chromosome were performed as already described in point 3.2.4.2. regarding the construction of the conditional mutant COLpcad0675.

Table 3.1. List of strains and plamids used in this study

Strain/Plasmid	Description	Source or Reference
E. coli		
DH5α	*recA endA1 gyrA*96 *thi*-1 *hsdR*17 *supE*44 *relA*1 Φ80 Δ*lacZ*ΔM15	Invitrogen
BL21 (DE3)	B F$^-$ *ompT gal dcm lon hsdS$_B$*($r_B^- m_B^-$) λ(DE3 [*lacI lacUV5-T7p07 ind1 sam7 nin5*]) [*malB*$^+$]$_{K-12}$(λ^S)	Novagen
BTH101	F-, *cya-99*, *araD139, galE15, galK16, rpsL1 (Str^r)*, *hsdR2, mcrA1, mcrB1*	Euromedex
BL21(DE3)+pET28a-0677-His$_6$	BL21(DE3) strain expressing SACOL0677-His$_6$	This study
BL21(DE3)+pET28a-0676-His$_6$	BL21(DE3) strain expressing SACOL0676-His$_6$	This study
BL21(DE3)+pET28a-0677-0676-His$_6$	BL21(DE3) strain expressing SACOL0677B-His$_6$	This study
BL21(DE3)+pET28a- His$_6$-0677-0676	BL21(DE3) strain expressing His$_6$-SACOL0677-0676	This study
S. aureus		
COL	Homogeneous Mc^r, Em^s	Rockefeller University
RN4220	Mc^s , restriction negative	R. Novick
F9	COL (*murF*::pRS2), Em^r	(58)
F9H	COL (*murF*::pRS2), Em^r , Homo*	(58)
Overexpression mutants		
COL+pBCB8-0677	COL with SACOL0677 under pcad control in replicative vector pBCB8, Kan^r , Neo^r	This study
COL+pBCB8-0676	COL with SACOL0676 under pcad control in replicative vector pBCB8, Kan^r , Neo^r	This study

COL+pBCB8-0677-0676	COL with SACOL0677B under pcad control in replicative vector pBCB8, Kan^r , Neo^r	This study
COLspac*murF*+pBCB8-0677-0676	COLspac*murF* with SACOL0677-0676 under pcad control in replicative vector pBCB8, Kan^r , Neo^r	This study
Conditional mutant		
COLpcad0675	COL with SACOL0675 placed under pcad control	This study
Deletion mutant		
COLΔ0677-0676	COL deletion mutant for genes SACOL0677 and SACOL0676	This study
Plasmids		
pKNT25	BACTH vector for fusions to the N-terminus of T25, Kan^r	Euromedex
pKT25	BACTH vector for fusions to the C-terminus of T25, Kan^r	Euromedex
pUT18	BACTH vector for fusions to the N-terminus of T18, Amp^r	Euromedex
pUT18C	BACTH vector for fusions to the C-terminus of T18, Amp^r	Euromedex
pKT25-Zip	BACTH vector – Positive control encoding Zip-T25, Kan^r	Euromedex
pUT18C-Zip	BACTH vector – Positive control encoding Zip-T18, Amp^r	Euromedex
pKNT25-0676	pKNT25 vector containing T25-SACOL0676 N-terminal fusion	This study
pUT18-0676	pUT18 vector containing T18-SACOL0676 N-terminal fusion	This study
pKT25-0676	pKNT25 vector containing T25-SACOL0676 C-terminal fusion	This study
pUT18C-*0676*	pKNT25 vector containing T18-SACOL0676 C-terminal fusion	This study
pET28a	Expression vector with T7/lac promoter, N-terminal His-tag, thrombin cleavage site, C-terminal His-tag; Kan^r	Invitrogen
pET28a-0677-His_6	pET28a expressing SACOL0677-His_6	This study
pET28a-0676-His_6	pET28a expressing SACOL0676-His_6	This study
pET28a-0677-0676-His_6	pET28a expressing SACOL0677-SACOL0676-His_6	This study
pET28a-His_6-677-0676	pET28a expressing His_6-SACOL0677-SACOL0676	This study
pBCB8	*S. aureus* replicative vector with pcad inducible promoter, Amp^r, Kan^r	R. Sobral / M. Pinho (unpublished)
pBCB8-0677	pBCB8 vector with SACOL0677 and rbs fused to pcad promoter, Amp^r , Kan^r	This study
pBCB8-0676	pBCB8 vector with SACOL0676 and rbs fused to pcad promoter, Amp^r , Kan^r	This study
pBCB8-0677-0676	pBCB8 vector with SACOL0677-0676 and their rbs fused to pcad promoter, Amp^r , Kan^r	This study
pMAD	*E. coli-S. aureus* shuttle, allelic replacement, thermosensitive origin of replication, Amp^r, Ery^r	(273)
pBCB8-0675	pBCB8 with SACOL0675 under the control of pcad inducible promoter	This study
pMADup0675::pcad0675	pMAD cloned with pcad inducible promoter flanked by SACOL0675, downstream, and the gene's upstream region, upstream	This study
pMADΔ0677-0676	*E.coli-S. aureus* shuttle vector pMAD containing a overlap fragment corresponding to the regions upstream and downstream SACOL0677-0676, excluding SACOL0677-0676 genes	This study

Table 3.2. List of primers used in this study

Primer ID	Sequence 5'→3'	Source or Reference
Bacterial two-hybrid system		
p2H1F	GGGCCTGCAGCATGACTAAAACACTTGAATTAAG	This study
p2H2R	GCGGAATTCCCTTTCTTATCTTCAAATAAAACAG	This study
p2H3F	GGGCTGCAGCATGACTAAAACACTTGAATTAAG	This study
p2H5F	GGGGCTGCAGCGATGACTAAAACACTTGAATTAAG	This study
p2H6R	GGCGAATTCATTTCTTATCTTCAAATAAAACAG	This study
p2H8R	GCGGAATTCCCCTATTTCTTATCTTCAAATAAAACAG	This study
p2H9F	GGGCCTGCAGCATGAGTAAAATAAACCACATCAC	This study
p2H10R	GCGGAATTCCCAATTGATAAAGATTTGATGAGTTCG	This study
p2H11F	GGGCTGCAGCATGAGTAAAATAAACCACATCAC	This study
p2H13F	GGGGCTGCAGCGATGAGTAAAATAAACCACATCAC	This study
p2H14R	GGCGAATTCAAATTGATAAAGATTTGATGAGTTCG	This study
p2H16R	GGGGAATTCTAAATTGATAAAGATTTGATGAGTTCG	This study
SACOL0676, SACOL0677 and SACOL0677-0676 His_6-tag fusions		
p1	GCGCCATGGGTAGTAAAATAAACCACATCAC	This study
p2	GCGCTCGAGAATTGATAAAGATTTGATGAG	This study
p3	GCGCCATGGGTACTAAAACACTTGAATTAAG	This study
p4	GCGCTCGAGTTTCTTATCTTCAAATAAAAC	This study
p5	GCGCATATGAGTAAAATAAACCACATCAC	This study
p6	GCGCTCGAGCTATTTCTTATCTTCAAATAAAAC	This study
SACOL0676, SACOL0677 and SACOL0677-0676 overexpression mutants		
p13	GGGGGGATCCCGATATATAGTGTGAAAGGAGG	This study
p14	GGGGGAATTCGAATATGTCCTCCTGATTAAATTG	This study
p15	GGGGCCCGGGCAGGAGGACATATTCATGAC	This study
p16	GGGGCCCGGGCGCTTTCTTTATATCTATTTC	This study
p75	GCATCCCTGCAGATATATAGTGTGAAAGGAGG	This study
p77	TGCGAAGGATCCTAGACAATCATGATGAAAGTC	This study
Conditional mutant COLpcad0675		
p106	CGGCGGAATTCCAAGTTAAAATGATAAGC	This study
p107	TAAGGATCCTTCTATATCATTGGTGTCC	This study
p103	GCGCCATGGAAGTGTCTTAATCATAGC	This study
p104	AAATACACTTGAATAAGTGCAATATACAACTCATAATG	This study
p105	CATTATGAGTTGTATATTGCACTTATTCAAGTGTATTT	This study
SACOL0677-0676 deletion mutant		
p17	GCGCTTTCTTTATATCTATTTCTTTTTACTCATATTTTAAAACCTCCT	This study
p18	AGGAGGTTTTAAAATATGAGTAAAAAGAAATAGATATAAAGAAAGCGC	This study
p19	CGCGGATCCTGCAGTTTAGCTACTGATGG	This study
p20	CATGCCATGGCCATGCCAAGTATACCGCC	This study
EMSA assays		
p21	CGTTCAGATTTTATCTTGAGC	This study
p22	GTGATGTGGTTTATTTTACTC	This study
p23	CACCCTAGACTTTCATCATG	This study
p24	GGATAGGAATAAGCATTCC	This study
p63	CGGTTCAAAGCATCCATTAA	This study
p85	CACCCGGGAGGTCAGTGACATATGTC	This study

3.2.5. Determination of *S. aureus* oxacillin resistance

Cultures of *S. aureus* were grown in the absence or in the presence of the appropriate concentration of inducer and of antibiotics. An aliquot of the overnight cultures was centrifuged at 5000 x *g* during 2 min and cells were ressupended in the same volume of fresh TSB. The pellets were

washed three times to remove traces of antibiotic and/or inducer. Subsequently, the washed cultures were swabbed on TSA and TSA supplemented with the appropriate concentration of the inducer (as indicated) and oxacillin diffusion disks (1mg) were placed on the plates. After an incubation of 48 hours at 37°C the growth inhibition halos were measured.

3.2.6. Bacterial two-hybrid system

The bacterial adenylate cyclase two-hybrid (BACTH) system was used (Euromedex) (274). This system includes four plasmids: pUT18, pUT18C, pKNT25 and pKT25, that enable fusions to the N- or C-terminus of T18 or T25 fragments of the catalytic domain of adenylate cyclase (CyaA) from *Bordetella pertussis.*

The SACOL0677 and SACOL0676 genes were amplified by PCR with the primers listed (Table 3.2) and cloned into the pUT18C, pUT18, pKNT25 and pKT25 vectors using the EcoRI and PstI restriction enzymes (Table 3.1).

The correct sequence of all the DNA fragments cloned was determined by DNA sequencing.
Adenylate cyclase (Cya)-deficient *E. coli* BTH101 $CaCl_2$-competent cells were co-transformed with plasmids expressing the different T18 and T25 hybrid proteins. Co-transformants were selected on LA plates supplemented with Ampicillin (100 μg/ml) and Kanamycin (50 μg/ml), grown at 30 °C, and three representative colonies were isolated for further experiments to exclude clone-by-clone variation. The strain BTH101 co-transformed with plasmids pUT18C-zip and pKT25-zip encoding two leucine zipper domains that strongly interact was used as positive control.

To test the interactions, co-transformants were grown overnight at 30ºC in LA medium supplemented with IPTG (0.5 mM), ampicillin (100 μg/ml), kanamycin (50 μg/ml) and the chromogenic substrate 5-bromo-4-chloro-indolyl-β-D-galactoside (X-gal; 40 μg/ml). Additionally, the same co-transformants were streaked on MacConkey agar supplemented with maltose (1 %), IPTG (0.5 mM), X-gal (40 μg/ml), ampicillin (100 μg/ml) and kanamycin (50 μg/ml). Plates were incubated at 30ºC for 48 hours. Development of blue colonies on LA-X-gal plates and pink colonies on MacConkey-maltose plates indicated protein-protein interaction.

3.2.7.SACOL0676 Electrophoretic mobility shift assays (EMSA)

DNA fragments encompassing the putative promoter regions of the SACOL0677-0676 operon and of SACOL0675 were amplified by PCR using the pair of primers p21 and p22 (258 bp) and the pair p23 and p24 (208 bp) respectively (Table 3.2). An internal fragment of *pheS* gene was amplified using p63 and p85 (353 bp). Increasing concentrations of the recombinant protein SACOL0676-His_6 were incubated with 100 ng of the DNA fragments in 1x EMSA Buffer (10 mM Tris HCl (pH 8.0) 150 mM KCl, 5mM EDTA, 0.1% Triton X-100 and 12.5% glycerol) for 30 min at room temperature. The samples were loaded onto a 1% agarose gel in the presence of GreenSafe (NZYTech) DNA intercalator following the manufacturer's recommendations, and 100V were applied for 30 min.

3.2.8. Overproduction and purification of SACOL0676, SACOL0677 and SACOL0677-0676 recombinant proteins

Overnight cultures of BL21(DE3)+pET28a-0677-His_6, BL21(DE3)+pET28a-0676-His_6 and BL21(DE3)+pET28a-0677-0676-His_6 in LB supplemented with kanamycin (30 µg/ml), was used to inoculate 500 ml of LB supplemented with antibiotic. Growth was carried out at 37ºC to an OD_{600}=0.7. At this point, IPTG was added to 1mM and the culture was grown for four additional hours. Cells were harvested and the pellets were resuspended in phosphate buffer pH7.0 (0.1 M), guanidinium chloride (GndHCl) (3 M) (Fisher BioReagents, Pittsburgh, Pennsylvania, USA) to improve the protein yield in the soluble fraction. The cell suspensions were sonicated on ice at 80% amplitude and 0.5 cycle with 1 minu cycles, for 10 times, using a Hielscher UP200S Ultrasonic Lab Homogenizer and a S3 sonotrode (Teltow, Germany). The sonicated solutions were centrifuged at 20000 x *g* at 4ºC for 1 hour. The supernatant was purified in a 5 ml-HisTrap column (GE Healthcare Life Sciences, USA) following the manufacturer's instructions. Briefly, the elution of the proteins was accomplished by a discountinuous gradient of 40, 100, 200 and 400 mM imidazole in phosphate buffer pH 7.0 (0.1 M). A sample of each fraction was analysed by SDS-PAGE. Fractions containing recombinant protein almost without the presence of contaminants were pooled and dialyzed using SnakeSkin dialysis tubing, 3.5K MWCO against phosphate buffer pH 7.0 (0.1 M) at 4ºC, overnight. Protein concentration was determined using Pierce BCA Protein Assay Kit (ThermoFisher Scientific).

3.2.9. Overproduction and purification of SACOL0676-His_6 for NMR assays

The overeproduction and purification of SACOL0676-His_6 for NMR assays was performed as following: the *E. coli* BL21(DE3) + pET28a-0676-His_6 was grown in 2 L of ^{15}N-labelled M9 minimal medium with $^{15}NH_4Cl$ at 37ºC with aeration to an OD_{600} = 0.7. At this time IPTG (isopropyl-β-D-thiogalactopyranoside) was added to 1mM and the culture was grown for four additional hours. Cells were harvested and the pellets were resuspended in 30 ml of phosphate buffer pH7.0 (0.1M), guanidinium chloride (GndHCl) (3M) (Fisher BioReagents, Pittsburgh, Pennsylvania, USA). The suspensions were sonicated on ice at 80% amplitude and 0.5 cycle with 1min cycles 10 times using a Hielscher UP200S Ultrasonic Lab Homogenizer and a S3 sonotrode. The sonicated solutions were centrifuged at 20000 x *g* at 4ºC for 1 hour. The supernatants were purified using an ÄKTA Start chromatography system (GE Healthcare) and a HisTrap HP 5ml column (GE Healthcare). Elution was performed at a flow rate of 4 ml/min with phosphate buffer pH 7.0 (0.1 M), GndHCl 3 M and phosphate buffer pH 7.0 (0.1 M), 1 M Imidazole. The elution gradient performed was 0.75 M GndHCl vs 0.75 M Imidazole during 47.5 ml and 1 M Imidazole during 17.5 ml. Absorbance was detected at 280nm. Protein fractions were purified on a HiTrap 5ml desalting linked columns (GE Healthcare) in an ÄKTA Start chromatography system. The desalting was done against water. The desalted elution fractions were analyzed by SDS-PAGE. The desalted samples were frozen (-80ºC) and freeze-dried.

The freeze-dried eluted fractions were resuspended in 5 ml MQ water and purified by size-exclusion chromatography in a GE Healthcare Superdex™ 75 10/300 GL column using an Amersham

Pharmacia Biotec FPLC with a UV-900 unit (Buckinghamshire, United Kingdom). Absorbance values were monitored at 220 nm and 280 nm. Elution was performed at a flow rate of 0.5 ml/min with 0.1 M sodium phosphate, pH 7.0. The eluted fractions were analyzed by SDS-PAGE.

Protein concentration was determined using Pierce BCA Protein Assay Kit (ThermoFisher Scientific).

3.2.10. SACOL0676-His_6 protein NMR analysis in the presence of membrane mimetics

Protein ^{1}H-^{15}N HSQC spectra were acquired in the absence and in the presence of four different membrane mimetics: Sodium dodecyl sulphate (SDS), Triton X-100, 2,2,2 – Trifluoroethanol-*d2* (TFE) and Tween 20.

The protein stock (130.56 µM) was diluted to a final volume of 500 µL in the appropriate buffer with 10% D_2O and the respective detergent, yielding final concentrations of 14.2 µM of SACOL0676-His_6 protein and of the following of detergents: 0.1 g/ml Triton X-100 (Fischer Scientific, Loughborough, UK), 0.1 g/ml Tween20 (Sigma-Aldrich, St. Louis, MO, USA) and 50% (v/v) TFE. The spectra obtained in the presence of SDS were acquired under the same conditions but with two different concentrations of detergent (5 mM and 20 mM).

All NMR data was acquired using a Bruker AVANCE II 600MHz NMR equipped with a cryoprobe and processed using TopSpin.

3.3. Results

In the Chapter 2 of this dissertation it was identified, by transcriptomic analysis, an unknown system of *S. aureus*, constituted by SACOL0677, SACOL0676 and SACOL0675 genes, whose expression was highly up-regulated in a cell wall mutant. The up-regulation of SACOL0676 and SACOL0677 was triggered by the impairment of *rho* gene and is thought to be involved in the response of bacteria in dealing with a damage that can be lethal. In Chapter 3, we aimed to further characterize this system in order to understand its role in a cell facing a severe damage.

3.3.1. Identification of SACOL0677 and SACOL0676 by mass spectometry

The search for information about these ORFs in the databases demonstrated that according to different ORF analysis algorithms, discordant predictions were obtained for the same DNA sequence.

Depending on the initiation codon considered, for the *S. aureus* strains NEWMAN and NCTC8325, one single ORF was predicted, resulting in a protein with an estimated molecular weight of 12.7 KDa and for the *S. aureus* strains COL, MU50, MW2, N315, USA300 and MRSA 252, two ORFs were predicted, resulting in two proteins of estimated molecular weight values of 8.2 KDa and 7.6 KDa (Fig. 3.1).

This data raised the question whether this DNA sequence would originate a single protein, two independent proteins or even a regulatory RNA. To determine if the ORFs are indeed translated, crude

extracts of COL and mutant F9 were prepared and separated in denaturing conditions. In this assay, two bands corresponding to proteins with molecular weight values of approximately 12 and 7 KDa, values in agreement to the ones of the proteins that might be translated, were identified as overexpressed in the F9 mutant (Fig. 3.2, Box 1 and Box 2). The bands were excised from the gel and analysed by mass spectrometry. While the 12 KDa protein corresponded to the DNA-binding protein HU, the 7 KDa band retrieved a mixture of peptides encompassing the amino-acid sequence of both SACOL0677 and SACOL0676 proteins, indicating that the ORFs generate two independent proteins of 7.6 and 8.2 KDa respectively.

The retrieved sequence of peptides was not compatible with the translation of one single protein. The results showed that two independent proteins were indeed translated from the DNA sequence analysed.

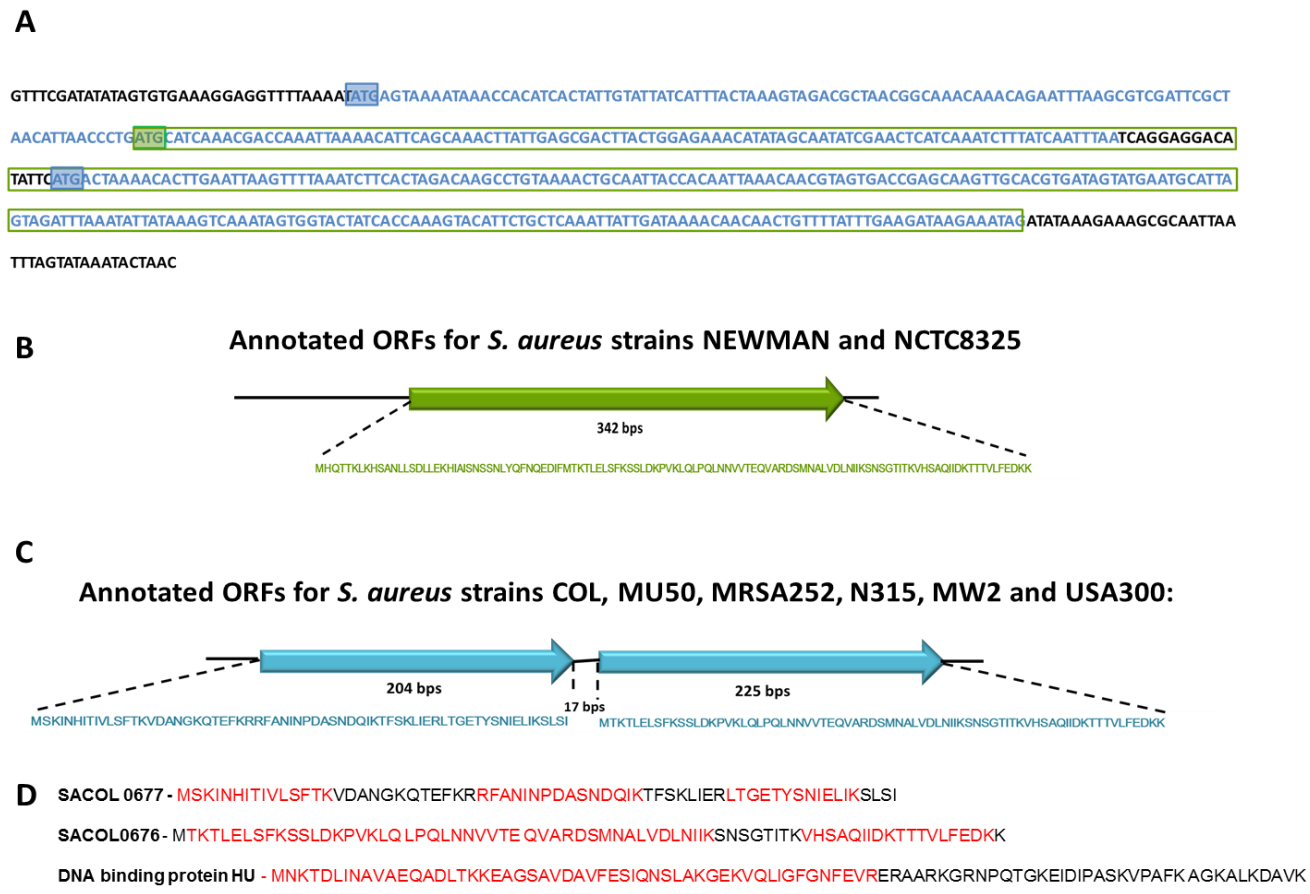

Fig. 3.2. Representation of the different algorithm predictions used for the translation of the DNA sequencing encompassing SACOL0676 and SACOL0677 in different *S. aureus* strains. A) DNA sequencing of the genomic region encompassing SACOL0676 and ScwA in all *S. aureus* strains analysed. In blue are represented both the ATG codons considered in the translation of two independent proteins. In green is represented the ATG codon considered in the translation of one single protein. **B)** Protein translated from the ATG considered in green and indication of the strains for which this translation was predicted. **C)** Proteins translated from the ATGs considered in blue and indication of the strains for which this translation was predicted. **D)** Peptides identified by mass spectrometry analysis are highlighted in red.

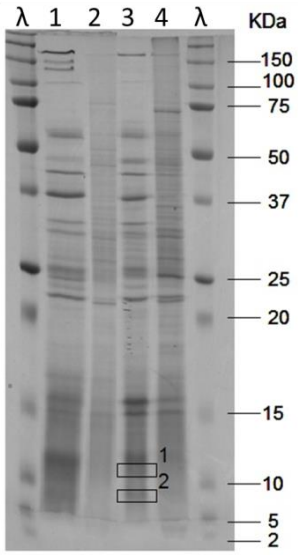

Fig. 3.2. COL and F9 crude extracts separated by SDS-PAGE. SDS-PAGE midi-gel of crude extracts of COL and F9 mutant. 1- COL cytoplasmic fraction, 2- COL pellet fraction, 3- F9 cytoplasmic fraction, 4- F9 pellet fraction. λ- Dual Xtra protein ladder (BioRad). Box 1 - band of ≈ 12KDa protein excised and analysed by mass spectrometry. Box 2 – band of ≈ 7 KDa protein excised and analysed by mass spectrometry.

3.3.2. *In silico* analysis of SACOL0677 and SACOL0676

In the former TIGR-CMR and in NCBI databases, SACOL0677 (204 bp) and SACOL0676 (225 bp) genes were unannotated and no functions were assigned to the respective proteins (protein of unknown function). The two genes are exclusive of staphylococcal species.

The most significant results obtained using the Blastp algorithm were of 40% amino acid identity of SACOL0677 with part of diguanilate cyclase from *Thermosipho melanesiensis* (with 305 residues) (Fig. 3.3, A), corresponding to a low complexity region and of 48% identity of SACOL0676 with a chemotaxis sensory transducer from *Synechococcus* sp (with 142 residues) (Fig. 3.3, B).

Diguanylate cyclase is an enzyme responsible for the synthesis of cyclic di-3',5'-guanylate (cyclic di-GMP) from two molecules of guanosine triphosphate (GTP). Cyclic di-GMP is a signaling molecule that acts on several physiological roles such as motility, virulence, biofilm formation and cell cycle progression (275).

A

```
CLUSTAL 2.1 multiple sequence alignment

SACOL0677       ------------------------------------------------------------
A6LL54_THEM4    MYNSGRLVENPNLANFITSEEYKIFDFSFFTVVPKSLFLKPLYTIIFFTVFLLMIFIVIS 60

SACOL0677       --MSKINHITIVLSFTKVDANGKQTEFKRRFANINPDASNDQIKTFSKLIERLTG--ETY 56
A6LL54_THEM4    YFVSRYITNRITVSLRKLSENMKKFE-KKEFKNINVDGFEDEIKTFLKVYNDVANELERY 119
                  :*:     *.:*: *:. * *: * *:.* *** *. :*:**** *: : ::.  * *

SACOL0677       SN------------IEL----IKSLSI-------------------------------- 67
A6LL54_THEM4    VENTELIIKNKTREIEIKNEKLRELSIKDELTGLYNRRFFNESFPKDCSLAFREKMYVNF 179
                 :            **:    ::.***

SACOL0677       ------------------------------------------------------------
A6LL54_THEM4    AIIDLDDFKVINDTYGHQAGDECLRVFSKMFKESFHRESDKYFRYGGEEFVVYYISKEKT 239

SACOL0677       ------------------------------------------------------------
A6LL54_THEM4    NFFEKLEKFRKEVERHILEYNGEKITFTISIGVVEEKQETSRYQDIISKADKNLYIAKNK 299

SACOL0677       ------
A6LL54_THEM4    GKNIVV 305
```

B

```
SACOL0676       ---------------------------------------------MTKTLELSFKSSL 13
Syncc9605_1536  MVACCGDRFTLTCLCLAEPIRRAGVGAATTEEEGLELVLRHKPSLLICTSDLETGYGMNL 60
                                                             *. ** .:  .*

SACOL0676       DKPVKLQLPQLNNVVT-----EQVARDSMNALVDLNIIKS--NSGTITKVHSAQIIDKTT 66
Syncc9605_1536  LRRVKAELPTCQLLIVLVRETQAVVQEAMQAYADAVIFKSSLGIGKGDFVQALQTLSEGG 120
                 : ** :**  : ::.     : *.:::*:* .*  *:**  .:*.   *:: * :.:

SACOL0676       TVLFEDKK-------------- 74
Syncc9605_1536  VYLPEEIRQLGAAQAPNPTCRR 142
                . * *: :
```

Fig. 3.3. Protein sequence alignments of SACOL 06767 and SACOL0676. A) SACOL0677 shares 40% of amino acid identity with diguanylate cyclase of *Thermosipho melanesiensis,* uniprot accession number A6LL54_THEM4 and **B)** SACOL0676 shares 48% of amino acid identity with a response regulator receiver domain protein (CheY-like), uniprot accession numer Q3AJE7_SYNSC. Alignments were performed using CLUSTAL 2.1 multiple sequence alignment.

3.3.3. Analysis of SACOL0677 and SACOL0676 protein interaction

The physical proximity of the genes, their putative organization as a transcriptional unit and the fact that both proteins are produced in response to the same trigger, suggests a functional relation between SACOL0677 and SACOL0676 that may depend on a physical interaction between them. To determine if the two proteins interact, forming a protein complex, SACOL0677-SACOL0676, two strategies were followed: co-purification assays and *in vivo* bacterial two-hybrid assay (BACTH system).

3.3.3.1. Co-purification assays

The two genes, SACOL0677-0676 were amplified from COL genome and cloned as a co-expression system in the expression vector pET28a, using the *E. coli* BL21(DE3) strain as expression host resulting in plasmid pET28a-0677-0676-His_6-tag, that allowed the production of recombinant proteins SACOL0677-SACOL0676, in which only SACOL0676 is fused to a His_6-tag. Cultures of

BL21(DE3)+pET28a-0677-0676-His_6-tag were grown in LB+Km (30 μg/ml), supplemented with IPTG (1 mM) and were purified by affinity chromatography with Ni-Nta resin.

The eluted fractions were analysed by SDS-PAGE and only one protein band of low molecular weight was observed (Fig. 3.4). Since the two proteins, SACOL0677 and SACOL0676, have very similar predicted molecular sizes (8.7 and 9.3 KDa including the His_6-tag), the band was extracted from the gel and analysed by Mass Spectrometry. This analysis retrieved a mixture of peptides that encompasses only the protein sequence of SACOL0676, the protein fused to the His_6-tag. This result suggests that the two proteins do not physically interact in the conditions tested. An alternative explanation for this result is that SACOL0676-His_6 may not be correctly folded preventing the bind of SACOL0677.

The co-purification assay was also performed with SACOL0677 fused to a His_6-tag and the result obtained also indicated lack of interaction (data not shown).

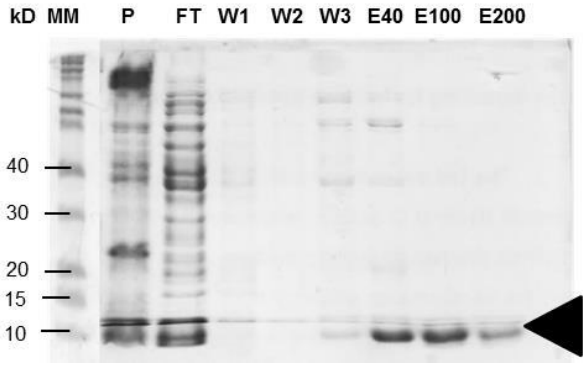

Fig. 3.4. SDS-PAGE of pET28a-0677-0676-His_6 tag proteins purification. SDS-PAGE (Tris-glycine buffer) of the eluted fractions of the pET28a-0677-0676-His_6 tag protein purification of Ni-NTA purification of *E. coli* + pET28a-0677-0676-His_6 tag protein extracts. MM-Novex sharp unstained protein standard; P-Pellet fraction; FT-Flowtrough; W1, W2 and W3- Washes 1, 2 and 3; E40 - Elution with 40mM Imidazol buffer; E100 - Elution with 100mM Imidazol buffer; E200 - Elution with 200mM Imidazol buffer. Black triangle indicates the bands analysed by mass spectrometry.

3.3.3.2. *In vivo* bacterial two hybrid assays (BACTH system)

The fact that no interaction was observed through the co-purification assays may be due to the specific conditions used in this in vitro assay, however, a negative result must not rule out completely the possibility of a physical interaction between the two proteins.

The Bacterial Two Hybrid system (BACTH) relies in the *in vivo* reconstitution of the two subunits, T18 and T25, of the catalytic domain of adenylate cyclase of *Bordetella pertussis*. For the adenylate cyclase to be functional, its two subunits, T25 and T18, need to be in physical proximity. In an *E. coli* strain defective for the production of adenylate cyclase (*cya- E. coli* BTH101 strain), a plasmid containing one subunit of adenylate cyclase fused to one of the proteins of interest is co-transformed with another plasmid containing the counterpart subunit fused to the second protein under test. If the two proteins physically interact, the two subunits T25 and T18 become in close proximity and cAMP is produced. The cAMP bound to the catabolite activator protein CAP is a pleiotropic transcriptional

regulator in *E. coli* that activates the transcription of several genes, including genes involved in lactose and maltose catabolism.

The capacity to utilize maltose and lactose as the unique carbon sources allows positive clones to be distinguished on indicator media supplemented with X-Gal (color blue develops) or on MacConkey maltose media (color pink develops).

The SACOL0677 and SACOL0676 genes were amplified from the *S. aureus* COL strain and were cloned in frame with the T25 and T18 adenylate cyclase subunits in the pT25 (pKNT25 and pKT25) and pT18 (pUT18 and pUT18C) vectors, both as N- or C-terminal fusions, respectively. The *E. coli* BTH101 strains were co-transformed with two plasmids, each one expressing the different T18 and T25 hybrid proteins in all possible combinations (Table 3.3). To screen for adenylate cyclase activity, all co-transformants were grown in indicator media LA-X-Gal and MacConkey-Maltose.

The positive control used was strain BTH101 co-transformed with plasmids pUT18C-zip and pKT25-zip, encoding two leucine zipper domains that strongly interact. The positive reaction was observed as development of intense pink colour on MacConkey maltose plates (Fig. 3.5).

Development of pink colour was only observed for the positive control of interaction, BTH101 co-transformed with pUT18C-zip and pKT25-zip, and for no other co-transformant (Fig. 3.5). The results of *In vivo* bacterial two-hybrid system technique indicated that SACOL0677 and SACOL0676 do not physically interact in the specific conditions tested.

Table 3.3. Constructed and assayed *E.coli* BTH101 co-transformants. The plasmid, the partner protein, the relative position of the fusion to the subunit of adenylate cyclase and the vector used in the construction of each plasmid is indicated for each co-transformant.

Co-transformant	Plasmid 1			Plasmid 2		
	Protein	Fusion	Vector	Protein	Fusion	Vector
AxF	SACOL0676	N- terminal	pKNT25	SACOL0677	N- terminal	pUT18
BxE	SACOL0676	N- terminal	pUT18	SACOL0677	N- terminal	pKNT25
CxH	SACOL0676	C- terminal	pKT25	SACOL0677	C- terminal	pUT18C
DxG	SACOL0676	C- terminal	pUT18C	SACOL0677	C- terminal	pKT25
AxH	SACOL0676	N- terminal	pKNT25	SACOL0677	C- terminal	pUT18C
BxG	SACOL0676	N- terminal	pUT18	SACOL0677	C- terminal	pKT25
CxF	SACOL0676	C- terminal	pKT25	SACOL0677	N- terminal	pUT18
DxE	SACOL0676	C- terminal	pUT18C	SACOL0677	N- terminal	pKNT25

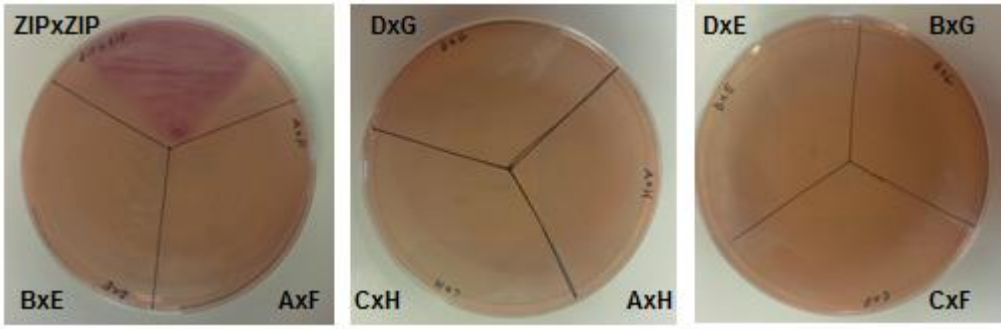

Fig. 3.5. MacConkey/maltose plates obtained after plating *E. coli* BTH101 co-transformants. Zip-Zip is the positive control that corresponds to the *E. coli* BTH101 co-transformed with pUT18C-zip and pKT25-zip plasmids. The other combinations correspond to all co-transformants constructed, listed in Table 3.3, to test the physical interaction between SACOL0677 and SACOL0676 proteins.

3.3.4. Impact of the overexpression of SACOL0677 and SACOL0676 proteins in growth of *S. aureus*

Although no physical interaction between the proteins was observed, SACOL0677 and SACOL0676 are most probably functionally related, due to their relative location and transcriptional pattern in the mutants F9 and F9H. In these mutants the massive overexpression of these two proteins may play a role in maintaining the fitness of a cell with a cell wall damage that, according to other mutants, impairs its growth. To identify the function of these proteins we adopted a strategy of expression modulation *in vivo*.

To address the individual and cumulative effects of the overexpression of the ORFs in the growth of the parental strain COL, two different strategies were followed: the overexpression of both ORFs under the control of the inducible pcad promoter from a replicative plasmid pBCB8, COL+pBCB8-0677-0676; and the overexpression of each ORF independently through the construction of two *S. aureus* overexpression mutants, COL+pBCB8-0677 and COL+pBCB8-0676, in which SACOL0677 and SACOL0676 are independently overexpressed.

Cultures of the mutants were grown in the presence of different concentrations of the inducer, $CdCl_2$ (from 0 to 1 µM) and the OD_{620nm} was monitored along time. As controls, the parental strain COL and the control strain COL+pBCB8 with the empty vector were grown in the same conditions (Fig. 3.6).

In the absence of inducer, the overexpression strain showed a growth rate lower than the growth rate of the parental strain COL but equivalent to the control strain COL+pBCB8, indicating that this decrease in the growth rate is due to the presence of pBCB8 plasmid and of antibiotic in the medium.

In the presence of increasing concentrations of inducer, the increasing overexpression of both SACOL0677 and SACOL0676 genes led to a continuous and consistent decrease in the growth rate.

A similar effect, although less pronounced, was obtained for the independent overexpression of the proteins (Fig. 3.6). Additionally, it was observed that the overexpression of both proteins resulted in an extension of the lag phase and that it was also more pronounced when both ORFs were overexpressed. These results showed a synergistic effect between both proteins in decreasing the growth rate and increasing the lag phase of COL strain. These results suggest that the overexpression

of SACOL0677 and SACOL0676 proteins contribute to the decrease of the fitness of the cell in the absence of cell wall damage.

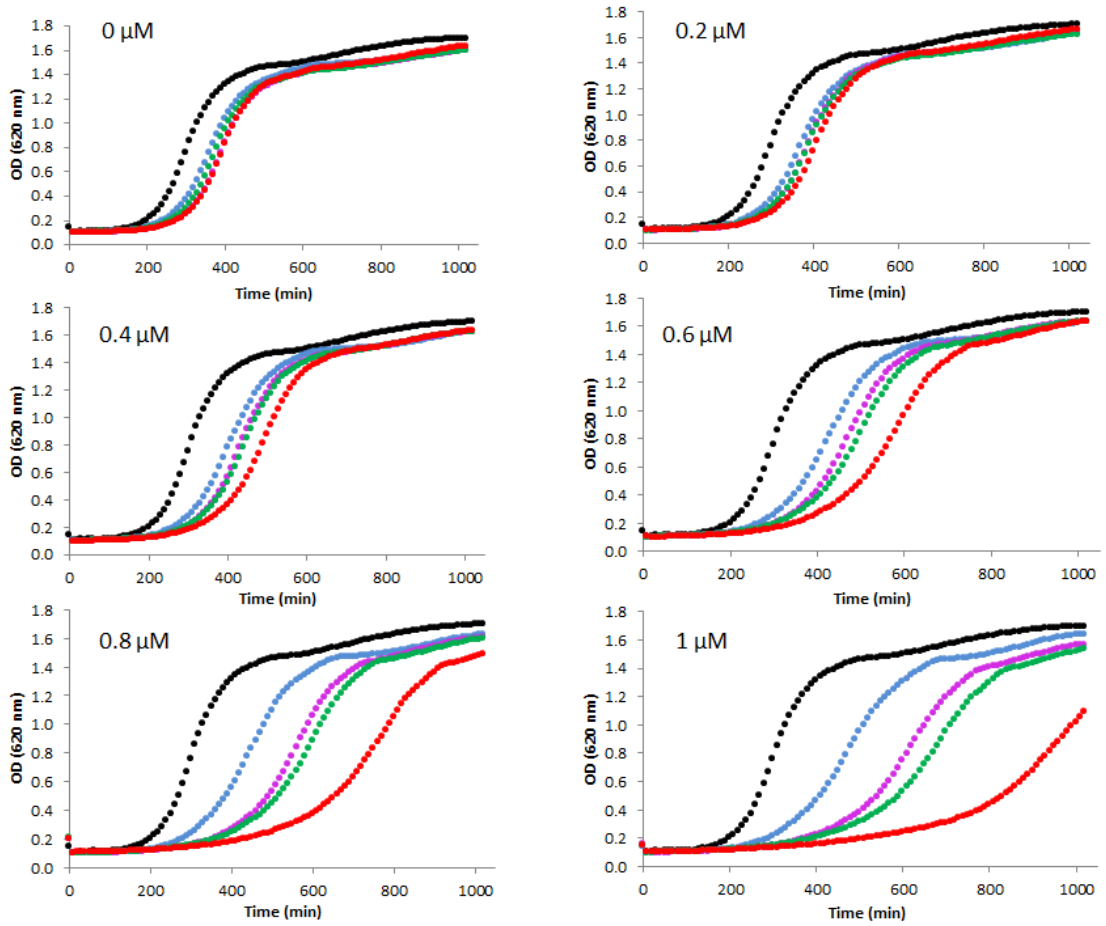

Fig. 3.6. Growth curves of SACOL0676, SACOL0677 and SACOL0677-0676 overexpression mutants. Growth curves for the parental strain COL (●); COL+pBCB8 (●), COL+pBCB8-0677 (●), COL+pBCB8-0676 (●) and COL+pBCB8-0677-0676 (●) in the presence of different concentrations of cadmium inducer.

3.3.5. Impact of the overexpression of SACOL0677 and SACOL0676 proteins in growth in the presence of a cell wall damage

One hypothesis for the negative impact of the overexpression of SACOL0677 and SACOL0676 on growth could be related with the absence of cell wall damage in COL. To verify whether the overexpression of the proteins is related with an increase in the fitness of the cell only in a situation of cell wall stress, the overexpression of SACOL0677 and SACOL0676 was performed for the conditional mutant COLspac*murF*, in the presence of a sub-inhibitory concentration of the inducer (5 µM IPTG). At this inducer concentration, the mutant is viable although it presents a decreased growth rate and incorporation of abnormal tripeptide in the cell wall (60). The overexpression mutant COLspac*murF* + pBCB8-0677-0676 was constructed and growth was monitored in the presence of a sub-optimal

concentration of IPTG (inducer of *murF* expression) and increasing concentrations of the $CdCl_2$ (inducer of SACOL0677 and SACOL0676 expression) (Fig. 3.7).

The results confirmed that, upon *murF* inhibition (Fig. 3.7 – grey curve), the growth rate and the value of optical density reached in stationary phase were negatively affected. An equivalent growth profile was obtained with the replicative vector pBCB8-0677-0676 without the induction of the SACOL0677 and SACOL0676 genes (Fig. 3.7 - light blue). As these genes are moderately induced, in the presence of 0.2 and 0.4 µM of $CdCl_2$ (Fig 3.7 – light green and blue curves, respectively), the lag phase increased but the culture attained higher values of optical density in stationary phase, in comparison with the mutant in the absence of the expression of the two genes. For 0.6 µM of $CdCl_2$ (Fig.3.7 – dark green curve), the strain presented a highly increased lag phase. For the higher concentrations of inducer 0.8 and 1 µM of $CdCl_2$ (Fig.3.7 – pink and red curves, respectively), the growth of the strain was totally abolished.

The results showed that for lower amounts of overexpression, the impact in the stationary phase was positive, which must be further addressed in the future, however, with higher overexpression, the impact on growth is negative or even lethal.

The results suggest that the overexpression of SACOL0677 and SACOL0676 must be related with the F9 specific impairment.

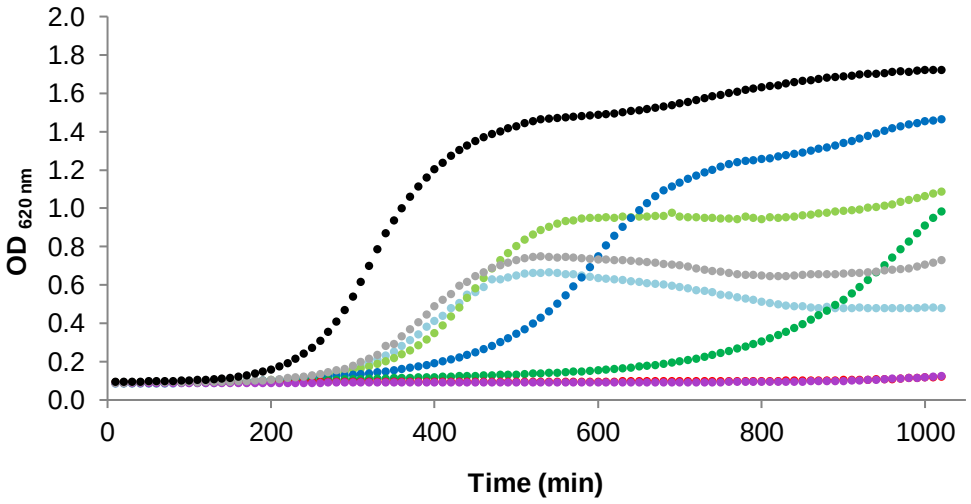

Fig. 3.7. Growth curves of COLspac*murF*+pBCB8-0677-0676 overexpression mutant. Growth curves of COLspac*murF*+pBCB8-0677-0676 (100 mM IPTG - optimal concentration) (●); COLspac*murF* (5 mM IPTG – sub-optimal concentration) (●), COLspac*murF* + pBCB8-0677-0676 (5mM IPTG + 0 µM $CdCl_2$) (●), COLspac*murF* + pBCB8-0677-0676 (5 mM IPTG + 0.2 µM $CdCl_2$) (●), COLspac*murF* + pBCB8-0677-0676 (5 mM IPTG + 0.4 µM $CdCl_2$) (●), COLspac*murF* + pBCB8-0677-0676 (5 mM IPTG + 0.6 µM $CdCl_2$) (●), COLspac*murF* + pBCB8-0677-0676 (5 mM IPTG + 0.8 µM $CdCl_2$) (●) and COLspac*murF* + pBCB8-0677-0676 (5 mM IPTG + 1 µM $CdCl_2$) (●).

3.3.6. Impact of the overexpression of SACOL0677 and SACOL0676 proteins in oxacillin resistance

The overexpression of SACOL0677 and SACOL0676 was observed in a mutant with decreased resistance to oxacillin which suggested that the two genes could be related with the observed phenotype of resistance. To address this question, the overexpression mutants in COL were tested for oxacillin resistance upon induction with 1 μM of $CdCl_2$ (Fig. 3.8) by disk diffusion.

The result showed that the overexpression of both SACOL0677 and SACOL0676, together, promoted the decrease in resistance to β-lactams. The independent overexpression of a single protein, alone, did not impact the resistance to oxacillin of the strain.

The results allowed to conclude that not only SACOL0677 and SACOL0676 were related with resistance to β-lactams in this mutant, as also the two proteins must functionally interact to promote this phenotype of decreased resistance.

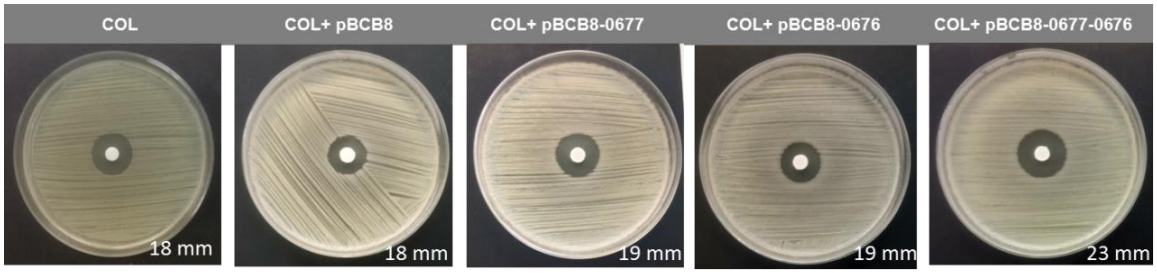

Fig. 3.8. Growth inhibition halos of SACOL0677-76 overexpression mutants. Growth inhibition halos for oxacillin (1 mg) obtained by disk diffusion for strain COL, the control COL+pBCB8 and the overexpression mutants COL+pBCB8-0677, COL+pBCB8-0676, COL+pBCB8-0677-0676. The values presented correspond to the diameter in mm. All the growth inhibition halos of the mutants were performed in the presence of 1 μM of $CdCl_2$.

3.3.7. Impact of the absence of SACOL0677 and SACOL0676 on growth

A complementary strategy to the overexpression of SACOL0677 and SACOL0676, adopted to characterize the role of the two genes, was to abolish their expression in the chromosome and observe the phenotype of the mutant responding to their absence.

A knock-out mutant for both genes, COLΔ0676-0677, was constructed using the allelic replacement vector pMAD. The impact of the abolishment of the genes was assessed by the monitorization of the OD_{620nm} along time. The growth curve obtained was coincident with the one of the parental strain COL showing that SACOL0677 and SACOL0676 genes are not essential and that their absence does not affect the growth of *S. aureus* in normal laboratory conditions (Fig. 3.9).

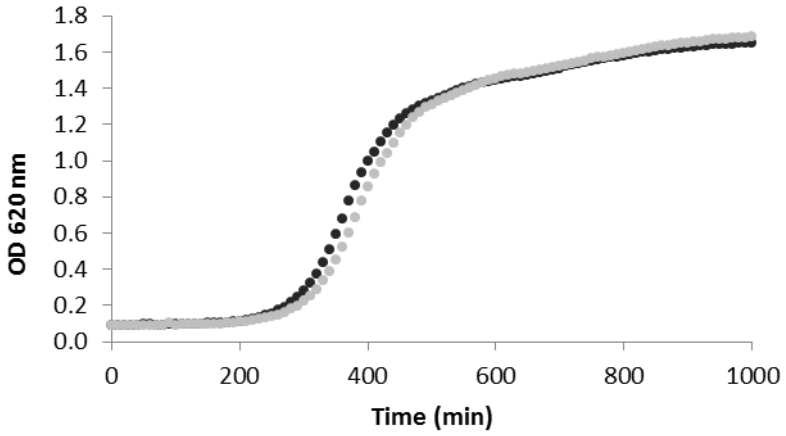

Fig. 3.9. Growth curve of the SACOL0677-0676 deletion mutant. Growth curves of COL (●) and of the mutant COLΔ0677-0676 in TSB (●).

3.3.8. Impact of the absence of SACOL0677 and SACOL0676 on resistance to antibiotics

To address the impact of SACOL0677 and SACOL0676 proteins in resistance to β-lactam antibiotics and to identify a cellular process in which these proteins could play a role, an antibiogram including several antimicrobial classes was performed for the knock-out mutant COLΔ0677-0676 and the parental strain COL. The antibiotic disks used were: oxacillin a β-lactam; sulphametoxazole, a sulphanilamide that interferes with folic acid synthesis; linezolid, an oxazolidinone that interferes with the initiation of protein synthesis; vancomycin, a glycopeptide that inhibits cell wall synthesis; erythromycin, a macrolide that interferes with aminoacyl translocation in the ribosome; gentamicin, an aminoglycoside that interrupts protein synthesis and clindamycin that inhibits ribosome translocation.
The result showed no alteration in the growth inhibition halo for none of the antibiotics tested (Fig. 3.10).

The observation of the same growth inhibition halo in the absence of SACOL0677 and SACOL0676 genes contrasts with the result previously obtained for the overexpression mutant COL + pBCB8-0677-0676 (Point 3.3.6.), in which the overexpression of both genes decreased the resistance level to oxacillin. These results demonstrated that the overexpression, but not the absence, of SACOL0677 and of SACOL0676 genes impacts β-lactam resistance.

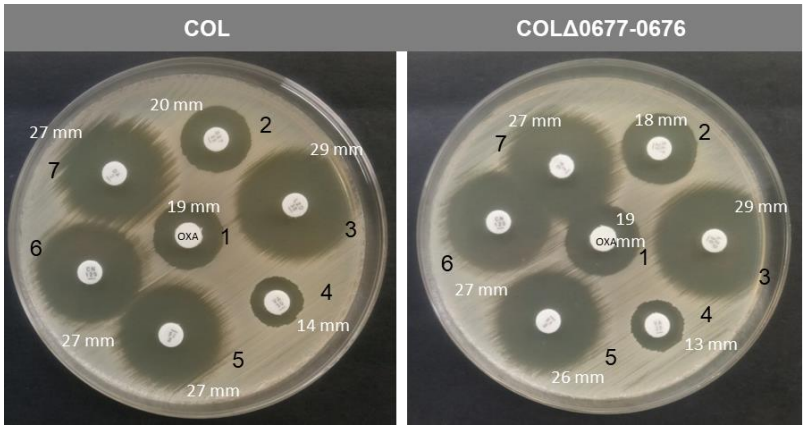

Fig. 3.10. Antibiogram of deletion mutant COLΔ0677-0676. Antibiogram of strain COL (left) and mutant COLΔ0677-0676 (right) performed for: 1- oxacillin (1 mg), 2- sulphametoxazole (25 μg), 3-Linezolid (30 μg), 4-Vancomycin (30 μg), 5- Erythromycin (15 μg), 6- Gentamicin (High level) (120 μg) 7-Clindamycin (2 μg).

3.3.9. SACOL0676 structural analysis

To determine the function of a protein, a useful common strategy is the elucidation of its structure, which may allow the identification of structural homologs and interaction partners in the databases. The structural elucidation of SACOL0676 protein by NMR was attempted using SACOL0676 recombinant protein overexpressed in strain *E. coli* BL21(DE3)+pET28a-0676 as a C-terminal His_6-tag fusion. Expression conditions were optimized for the maximum yield in minimal medium supplemented with $^{15}NH_4Cl$ for the acquisition of the ^{1}H-^{15}N-HSQC NMR spectrum. The acquired spectrum showed that, in the tested conditions, a poor signal dispersion a clear indication that the protein is unstructured in solution (Fig. 3.11).

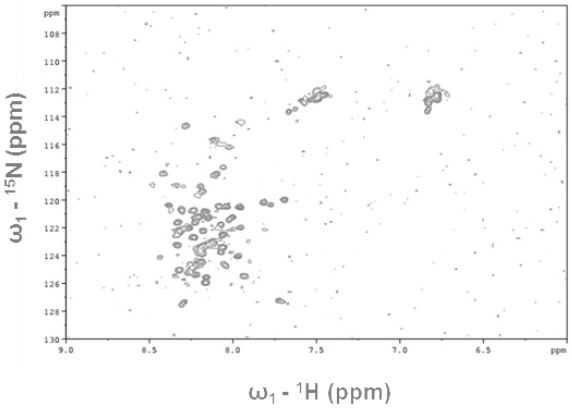

Fig. 3.11. ^{1}H-^{15}N-HSQC NMR spectrum of SACOL0676 protein in phosphate buffer (10 mM).

The secondary structure prediction tool (SWISS-MODEL) did not identify any topology for this protein but predicted the presence of a single alpha helix between residues 31 and 41. A more detailed analysis of this helix shows that it is amphipathic in nature, harbouring only hydrophilic

residues on one surface and only hydrophobic residues on the opposite side, a common motif in membrane-associated proteins (Fig. 3.12).

Following this observation, ^{1}H-^{15}N-HSQC spectra were acquired in the presence of the membrane mimetics Triton X-100, Tween 20, Trifluoroethanol (TFE) and sodium dodecyl sulphate (SDS) at concentrations below (5 mM) and above (20 mM) the SDS critical micelle concentration (CMC).

Preliminary results showed that SACOL0676 resonances shift in the presence of anionic detergents such as sodium dodecyl sulphate (SDS) and trifluoroethanol (TFE), which are mimetics of cellular membranes (Fig. 3.13 A, B and C). Additionally, in the presence of non-anionic detergents like Tween-20 and Triton X-100, chemical shift deviations are not observed (Fig. 3.13, D and E). These results support the hypothesis that SACOL0676 could bind to the membrane of *S. aureus.*

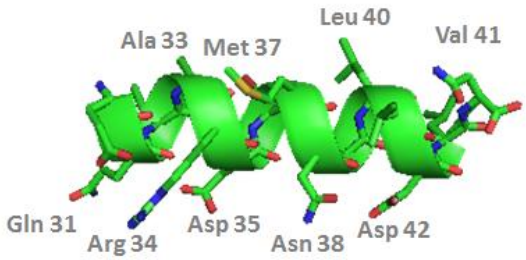

Fig. 3.12. Model prediction of an α-helix of SACOL0676. Model prediction (SWISS MODEL) of an α-helix of SACOL0676. of with amphipathic nature, characterized by the presence of hydrophilic residues located on one face of the helix (lower part) and the hydrophobic residues located on the opposite face of the helix (upper part) a common feature of membrane-associated proteins.

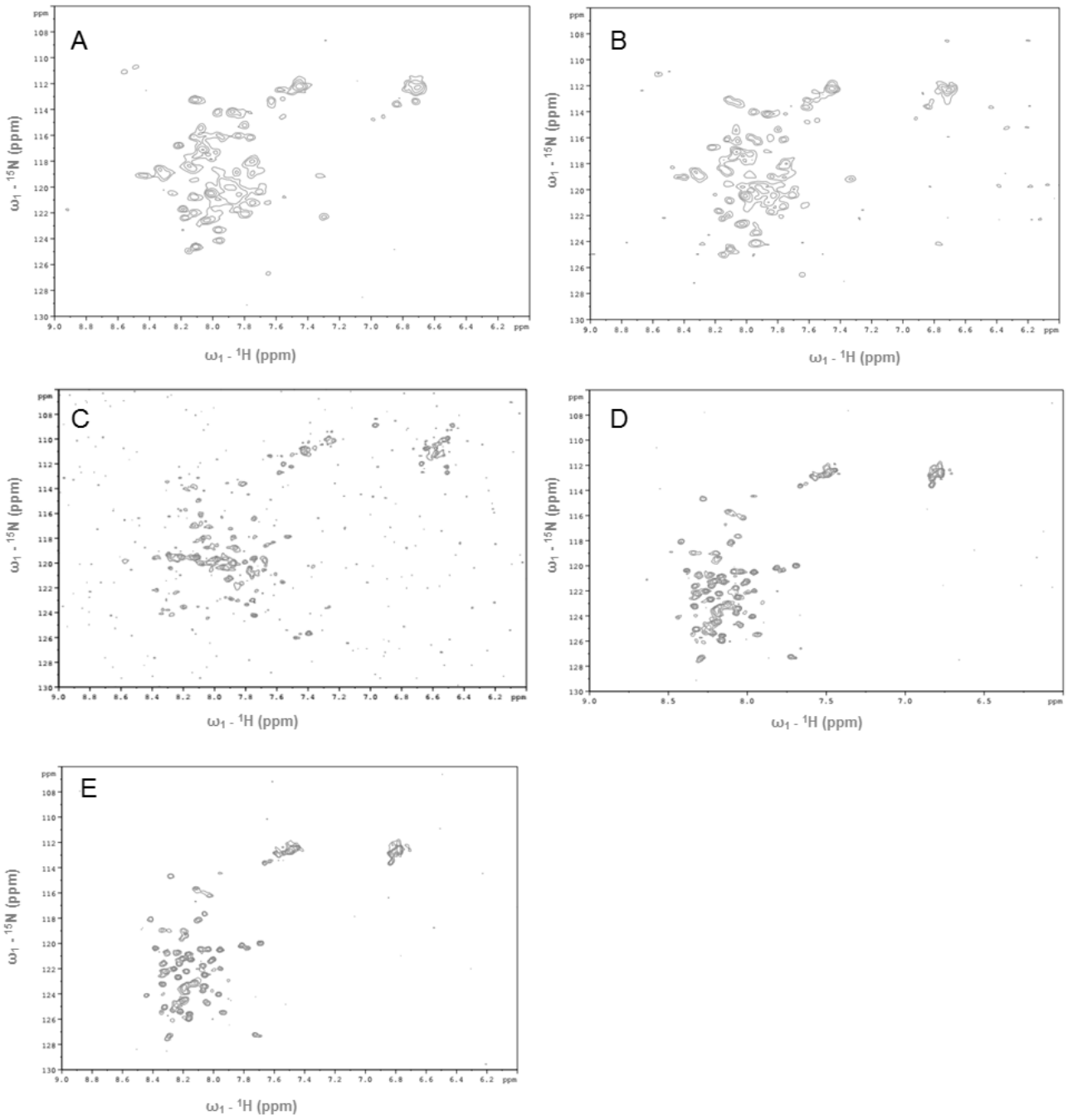

Fig. 3.13. ^{1}H-^{15}N-HSQC spectra of SACOL0676 protein in the presence of membrane mimetics. SACOL0676 protein in phosphate buffer (10 mM) **A)** in the presence of SDS (5 mM), **B)** in the presence of SDS (20 mM), **C)** in the presence of trifluoroethanol (TFE), **D)** in the presence of Triton X-100 and **E)** in the presence of Tween 20.

3.3.10. SACOL0676 and SACOL0677 association to DNA

During the purification steps of the SACOL0677 and SACOL0676 recombinant proteins, a UV absorbance spectrum of the eluted fractions was acquired. The spectrum revealed a maximum absorbance at 260 nm, indicating the presence of DNA.

To verify the hypothesis that these proteins could bind to DNA, SACOL0677 and SACOL0676 recombinant proteins were analysed, after purification, by agarose electrophoresis with DNA intercalator incorporated to visualize the presence of DNA in the sample. Additionally, all the samples were also treated with DNAse and suffered temperature denaturation (boiled samples).

A band of high intensity, compatible with the presence of DNA, was present in SACOL0677 and in SACOL0676 samples. The intensity of this band decreased following the treatment with DNAse which strongly corroborates the presence of DNA associated to the proteins (Fig. 3.14). The boiling treatment applied to the samples seemed to alter the capacity of the proteins to bind DNA. The fainter bands observed in the gel disappeared with the boiling process suggesting that denaturing the proteins inhibited their binding capacity (Fig. 3.14). To discard the possibility that the presence of DNA could be an artefact from the purification method, the same protocol was performed to purify Atl-H, which is a truncated version of the Atl protein, an autolysin of S.*aureus.* This truncation maintains only the domains that are known not to bind to DNA. No DNA was retrieved in this sample (Fig. 3.14), showing that the results obtained for SACOL0677 and SACOL0676 were not an artifact of the technique and that SACOL0677 and SACOL0676 are able to bind DNA.

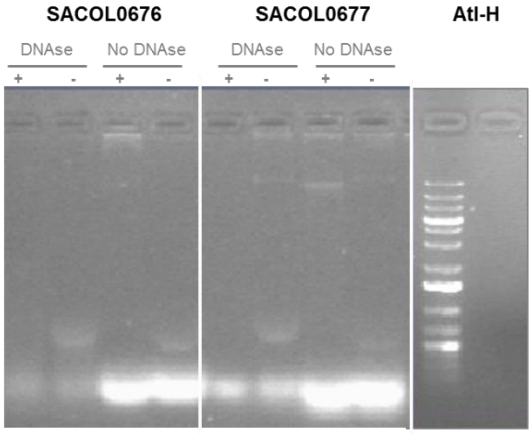

Fig. 3.14. Agarose gel electrophoresis of the purified SACOL0677 and SACOL0676 recombinant proteins. SACOL0677 and SACOL0676 recombinant proteins in the presence or absence of DNAse treatment. For each test the sample was boiled (+) and not-boiled (-). Atl H was purified with the same conditions and separated in agarose gel electrophoresis as control of the purification method.

3.3.11. SACOL0676 electrophoretic mobility shift assay

Following the previous result, that suggests that SACOL0676 protein binds to DNA, the fact that the predicted alpha helix of SACOL0676 has a hydrophilic surface and also due to the high isoelectric point estimated for SACOL0676 (PI = 9.9), the association of the protein to DNA was analysed through Electrophoretic Mobility Shift Assay (EMSA), in which the migration of protein-DNA complex in a gel is retarded in comparison to the migration of the DNA.

A form of regulation of gene expression is through the binding of a regulatory protein to the promotor region of its own gene. Thus, the EMSA assay was performed using the recombinant protein SACOL0676-His_{6}-tag and DNA fragments encompassing the putative promoter sequence of SACOL0677-SACOL0676 and the promoter sequence of SACOL0675 which is located downstream of SACOL0677 and was found to be also overexpressed in F9 transcriptomic data (Fig. 3.15). An unspecific double stranded DNA sequence (internal fragment of *pheS* gene) was used as control.

The DNA fragments were incubated with increasing concentrations of the purified SACOL0676 protein (0.5 to 2.5 μM) in the presence of binding buffer (Tris pH 7.5 -100 mM, KCl -500 mM, DTT (Dithiothreitol)-10 mM). After incubation, the mixture was separated in a 1% agarose electrophoresis and visualized by EtBr staining. The results showed that, in the conditions tested, no interaction occurs between the SACOL0676 protein and the DNA fragments tested (Fig. 3.16).

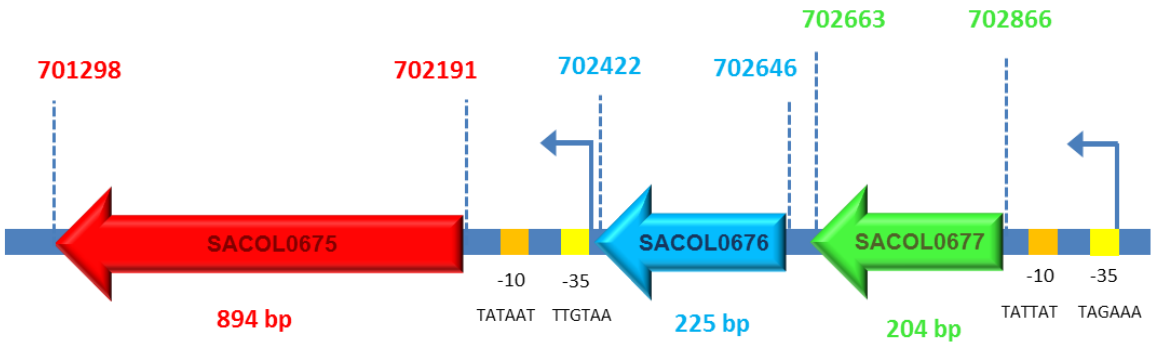

Fig. 3.15. Representation of the SACOL0677, SACOL0676 and SACOL0675 genes and their relative position in the chromosome of the *S. aureus* COL strain. The DNA strand is shown in blue and depicted in the promoter are the putative -10 and -35 elements with the corresponding sequence and genome coordinates.

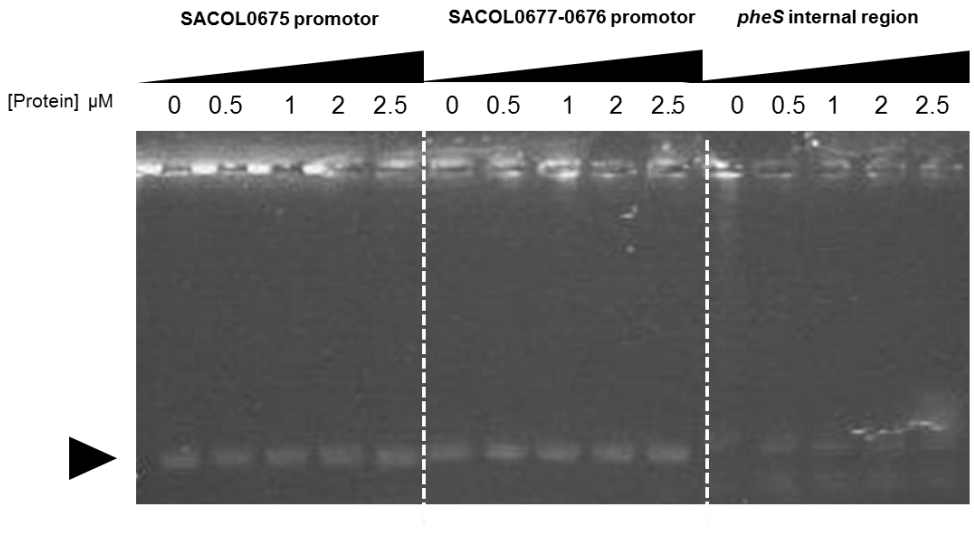

Fig. 3.16. Gel shift assays for SACOL0676 protein. Gel shift assays for SACOL0676 protein in the presence of three different DNA fragments: the fragment encompassing the SACOL0675 putative promotor, the fragment encompassing the SACOL0677-0676 putative promotor and an unrelated DNA fragment of an internal region of the *pheS* gene. All samples contain 100 ng of the corresponding DNA fragment.

3.3.12. *In silico* analysis of SACOL0675

The transcriptomic analysis of F9 and F9H mutants (Chapter 2), revealed the massive overexpression of SACOL0677 (F9: 210.08 fold; F9H: 293.43 fold) and SACOL0676 (F9: 140.11 fold; F9H: 189.96 fold) genes but also, although moderate, overexpression (F9: 2.38 fold; F9H: 3.35 fold) of the immediately downstream gene, SACOL0675, which function is anotated in the databases as unknown.

The SACOL0675 gene encodes a predicted protein of 32.4 KDa protein with 10 transmembrane α-helixes (Fig. 3.18, A and B) (https://www.ncbi.nlm.nih.gov/Structure/cdd/wrpsb.cgi) identified two EamA domains of opposite folding, which is thought to be the result of internal gene duplication followed by a fusion of the two genes. This feature is a signature of the drug/metabolite exporter (DME) family of the drug/metabolite transporter (DMT) superfamily. The DME family is large group of proteins exhibiting 10 membrane-spanning α-helixes. SACOL0675, however, lacks the characteristic 5+5 dual topology: its N-terminal α-helix is cytoplasmic while the remaining nine are membrane-spanners ending on an extracellular C-terminal (276).

In-depth *in silico* analysis of SACOL0675 revealed a putative transmembrane pore, further suggesting a role as a metabolite transporter (Fig. 3.18, C and D). The employed software, PoreWalker (https://www.ebi.ac.uk/thornton-srv/software/PoreWalker/), traces a hypothetical trajectory by accommodating a spherical probe of regulable radius along the center of the predicted pore (277).

The pore is composed of uncharged amino acids. Both the extracellular and cytoplasmic openings are hydrophilic with Ser and Thr residues prone to phosphorylation. The center, however, can be divided into two regions: an alternating hydrophobic/hydrophilic region at the extracellular end (Met-Ala-Thr-Thr-Phe-Asn-Leu) and an exclusive hydrophobic region at the cytoplasmic end (Val-Leu-Leu).

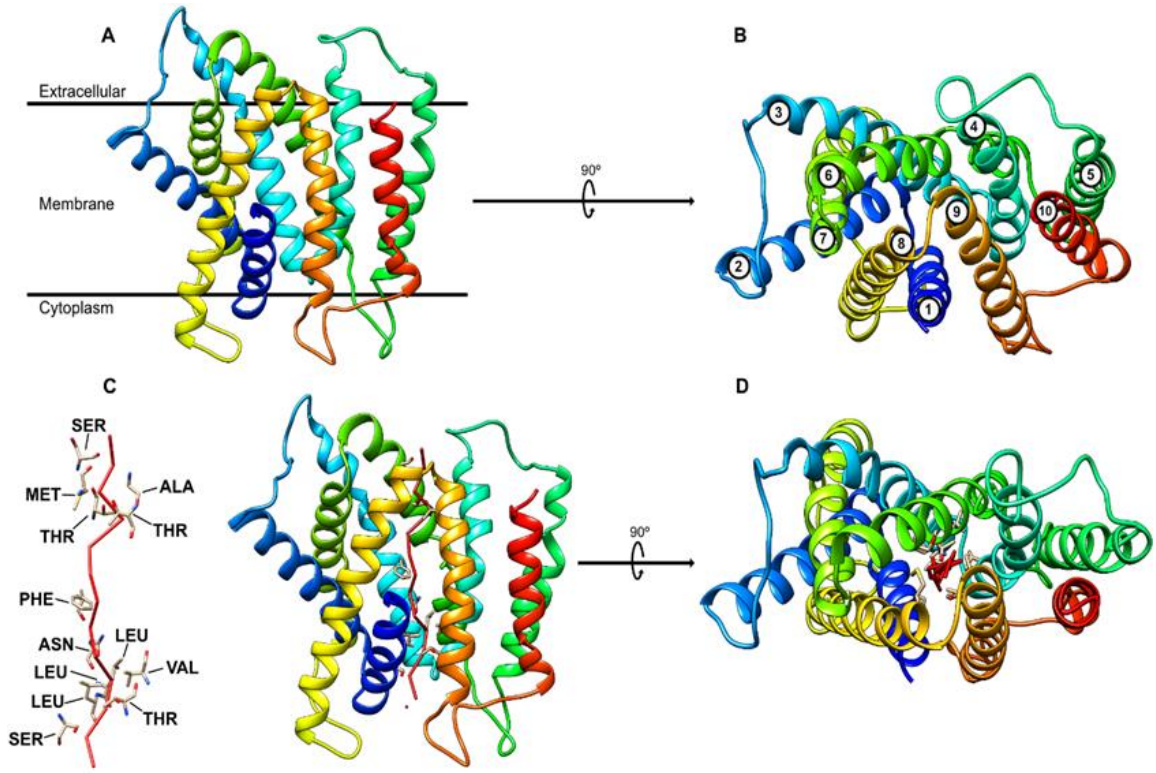

Fig. 3.17. Model structure of SACOL0675 protein. Model structure of SACOL0675 protein with 10 α-helix domains, one predicted to be cytoplasmic (1) and the remaining nine (2-10) being membrane-spanning. **A)** Prediction of the subcellular location of the secondary structure of SACOL0675. **B)** Top-down view of the α-helixes. **C)** Hypothetical metabolite trajectory is highlighted by a red line. Pore-lining residues are represented by their respective side-chain (left). Trajectory superimposed with the secondary structure (right). **D)** Top-down view of the metabolite trajectory (277). https://www.ebi.ac.uk/thornton-srv/software/PoreWalker/

3.3.13. Impact of the absence of SACOL0675 in growth

The *In silico* model suggested that SACOL0675 may act as an importer or exporter of metabolites. Additionally, being a transmembrane protein, with residues prone to be phosphorylated on the cytoplasmic side, also suggests that SACOL0675 could be a sensor triggered by an external stimuli that is transferred to the internal side by a signal cascade to the remaining partners SACOL0677 and SACOL0676.

To address the function of SACOL0675, a conditional mutant COLpcad0675 was constructed by a two-step approach using the allelic replacement vector pMAD. First the SACOL0675 gene (including the RBS) was cloned into the replicative vector pBCB8, downstream of the pcad inducible promoter, generating plasmid pBCB8-0675. Subsequently, a 1536 bp fragment corresponding to pcad0675 was amplified from pBCB-80675 and fused to a 703-bp fragment including SACOL0676 and SACOL0677 to guarantee that these two genes did not become impaired. The resulting 2239 bp fragment was cloned into the allelic replacement vector pMAD. The pMADΔ0675, was co-integrated into and excised from the chromosomal DNA of COL through non-redundant Campbell recombination events, resulting

in the chromosomal copy of SACOL0675 being placed under the transcriptional control of pcad. (Fig. 3.18)

Growth curves of the conditional mutant were determined in the absence and in the presence of increasing concentrations of the inducer (0.4, 0.8 and 1.5 µM of $CdCl_2$) (Fig. 3.19). The results showed that all the growth curves were overlapping with COL growth curve which indicated that in the absence of SACOL0675 (0 µM of $CdCl_2$), the strain is able to grow and divide properly. Thus, SACOL0675 was shown not to be an essential gene and its expression was not needed for growth in normal conditions in rich medium.

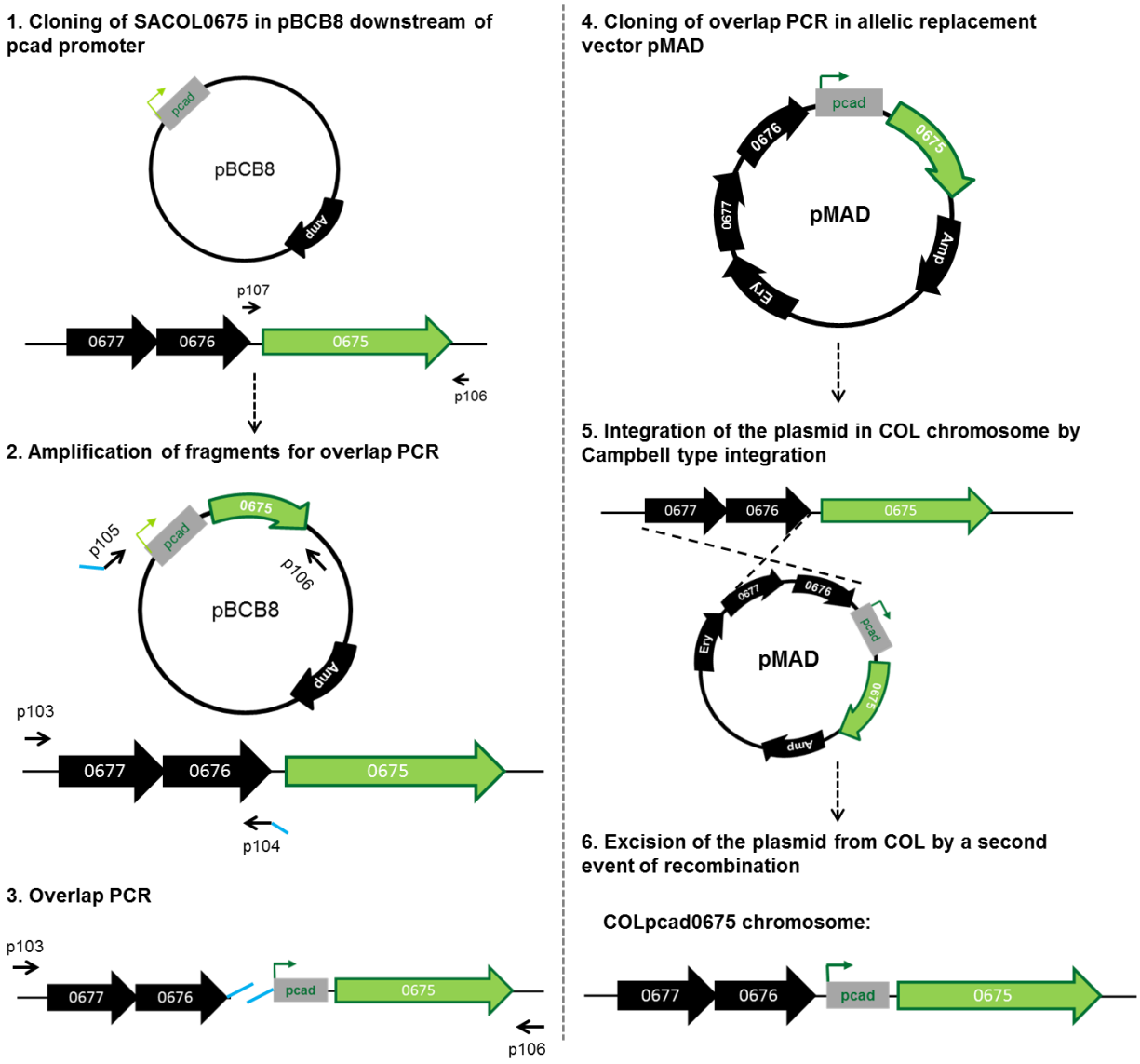

Fig. 3.18. Construction of COLpcad0675. Schematic depiction of the construction of the conditional mutant COLpcad0675. The fragments amplified in each step and the primers used are indicated in the figure.

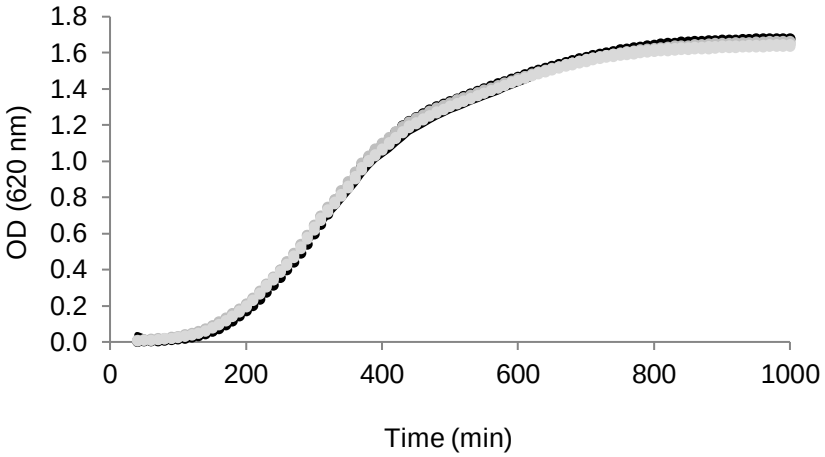

Fig. 3.19. Growth curves of conditional mutant COLpcad0675. Growth curves of COL (●) and the conditional mutant COLpcad0675 in the absence of the inducer (●) and in the presence of increasing concentrations of the inducer $CdCl_2$: COLpcad0675 + 0.2 µM (●), COLpcad0675 + 0.4 µM (●), COLpcad0675 + 0.6 µM (●),COLpcad0675 + 0.8 µM ( ) and COLpcad0675 + 1 µM (o).

3.3.14. Impact of the absence of SACOL0675 in growth with oxacillin

The SACOL0675 gene was found to be overexpressed in a mutant with the cell wall impaired. In order to address if SACOL0675 could play a role in the presence of a stimulus, such as the impairment of the cell wall, the conditional mutant was grown in the presence of oxacillin at 25 µg/ml (sub-MIC) and with increasing concentrations of the $CdCl_2$ inducer. This oxacillin concentration was chosen since it impacted the growth of the parental strain COL but without its complete abolishment (Fig. 3.19).

The results showed that under the lower concentrations of the inducer (no inducer and 0.2 µM), the lower expression of SACOL0675 negatively impacted the growth in the presence of oxacillin. As the concentration of inducer increased (0.4 and 0.2 µM), the growth profile became equivalent to the original growth profile of COL in the presence of oxacillin suggesting that these concentrations of inducer resulted in a expression of SACOL0675 gene similar to the native levels. Surprisingly, for the higher concentrations of the inducer (0.6 and 0.8 µM $CdCl_2$), the growth of the mutant surpassed the growth of the parental strain in the presence of oxacillin (Fig. 3.20). These results showed that the level of expression of SACOL0675 does not affect *S. aureus* growth in normal growth conditions however it is important in a condition of antibiotic stress.

This may suggest the involvement of SACOL0675 in a signaling mechanism of the cell to sense exterior conditions or a specific damage and probably translocating the signal to effector proteins allowing the cell to adapt.

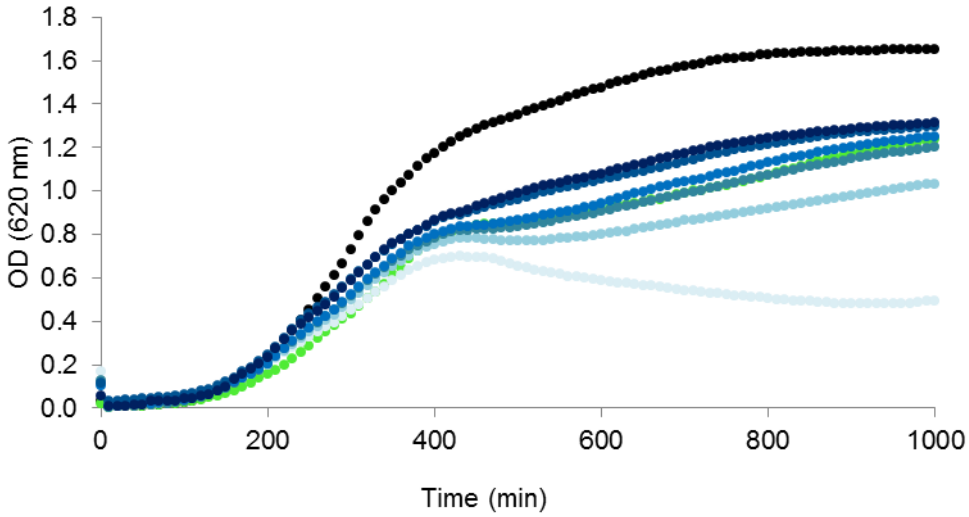

Fig. 3.20. Growth curves of conditional mutant COLpcad0675 in the presence of oxacillin. COL in the absence of oxacillin (●) and COL in the presence of oxacillin (25 µg/ml) (●) and the conditional mutant COLpcad0675 in the presence of oxacillin (25 µg/ml) and of increasing concentrations of the inducer $CdCl_2$: COLpcad0675 + 0 µM (●), COLpcad0675 + 0.2 µM (●), COLpcad0675 + 0.4 µM (●),COLpcad0675 + 0.8 µM (●) and COLpcad0675 + 1 µM (●).

3.3.15. Impact of the absence of SACOL0675 in oxacillin resistance

SACOL0675 was shown to be important for the cell to grow in the presence of oxacillin and this observation raised the hypothesis that SACOL0675 could be directly involved in the mechanism of resistance to oxacillin. To address this hypothesis, oxacillin growth inhibition halos were performed for the conditional mutant in the presence of increasing concentrations of the inducer.

The results showed that the diameter of the growth inhibition halos was similar to the one of the parental strain COL, independently of the inducer concentration used (Fig. 3.21). The absence of the SACOL0675 protein, although shown to impact growth in the presence of oxacillin, was not directly related with the mechanism of resistance to beta-lactams itself, at least, at the oxacillin concentration used.

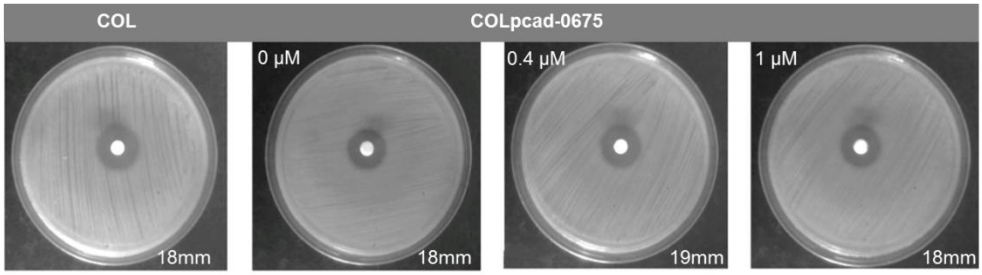

Fig. 3.21. Growth inhibition halos for conditional mutant COLpcad0675. Growth inhibition halos of oxacillin (1 mg) obtained by disk diffusion for strain COL and the COLpcad0675 mutant. The concentrations of the $CdCl_2$ used are indicated. The values presented correspond to the diameter of the halo in mm.

3.4. Discussion

In Chapter 2 of this Thesis, two short (~200 pbs) genes of unknown function were identified, by microarrays, as being massively overexpressed, about 1000 fold, in the cell wall mutant F9 (58). The *murF* gene of this strain is impaired by a plasmid insertion at the 5´end and, as a consequence, the strain accumulated tripeptide in the cell wall, lacking the terminal D-alanyl-D-alanine, instead of the normal pentapeptide. A similar impairment was previously achieved through the controlled down-regulation of *murF* gene in the conditional mutant COLspac*murF* (59) culminating with the observation that the lack of *murF* expression was lethal for the bacteria. In contrast with the conditional mutant, in F9, the same percentage of incorporation of tripeptide was not lethal and also did not cause any impact on growth.

These two small genes stood out in the transcriptomic data as possible players in the capacity of the F9 mutant to survive to severe cell wall damage.

Given that these two genes were described as being highly overexpressed in a *rho* knock-out mutant (253), and since F9 mutant has a loss-of-function mutation in *rho* gene, the impairment of *rho* gene is most probably triggering the overexpression of the genes. This mechanism raised the hypothesis that F9 mutant may be profiting from this indirectly-caused overexpression to overcome the cell wall damage that would otherwise be lethal.

In this Chapter we presented preliminary data that was obtained with the aim to understand the function of these genes and, ultimately, to disclose their role in bacterial cells exposed to a stress to its first defensive barrier and surely one of its most important structures, the peptidoglycan.

The first step of this work consisted in proving that the nucleotide sequence annotated in the databases for strain COL actually encompassed two genes, SACOL0676 and SACOL0677*,* and that both are indeed translated in proteins. The only putative promoter identified upstream of SACOL0676 and the presence of two canonical RBSs suggested that the translation of the sequence results in two independent proteins. A band with the expected size of the proteins (~8 KDa) was excised from a gel containing crude extracts of the mutant F9. Mass spectrometry analysis confirmed the translation of two proteins from the nucleotide sequence, as predicted in COL genome annotation, since the peptides identified were compatible with the translation of two independent proteins and not compatible with the peptide sequence expected if a single protein was generated. Since the nucleotide sequence was shown to originate two independent proteins, we hypothesize that an automatic annotation issue must have mistakenly identified only SACOL0676*,* and not SACOL0677*,* in the transcriptomic data of the *rho* knock-out mutant in the background of strain HG001 (253).

Blast alignments of the protein sequences with the sequences available in the databases have not retrieved homologues and it was not possible to identify specific sequence domains with the several algorithms tested. The only matches found were of 40% identity for SACOL0677 with part of a diguanilate cyclase from *Thermosipho melanesiensis* and of 48% identity for SACOL0676 with a chemotaxis sensory transducer from *Synechococcus* sp.

Diguanylate cyclase is an enzyme responsible for the synthesis of cyclic di-3',5'-guanylate (cyclic di-GMP) from two molecules of guanosine triphosphate (GTP). Cyclic di-GMP is a nucleotide second messenger involved in the regulation of numerous processes in bacteria such as motility inhibition and

induction of sessility. The nucleotide messenger is related with biofilm development and is suggested to play a role in bacterial surface sensing and adhesion (278).

In *S. aureus,* only one gene, *gdpS* (SACOL0809) is known to encode a protein with a degenerate GGDEF domain, the typical domain of diguanylate cyclases, but phosphodiesterases (PDEs), the enzymes that degrade Cyclic-di GMP, or known receptors or riboswitches to which this messenger could bind, remain unknown (278).

In Firmicutes, several cyclic di-GMP riboswitches are predicted, which anticipates that this mechanism of regulation plays an important role in cyclic-di-GMP signaling in these organisms probably to control functions that are yet unknown (279).

These protein sequence homologies led us to hypothesize that SACOL0677 and SACOL0676 could be part of a signaling pathway, so far unknown in *S. aureus,* involving cyclic-di-GMP, which could allow the bacteria to overcome a cell wall stress.

Protein-DNA association assays suggested that both SACOL0677 and SACOL0676 proteins are able to bind DNA, although we were until now not able to determine the sequence specificity of the DNA to which they bind. The proteins did not bind to the DNA sequences tested, that included their own promoter sequences. Additionally, results from NMR assays, strongly suggest that SACOL0676 binds to the bacterial membrane. These observations, although preliminary, strengthened the hypothesis that the genes SACOL0677, SACOL0676 and the transmembrane partner SACOL0675 may encode a three-component system, related with cell wall stress that could transduce the signal in a cyclic-di-GMP dependent cascade.

Two component signaling transducing systems (TCS) are widely distributed mechanisms that allow microorganisms to sense and respond to environmental changes. TCS are much more common in bacteria than in any other domain of life. Canonically, the system is composed of a membrane bound sensor, typically a histidine-kinase and a response regulator that mediates the cellular response (280).

In Firmicutes, a very common variation of the TCS is the existence of a protein that acts as a signaling module, senses an environmental variation and activates a neighboring TCS in a so-called three component system (280). Three component systems can interact with pathways involving cyclic-di-GMP. In TCS the majority of the partners of the response regulators consist in a DNA-binding domain that functions as a transcriptional regulator but some contain enzymatic domains that are commonly involved in second messenger homeostasis, such as c-di-GMP. This is the case of the PleD response regulator of *Caulobacter* sp. that belongs to a subfamily that contains a GGDEF-type output domain with diguanylate cyclase activity. Despite more rare, some response regulators also have RNA binding activity which typically regulate transcription by inhibition of termination at Rho-independent terminators (281).

The results obtained for SACOL0677 and SACOL0676 with the bacterial two-hybrid system and by co-purification assays did not show a direct physical interaction between the proteins which does not rule out a possible functional interaction as the one expected in a three component system, or an eventual interaction after modification of the partner proteins, for instance, if the proteins must be phosphorylated to interact, which should be addressed in the future.

To understand if this system may be directly involved in resistance to β-lactams, or with the damage in the cell wall, the proteins SACOL0677 and SACOL0676 were overexpressed in the COLspac*murF* mutant, at suboptimal concentrations of inducer, to mimic the cell wall damage of the F9 mutant. The overproduction of the proteins did not contribute to solve the impairment in growth caused by the *murF* down-regulation. Instead, it even promoted a decrease in the growth rate, similar to the one found for the COL overexpression mutants COL+pBCB8-0677, COL+pBCB8-0676 and COL+pBCB8-0677-0676. Firstly, these results indicate that the expression of these genes must be tightly regulated since their overexpression has detrimental effects for the cell, and that the two proteins may act synergistically, as the decrease in growth is higher when of both proteins are overproduced. Secondly, the fact that F9 mutant has an unaltered growth rate, although with high levels of expression of both SACOL0676 and SACOL0677, in contrast with COL and COLspac*murF,* in which the expression of these genes caused a dramatic negative impact on the growth rate, suggests that these genes could be related with the specific damage occurring in F9.

Curiously, abolishment of the expression of both SACOL0677 and SACOL0676 genes did not have an impact on the growth profile of the strain, and did not have an effect on the resistance phenotype to oxacillin. Several other classes of antibiotics were tested, and for none was the phenotype of resistance altered.

Contrarily to what was observed for SACOL0677 and SACOL0676, the results obtained for the conditional mutant COLpcad0675 indicated that the absence of SACOL0675 did not have an impact on the β-lactam resistance level, however, the expression of the gene was needed for the normal growth of the mutant in the presence of oxacillin. These results did not rule out a role for SACOL0675 in a signaling pathway, in which it acts as an external sensor but might be evidencing its role as a cellular exporter, which would have more impact in liquid medium, and in growth, than in solid medium.

To this point we were not able to identify the pathway in which SACOL77-76-75 system is involved and consequently its role in F9 mutant, but our preliminary results suggest the importance of the system for *S. aureus* facing a cell wall damage and have uncovered new routes to pursue.

As a next step in this work, we aim to identify the DNA sequences to which SACOL0677 and SACOL0676 bind to clarify the pathways in which this system is involved. The identification of the DNA sequence could be performed using the IDAP-seq technique, which stands for *in vitro* DNA affinity purification combined with massive next-generation sequencing (282). In this technique, the recombinant proteins are overproduced and purified and combined with genomic DNA. Then, the Protein-DNA complex is cross-linked and pulled-down by immunoprecipitation. The protein is digested and the DNA is sequenced by high throughput sequencing.

Chapter 4
General Discussion

Staphylococcus aureus is a Gram-positive commensal bacterium that can colonize humans asymptomatically but can also become one of the most feared pathogens, namely the methicillin resistant *S. aureus* (MRSA) strains that are resistant to β-lactam antibiotics and virtually resistant to all antimicrobial classes presently available in the clinic. The main target of the β-lactam antibiotics is the cell wall assembly, specifically the transpeptidation step, which is performed by the penicillin binding proteins (PBPs) that are inactivated by this class of antibiotics. Thus, over the half century, the studies on the peptidoglycan biosynthetic pathway and on resistance to β-lactams have been carried out in parallel.

In earlier studies in our laboratory, an *S. aureus* plasmid insertional mutant named F9, was constructed for the *murF* gene in the background of the MRSA strain COL. The MurF protein is a ligase responsible for the addition of the terminal D-alanyl-D-alanine residues to the stem peptide of peptidoglycan. The *murF* insertional mutation lead to an abnormal peptidoglycan composition, with incorporated abnormal tripeptide, a cell wall damage that is described to be lethal in other *murF* mutants (59). The F9 mutant was characterized by a decreased level of resistance to β-lactam antibiotics and by the presence of highly resistant subpopulations of revertants. One of these revertant strains was isolated and named homostar mutant F9H.

Although F9 was unable to correct the primary cell wall defect, and despite the decreased resistance to β-lactams, the mutant strain survives and presents a normal growth rate, suggesting the existence of a molecular mechanism that allows the cell to overcome the fatal damage.

Mutant F9 belongs to a collection of thirty independent mutants that were constructed following the same plasmid insertion methodology. Multiple copies of the inserted plasmid were found to be present in tandem in the chromosome of all the insertion mutants constructed. The thirty strains were analyzed by restriction mapping and the number of plasmid insertions varied for each mutant and ranged from five to more than twenty seven. Only 10% of the isolates showed decreased resistance to β-lactams, corresponding to mutants F9, F20 and F26. The remaining isolates of the collection maintained a high and homogeneous level of resistance to β-lactams, identical to the parental strain COL and a normal composition of the cell wall, without accumulation of tripeptide.

Whole genome sequencing of the F9 and F9H mutants revealed one common mutation in the genome of F9, in the coding region of the *rho* gene that encodes the Rho transcription terminator factor and one mutation unique to F9H, in the coding region of *pheS* gene that encodes the α-subunit of phenylalanyl-tRNA synthetase.

Regarding the mutation in *rho*, the three insertion mutants with decreased levels of resistance to β-lactams, F9, F20 and F26, were found to harbor mutations in the *rho* gene that although different, were all loss-of-function mutations. The complementation of the three mutants with a replicative plasmid, in which the expression of wild-type copies of the *rho* gene can be controlled by the presence of an inducer, was able to revert the level of resistance to β-lactams to the level of the parental strain COL.

However, through the construction and analysis of *rho* mutants in the background of several strains, we determined that the impairment of *rho*, *per se*, did not translate in an alteration of the resistance level. This was verified for strains COL and COL-S, in which the *mecA* gene was excised, and for strain HDE288, an MRSA with a lower level of resistance and with a SCC*mec* different from COL and harboring the *mecA* regulatory genes. The results showed that in any of these cases did the impairment in *rho* promoted a reduction or an increase in the level of resistance, suggesting that the implication of Rho in β-lactams resistance was a specific feature of the F9 mutant and of its specific genetic damage. We also demonstrated by western-blotting that the mechanism through which Rho mediates the reversion of resistance, in the *rho* complementation mutant, was independent of the production of PBP2A.

The three mutants, F9, F20 and F26, with decreased resistance, were also characterized by a lower number of plasmid tandem insertions in the chromosome in comparison with the insertion mutants that retained high level resistance to β-lactams. Complementation assays of F9 and F9H with the *rho* wild type gene, provided in a replicative plasmid, and chromosome restriction mapping of these mutants revealed that Rho expression resulted in the chromosomal tandem amplification of the plasmid interrupting *murF* gene. This genetic recombination event allowed for the reversal of the resistance phenotype of F9 mutant and for the decrease of the accumulated abnormal tripeptide in the cell wall, observed by RP-HPLC analysis of the peptidoglycan structure.

Sequencing of the *murF* gene in the chromosome of the insertion mutants F1 and F9 suggested that the mutant that retained the high level of resistance to the β-lactams, F1, had the *murF* gene fully restored, which may have occurred during the subsequent events of recombination. The restoration of the complete *murF* gene probably did not happened in the F9 mutant. Despite the F9 strain had already been sequenced using the 454 platform, to undoubtedly determine the number of tandem repetitions in the genome of F9 and F1 mutants and how the tandem repetitions are structurally organized, it would be essential to perform whole genome sequencing for these strains using a third generation sequencing technique such as the PacBio SMRT or the Oxford Nanopore technologies.

Despite based on different detected signals, fluorescence and ionic current, respectively, both technologies present the capacity to provide long reads, in the order of thousands of bases, using single molecule technology (283-285). This approach would allow the sequencing of the F9 and F1 mutants genome, surpassing the alignment and assembly ambiguities that occur for repeat regions when sequencing platforms that are based in short reads are used. The capacity to provide long reads would allow to determine the exact number of tandem repeats in the genome and their precise organization which would provide details on the process of recombination that took place and, ultimately, in the F1 mutant, to confirm the full restoration of the *murF* gene. Moreover, the existence of an inverted repeat region (palindrome) at the 3´-end of the *murF* gene, could have originated a tandem inversion duplication of the *murF* gene. If this genetic event occurred, it is possible that some *murF* repeated sequences are inverted in the genome. The inversion process occurs when, due to breaks in the DNA, the strand end snaps back and the inverted sequence base pairs with the reverse complement of itself in the same strand, creating a hairpin that functions as a template for the repair

system (286). The use of a third generation sequencing technology, would allow to address this hypothesis.

Independently of the full restoration of the full *murF*, our results showed that Rho is essential for the tandem amplification of the pRS2 plasmid which is interrupting *murF* gene in the chromosome which usually happens by a homologous recombination process.

Moreover, tandem amplification in the chromosome is a strategy found in bacteria as a way to increase resistance and was already described in the literature although more specifically for antibiotic resistance genes. For instance, the analysis of the genome of the CA-MRSA strain USA300, grown for several days in the presence of growing concentrations of oxacillin, revealed that the *mecA* gene was repeated in tandem in the chromosome (10 copies), and single nucleotide polymorphisms were found in *gdpP*, *clpX*, *guaA*, and *camS* genes (287). Furthermore, the amplification of genes in the chromosome is a widely distributed process in many species of bacteria and other organisms. This process is an evolutionary tool to generate the genomic variability necessary for the adaptation to new conditions and stresses, in some cases with amplifications in the order of several megabases (288).

In the case of the amplification of a plasmid containing a fragment of *murF* gene, that is lacking the initial region of the gene, it seems more likely that the high rate of transcription in that genomic region, which was shown by Northern-blotting analysis of F1 and F9 mutants, led to conflicts between the transcription and replication machineries that were properly solved through homologous recombination. Since the process of homologous recombination could allow for the reestablishment of a full *murF* gene enabling the reversion of the resistance phenotype, the genetic amplification mechanism allowed the cell to circumvent the cell wall damage and consequently the impaired resistance.

The exacerbated homologous recombination only happened in the presence of a functional *rho* gene, since the number of plasmid insertions in the genomes of the mutants harboring a loss-of-function mutation in *rho*, reflects the initial copies that integrated the genome upon the transduction event.

In this way, this work allowed to suggest a new, direct or indirect, role for the Rho transcription termination factor in the mechanism of homologous recombination. Several physiological roles other than termination of transcription have been attributed to Rho, but so far, to the best of our knowledge, not related to the mechanism of homologous recombination. The homologous recombination between long repetitive sequences is mainly dependent on *recA* gene (288). The fact that Rho is a member of the RecA family may disclose the hypothesis of a direct function of Rho in homologous recombination (216). Despite the involvement of Rho factor in homologous recombination was demonstrated, the pathway through which it occurs remains elusive.

Concerning the mutation in *pheS* gene*,* exclusive of the resistant homostar mutant F9H, we have demonstrated, through the construction of an F9::pcad*pheS* conditional mutant and through the construction of F9H+pBCB8*pheS* overexpression mutant, that this genetic impairment was responsible for the reversion of the oxacillin susceptible phenotype of F9 by triggering a mechanism of stringent response. Besides all the advances that have been made, stringent response remains a poorly known mechanism and it is not completely understood how it exerts the reversion of the resistance

phenotype. The fact that the F9H mutant managed to decrease the accumulation of tripeptide, should explain the reversion of phenotype, but the pathway that led to this deaccumulation remains elusive.

Unexpectedly, the mutants F9, F20 and F26 were able to survive without growth impairments, although presenting a defective cell wall with a level of tripeptide incorporation similar to the previously characterized *murF* conditional mutant, that showed a decrease in the growth rate proportional to the amount of tripeptide incorporated in the cell wall (59). The comparison of the different growth phenotypes of these two strains, that present a comparable genetic defect, led us to hypothesize that the F9 mutant, and its similar mutants F20 and F26, developed a mechanism that allows the cell to survive to *murF* impairment. To further explore this hypothesis, we analysed the transcriptome of F9 and compared it to the transcriptome of COL strain. The transcriptome of F9H was also analysed to clarify the paths that are affected by stringent response.

The transcriptome of strains F9 and F9H was firstly compared with the available transcriptomic data of the *rho* knock-out mutant, HG001Δ*rho*, a mutant derived from the MSSA strain NCTC8325 but, that contrarily to its parental strain, has the SigB-activating phosphatase RsbU active. This transcriptome comparison, despite the differences in the methodology and in the strain used, had the aim to classify in a separate group, the genes which expression was altered in response to Rho impairment. Comparison between the transcriptomes of F9 and F9H would then allow to identify the genes that are related with stringent response. Finally, the genes that were left after the previous analysis would be associated with survival to cell wall damage. The genes identified by transcriptomic analysis of F9 and F9H were in this way divided in three groups: i) the genes which expression was altered as a result of the *rho* mutation, by comparing with the transcriptome of HG001Δ*rho* mutant; ii) the genes which expression was altered in response to *pheS* mutation, by comparing the transcriptomes of F9 and F9H; iii) the genes which expression was altered in response to *murF* mutation, by comparing with the transcription in COL and including all the genes that did not fit in the previous groups.

A total of 22 genes with altered expression had no counterpart in the *rho* knock-out mutant and were mostly related with methicillin resistance and prophages of COL strain. These genes were assigned as *murF* related since the direction of expression is similar in F9 and in F9H.

Additionally, 61 genes were found to be differentially expressed in F9 and in F9H but not in HG001Δ*rho* disclosing a possible direct association between these genes and *murF* impairment.

Regarding this group, the majority of the genes overexpressed were ABC (ATP binding cassette) transporters and other membrane transporters related with different substrates such as ions, iron compounds, amino acids and virulence factors. The *icaADBC* operon, related with biofilm formation and genes of the branched chained amino acids biosynthesis pathway, were found to be down-regulated.

One of the most intriguing results is the fact that the genes of the “cell wall stimulon” were not affected upon the impairment of *murF.* Our main hypothesis for this fact is related with the adaptive state of bacteria to this damage in the F9 insertion mutant. The genes of the “cell wall stimulon” are a group of genes whose expression is altered as a consequence of a damage in the cell wall, being thus involved in the response to this damage. The genes of the cell wall stimulon were found to be affected

in the *murF* conditional mutant grown at suboptimal concentrations of the inducer (60), that presents a similar rate of accumulation of tripeptide at the cell wall (about 7%) than F9. In the case of the conditional mutant, this percentage of accumulation of tripeptide was sufficient to impair the viability of the mutant, and the "cell wall stimulon" is triggered, which did not happen in F9. This difference could be due to the fact that the impairment of *murF* gene in F9 results from a stable mutation to which the bacteria has adapted, whereas in the case of the conditional mutant, the bacteria must adapt to the intermittent damage each time the inducer is removed. In fact, the transcriptomic results of *murF* impairment in F9 can be considered as a later stage of response than those of the conditional mutant when grown at suboptimal concentrations of the inducer. This result seems to suggest that the triggering of the "cell wall stimulon" upon cell wall damage is a first level of response of bacteria until the cell adapts to the new condition. After adaptation, the cell should be able to restore the transcription of these genes to basal levels.

Regarding the *rho* impairment, the transcriptomic data revealed the altered expression of 46 genes. The list of the most upregulated genes included the *comEC* and the *comK*, related with genetic competence and the *radC* gene which is described as being involved in the recombinational repair of DNA strand breaks associated with the replication fork. This data suggested that *rho* gene regulates the expression of *radC* gene. Thus the *radC* altered expression may be involved in the process of homologous recombination that is responsible for the amplification of the copies of inserted plasmid.

One hypothesis is that the normal expression of *radC* may be unsufficient to repair the DNA damage that could arise from transcription-replication conflicts promoting a higher rate of homologous recombination found in the mutants with higher number of plasmids in tandem in the chromosome. On the other hand, the *radC* overexpression in F9 resulting from the *rho* impairment could lead to higher degree of DNA repair limiting the homologous recombination process in this mutant. It would be important in a near future to address the involvement of *radC* in this process through the assessment of its functional relation with *rho*. In order to address this functional interaction, a *radC* knock-out mutant should be constructed in the family of *rho* overexpression mutants such as F9+pBCB8*rho* and assess the number of plasmid insertions by performing new restriction mapping analysis. Since the F9 strain seems to have an unknown limiting factor, other than the altered expression of *radC,* for the amplification of the plasmid by homologous recombination, and that this may be the reason why the number of copies did not increase as much as in the F9H background upon copies of *rho* were given in a plasmid, the *radC* knock-out mutant must also be constructed in the F9H+pBCB8*rho* overexpression mutant. Such construction could be performed using the pMAD-Cm allelic replacement vector containing the *cat* gene from pSK236 (101). Additionally, *radC* overexpression mutants should be constructed in the background of the highly resistant mutants of the F1-F30 collection and these should be analysed by restriction mapping for the determination of copies in tandem of pRS2. For this, *radC* would be cloned under the transcriptional control of pcad promoter in replicative plasmid pBCB8.

This mutant will allow to observe the effect of provide copies of *radC* in a background with no impairment of *rho* gene.

Regarding the pathway of stringent response triggered in F9H, the comparison of the transcriptomic data of F9H and F9 suggested that the pathway through which stringent response

exerts this reversion, might depend on the *pyr* operon that encodes the enzymes of the biosynthesis of pyrimidines. In other bacterial species, such as in *Lactococcus lactis,* an association between the biosynthesis of pyrimidines, the integrity of the cell wall and the levels of the alarmone (p)ppGpp, the first messenger of stringent response, was already demonstrated. A survey for lysozyme resistant mutants identified a *guaA* mutant. This gene encodes an enzyme responsible for the formation of guanosine monophosphate (GMP) and consequently important in the synthesis of the alarmone (p)ppGpp. The mutation in *guaA* results in the decrease of the expression of the *pyr* operon, which maintains L-aspartate free to be utilized in peptidoglycan biosynthesis, since in this species, the cross linking between adjacent peptides is formed by L-asp bridges (271). We hypothesize that in the case of the F9H mutant, the stringent response, through the alarmone (p)ppGpp, may inhibit one or more of the enzymes of the GTP biosynthetic pathway, as occurs in other bacteria, and as is known to happen in the regulatory mechanism of (p)ppGpp, leading to an increase in the transcription of the *pyr* operon, which suggests an important interconnection between the purines and pyrimidines metabolism pathways. The increase in the *pyr* operon expression lead to higher production of 2'-Deoxyuridine 5'-triphosphate (dUTP), a pyrimidine derivative, used in the formation of uridine-5'-diphosphate-*N*-acetylglucosamine (UDP-GlcNAc) in the first cytoplasmic step of the peptidoglycan biosynthetic pathway. This observation may unveil the role of *pyr* operon and suggests a new element to be considered in further investigation on the topic of stringent response. We additionally anticipate the importance of the hypothetical protein SACOL1218 located immediately downstream of *pyrE* gene and with the same pattern of transcription response. In order to address this hypothesis we aim to construct a conditional mutant F9H::pcad*pyrR* in which the chromosomal copy of the regulator element of the *pyr* operon is placed under the transcriptional control of the pcad inducible promotor. The analysis of the muropeptides will be performed by RP-HPLC in order to verify if down-regulating the expression of the *pyrR* regulator promotes an increase in the tripeptide accumulated at cell wall.

However, the pathway of biosynthesis of pyrimidines is linked to many other pathways and a reduction in the expression of *pyrR* may affect the phenotype of accumulation of tripeptide in an indirect way

Another hypothesis is that the lower metabolism induced by stringent response, and the consequent lower growth rate, provides more time for the cell to produce pentapeptide and to drain the tripeptide which accumulates due to low levels of MurF enzyme. The leak of the intermediates of peptidoglycan biosynthesis could be the reason for the increase in the expression of the *pyr* operon genes since unlocking the pathway requires a higher production of 2'-Deoxyuridine 5'-triphosphate (dUTP). To verify this hypothesis, in which the increase in the expression of *pyr* operon genes is a consequence of the decrease in the accumulation of tripeptide by stringent response, we aim to promote the decrease of the growth rate of the F9 insertion mutant and analyze the muropeptide composition of the mutant to determine if a decrease in the rate of formation of peptidoglycan is sufficient to promote a decrease in the tripeptide accumulated at the cell wall.

The decrease in growth rate will be achieved by growing bacteria in minimal medium, at a lower temperature or at a lower aeration rate.

The transcriptomic analysis particularly highlighted two short-sequence genes, SACOL0676 and SACOL0677 consecutively located in the chromosome, annotated as hypothetical proteins, as being overexpressed more than 200 fold in F9 and F9H. These genes are exclusive of staphylococcal species and have almost no homology to sequences available in the databases. One of the genes, SACOL0677 showed low sequence homology with part of a diguanylate cyclase of *Thermosipho melanesiensis* and SACOL0676 with a response regulator receiver domain protein of *Synechococcus* sp. We have demonstrated that these ORFs are transcribed into two proteins. Immediately downstream, a third gene, that encodes a large protein with 10 transmembrane domains, was also found to be overexpressed both in F9 and F9H mutants. The protein includes two EamA domains with opposite folding which is a common feature of a drug/metabolite exporter. In order to understand their function, several genetic and biochemical approaches were pursued. Our findings showed the ability of SACOL0676 and SACOL0677 proteins to bind to DNA, suggesting that they may act as transcriptional regulators. NMR analysis performed in the presence of membrane mimetics, indicated that SACOL0676 may associate to the phospholipidic membrane of *S. aureus*. The integration of these preliminary results allowed us to suggest that the SACOL0676-0677-0675 may consist of a three component system, which would be transcriptionally activated as a response to the *rho* impairment and could be involved in the sensing of the damage at the cell surface and on the corresponding signal transduction. The transmembrane protein SACOL0675 could act as a sensor partner that transduces the signal to the response regulators or effectors SACOL0676 and SACOL0677. The homology of SACOL0677 with a diguanylate cyclase further extended the hypothesis that this system could transduce a signal in a cyclic-di-GMP dependent cascade.

Furthermore, we constructed mutants of SACOL0676 and/or SACOL0677 in COL strain and observed that the induction of these genes was highly detrimental for the cell viability, in a dose dependent manner, which indicates that the expression of these genes must be tightly controlled in the cell. The altered expression of these three determinants in F9 and F9H was most probably triggered by the impairment of *rho* gene, but unexpectedly, did not have the same growth impairment effect as it did for COL strain. This result allowed us to put forward the hypothesis that the overexpression of the SACOL0676/0677 system may have an important role in the adaptation of the cell to a lethal stress. So, it would be very important to identify partners of this system. As a next step in this work, we aim to identify the DNA sequences to which SACOL0677 and SACOL0676 bind to clarify the pathways in which this system is involved. The identification of the DNA sequence would be performed using the IDAP-seq technique, which stands for *in vitro* DNA affinity purification, combined with massive next-generation sequencing (282). In this technique, the recombinant proteins are overproduced, purified and combined with fragmented genomic DNA. Then, the Protein-DNA complex is cross-linked and pulled-down by immunoprecipitation. The protein is digested and the retrieved DNA is sequenced by high throughput sequencing.

The DNA binding capacity of SACOL0677 and SACOL0676 will be used in an attempt to elucidate the structure of the proteins by performing NMR of the proteins in the presence of DNA. Due to the DNA binding capacity of the proteins, the presence of DNA may stabilize the proteins or contribute to its proper folding.

Additionally, the construction of a conditional mutant COLpcad0675 showed that the impairment or absence of SACOL0675 did not have an impact on growth neither on the β-lactams resistance level.

However, the expression of the gene was essential for the normal growth of COL in the presence of sub-inhibitory concentrations of oxacillin in liquid medium. The fact that SACOL0675 has a role in resistance to oxacillin in liquid medium, but not in solid medium, suggests a role for the protein as an exporter of an yet unknown compound to the external medium that would be important for *S. aureus* survival to sub-inhibitory concentrations of oxacillin or, as an exporter of a toxic component that may accumulate inside the cells as a product of the challenge with oxacillin. However, this did not exclude a role for SACOL0675 has a sensory domain of a three-component system.

Firstly, in order to determine if SACOL0675 exports a compound that may act as a signal for the neighboring cells in the population, we will grow cells of the conditional mutant COL in the presence of a sub-inhibitory concentration of oxacillin. At this point, the culture will be filtered and the medium recovered. Another culture of COLpcad0675 will be inoculated in the previously recovered medium with the same oxacillin challenge and in the absence of inducer. If the cells are able to resist to the oxacillin challenge, this will indicate that the medium contains a signaling compound, exported by the first batch of cells grown, that allows bacteria to survive to the antibiotic sub-inhibitory concentration.

Altogether, the results obtained in this thesis, provided new insights on the complex dynamic of cell wall integrity and resistance to β-lactams in *S. aureus* and allowed the addition of one new player to this equation: the Rho factor. This work allowed to observe the diversity of successful strategies that *S. aureus* employs to overcome challenges, such as cell wall damage. On one hand, the expression of *rho* triggered homologous recombination events, leading to the tandem amplification of the plasmid in the chromosome that resulted in the reestablishment of the level of high resistance in the mutants, probably through the restore of a full *murF* gene. On the other hand, when *rho* gene was impaired, there was no amplification of the plasmid copies, a process that seems essential for the strain to solve the decreased resistance. Yet, even in the presence of a mutated *rho* gene, the strain was still able to survive to the otherwise lethal damage, although not being able to correct the primary cell wall defect.

This capacity may be due to the putative SACOL0676-0677-0675 system which expression is triggered by *rho* impairment and that we suggested may form a three component system involved in the survival of *S. aureus* to cell wall damage.

Lastly, another successful strategy of *S. aureus* to survive antibiotic challenge and cell wall damage that was highlighted in our study was the mechanism of stringent response, usually triggered by nutrient limiting conditions that resulted in the repair of the cell wall defect and in the reversion of the phenotype of resistance.

References

1. A. Ogston, Report upon Micro-Organisms in Surgical Diseases. *Br Med J* **1**, 369.b362-375 (1881).
2. F. J. Rosenbach (1884) Mikro-organismen bei den Wund-Infections-Krankheiten des Menschen. (Wiesbaden JF Bergmann), p 18.
3. S. Karl-Heinz, J. A. Bell, *BERGEY'S MANUAL OF Systematic Bacteriology*. W. B. Whitman, Ed. (Springer, ed. 2nd, 2009), vol. 3, pp. 1422.
4. W. Yu, H. K. Kim, S. Rauch, O. Schneewind, D. Missiakas, Pathogenic conversion of coagulase-negative staphylococci. *Microbes Infect* **19**, 101-109 (2017).
5. A. Sakr, F. Brégeon, J. L. Mège, J. M. Rolain, O. Blin, *Staphylococcus aureus* Nasal Colonization: An Update on Mechanisms, Epidemiology, Risk Factors, and Subsequent Infections. *Front Microbiol* **9**, 2419 (2018).
6. A. F. Brown, J. M. Leech, T. R. Rogers, R. M. McLoughlin, *Staphylococcus aureus* Colonization: Modulation of Host Immune Response and Impact on Human Vaccine Design. *Front Immunol* **4**, 507 (2014).
7. B. Krismer, C. Weidenmaier, A. Zipperer, A. Peschel, The commensal lifestyle of *Staphylococcus aureus* and its interactions with the nasal microbiota. *Nat Rev Microbiol* **15**, 675-687 (2017).
8. J. J. Yang *et al.*, Commensal *Staphylococcus aureus* Provokes Immunity to Protect against Skin Infection of Methicillin-Resistant *Staphylococcus aureus*. *Int J Mol Sci* **19** (2018).
9. A. G. Peres, J. Madrenas, The broad landscape of immune interactions with *Staphylococcus aureus*: from commensalism to lethal infections. *Burns* **39**, 380-388 (2013).
10. S. Y. Tong, J. S. Davis, E. Eichenberger, T. L. Holland, V. G. Fowler, Jr., *Staphylococcus aureus* infections: epidemiology, pathophysiology, clinical manifestations, and management. *Clin Microbiol Rev* **28**, 603-661 (2015).
11. E. J. G. Pollitt, P. T. Szkuta, N. Burns, S. J. Foster, *Staphylococcus aureus* infection dynamics. *PLoS Pathog* **14**, e1007112 (2018).
12. E. F. Kong, J. K. Johnson, M. A. Jabra-Rizk, Community-Associated Methicillin-Resistant *Staphylococcus aureus*: An Enemy amidst Us. *PLoS Pathog* **12**, e1005837 (2016).
13. A. R. Richardson, Virulence and Metabolism. *Microbiol Spectr* **7** (2019).
14. H. Li, Y. Ding, L. Lan, Transcriptional profiling of CcpE-regulated genes in *Staphylococcus aureus*. *Genom Data* **5**, 157-158 (2015).
15. T. Geiger, C. Wolz, Intersection of the stringent response and the CodY regulon in low GC Gram-positive bacteria. *Int J Med Microbiol* **304**, 150-155 (2014).
16. C. Jenul, A. R. Horswill, Regulation of *Staphylococcus aureus* Virulence. *Microbiol Spectr* **6** (2018).
17. A. A. Mashruwala, A. V. Guchte, J. M. Boyd, Impaired respiration elicits SrrAB-dependent programmed cell lysis and biofilm formation in *Staphylococcus aureus*. *Elife* **6** (2017).
18. Q. Liu, W. S. Yeo, T. Bae, The SaeRS Two-Component System of *Staphylococcus aureus*. *Genes (Basel)* **7** (2016).
19. B. Fournier, A. Klier, G. Rapoport, The two-component system ArlS-ArlR is a regulator of virulence gene expression in *Staphylococcus aureus*. *Mol Microbiol* **41**, 247-261 (2001).
20. A. Kuipers *et al.*, The *Staphylococcus aureus* polysaccharide capsule and Efb-dependent fibrinogen shield act in concert to protect against phagocytosis. *Microbiology* **162**, 1185-1194 (2016).
21. C. von Eiff *et al.*, Distribution of capsular and surface polysaccharide serotypes of *Staphylococcus aureus*. *Diagn Microbiol Infect Dis* **58**, 297-302 (2007).
22. M. Rajagopal, S. Walker, Envelope Structures of Gram-Positive Bacteria. *Curr Top Microbiol Immunol* **404**, 1-44 (2017).
23. W. Vollmer, D. Blanot, M. A. de Pedro, Peptidoglycan structure and architecture. *FEMS Microbiol Rev* **32**, 149-167 (2008).
24. V. R. Matias, T. J. Beveridge, Cryo-electron microscopy of cell division in *Staphylococcus aureus* reveals a mid-zone between nascent cross walls. *Mol Microbiol* **64**, 195-206 (2007).
25. J. G. Swoboda, J. Campbell, T. C. Meredith, S. Walker, Wall teichoic acid function, biosynthesis, and inhibition. *Chembiochem* **11**, 35-45 (2010).
26. S. Brown, J. P. Santa Maria, Jr., S. Walker, Wall teichoic acids of gram-positive bacteria. *Annu Rev Microbiol* **67**, 313-336 (2013).

27. Y. G. Chan, M. B. Frankel, V. Dengler, O. Schneewind, D. Missiakas, *Staphylococcus aureus* mutants lacking the LytR-CpsA-Psr family of enzymes release cell wall teichoic acids into the extracellular medium. *J Bacteriol* **195**, 4650-4659 (2013).
28. F. C. Neuhaus, J. Baddiley, A continuum of anionic charge: structures and functions of D-alanyl-teichoic acids in gram-positive bacteria. *Microbiol Mol Biol Rev* **67**, 686-723 (2003).
29. N. Mistretta *et al.*, Glycosylation of *Staphylococcus aureus* cell wall teichoic acid is influenced by environmental conditions. *Sci Rep* **9**, 3212 (2019).
30. D. Gerlach *et al.*, Methicillin-resistant *Staphylococcus aureus* alters cell wall glycosylation to evade immunity. *Nature* **563**, 705-709 (2018).
31. S. Brown *et al.*, Methicillin resistance in *Staphylococcus aureus* requires glycosylated wall teichoic acids. *Proc Natl Acad Sci U S A* **109**, 18909-18914 (2012).
32. J. Schade, C. Weidenmaier, Cell wall glycopolymers of Firmicutes and their role as nonprotein adhesins. *FEBS Lett* **590**, 3758-3771 (2016).
33. S. K. Mazmanian, G. Liu, H. Ton-That, O. Schneewind, *Staphylococcus aureus* sortase, an enzyme that anchors surface proteins to the cell wall. *Science* **285**, 760-763 (1999).
34. A. Ruzin *et al.*, Further evidence that a cell wall precursor [C(55)-MurNAc-(peptide)-GlcNAc] serves as an acceptor in a sorting reaction. *J Bacteriol* **184**, 2141-2147 (2002).
35. O. Schneewind, D. Missiakas, Sortases, Surface Proteins, and Their Roles in *Staphylococcus aureus* Disease and Vaccine Development. *Microbiol Spectr* **7** (2019).
36. P. Giesbrecht, T. Kersten, H. Maidhof, J. Wecke, Staphylococcal cell wall: morphogenesis and fatal variations in the presence of penicillin. *Microbiol Mol Biol Rev* **62**, 1371-1414 (1998).
37. I. G. Boneca, Z. H. Huang, D. A. Gage, A. Tomasz, Characterization of *Staphylococcus aureus* cell wall glycan strands, evidence for a new beta-N-acetylglucosaminidase activity. *J Biol Chem* **275**, 9910-9918 (2000).
38. T. R. Walsh, R. A. Howe, The prevalence and mechanisms of vancomycin resistance in *Staphylococcus aureus*. *Annu Rev Microbiol* **56**, 657-675 (2002).
39. Y. Asano, T. L. Lubbehusen, Enzymes acting on peptides containing D-amino acid. *J Biosci Bioeng* **89**, 295-306 (2000).
40. R. Sobral, A. Tomasz, The Staphylococcal Cell Wall. *Microbiol Spectr* **7** (2019).
41. B. L. de Jonge, Y. S. C hang, D. Gage, A. Tomasz, Peptidoglycan composition of a highly methicillin-resistant *Staphylococcus aureus* strain. The role of penicillin binding protein 2A. *J Biol Chem* **267**, 11248-11254 (1992).
42. B. L. de Jonge, Y. S. Chang, D. Gage, A. Tomasz, Peptidoglycan composition of a highly methicillin-resistant *Staphylococcus aureus* strain. The role of penicillin binding protein 2A. *J Biol Chem* **267**, 11248-11254 (1992).
43. M. Jarick *et al.*, The serine/threonine kinase Stk and the phosphatase Stp regulate cell wall synthesis in *Staphylococcus aureus*. *Sci Rep* **8**, 13693 (2018).
44. P. Glanzmann, J. Gustafson, H. Komatsuzawa, K. Ohta, B. Berger-Bachi, glmM operon and methicillin-resistant glmM suppressor mutants in *Staphylococcus aureus*. *Antimicrob Agents Chemother* **43**, 240-245 (1999).
45. J. T. Park, Uridine-5'-pyrophosphate derivatives. III. Amino acid-containing derivatives. *J Biol Chem* **194**, 897-904 (1952).
46. H. Barreteau *et al.*, Cytoplasmic steps of peptidoglycan biosynthesis. *FEMS Microbiol Rev* **32**, 168-207 (2008).
47. E. J. Lugtenberg, A. v Schijndel-van Dam, Temperature-sensitive mutants of *Escherichia coli* K-12 with low activities of the L-alanine adding enzyme and the D-alanyl-D-alanine adding enzyme. *J Bacteriol* **110**, 35-40 (1972).
48. C. A. Smith, Structure, function and dynamics in the mur family of bacterial cell wall ligases. *J Mol Biol* **362**, 640-655 (2006).
49. Y. Sheng *et al.*, Structural and functional similarities in the ADP-forming amide bond ligase superfamily: implications for a substrate-induced conformational change in folylpolyglutamate synthetase. *J Mol Biol* **302**, 427-440 (2000).
50. J. A. Bertrand *et al.*, Crystal structure of UDP-N-acetylmuramoyl-L-alanine:D-glutamate ligase from *Escherichia coli*. *Embo j* **16**, 3416-3425 (1997).
51. M. S. Anderson, S. S. Eveland, H. R. Onishi, D. L. Pompliano, Kinetic mechanism of the *Escherichia coli* UDPMurNAc-tripeptide D-alanyl-D-alanine-adding enzyme: use of a glutathione S-transferase fusion. *Biochemistry* **35**, 16264-16269 (1996).
52. T. A. Figueiredo *et al.*, Identification of genetic determinants and enzymes involved with the amidation of glutamic acid residues in the peptidoglycan of *Staphylococcus aureus*. *PLoS Pathog* **8**, e1002508 (2012).

53. D. Munch *et al.*, Identification and in vitro analysis of the GatD/MurT enzyme-complex catalyzing lipid II amidation in *Staphylococcus aureus*. *PLoS Pathog* **8**, e1002509 (2012).
54. E. Ito, J. L. Strominger, Enzymatic synthesis of the peptide in bacterial uridine nucleotides. VII. Comparative biochemistry. *J Biol Chem* **248**, 3131-3136 (1973).
55. C. T. Walsh, Enzymes in the D-alanine branch of bacterial cell wall peptidoglycan assembly. *J Biol Chem* **264**, 2393-2396 (1989).
56. K. Duncan, J. van Heijenoort, C. T. Walsh, Purification and characterization of the D-alanyl-D-alanine-adding enzyme from *Escherichia coli. Biochemistry* **29**, 2379-2386 (1990).
57. B. L. de Jonge, Y. S. Chang, N. Xu, D. Gage, Effect of exogenous glycine on peptidoglycan composition and resistance in a methicillin-resistant *Staphylococcus aureus* strain. *Antimicrob Agents Chemother* **40**, 1498-1503 (1996).
58. R. G. Sobral *et al.*, Normally functioning murF is essential for the optimal expression of methicillin resistance in *Staphylococcus aureus*. *Microb Drug Resist* **9**, 231-241 (2003).
59. R. G. Sobral, A. M. Ludovice, H. de Lencastre, A. Tomasz, Role of murF in cell wall biosynthesis: isolation and characterization of a murF conditional mutant of *Staphylococcus aureus*. *J Bacteriol* **188**, 2543-2553 (2006).
60. R. G. Sobral *et al.*, Extensive and genome-wide changes in the transcription profile of *Staphylococcus aureus* induced by modulating the transcription of the cell wall synthesis gene murF. *J Bacteriol* **189**, 2376-2391 (2007).
61. Y. J. An, C. S. Jeong, J. H. Yu, K. M. Chung, S. S. Cha, Purification, crystallization and preliminary X-ray crystallographic analysis of the UDP-N-acetylmuramoyl-tripeptide-D-alanyl-D-alanine ligase (MurF) from *Acinetobacter baumannii*. *Acta Crystallogr F Struct Biol Commun* **70**, 976-978 (2014).
62. K. L. Longenecker *et al.*, Structure of MurF from *Streptococcus pneumoniae* co-crystallized with a small molecule inhibitor exhibits interdomain closure. *Protein Sci* **14**, 3039-3047 (2005).
63. Y. G. Gu *et al.*, Structure-activity relationships of novel potent MurF inhibitors. *Bioorg Med Chem Lett* **14**, 267-270 (2004).
64. M. Hrast *et al.*, Design, synthesis and evaluation of second generation MurF inhibitors based on a cyanothiophene scaffold. *Eur J Med Chem* **73**, 83-96 (2014).
65. J. N. Sangshetti, S. S. Joshi, R. H. Patil, M. G. Moloney, D. B. Shinde, Mur Ligase Inhibitors as Anti-bacterials: A Comprehensive Review. *Curr Pharm Des* **23**, 3164-3196 (2017).
66. M. Jukic, S. Gobec, M. Sova, Reaching toward underexplored targets in antibacterial drug design. *Drug Dev Res* **80**, 6-10 (2019).
67. Y. Higashi, G. Siewert, J. L. Strominger, Biosynthesis of the peptidoglycan of bacterial cell walls. XIX. Isoprenoid alcohol phosphokinase. *J Biol Chem* **245**, 3683-3690 (1970).
68. M. Ikeda, M. Wachi, H. K. Jung, F. Ishino, M. Matsuhashi, The *Escherichia coli* mraY gene encoding UDP-N-acetylmuramoyl-pentapeptide: undecaprenyl-phosphate phospho-N-acetylmuramoyl-pentapeptide transferase. *J Bacteriol* **173**, 1021-1026 (1991).
69. A. Bouhss, D. Mengin-Lecreulx, D. Le Beller, J. Van Heijenoort, Topological analysis of the MraY protein catalysing the first membrane step of peptidoglycan synthesis. *Mol Microbiol* **34**, 576-585 (1999).
70. T. Mohammadi *et al.*, Identification of FtsW as a transporter of lipid-linked cell wall precursors across the membrane. *Embo j* **30**, 1425-1432 (2011).
71. S. Rohrer, K. Ehlert, M. Tschierske, H. Labischinski, B. Berger-Bachi, The essential *Staphylococcus aureus* gene fmhB is involved in the first step of peptidoglycan pentaglycine interpeptide formation. *Proc Natl Acad Sci U S A* **96**, 9351-9356 (1999).
72. H. Maidhof, B. Reinicke, P. Blümel, B. Berger-Bächi, H. Labischinski, femA, which encodes a factor essential for expression of methicillin resistance, affects glycine content of peptidoglycan in methicillin-resistant and methicillin-susceptible *Staphylococcus aureus* strains. *J Bacteriol* **173**, 3507-3513 (1991).
73. M. Matsuhashi, C. P. Dietrich, J. L. Strominger, Incorporation of glycine into the cell wall glycopeptide in *Staphylococcus aureus*: role of sRNA and lipid intermediates. *Proc Natl Acad Sci U S A* **54**, 587-594 (1965).
74. J. M. Monteiro *et al.*, The pentaglycine bridges of *Staphylococcus aureus* peptidoglycan are essential for cell integrity. *Sci Rep* **9**, 5010 (2019).
75. A. M. Stranden, K. Ehlert, H. Labischinski, B. Berger-Bachi, Cell wall monoglycine cross-bridges and methicillin hypersusceptibility in a femAB null mutant of methicillin-resistant *Staphylococcus aureus*. *J Bacteriol* **179**, 9-16 (1997).

76. U. Henze, T. Sidow, J. Wecke, H. Labischinski, B. Berger-Bachi, Influence of femB on methicillin resistance and peptidoglycan metabolism in *Staphylococcus aureus*. *J Bacteriol* **175**, 1612-1620 (1993).
77. B. V. Goncalves *et al.*, The role of MurT C-terminal domain in the amidation of *Staphylococcus aureus* peptidoglycan. *Antimicrob Agents Chemother* (2019).
78. A. Zapun *et al.*, In vitro reconstitution of peptidoglycan assembly from the Gram-positive pathogen *Streptococcus pneumoniae*. *ACS Chem Biol* **8**, 2688-2696 (2013).
79. T. A. Figueiredo, A. M. Ludovice, R. G. Sobral, Contribution of peptidoglycan amidation to beta-lactam and lysozyme resistance in different genetic lineages of *Staphylococcus aureus*. *Microb Drug Resist* **20**, 238-249 (2014).
80. M. G. Pinho, J. Errington, Dispersed mode of *Staphylococcus aureus* cell wall synthesis in the absence of the division machinery. *Mol Microbiol* **50**, 871-881 (2003).
81. D. J. Scheffers, M. G. Pinho, Bacterial cell wall synthesis: new insights from localization studies. *Microbiol Mol Biol Rev* **69**, 585-607 (2005).
82. J. M. Ghuysen, Serine beta-lactamases and penicillin-binding proteins. *Annu Rev Microbiol* **45**, 37-67 (1991).
83. P. Reed, H. Veiga, A. M. Jorge, M. Terrak, M. G. Pinho, Monofunctional transglycosylases are not essential for *Staphylococcus aureus* cell wall synthesis. *J Bacteriol* **193**, 2549-2556 (2011).
84. Q. M. Wang *et al.*, Identification and characterization of a monofunctional glycosyltransferase from *Staphylococcus aureus*. *J Bacteriol* **183**, 4779-4785 (2001).
85. N. H. Georgopapadakou, B. A. Dix, Y. R. Mauriz, Possible physiological functions of penicillin-binding proteins in *Staphylococcus aureus*. *Antimicrob Agents Chemother* **29**, 333-336 (1986).
86. B. Hartman, A. Tomasz, Altered penicillin-binding proteins in methicillin-resistant strains of *Staphylococcus aureus*. *Antimicrob Agents Chemother* **19**, 726-735 (1981).
87. C. Goffin, J. M. Ghuysen, Multimodular penicillin-binding proteins: an enigmatic family of orthologs and paralogs. *Microbiol Mol Biol Rev* **62**, 1079-1093 (1998).
88. X. Fan *et al.*, Diversity of penicillin-binding proteins. Resistance factor FmtA of *Staphylococcus aureus*. *J Biol Chem* **282**, 35143-35152 (2007).
89. A. Wada, H. Watanabe, Penicillin-binding protein 1 of *Staphylococcus aureus* is essential for growth. *J Bacteriol* **180**, 2759-2765 (1998).
90. S. F. Pereira, A. O. Henriques, M. G. Pinho, H. de Lencastre, A. Tomasz, Role of PBP1 in cell division of *Staphylococcus aureus*. *J Bacteriol* **189**, 3525-3531 (2007).
91. P. Reed *et al.*, *Staphylococcus aureus* Survives with a Minimal Peptidoglycan Synthesis Machine but Sacrifices Virulence and Antibiotic Resistance. *PLoS Pathog* **11**, e1004891 (2015).
92. S. F. Pereira, A. O. Henriques, M. G. Pinho, H. de Lencastre, A. Tomasz, Evidence for a dual role of PBP1 in the cell division and cell separation of *Staphylococcus aureus*. *Mol Microbiol* **72**, 895-904 (2009).
93. T. A. Łeski, A. Tomasz, Role of penicillin-binding protein 2 (PBP2) in the antibiotic susceptibility and cell wall cross-linking of *Staphylococcus aureus*: evidence for the cooperative functioning of PBP2, PBP4, and PBP2A. *J Bacteriol* **187**, 1815-1824 (2005).
94. M. G. Pinho, S. R. Filipe, H. de Lencastre, A. Tomasz, Complementation of the essential peptidoglycan transpeptidase function of penicillin-binding protein 2 (PBP2) by the drug resistance protein PBP2A in *Staphylococcus aureus*. *J Bacteriol* **183**, 6525-6531 (2001).
95. M. G. Pinho, H. de Lencastre, A. Tomasz, An acquired and a native penicillin-binding protein cooperate in building the cell wall of drug-resistant staphylococci. *Proc Natl Acad Sci U S A* **98**, 10886-10891 (2001).
96. V. Srisuknimit, Y. Qiao, K. Schaefer, D. Kahne, S. Walker, Peptidoglycan Cross-Linking Preferences of *Staphylococcus aureus* Penicillin-Binding Proteins Have Implications for Treating MRSA Infections. *J Am Chem Soc* **139**, 9791-9794 (2017).
97. M. G. Pinho, H. de Lencastre, A. Tomasz, Cloning, characterization, and inactivation of the gene pbpC, encoding penicillin-binding protein 3 of *Staphylococcus aureus*. *J Bacteriol* **182**, 1074-1079 (2000).
98. R. Kylvaja, T. Ojalehto, V. Kainulainen, R. Virkola, B. Westerlund-Wikstrom, Penicillin binding protein 3 of *Staphylococcus aureus* NCTC 8325-4 binds and activates human plasminogen. *BMC Res Notes* **9**, 389 (2016).
99. K. Sieradzki, M. G. Pinho, A. Tomasz, Inactivated pbp4 in highly glycopeptide-resistant laboratory mutants of *Staphylococcus aureus*. *J Biol Chem* **274**, 18942-18946 (1999).

100. Y. Qiao *et al.*, Detection of lipid-linked peptidoglycan precursors by exploiting an unexpected transpeptidase reaction. *J Am Chem Soc* **136**, 14678-14681 (2014).
101. G. Memmi, S. R. Filipe, M. G. Pinho, Z. Fu, A. Cheung, *Staphylococcus aureus* PBP4 is essential for beta-lactam resistance in community-acquired methicillin-resistant strains. *Antimicrob Agents Chemother* **52**, 3955-3966 (2008).
102. S. M. Hamilton *et al.*, High-Level Resistance of *Staphylococcus aureus* to beta-Lactam Antibiotics Mediated by Penicillin-Binding Protein 4 (PBP4). *Antimicrob Agents Chemother* **61** (2017).
103. D. Lim, N. C. Strynadka, Structural basis for the beta lactam resistance of PBP2a from methicillin-resistant *Staphylococcus aureus*. *Nat Struct Biol* **9**, 870-876 (2002).
104. K. V. Mahasenan *et al.*, Conformational Dynamics in Penicillin-Binding Protein 2a of Methicillin-Resistant *Staphylococcus aureus*, Allosteric Communication Network and Enablement of Catalysis. *J Am Chem Soc* **139**, 2102-2110 (2017).
105. A. Bera, R. Biswas, S. Herbert, F. Gotz, The presence of peptidoglycan O-acetyltransferase in various staphylococcal species correlates with lysozyme resistance and pathogenicity. *Infect Immun* **74**, 4598-4604 (2006).
106. A. C. Pushkaran *et al.*, Understanding the Structure-Function Relationship of Lysozyme Resistance in *Staphylococcus aureus* by Peptidoglycan O-Acetylation Using Molecular Docking, Dynamics, and Lysis Assay. *J Chem Inf Model* **55**, 760-770 (2015).
107. O. Irazoki, S. B. Hernandez, F. Cava, Peptidoglycan Muropeptides: Release, Perception, and Functions as Signaling Molecules. *Front Microbiol* **10**, 500 (2019).
108. D. J. Tipper, Mechanism of autolysis of isolated cell walls of *Staphylococcus aureus*. *J Bacteriol* **97**, 837-847 (1969).
109. M. Schindler, Y. Assaf, N. Sharon, D. M. Chipman, Mechanism of lysozyme catalysis: role of ground-state strain in subsite D in hen egg-white and human lysozymes. *Biochemistry* **16**, 423-431 (1977).
110. A. S. Brott, A. J. Clarke, Peptidoglycan O-Acetylation as a Virulence Factor: Its Effect on Lysozyme in the Innate Immune System. *Antibiotics (Basel)* **8** (2019).
111. W. Vollmer, B. Joris, P. Charlier, S. Foster, Bacterial peptidoglycan (murein) hydrolases. *FEMS Microbiol Rev* **32**, 259-286 (2008).
112. R. Sharma, P. R. Sharma, M. L. Choudhary, A. Pande, G. S. Khatri, Cytoplasmic expression of mature glycylglycine endopeptidase lysostaphin with an amino terminal hexa-histidine in a soluble and catalytically active form in *Escherichia coli*. *Protein Expr Purif* **45**, 206-215 (2006).
113. M. Sugai, T. Akiyama, H. Komatsuzawa, Y. Miyake, H. Suginaka, Characterization of sodium dodecyl sulfate-stable *Staphylococcus aureus* bacteriolytic enzymes by polyacrylamide gel electrophoresis. *J Bacteriol* **172**, 6494-6498 (1990).
114. T. Oshida, A. Tomasz, Isolation and characterization of a Tn551-autolysis mutant of *Staphylococcus aureus*. *J Bacteriol* **174**, 4952-4959 (1992).
115. S. J. Foster, Molecular characterization and functional analysis of the major autolysin of *Staphylococcus aureus* 8325/4. *J Bacteriol* **177**, 5723-5725 (1995).
116. I. R. Grilo, A. M. Ludovice, A. Tomasz, H. de Lencastre, R. G. Sobral, The glucosaminidase domain of Atl - the major *Staphylococcus aureus* autolysin - has DNA-binding activity. *Microbiologyopen* **3**, 247-256 (2014).
117. J. Kajimura *et al.*, Identification and molecular characterization of an N-acetylmuramyl-L-alanine amidase Sle1 involved in cell separation of *Staphylococcus aureus*. *Mol Microbiol* **58**, 1087-1101 (2005).
118. M. B. Frankel, A. P. Hendrickx, D. M. Missiakas, O. Schneewind, LytN, a murein hydrolase in the cross-wall compartment of *Staphylococcus aureus*, is involved in proper bacterial growth and envelope assembly. *J Biol Chem* **286**, 32593-32605 (2011).
119. L. Ramadurai, K. J. Lockwood, M. J. Nadakavukaren, R. K. Jayaswal, Characterization of a chromosomally encoded glycylglycine endopeptidase of *Staphylococcus aureus*. *Microbiology* **145 (Pt 4)**, 801-808 (1999).
120. G. Memmi, D. R. Nair, A. Cheung, Role of ArlRS in autolysis in methicillin-sensitive and methicillin-resistant *Staphylococcus aureus* strains. *J Bacteriol* **194**, 759-767 (2012).
121. K. H. Groicher, B. A. Firek, D. F. Fujimoto, K. W. Bayles, The *Staphylococcus aureus* lrgAB operon modulates murein hydrolase activity and penicillin tolerance. *J Bacteriol* **182**, 1794-1801 (2000).
122. L. Zheng, M. Yan, F. Fan, Y. Ji, The Essential WalK Histidine Kinase and WalR Regulator Differentially Mediate Autolysis of *Staphylococcus aureus* RN4220. *J Nat Sci* **1** (2015).

123. M. P. Trotonda, Y. Q. Xiong, G. Memmi, A. S. Bayer, A. L. Cheung, Role of mgrA and sarA in methicillin-resistant *Staphylococcus aureus* autolysis and resistance to cell wall-active antibiotics. *J Infect Dis* **199**, 209-218 (2009).
124. D. F. Fujimoto, K. W. Bayles, Opposing roles of the *Staphylococcus aureus* virulence regulators, Agr and Sar, in Triton X-100- and penicillin-induced autolysis. *J Bacteriol* **180**, 3724-3726 (1998).
125. O. Goldmann, E. Medina, *Staphylococcus aureus* strategies to evade the host acquired immune response. *Int J Med Microbiol* **308**, 625-630 (2018).
126. C. C. Fuda, J. F. Fisher, S. Mobashery, Beta-lactam resistance in *Staphylococcus aureus*: the adaptive resistance of a plastic genome. *Cell Mol Life Sci* **62**, 2617-2633 (2005).
127. A. A. Medeiros, Evolution and dissemination of beta-lactamases accelerated by generations of beta-lactam antibiotics. *Clin Infect Dis* **24 Suppl 1**, S19-45 (1997).
128. E. P. Abraham, E. Chain, An enzyme from bacteria able to destroy penicillin. 1940. *Rev Infect Dis* **10**, 677-678 (1988).
129. C. H. Rammelkamp, T. Maxon, Resistance of *Staphylococcus aureus* to the action of penicillin. *Proc. Royal Soc. Expert. Biol. Med.* **51**, 386-389 (1942).
130. G. N. Rolinson, S. Stevens, F. R. Batchelor, J. C. Wood, E. B. Chain, Bacteriological studies on a new penicillin-BRL. 1241. *Lancet* **2**, 564-567 (1960).
131. M. P. Jevons, "Celbenin" - resistant Staphylococci. *Br Med J* **1**, 124-125 (1961).
132. K. G. Dyke, M. P. Jevons, M. T. Parker, Penicillinase production and intrinsic resistance to penicillins in Staphylococcus aures. *Lancet* **1**, 835-838 (1966).
133. L. D. Sabath, S. J. Wallace, D. A. Gerstein, Suppression of intrinsic resistance to methicillin and other penicillins in *Staphylococcus aureus*. *Antimicrob Agents Chemother* **2**, 350-355 (1972).
134. S. R. Gill *et al.*, Insights on evolution of virulence and resistance from the complete genome analysis of an early methicillin-resistant *Staphylococcus aureus* strain and a biofilm-producing methicillin-resistant Staphylococcus epidermidis strain. *J Bacteriol* **187**, 2426-2438 (2005).
135. D. J. Diekema *et al.*, Survey of infections due to Staphylococcus species: frequency of occurrence and antimicrobial susceptibility of isolates collected in the United States, Canada, Latin America, Europe, and the Western Pacific region for the SENTRY Antimicrobial Surveillance Program, 1997-1999. *Clin Infect Dis* **32 Suppl 2**, S114-132 (2001).
136. W. A. McGuinness, N. Malachowa, F. R. DeLeo, Vancomycin Resistance in *Staphylococcus aureus*. *Yale J Biol Med* **90**, 269-281 (2017).
137. S. Gardete, A. Tomasz, Mechanisms of vancomycin resistance in *Staphylococcus aureus*. *J Clin Invest* **124**, 2836-2840 (2014).
138. K. A. Rodvold, K. W. McConeghy, Methicillin-resistant *Staphylococcus aureus* therapy: past, present, and future. *Clin Infect Dis* **58 Suppl 1**, S20-27 (2014).
139. S. Stefani, D. Bongiorno, G. Mongelli, F. Campanile, Linezolid Resistance in Staphylococci. *Pharmaceuticals (Basel)* **3**, 1988-2006 (2010).
140. A. J. Sabat *et al.*, Daptomycin Resistant *Staphylococcus aureus* Clinical Strain With Novel Non-synonymous Mutations in the mprF and vraS Genes: A New Insight Into Daptomycin Resistance. *Front Microbiol* **9**, 2705 (2018).
141. M. Yousefi *et al.*, Identification of tigecycline- and vancomycin-resistant *Staphylococcus aureus* strains among patients with urinary tract infection in Iran. *New Microbes New Infect* **19**, 8-12 (2017).
142. S. W. Long *et al.*, PBP2a mutations causing high-level Ceftaroline resistance in clinical methicillin-resistant *Staphylococcus aureus* isolates. *Antimicrob Agents Chemother* **58**, 6668-6674 (2014).
143. G. Morroni *et al.*, High Rate of Ceftobiprole Resistance among Clinical Methicillin-Resistant *Staphylococcus aureus* Isolates from a Hospital in Central Italy. *Antimicrob Agents Chemother* **62** (2018).
144. E. M. Harrison *et al.*, Genomic identification of cryptic susceptibility to penicillins and beta-lactamase inhibitors in methicillin-resistant *Staphylococcus aureus*. *Nat Microbiol* (2019).
145. K. Bush, Past and Present Perspectives on beta-Lactamases. *Antimicrob Agents Chemother* **62** (2018).
146. K. Bush, P. A. Bradford, beta-Lactams and beta-Lactamase Inhibitors: An Overview. *Cold Spring Harb Perspect Med* **6** (2016).
147. N. H. Georgopapadakou, Penicillin-binding proteins and bacterial resistance to beta-lactams. *Antimicrob Agents Chemother* **37**, 2045-2053 (1993).

148. I. Massova, S. Mobashery, Kinship and diversification of bacterial penicillin-binding proteins and beta-lactamases. *Antimicrob Agents Chemother* **42**, 1-17 (1998).
149. R. K. Voladri, D. S. Kernodle, Characterization of a chromosomal gene encoding type B beta-lactamase in phage group II isolates of *Staphylococcus aureus*. *Antimicrob Agents Chemother* **42**, 3163-3168 (1998).
150. J. E. Olsen, H. Christensen, F. M. Aarestrup, Diversity and evolution of blaZ from *Staphylococcus aureus* and coagulase-negative staphylococci. *J Antimicrob Chemother* **57**, 450-460 (2006).
151. S. J. Rowland, K. G. Dyke, Tn552, a novel transposable element from *Staphylococcus aureus*. *Mol Microbiol* **4**, 961-975 (1990).
152. C. J. Hackbarth, H. F. Chambers, blaI and blaR1 regulate beta-lactamase and PBP 2a production in methicillin-resistant *Staphylococcus aureus*. *Antimicrob Agents Chemother* **37**, 1144-1149 (1993).
153. S. R. Clarke, K. G. Dyke, The signal transducer (BlaRI) and the repressor (BlaI) of the *Staphylococcus aureus* beta-lactamase operon are inducible. *Microbiology* **147**, 803-810 (2001).
154. P. D. Gregory, R. A. Lewis, S. P. Curnock, K. G. Dyke, Studies of the repressor (BlaI) of beta-lactamase synthesis in *Staphylococcus aureus*. *Mol Microbiol* **24**, 1025-1037 (1997).
155. H. Z. Zhang, C. J. Hackbarth, K. M. Chansky, H. F. Chambers, A proteolytic transmembrane signaling pathway and resistance to beta-lactams in staphylococci. *Science* **291**, 1962-1965 (2001).
156. R. A. Lewis, S. P. Curnock, K. G. Dyke, Proteolytic cleavage of the repressor (BlaI) of beta-lactamase synthesis in *Staphylococcus aureus*. *FEMS Microbiol Lett* **178**, 271-275 (1999).
157. B. J. Hartman, A. Tomasz, Low-affinity penicillin-binding protein associated with beta-lactam resistance in *Staphylococcus aureus*. *J Bacteriol* **158**, 513-516 (1984).
158. E. M. Harrison *et al.*, A Staphylococcus xylosus isolate with a new mecC allotype. *Antimicrob Agents Chemother* **57**, 1524-1528 (2013).
159. G. K. Paterson *et al.*, The newly described *mecA* homologue, mecALGA251, is present in methicillin-resistant *Staphylococcus aureus* isolates from a diverse range of host species. *J Antimicrob Chemother* **67**, 2809-2813 (2012).
160. K. Becker *et al.*, Plasmid-Encoded Transferable mecB-Mediated Methicillin Resistance in *Staphylococcus aureus*. *Emerg Infect Dis* **24**, 242-248 (2018).
161. S. Schwendener, V. Perreten, The integrase of the *Macrococcus caseolyticus* resistance island mecD (McRImecD) inserts DNA site-specifically into *Staphylococcus* and *Bacillus* chromosomes. *Mol Microbiol* **110**, 455-468 (2018).
162. M. D. Song, M. Wachi, M. Doi, F. Ishino, M. Matsuhashi, Evolution of an inducible penicillin-target protein in methicillin-resistant *Staphylococcus aureus* by gene fusion. *FEBS Lett* **221**, 167-171 (1987).
163. G. L. Archer, D. M. Niemeyer, Origin and evolution of DNA associated with resistance to methicillin in staphylococci. *Trends Microbiol* **2**, 343-347 (1994).
164. S. Tsubakishita, K. Kuwahara-Arai, T. Sasaki, K. Hiramatsu, Origin and molecular evolution of the determinant of methicillin resistance in staphylococci. *Antimicrob Agents Chemother* **54**, 4352-4359 (2010).
165. J. Rolo *et al.*, Evidence for the evolutionary steps leading to *mecA*-mediated beta-lactam resistance in staphylococci. *PLoS Genet* **13**, e1006674 (2017).
166. M. Miragaia, Factors Contributing to the Evolution of *mecA*-Mediated beta-lactam Resistance in Staphylococci: Update and New Insights From Whole Genome Sequencing (WGS). *Front Microbiol* **9**, 2723 (2018).
167. Y. Katayama, T. Ito, K. Hiramatsu, A new class of genetic element, staphylococcus cassette chromosome mec, encodes methicillin resistance in *Staphylococcus aureus*. *Antimicrob Agents Chemother* **44**, 1549-1555 (2000).
168. S. Boundy *et al.*, Characterization of the *Staphylococcus aureus* rRNA methyltransferase encoded by orfX, the gene containing the staphylococcal chromosome Cassette mec (SCCmec) insertion site. *J Biol Chem* **288**, 132-140 (2013).
169. A. Misiura *et al.*, Roles of two large serine recombinases in mobilizing the methicillin-resistance cassette SCCmec. *Mol Microbiol* **88**, 1218-1229 (2013).
170. P. Arede, C. Milheirico, H. de Lencastre, D. C. Oliveira, The anti-repressor MecR2 promotes the proteolysis of the mecA repressor and enables optimal expression of beta-lactam resistance in MRSA. *PLoS Pathog* **8**, e1002816 (2012).

171. C. Milheirico, D. C. Oliveira, H. de Lencastre, Update to the multiplex PCR strategy for assignment of mec element types in *Staphylococcus aureus*. *Antimicrob Agents Chemother* **51**, 3374-3377 (2007).
172. C. Milheirico, D. C. Oliveira, H. de Lencastre, Multiplex PCR strategy for subtyping the staphylococcal cassette chromosome mec type IV in methicillin-resistant *Staphylococcus aureus*: 'SCCmec IV multiplex'. *J Antimicrob Chemother* **60**, 42-48 (2007).
173. P. G. Higgins, A. E. Rosato, H. Seifert, G. L. Archer, H. Wisplinghoff, Differential expression of ccrA in methicillin-resistant *Staphylococcus aureus* strains carrying staphylococcal cassette chromosome mec type II and IVa elements. *Antimicrob Agents Chemother* **53**, 4556-4558 (2009).
174. V. K. Sharma, C. J. Hackbarth, T. M. Dickinson, G. L. Archer, Interaction of native and mutant MecI repressors with sequences that regulate mecA, the gene encoding penicillin binding protein 2a in methicillin-resistant staphylococci. *J Bacteriol* **180**, 2160-2166 (1998).
175. G. L. Archer, J. M. Bosilevac, Signaling antibiotic resistance in staphylococci. *Science* **291**, 1915-1916 (2001).
176. K. Murakami, A. Tomasz, Involvement of multiple genetic determinants in high-level methicillin resistance in *Staphylococcus aureus*. *J Bacteriol* **171**, 874-879 (1989).
177. B. Berger-Bachi, A. Strassle, F. H. Kayser, Characterization of an isogenic set of methicillin-resistant and susceptible mutants of *Staphylococcus aureus*. *Eur J Clin Microbiol* **5**, 697-701 (1986).
178. B. J. Hartman, A. Tomasz, Expression of methicillin resistance in heterogeneous strains of *Staphylococcus aureus*. *Antimicrob Agents Chemother* **29**, 85-92 (1986).
179. M. Andrade-Figueiredo, T. C. Leal-Balbino, Clonal diversity and epidemiological characteristics of *Staphylococcus aureus*: high prevalence of oxacillin-susceptible mecA-positive *Staphylococcus aureus* (OS-MRSA) associated with clinical isolates in Brazil. *BMC Microbiol* **16**, 115 (2016).
180. S. Giannouli *et al.*, Detection of mutations in the FemXAB protein family in oxacillin-susceptible mecA-positive *Staphylococcus aureus* clinical isolates. *J Antimicrob Chemother* **65**, 626-633 (2010).
181. Y. Katayama, H. Z. Zhang, D. Hong, H. F. Chambers, Jumping the barrier to beta-lactam resistance in *Staphylococcus aureus*. *J Bacteriol* **185**, 5465-5472 (2003).
182. J. Kornblum, B. J. Hartman, R. P. Novick, A. Tomasz, Conversion of a homogeneously methicillin-resistant strain of *Staphylococcus aureus* to heterogeneous resistance by Tn551-mediated insertional inactivation. *Eur J Clin Microbiol* **5**, 714-718 (1986).
183. B. Berger-Bächi, Insertional inactivation of staphylococcal methicillin resistance by Tn551. *J Bacteriol* **154**, 479-487 (1983).
184. B. L. de Jonge *et al.*, Altered muropeptide composition in *Staphylococcus aureus* strains with an inactivated femA locus. *J Bacteriol* **175**, 2779-2782 (1993).
185. H. Lencastre, A. Tomasz, Reassessment of the number of auxiliary genes essential for expression of high-level methicillin resistance in Staphylococcus aureus. *Antimicrob Agents and Chemother* **38**, 2590-2598 (1994).
186. A. M. Ludovice, S. W. Wu, H. de Lencastre, Molecular cloning and DNA sequencing of the *Staphylococcus aureus* UDP-N-acetylmuramyl tripeptide synthetase (*murE*) gene, essential for the optimal expression of methicillin resistance. *Microb Drug Resist* **4**, 85-90 (1998).
187. A. Ornelas-Soares, H. de Lencastre, B. L. de Jonge, A. Tomasz, Reduced methicillin resistance in a new *Staphylococcus aureus* transposon mutant that incorporates muramyl dipeptides into the cell wall peptidoglycan. *J Biol Chem* **269**, 27246-27250 (1994).
188. R. A. Forsyth *et al.*, A genome-wide strategy for the identification of essential genes in *Staphylococcus aureus*. *Mol Microbiol* **43**, 1387-1400 (2002).
189. F. Jacob-Dubuisson, A. Mechaly, J. M. Betton, R. Antoine, Structural insights into the signalling mechanisms of two-component systems. *Nat Rev Microbiol* **16**, 585-593 (2018).
190. M. Kawada-Matsuo, Y. Yoshida, N. Nakamura, H. Komatsuzawa, Role of two-component systems in the resistance of *Staphylococcus aureus* to antibacterial agents. *Virulence* **2**, 427-430 (2011).
191. R. P. Novick, Autoinduction and signal transduction in the regulation of staphylococcal virulence. *Mol Microbiol* **48**, 1429-1449 (2003).
192. K. Sureka *et al.*, Positive feedback and noise activate the stringent response regulator rel in mycobacteria. *PLoS One* **3**, e1771 (2008).

193. M. Kawada-Matsuo *et al.*, Three distinct two-component systems are involved in resistance to the class I bacteriocins, Nukacin ISK-1 and nisin A, in *Staphylococcus aureus*. *PLoS One* **8**, e69455 (2013).
194. S. Utaida *et al.*, Genome-wide transcriptional profiling of the response of *Staphylococcus aureus* to cell-wall-active antibiotics reveals a cell-wall-stress stimulon. *Microbiology* **149**, 2719-2732 (2003).
195. M. Kuroda *et al.*, Two-component system VraSR positively modulates the regulation of cell-wall biosynthesis pathway in *Staphylococcus aureus*. *Mol Microbiol* **49**, 807-821 (2003).
196. S. Boyle-Vavra, S. Yin, D. S. Jo, C. P. Montgomery, R. S. Daum, VraT/YvqF is required for methicillin resistance and activation of the VraSR regulon in *Staphylococcus aureus*. *Antimicrob Agents Chemother* **57**, 83-95 (2013).
197. M. Falord, G. Karimova, A. Hiron, T. Msadek, GraXSR proteins interact with the VraFG ABC transporter to form a five-component system required for cationic antimicrobial peptide sensing and resistance in *Staphylococcus aureus*. *Antimicrob Agents Chemother* **56**, 1047-1058 (2012).
198. A. Delaune *et al.*, The WalKR system controls major staphylococcal virulence genes and is involved in triggering the host inflammatory response. *Infect Immun* **80**, 3438-3453 (2012).
199. S. Dubrac, I. G. Boneca, O. Poupel, T. Msadek, New insights into the WalK/WalR (YycG/YycF) essential signal transduction pathway reveal a major role in controlling cell wall metabolism and biofilm formation in *Staphylococcus aureus*. *J Bacteriol* **189**, 8257-8269 (2007).
200. A. Hiron, M. Falord, J. Valle, M. Debarbouille, T. Msadek, Bacitracin and nisin resistance in *Staphylococcus aureus*: a novel pathway involving the BraS/BraR two-component system (SA2417/SA2418) and both the BraD/BraE and VraD/VraE ABC transporters. *Mol Microbiol* **81**, 602-622 (2011).
201. A. Katz, S. Elgamal, A. Rajkovic, M. Ibba, Non-canonical roles of tRNAs and tRNA mimics in bacterial cell biology. *Mol Microbiol* **101**, 545-558 (2016).
202. J. Shepherd, M. Ibba, Direction of aminoacylated transfer RNAs into antibiotic synthesis and peptidoglycan-mediated antibiotic resistance. *FEBS Lett* **587**, 2895-2904 (2013).
203. T. Geiger *et al.*, Role of the (p)ppGpp synthase RSH, a RelA/SpoT homolog, in stringent response and virulence of *Staphylococcus aureus*. *Infect Immun* **78**, 1873-1883 (2010).
204. M. C. Manav *et al.*, Structural basis for (p)ppGpp synthesis by the *Staphylococcus aureus* small alarmone synthetase RelP. *J Biol Chem* **293**, 3254-3264 (2018).
205. C. C. Boutte, S. Crosson, Bacterial lifestyle shapes stringent response activation. *Trends Microbiol* **21**, 174-180 (2013).
206. A. O. Gaca, C. Colomer-Winter, J. A. Lemos, Many means to a common end: the intricacies of (p)ppGpp metabolism and its control of bacterial homeostasis. *J Bacteriol* **197**, 1146-1156 (2015).
207. M. M. Mwangi *et al.*, Whole-genome sequencing reveals a link between beta-lactam resistance and synthetases of the alarmone (p)ppGpp in *Staphylococcus aureus*. *Microb Drug Resist* **19**, 153-159 (2013).
208. J. Dordel *et al.*, Novel determinants of antibiotic resistance: identification of mutated loci in highly methicillin-resistant subpopulations of methicillin-resistant *Staphylococcus aureus*. *MBio* **5**, e01000 (2014).
209. M. Pardos de la Gandara *et al.*, Genetic Determinants of High-Level Oxacillin Resistance in Methicillin-Resistant *Staphylococcus aureus*. *Antimicrob Agents Chemother* **62** (2018).
210. S. Aedo, A. Tomasz, Role of the Stringent Stress Response in the Antibiotic Resistance Phenotype of Methicillin-Resistant *Staphylococcus aureus*. *Antimicrob Agents Chemother* **60**, 2311-2317 (2016).
211. C. Milheirico, H. de Lencastre, A. Tomasz, Full-Genome Sequencing Identifies in the Genetic Background Several Determinants That Modulate the Resistance Phenotype in Methicillin-Resistant *Staphylococcus aureus* Strains Carrying the Novel mecC Gene. *Antimicrob Agents Chemother* **61** (2017).
212. C. K. Kim, C. Milheirico, H. de Lencastre, A. Tomasz, Antibiotic Resistance as a Stress Response: Recovery of High-Level Oxacillin Resistance in Methicillin-Resistant *Staphylococcus aureus* "Auxiliary" (fem) Mutants by Induction of the Stringent Stress Response. *Antimicrob Agents Chemother* **61** (2017).
213. S. Rohrer, B. Berger-Bächi, FemABX peptidyl transferases: a link between branched-chain cell wall peptide formation and beta-lactam resistance in gram-positive cocci. *Antimicrob Agents Chemother* **47**, 837-846 (2003).

214. Y. d'Aubenton Carafa, E. Brody, C. Thermes, Prediction of rho-independent *Escherichia coli* transcription terminators. A statistical analysis of their RNA stem-loop structures. *J Mol Biol* **216**, 835-858 (1990).
215. J. W. Roberts, Termination factor for RNA synthesis. *Nature* **224**, 1168-1174 (1969).
216. E. Skordalakes, J. M. Berger, Structure of the Rho transcription terminator: mechanism of mRNA recognition and helicase loading. *Cell* **114**, 135-146 (2003).
217. A. Ray-Soni, M. J. Bellecourt, R. Landick, Mechanisms of Bacterial Transcription Termination: All Good Things Must End. *Annu Rev Biochem* **85**, 319-347 (2016).
218. E. J. Steinmetz, T. Platt, Evidence supporting a tethered tracking model for helicase activity of *Escherichia coli* Rho factor. *Proc Natl Acad Sci U S A* **91**, 1401-1405 (1994).
219. P. Mitra, G. Ghosh, M. Hafeezunnisa, R. Sen, Rho Protein: Roles and Mechanisms. *Annu Rev Microbiol* **71**, 687-709 (2017).
220. S. K. Tomar, I. Artsimovitch, NusG-Spt5 proteins-Universal tools for transcription modification and communication. *Chem Rev* **113**, 8604-8619 (2013).
221. C. M. Burns, W. L. Nowatzke, J. P. Richardson, Activation of Rho-dependent transcription termination by NusG. Dependence on terminator location and acceleration of RNA release. *J Biol Chem* **274**, 5245-5251 (1999).
222. J. Chalissery, S. Banerjee, I. Bandey, R. Sen, Transcription termination defective mutants of Rho: role of different functions of Rho in releasing RNA from the elongation complex. *J Mol Biol* **371**, 855-872 (2007).
223. R. S. Washburn, A. Marra, A. P. Bryant, M. Rosenberg, D. R. Gentry, rho is not essential for viability or virulence in *Staphylococcus aureus*. *Antimicrob Agents Chemother* **45**, 1099-1103 (2001).
224. A. Nagel *et al.*, Inhibition of Rho Activity Increases Expression of SaeRS-Dependent Virulence Factor Genes in *Staphylococcus aureus*, Showing a Link between Transcription Termination, Antibiotic Action, and Virulence. *MBio* **9** (2018).
225. R. S. Washburn, M. E. Gottesman, Transcription termination maintains chromosome integrity. *Proc Natl Acad Sci U S A* **108**, 792-797 (2011).
226. W. Gan *et al.*, R-loop-mediated genomic instability is caused by impairment of replication fork progression. *Genes Dev* **25**, 2041-2056 (2011).
227. S. Hamperl, K. A. Cimprich, Conflict Resolution in the Genome: How Transcription and Replication Make It Work. *Cell* **167**, 1455-1467 (2016).
228. S. Hamperl, K. A. Cimprich, The contribution of co-transcriptional RNA:DNA hybrid structures to DNA damage and genome instability. *DNA Repair (Amst)* **19**, 84-94 (2014).
229. J. T. Wade, D. C. Grainger, "Pervasive transcription: illuminating the dark matter of bacterial transcriptomes" in Nat Rev Microbiol. (England, 2014), vol. 12, pp. 647-653.
230. M. H. de Smit, P. W. Verlaan, J. van Duin, C. W. Pleij, Intracistronic transcriptional polarity enhances translational repression: a new role for Rho. *Mol Microbiol* **69**, 1278-1289 (2008).
231. C. J. Cardinale *et al.*, Termination factor Rho and its cofactors NusA and NusG silence foreign DNA in *E. coli*. *Science* **320**, 935-938 (2008).
232. P. Nicolas *et al.*, Condition-dependent transcriptome reveals high-level regulatory architecture in *Bacillus subtilis*. *Science* **335**, 1103-1106 (2012).
233. S. E. Irving, R. M. Corrigan, Triggering the stringent response: signals responsible for activating (p)ppGpp synthesis in bacteria. *Microbiology* **164**, 268-276 (2018).
234. G. Kraemer, J. Iandolo, High-Frequency Transformation of *Staphylococcus aureus* by Electroporation. *Curr Microbiol* **21**, 373-376 (1990).
235. P. D. Fey *et al.*, A genetic resource for rapid and comprehensive phenotype screening of nonessential *Staphylococcus aureus* genes. *MBio* **4**, e00537-00512 (2013).
236. J. Rolo *et al.*, High genetic diversity among community-associated *Staphylococcus aureus* in Europe: results from a multicenter study. *PLoS One* **7**, e34768 (2012).
237. J. Messing, New M13 vectors for cloning. *Methods Enzymol* **101**, 20-78 (1983).
238. S. Gardete, H. de Lencastre, A. Tomasz, A link in transcription between the native pbpB and the acquired *mecA* gene in a strain of *Staphylococcus aureus*. *Microbiology* **152**, 2549-2558 (2006).
239. H. de Lencastre *et al.* (1994) Methicillin-resistant*Staphylococcus aureus* disease in a portuguese hospital: Characterization of clonal types by a combination of DNA typing methods. pp 64-73.
240. D. R. Bentley, Whole-genome re-sequencing. *Curr Opin Genet Dev* **16**, 545-552 (2006).
241. L. W. Hillier *et al.*, Whole-genome sequencing and variant discovery in C. elegans. *Nat Methods* **5**, 183-188 (2008).

242. F. Poly *et al.*, Genome sequence of a clinical isolate of Campylobacter jejuni from Thailand. *Infect Immun* **75**, 3425-3433 (2007).
243. G. J. Velicer *et al.*, Comprehensive mutation identification in an evolved bacterial cooperator and its cheating ancestor. *Proc Natl Acad Sci U S A* **103**, 8107-8112 (2006).
244. B. L. de Jonge, Y. S. Chang, D. Gage, A. Tomasz, Peptidoglycan composition in heterogeneous Tn551 mutants of a methicillin-resistant *Staphylococcus aureus* strain. *J Biol Chem* **267**, 11255-11259 (1992).
245. V. Bidnenko *et al.*, Termination factor Rho: From the control of pervasive transcription to cell fate determination in *Bacillus subtilis*. *PLoS Genet* **13**, e1006909 (2017).
246. U. Mader *et al.*, *Staphylococcus aureus* Transcriptome Architecture: From Laboratory to Infection-Mimicking Conditions. *PLoS Genet* **12**, e1005962 (2016).
247. C. E. Bogden, D. Fass, N. Bergman, M. D. Nichols, J. M. Berger, The structural basis for terminator recognition by the Rho transcription termination factor. *Mol Cell* **3**, 487-493 (1999).
248. G. E. Christie *et al.*, The complete genomes of *Staphylococcus aureus* bacteriophages 80 and 80α--implications for the specificity of SaPI mobilization. *Virology* **407**, 381-390 (2010).
249. D. McDevitt, E. R. Wann, T. J. Foster, Recombination at the coagulase locus in *Staphylococcus aureus*: plasmid integration and amplification. *J Gen Microbiol* **139**, 695-706 (1993).
250. A. B. Reams, J. R. Roth, Mechanisms of gene duplication and amplification. *Cold Spring Harb Perspect Biol* **7**, a016592 (2015).
251. J. W. Savopoulos *et al.*, Identification, cloning, and expression of a functional phenylalanyl-tRNA synthetase (pheRS) from *Staphylococcus aureus*. *Protein Expr Purif* **21**, 470-484 (2001).
252. S. S. Elbaramawi *et al.*, Exploring the binding sites of *Staphylococcus aureus* phenylalanine tRNA synthetase: A homology model approach. *J Mol Graph Model* **73**, 36-47 (2017).
253. U. Mäder *et al.*, *Staphylococcus aureus* Transcriptome Architecture: From Laboratory to Infection-Mimicking Conditions. *PLoS Genet* **12**, e1005962 (2016).
254. C. G. Korea *et al.*, Staphylococcal Esx proteins modulate apoptosis and release of intracellular *Staphylococcus aureus* during infection in epithelial cells. *Infect Immun* **82**, 4144-4153 (2014).
255. M. R. Stapleton *et al.*, Characterization of IsaA and SceD, two putative lytic transglycosylases of *Staphylococcus aureus*. *J Bacteriol* **189**, 7316-7325 (2007).
256. H. K. Miller *et al.*, The extracytoplasmic function sigma factor sigmaS protects against both intracellular and extracytoplasmic stresses in *Staphylococcus aureus*. *J Bacteriol* **194**, 4342-4354 (2012).
257. H. Wang *et al.*, Dual-Targeting Small-Molecule Inhibitors of the *Staphylococcus aureus* FMN Riboswitch Disrupt Riboflavin Homeostasis in an Infectious Setting. *Cell Chem Biol* **24**, 576-588.e576 (2017).
258. A. Fagerlund, P. E. Granum, L. S. Havarstein, *Staphylococcus aureus* competence genes: mapping of the SigH, ComK1 and ComK2 regulons by transcriptome sequencing. *Mol Microbiol* **94**, 557-579 (2014).
259. L. Attaiech, C. Granadel, J. P. Claverys, B. Martin, RadC, a misleading name? *J Bacteriol* **190**, 5729-5732 (2008).
260. C. J. Saveson, S. T. Lovett, Tandem repeat recombination induced by replication fork defects in *Escherichia coli* requires a novel factor, RadC. *Genetics* **152**, 5-13 (1999).
261. L. G. Klinkenberg, J. H. Lee, W. R. Bishai, P. C. Karakousis, The stringent response is required for full virulence of *Mycobacterium tuberculosis* in guinea pigs. *J Infect Dis* **202**, 1397-1404 (2010).
262. T. Geiger *et al.*, The stringent response of *Staphylococcus aureus* and its impact on survival after phagocytosis through the induction of intracellular PSMs expression. *PLoS Pathog* **8**, e1003016 (2012).
263. C. D. Majerczyk *et al.*, Direct targets of CodY in *Staphylococcus aureus*. *J Bacteriol* **192**, 2861-2877 (2010).
264. M. Fang, C. E. Bauer, Regulation of stringent factor by branched-chain amino acids. *Proc Natl Acad Sci U S A* **115**, 6446-6451 (2018).
265. E. Nudler, RNA polymerase backtracking in gene regulation and genome instability. *Cell* **149**, 1438-1445 (2012).
266. J. Gowrishankar, J. K. Leela, K. Anupama, R-loops in bacterial transcription: their causes and consequences. *Transcription* **4**, 153-157 (2013).
267. A. Aguilera, H. Gaillard, Transcription and recombination: when RNA meets DNA. *Cold Spring Harb Perspect Biol* **6** (2014).

268. J. K. Leela, A. H. Syeda, K. Anupama, J. Gowrishankar, Rho-dependent transcription termination is essential to prevent excessive genome-wide R-loops in *Escherichia coli*. *Proc Natl Acad Sci U S A* **110**, 258-263 (2013).
269. A. Grylak-Mielnicka, V. Bidnenko, J. Bardowski, E. Bidnenko, Transcription termination factor Rho: a hub linking diverse physiological processes in bacteria. *Microbiology* **162**, 433-447 (2016).
270. R. Menouni, S. Champ, L. Espinosa, M. Boudvillain, M. Ansaldi, Transcription termination controls prophage maintenance in *Escherichia coli* genomes. *Proc Natl Acad Sci U S A* **110**, 14414-14419 (2013).
271. A. Solopova *et al.*, Regulation of Cell Wall Plasticity by Nucleotide Metabolism in *Lactococcus lactis*. *J Biol Chem* **291**, 11323-11336 (2016).
272. E. Skordalakes, A. P. Brogan, B. S. Park, H. Kohn, J. M. Berger, Structural mechanism of inhibition of the Rho transcription termination factor by the antibiotic bicyclomycin. *Structure* **13**, 99-109 (2005).
273. M. Arnaud, A. Chastanet, M. Debarbouille, New vector for efficient allelic replacement in naturally nontransformable, low-GC-content, gram-positive bacteria. *Appl Environ Microbiol* **70**, 6887-6891 (2004).
274. G. Karimova, J. Pidoux, A. Ullmann, D. Ladant, A bacterial two-hybrid system based on a reconstituted signal transduction pathway. *Proc Natl Acad Sci U S A* **95**, 5752-5756 (1998).
275. U. Jenal, A. Reinders, C. Lori, Cyclic di-GMP: second messenger extraordinaire. *Nat Rev Microbiol* **15**, 271-284 (2017).
276. L. J. McGuffin *et al.*, IntFOLD: an integrated web resource for high performance protein structure and function prediction. *Nucleic Acids Res* **47**, W408-W413 (2019).
277. M. Pellegrini-Calace, T. Maiwald, J. M. Thornton, PoreWalker: a novel tool for the identification and characterization of channels in transmembrane proteins from their three-dimensional structure. *PLoS Comput Biol* **5**, e1000440 (2009).
278. E. B. Purcell, R. Tamayo, Cyclic diguanylate signaling in Gram-positive bacteria. *FEMS Microbiol Rev* **40**, 753-773 (2016).
279. U. Römling, M. Y. Galperin, M. Gomelsky, Cyclic di-GMP: the first 25 years of a universal bacterial second messenger. *Microbiol Mol Biol Rev* **77**, 1-52 (2013).
280. T. Mascher, J. D. Helmann, G. Unden, Stimulus perception in bacterial signal-transducing histidine kinases. *Microbiol Mol Biol Rev* **70**, 910-938 (2006).
281. C. P. Zschiedrich, V. Keidel, H. Szurmant, Molecular Mechanisms of Two-Component Signal Transduction. *J Mol Biol* **428**, 3752-3775 (2016).
282. J. L. Smith, A. D. Grossman, In Vitro Whole Genome DNA Binding Analysis of the Bacterial Replication Initiator and Transcription Factor DnaA. *PLoS Genet* **11**, e1005258 (2015).
283. S. Goldstein, L. Beka, J. Graf, J. L. Klassen, Evaluation of strategies for the assembly of diverse bacterial genomes using MinION long-read sequencing. *BMC Genomics* **20**, 23 (2019).
284. L. Gong *et al.*, Complete genome sequencing of the luminescent bacterium, Vibrio qinghaiensis sp. Q67 using PacBio technology. *Sci Data* **5**, 170205 (2018).
285. W. Song, T. Thomas, R. J. Edwards, Complete genome sequences of pooled genomic DNA from 10 marine bacteria using PacBio long-read sequencing. *Mar Genomics* (2019).
286. A. B. Reams, E. Kofoid, E. Kugelberg, J. R. Roth, Multiple pathways of duplication formation with and without recombination (RecA) in Salmonella enterica. *Genetics* **192**, 397-415 (2012).
287. L. A. Gallagher *et al.*, Tandem Amplification of the Staphylococcal Cassette Chromosome mec Element Can Drive High-Level Methicillin Resistance in Methicillin-Resistant *Staphylococcus aureus*. *Antimicrob Agents Chemother* **61** (2017).
288. L. Sandegren, D. I. Andersson, Bacterial gene amplification: implications for the evolution of antibiotic resistance. *Nat Rev Microbiol* **7**, 578-588 (2009).